

University of Southern Queensland
Faculty of Health, Engineering and Sciences
School of Engineering

**Peak flow estimation considering future climate scenarios
for flood resilience modelling of the Warrego Highway at
Laidley Creek**

A dissertation submitted by

Hayden Jago

In fulfilment of the requirements of
ENP4111 Professional Engineer Research Project

Towards the degree of
Bachelor of Engineering (Honours) (Civil)

Submitted: 4 November 2024

Abstract

The Warrego Highway at Laidley Creek is susceptible to inundation following periods of high catchment rainfall, causing the closure of a high priority connection within the state-controlled road network. Increased surface temperatures attributed to climate change are projected to increase the intensity of extreme rainfall events. It is therefore anticipated the extent of flooding from Laidley Creek will increase and events will become more frequent.

This study investigated the impact of increased high intensity rainfall on peak discharge characteristics using a semi-distributed node-reach runoff routing model developed in the RORB software package. The model parameters were calibrated against eight historic rainfall-runoff events encompassing a variety of peak magnitudes and event durations. The LIMB-BOM 2020 design rainfall envelope was factored to account for the projected median rises in surface temperature across two emissions scenarios at three projection horizons. Current and projected design event discharges were estimated using the Monte Carlo stochastic simulation method and compared to the estimates obtained by independent techniques including flood frequency analysis and regionalised regression methods.

The simulated discharges closely corresponded to the independent estimates for the 2% and 1% AEP events, indicating the model was accurately calibrated for low frequency, high flow events. The model projected rises in the median design discharge of 51% and 49% for the 2% and 1% AEP events respectively by 2090. However, uncertainty in the results increased for the higher frequency events, with less alignment between the independent estimates and the simulated flows.

The hydrologic simulations completed in this project form the first component of a proposed site investigation into the current and future flood resilience of the Warrego Highway at Laidley Creek. An accompanying hydraulic investigation of the existing bridge crossing section is recommended to complete the investigation.

University of Southern Queensland
School of Engineering
ENP4111 Professional Engineer Research Project

(This is a 2-unit research project in the Bachelor of Engineering Honours Program)

Limitations of Use

The Council of the University of Southern Queensland, its Academic Affairs, and the staff of the University of Southern Queensland, do not accept any responsibility for the truth, accuracy or completeness of material contained within or associated with this dissertation.

Persons using all or any part of this material do so at their own risk, and not at the risk of the Council of the University of Southern Queensland, its Faculty of Health, Engineering and Science or the staff of the University of Southern Queensland.

This dissertation reports an educational exercise and has no purpose or validity beyond this exercise. The sole purpose of this dissertation project is to contribute to the overall education within the student's chosen degree program. This document, the associated hardware, software, drawings, and any other material set out in the associated appendices should not be used for any other purpose: if they are so used, it is entirely at the risk of the user.

University of Southern Queensland
School of Engineering
ENP4111 Professional Engineer Research Project


Certification of Dissertation

I certify that the ideas, designs and experimental work, results, analyses and conclusions set out in this dissertation are entirely my own effort, except where otherwise indicated and acknowledged.

I further certify that the work is original and has not been previously submitted for assessment in any other course or institution, except where specifically stated.



Hayden Jago

Student Number: 

Date: 4 November 2024

Acknowledgements

There are several people who have supported me during this research project that I wish to acknowledge. The accomplishment that is the culmination of this report would not have been possible without them.

Firstly, I express the sincerest of thanks to my supervisor, Dr Sreeni Chadalavada, for his support of my project and his patience during my research journey. Additionally, I am grateful for the teaching and assistance provided by the academic and technical staff at USQ during my four years of enrolment.

Thank you to my colleagues at the Department of Transport and Main Roads who have mentored me during my final year internship.

Finally, thank you to my family, especially Mum, Dad and Mia, whose wholehearted love, patience and understanding has been my greatest support during this extremely demanding period of my life. Thanks so much, love you.

Table of Contents

Abstract	ii
Limitations of Use	iii
Certificate of Dissertation	iv
Acknowledgements	v
List of Tables	xi
List of Figures	xii
Abbreviations	xvi
1. Introduction	1
1.1 Overview	1
1.2 Background	1
1.3 Scope for research	2
1.4 Research objectives.....	2
1.5 Project benefits.....	3
2. Literature Review	4
2.1 Introduction.....	4
2.2 Laidley Creek catchment	4
2.2.1 Catchment geography and flow characteristics	4
2.2.2 Catchment land uses	7
2.2.3 Warrego Highway crossing of Laidley Creek	8
2.2.4 Flood history of Laidley Creek at the Warrego Highway	9
2.3 Regional hydrologic modelling.....	12
2.3.1 Overview	12
2.3.2 Introduction to Australian Rainfall and Runoff 2019 (ARR 2019).....	13
2.3.3 Design floods and rainfall events	14
2.3.4 Event terminology	15
2.3.5 Flood event criteria for the state-controlled road network	16
2.4 Input data for hydrologic modelling	18

2.4.1	Observed stream discharge data	18
2.4.2	Observed rainfall data.....	20
2.4.3	Design rainfall data.....	22
2.4.3.1	<i>Revised LIMB 2020 IFDs</i>	23
2.5	Conversion of rainfall to runoff in regional catchments	24
2.5.1	Catchment rainfall and streamflow relationships	24
2.5.2	Design rainfall Areal Reduction Factor	25
2.5.3	Rainfall temporal patterns	26
2.5.4	Catchment losses	28
2.6	Hydrologic modelling methods.....	31
2.6.1	At-site flood frequency analysis	31
2.6.1.1	<i>Annual maximum series</i>	32
2.6.1.2	<i>Log-Pearson III distribution</i>	34
2.6.2	Runoff routing	35
2.6.2.1	<i>Node-reach model features</i>	38
2.6.2.2	<i>Subcatchment area delineation</i>	38
2.6.2.3	<i>Non-linear storage routing</i>	38
2.6.3	Continuous catchment simulation models	39
2.6.4	Regression methods of analysis.....	40
2.6.4.1	<i>Parametric regression</i>	40
2.6.4.2	<i>Quantile regression</i>	40
2.7	Future climate considerations	41
2.7.1	Overview of climate change	41
2.7.2	Future climate impacts on hydrologic components.....	44
2.7.2.1	<i>Event intensity and frequency</i>	44
2.7.2.2	<i>Temporal patterns</i>	44
2.7.3	Direct climate impacts within the Lockyer Valley region.....	44
2.7.4	Design recommendations for future flood estimation	46

2.7.4.1	<i>DTMR climate change risk assessment framework</i>	48
2.8	Summary	48
3.	Methodology	50
3.1	Introduction	50
3.2	Design methodology overview	50
3.2.1	Preliminary methodology scope	50
3.2.2	Best practice modelling considerations	51
3.3	Data acquisition and preparation	52
3.3.1	Catchment geographic spatial data	52
3.3.2	Gauged streamflow data	56
3.3.2.1	<i>Rating curve and control evaluation for 143229A (Warrego Highway)</i>	58
3.3.2.2	<i>Rating curve and control evaluation for 143209B (Mulgowie)</i>	60
3.3.3	Observed rainfall data	62
3.3.3.1	<i>Daily observed rainfall totals</i>	62
3.3.3.2	<i>Hourly observed rainfall</i>	64
3.3.4	Design rainfall event parameters	64
3.3.4.1	<i>LIMB-BOM IFD enveloped dataset</i>	64
3.3.4.2	<i>Projected future climate IFD datasets</i>	64
3.3.4.3	<i>ARR Datahub parameters</i>	65
3.3.5	Finalisation of the design methodology scope	65
3.4	Semi-distributed runoff routing model development	65
3.4.1	Catchment model generation from spatial data	65
3.4.2	Generation of calibration storm files from previous observed events	68
3.4.3	Calibration of the RORB model parameters	71
3.4.3.1	<i>Calibrated events with closely replicated peak flows</i>	74
3.4.3.2	<i>Problematic or uncertain calibration events</i>	77
3.4.4	Current and future design flow simulations	79
3.4.4.1	<i>Ensemble simulation method</i>	80

3.4.4.2	<i>MC simulation method</i>	81
3.5	Bayesian Flood Frequency Analysis.....	82
3.5.1	Initial plotting position from annual maximum series.....	82
3.5.2	Fitted distribution functions.....	83
3.5.3	Bayesian parameter estimation.....	85
3.5.4	FFA design discharge results.....	86
3.6	Regression methods of peak flow estimation	86
3.6.1	RFFE method.....	86
3.6.2	P&W method	88
3.7	Research methodology evaluation	90
3.8	Summary.....	90
4.	Results	91
4.1	Design discharge simulation for current climate conditions.....	91
4.2	Design discharge simulation for future climate scenarios	93
4.3	Sensitivity analysis of the model parameters.....	95
5.	Discussion.....	97
5.1	Independent sanity validation of the results.....	97
5.1.1	Comparison of current design discharge simulation	97
5.1.2	Comparison of design discharges for future climate scenarios	98
5.2	Limitations of the results	99
5.2.1	Data limitations.....	99
5.2.1.1	<i>Uncertainty in the climate projections</i>	100
5.2.1.2	<i>Inadequate catchment coverage from rainfall stations</i>	100
5.2.1.3	<i>Duration of the gauged streamflow record</i>	101
5.2.1.4	<i>Simplification of catchment spatial features</i>	102
5.2.2	Modelling limitations	102
5.2.2.1	<i>Calibration uncertainty</i>	102
5.2.2.2	<i>Simulation uncertainty</i>	104

5.5.2.3	<i>Validation uncertainty</i>	105
5.2.2.4	<i>Limited consideration of time variable components</i>	105
5.3	Potential model improvements	105
6.	Conclusion	107
6.1	Summary of results	107
6.2	Recommended future work	108
	References	109
	Appendix A: Project specification and work plan (topic later refined)	116
	Appendix B: Rainfall station datasets coverage	121
	Appendix C: Design rainfall IFDs at Laidley Creek catchment centroid	123
	Appendix D: ARR Datahub files - Laidley Creek catchment	131
	Appendix E: RORB catchment file	137
	Appendix F: Calibration storm event files	143
	Appendix G: Design discharge simulation sets	167
	Appendix H: Sensitivity analysis of model parameters using 2020 outputs	178
	Appendix I: Flood frequency analysis – RMC outputs	182

List of Tables

Table 2.1: Observed Laidley Creek overtopping events of Warrego Highway	12
Table 2.2: East Coast North burst loading proportion by duration (Jordan, Seed & Nathan 2019)	28
Table 2.3: Rate of change α in rainfall intensity per degree of temperature rise ($\%/^{\circ}\text{C}$) and 66% certainty range in the value (Wasko et al. 2024)	47
Table 2.4: Mean surface temperature increase projections ΔT for design RCP scenarios relative to 1961-1990 baseline (Wasko et al. 2024)	47
Table 2.5: Mean annual temperature rise ($^{\circ}\text{C}$) relative to reference period 1986 – 2005 for Lockyer Valley (Queensland Government 2024)	48
Table 3.1: Distribution of data quality by classification at 143229A station.....	58
Table 3.2: Extreme rainfall events used to calibrate RORB model parameters.....	69
Table 3.3: Best-fit and average parameters for RORB calibration events	79
Table 3.4: Posterior mode FFA discharges (m^3/s) for suitable distributions	86
Table 3.5: 143229A discharges estimates from RFFE method.....	88
Table 3.6: 143229A discharge estimates from P&W method for current climate.....	89
Table 3.7: 143229A discharge estimates from P&W equations for RCP 4.5 scenarios	89
Table 3.8: 143229A discharge estimates from P&W equations for RCP 8.5 scenarios	89
Table 4.1: Simulated design discharges for current climate scenario (2020 envelope).....	91
Table 4.2: Simulated median discharge estimates for RCP 4.5 scenarios and percentage increase compared to current climate simulated median	93
Table 4.3: Simulated median discharge estimates for RCP 8.5 scenarios and percentage increase compared to current climate simulated median	93
Table 4.4: Sensitivity analysis of model parameters – current climate simulation.....	96
Table 5.1: Comparison of current climate simulation with independent estimates (m^3/s)	97
Table 5.2: Comparison of RCP 4.5 scenario simulations with P&W estimates (m^3/s).....	98
Table 5.3: Comparison of RCP 8.5 scenario simulations with P&W estimates (m^3/s).....	99

List of Figures

Figure 2.1: Upper reaches of the Laidley Creek Catchment surrounded by Little Liverpool Range (foreground) and Mistake Mountains (background) (Starkey 2023).....	5
Figure 2.2: Laidley Creek crossing at Thornton (Lockyer Valley Regional Council 2024b) ..	5
Figure 2.3: Thornton crossing overtopped during May 2022 flood event (Lockyer Valley Regional Council 2022b)	6
Figure 2.4: Sandy Creek floodplain at Forest Hill (Lockyer Valley Regional Council 2024b)	6
Figure 2.5: Upper reaches of the Laidley Creek Catchment surrounded by Little Liverpool Range (foreground) and Mistake Mountains (background) (Starkey 2023)	7
Figure 2.6: Laidley Creek catchment outlet at 143229A gauging station adjacent to Warrego Highway (Department of Resources 2024a).....	9
Figure 2.7: Thornton crossing overtopped during May 2022 flood event (Lockyer Valley Regional Council 2022b)	10
Figure 2.8: Sandy Creek floodplain at Forest Hill (Lockyer Valley Regional Council 2024b)	10
Figure 2.9: Laidley Creek flows overtopping Warrego Highway on 13/05/2022 (Department of Transport and Main Roads 2022a)	11
Figure 2.10: Widespread inundation of the Laidley Creek floodplain adjacent to the Warrego Highway during the January 2011 flood event (Lacey 2011)	11
Figure 2.11: ARR 2019 Preferred Terminology (Bates et al. 2019).....	15
Figure 2.12: Illustration of freeboard between roadway surface and cross drainage flows (Institute of Public Works Engineering Australasia 2017)	16
Figure 2.13: Recommended design event AEPs for cross drainage road flood immunity (Weeks, Babister & Retallick 2023)	17
Figure 2.14: Example rating curve generated from gauged data (Bates et al. 2019)	19
Figure 2.15: Source of incremental error through rating curve extrapolation at high discharges (Bates et al. 2019)	20
Figure 2.16: Design Rainfall Intensity IFD chart (example) (Bureau of Meteorology 2016b)	23
Figure 2.17: Short duration ARF equation for all locations in Australia (Babister et al. 2016)	26
Figure 2.18: Long duration ARF parametric equation for Laidley Creek (Babister et al. 2016)	26

Figure 2.19: Example event cumulative burst distributions (Jordan, Seed & Nathan 2019)	27
Figure 2.20: IL/CL model application to hyetograph (Ball, Weinmann & Boyd 2019)	29
Figure 2.21: Median initial loss distribution for Australia (Ball, Weinmann & Boyd 2019)	29
Figure 2.22: Continuous loss distribution in Australia (Ball, Weinmann & Boyd 2019)	30
Figure 2.23: Burst and storm initial losses (Ball, Weinmann & Boyd 2019)	31
Figure 2.24: Time series plot of discharge data (Holland, Herschy & Archer 1998)	32
Figure 2.25: Storage and travel impacts between inflow and outflow hydrographs (Ball, Weinmann & Boyd 2019)	36
Figure 2.26: Node-reach runoff routing model processes (Ball, Weinmann & Boyd 2019)	37
Figure 2.27: Projected CO ₂ emissions (mass, left) and CO ₂ atmospheric concentration (ppm, right) for RCPs until 2100 (Van Vuuren et al. 2011).	42
Figure 2.28: Project global temperature rises associated with the RCP climate scenarios relative to the 1961-1990 baseline (Wasko et al. 2024)	43
Figure 2.29: Annual mean temperature anomaly in Queensland between 1910 and 2023 based on 30 year average from 1961 to 1990 (Bureau of Meteorology 2024a)	45
Figure 3.1: Poor alignment of Laidley Creek using the rasterised threshold flow accumulation method	54
Figure 3.2: Laidley Creek catchment boundary delineated from ridgelines identified in the 25 metre contour overlay	55
Figure 3.3: Laidley Creek catchment with centroid location, major stream network and gauging stations shown	56
Figure 3.4: Site details for the 143229A and 143209B streamgauges extracted from the WMIP (Department of Regional Development, Manufacturing & Water 2024)	57
Figure 3.5: Monthly maximum streamflow record for 143229A gauge [generated from data produced by (Department of Regional Development, Manufacturing & Water 2024)]	57
Figure 3.6: 143229A Warrego Highway hydraulic control and surrounding stream section (Department of Regional Development, Manufacturing & Water 2024)	59
Figure 3.7: Well defined site rating curve from individual gaugings for 143229A station (Department of Regional Development, Manufacturing & Water 2024)	60
Figure 3.8: 143209B Mulgowie hydraulic control and surrounding stream section (Department of Regional Development, Manufacturing & Water 2024)	60

Figure 3.9: Site rating curve with significantly varied gaugings for 143209B station (Department of Regional Development, Manufacturing & Water 2024)	61
Figure 3.10: Full (green) and partial (yellow) rainfall station event record status	63
Figure 3.11: Suitable displacement between actual subcatchment centroids (black) and snapped centroid nodes to adjacent stream network (orange)	66
Figure 3.12: Partitioned subcatchments and adjusted stream reaches for RORB catchment file development.....	67
Figure 3.13: May 2022 event rainfall (mm) isohyetal distribution from active station datasets (stars).....	70
Figure 3.14: Calculated hydrograph (red) for February 2022 event using regionalised $k_c =$ 22.48.....	72
Figure 3.15: Calculated hydrograph (red) for May 2022 event using regionalised $k_c = 22.48$	72
Figure 3.16: Lateral separation between calculated and observed hydrographs for January 2013 event.....	73
Figure 3.17: Calibrated hydrograph for November 2008 event.....	74
Figure 3.18: Calibrated hydrograph for January 2011 event	74
Figure 3.19: Calibrated hydrograph for January 2013 event	75
Figure 3.20: Calibrated hydrograph for March 2017 event	75
Figure 3.21: Calibrated hydrograph for February 2022 event	76
Figure 3.22: Calibrated hydrograph for January 2024 event	76
Figure 3.23: Calibrated hydrograph for May 1996 event	77
Figure 3.24: Calibrated hydrograph for May 2022 event	78
Figure 3.25: 5% AEP, 48 hour Ensemble simulation event hydrographs	80
Figure 3.26: Sample set of runoff frequency curves generated from MC simulation	81
Figure 3.27: 143229A annual maximum discharge series 1991 – 2023.....	82
Figure 3.28: 143229A Laidley Creek at Warrego Highway AM series input and plotting position graph generated in RMC-BestFit	83
Figure 3.29: LP3, Gamma and Weibull distributions fitted to AM series with outlier flows identified	84
Figure 3.30: Posterior mode and confidence intervals of the Bayesian parametric estimation method for the LP3 distribution.....	85
Figure 3.31: RFFE input tool for 143229A catchment characteristics	87

Figure 4.1: Distribution of MC simulated peak discharges for current climate scenario	92
Figure 4.2: Distribution of sample 1% AEP event discharges for current IFDs and RCP 8.5 scenarios.....	94
Figure 4.3: Median 1% AEP peak discharges for RCP 4.5 and 8.5 scenarios to 2090	95
Figure 5.1: Reduction of central catchment daily rainfall station coverage from May 1996 (left) to February 2022 (right).....	101
Figure 5.2: Level of calibration accuracy for various flow magnitudes during January 2011 event.....	103

Abbreviations

AADT	Average Annual Daily Traffic
AATOS	Average Annual Time of Submergence
AIC	Akaike Information Criteria
AEP	Annual Exceedance Probability
AHD	Australian Height Datum
AM	Annual Maximum
ARF	Areal Reduction Factor
ARI	Average Recurrence Interval
ARR	Australian Rainfall and Runoff: A Guide to Flood Estimation
BIC	Bayesian Information Criteria
BOM	Bureau of Meteorology
CCNHRA	Climate Change and Natural Hazards Risk Assessment
CL	Continuing Loss
DDD	Darling Downs District
DEM	Digital Elevation Model
DRDMW	Department of Regional Development, Manufacturing and Water
DTMR	Department of Transport and Main Roads
EY	Exceedances per Year
FFA	Flood Frequency Analysis
FIP	Flood Information Portal
GCM	Global Circulation Model
GEV	Generalised Extreme Value
GP	Generalised Pareto
IDW	Inverse Distance Weighted
IFD	Intensity-Frequency-Distribution
IL	Initial Loss
IPCC	Intergovernmental Panel on Climate Change
LiDAR	Light Detection and Ranging
LIMB	Lockyer-Ipswich-Moreton Bay

LGA	Local Government Area
LVRC	Lockyer Valley Regional Council
LP3	Log Pearson Type III
MC	Monte Carlo
MLE	Maximum Likelihood Estimation
PILF	Potentially Influential Low Flow
POT	Peak-over-Threshold
P&W	Palmen and Weeks
QFCD	Queensland Future Climate Dashboard
QWMN	Queensland Water Modelling Network
RCP	Representative Concentration Pathway
RCM	Regional Climate Model
RFFE	Regional Flood Frequency Estimation
RMC	RMC-BestFit
RSME	Root Mean Square Error
SRTM	Shuttle Radar Topography Mission
WMIP	Water Monitoring Information Portal

1. Introduction

1.1 Overview

This research project intends to assess the impact of intensifying extreme rainfall events caused by climate change on critical transport infrastructure. For this project, the Warrego Highway crossing of Laidley Creek was selected as the case study location of interest. The site was chosen because of its historical record of flooding and its significance within the Southeast Queensland highway network controlled by the Department of Transport and Main Roads.

Defined within this introduction are the design objectives which guided the scope of literature reviewed to develop a thorough understanding of the multi-disciplinary topic, including hydrologic modelling technical recommendations and requirements. The objectives also guided the formation of a suitable research methodology, which considers modelling practices utilised by industry to ensure quality in the results obtained.

Throughout this report, the inputs sourced and outputs generated in response to each design objective are verified against supporting literature and independent methods of analysis to ensure the finalised results are as accurate as possible. The uncertainty and limitations associated with climate scenarios projections, as well as different modelling methods, are emphasised throughout this report. The results are presented in a format suitable for a future hydraulic investigation of the case study location as an extension to this research project.

1.2 Background

The Warrego Highway between Ipswich and Toowoomba supports approximately 26500 vehicle movements per day (Department of Transport and Main Roads 2023) as the primary connection for communities and freight between metropolitan Southeast Queensland and regional Southern Queensland.

The section of the highway corridor surrounding Laidley Creek is prone to inundation because of its low-lying elevation. Previous high rainfall events within the Laidley Creek catchment have resulted in major flooding, causing closures which prohibit traffic flow along a vital component of the state-controlled highway network.

The intensity of extreme rainfall is projected to increase in the coming decades due to raised surface temperatures attributed to climate change (Bureau of Meteorology & CSIRO 2022; Department of Transport and Main Roads 2024f).

Infrastructure upgrades to the Warrego Highway crossing of Laidley Creek have been explored to enhance flood immunity during peak events, in conjunction with improving motorist safety at a notoriously dangerous intersection. The lengthy period associated with the planning and design of upgrades to significant public infrastructure means accurate estimates indicative of future climate conditions are essential to achieving desired improvements to the site. Accurate planning and design is vital to prevent intensified damage to infrastructure from an evolving climate.

1.3 Scope for research

Broad projections of future climate conditions are widely published in literature and continually revised as modelling capabilities are improved. However, impacts of climate change on rainfall and the subsequent effects on catchment hydrology particularly at a regionalised scale are emerging, but remain less publicised.

It is hypothesised that inundation of the Warrego Highway crossing site will be exacerbated under future climate scenarios. However, no case study has yet to incorporate these projections as a component of a site specific hydrologic investigation of the Laidley Creek catchment. A clear gap in current knowledge exists with an ideal scope that underpins this project.

Hence, this research project aims to quantify the effects of increased extreme rainfall intensity on peak event discharge within the Laidley Creek catchment under multiple climate projection scenarios. It is intended this would be achieved through the development of a hydrologic model calibrated to the topography of the Laidley Creek catchment and current climate conditions. Revision of the model inputs representative of anticipated future rainfall intensities would yield updated design discharge estimates to be compared with current design discharges.

1.4 Research objectives

A series of sequential research objectives were established to advance the case study, as outlined below and expanded upon within the corresponding components of this report.

Objective 1: Background review of literature

Completion of a comprehensive review of literature to identify fundamental parameters, applications and assumptions covering the multi-disciplinary aspects associated with this project. Topics to be reviewed include catchment hydrology, climate science, transport engineering and infrastructure management. Academic, technical and government sources of reference material should be considered.

Objective 2: Documentation of the design research methodology

Documentation of a definitive research methodology that thoroughly describes the formation of a suitable hydrologic model, referencing the findings and assumptions introduced in the literature review.

Objective 3: Data acquisition and processing in preparation for technical modelling

Acquisition of high quality spatial and hydrologic data sets to produce a subcatchment model and storm event files compatible with a designated software platform.

Objective 4: Calibration of the design model

Generation of design discharge estimates from model specific parameters calibrated to historic peak flow events and verified against independent computational methods.

Objective 5: Simulation of future design discharges

Simulation of revised design discharge estimates representative of the impacts of climate change on hydrologic processes at a localised scale, such that the differences in hydrologic processes between current and future climate conditions are quantified.

Objective 6: Communication of the model outcomes

Preparation of this report communicating the development and findings of the research, including uncertainties in the outputs. An evaluation of the adopted research approach, specifically its strengths and limitations and a recommended course of action is incorporated.

1.5 Project benefits

Several beneficial outcomes are anticipated from undertaking this research project. Foremost is an enhanced understanding of current and future catchment hydrologic processes and interactions within the Laidley Creek catchment.

The design discharge estimates obtained through this research project are a crucial input for a two-dimensional hydraulic modelling study of the bridge crossing site. While outside the scope of this project, detailed hydraulic investigations are necessary to assess the current and future levels of flood immunity achieved by a bridge structure. The accuracy of these models is reliant on the accuracy of the results determined in the preceding hydrologic modelling (this report).

In addition to the intended use of the results of this research, an improved understanding of catchment hydrology could assist the development and revision of floodplain management strategies to reduce the impact of intensifying rainfall events on local communities.

2. Literature Review

2.1 Introduction

This chapter provides a synthesised background of literature reviewed across various topics relevant towards the development of various components of the project methodology. This review begins by introducing the characteristics of the Laidley Creek catchment and the Warrego Highway crossing at Laidley Creek. The application of Australian Rainfall and Runoff 2019 for modelling with observed and design events is explored. The application of event criteria for infrastructure design and management within the state controlled road network is examined. Then, the fundamental processes of regional hydrology that contribute to the generation of runoff from rainfall are reviewed. Subsequently, catchment flood modelling approaches representative of regional hydrologic processes are introduced, including at-site flood frequency analysis, runoff routing, continuous simulation and regression methods of analysis. The advantages and limitations of each approach are examined within the context of this research project. Future global climate change scenarios are introduced and the impacts on catchment hydrologic processes are contextualised to Australian conditions. Relevant published methodologies that detailing how future climate projections are incorporated within the hydrologic modelling for the design and management of state controlled road infrastructure are reviewed. Finally, this chapter concludes by outlining the evident knowledge gap that exists in current literature forming the basis of this dissertation.

2.2 Laidley Creek catchment

The Laidley Creek catchment is located within the Lockyer Valley Regional Council (LVRC) local government area (LGA) and the Darling Downs District (DDD) of the state-controlled road network managed by the Queensland Department of Transport and Main Roads (DTMR). The following sections outline the geographical characteristics of the catchment and the flood history at the catchment outlet adjacent to the Warrego Highway.

2.2.1 Catchment geography and overview of flow characteristics

The Laidley Creek catchment encompasses an area of 462 km² consisting of all the tributaries of Laidley Creek upstream of the Department of Regional Development, Manufacturing and Water (DRDMW) operated streamgauge 143229A titled ‘Laidley Creek at Warrego Highway’ (Department of Regional Development, Manufacturing & Water 2024). Nestled between the ridgelines of the Little Liverpool Range and the Mistake Mountains, Laidley Creek originates in steep, densely-vegetated terrain where elevations exceed 1000 - 1100 m AHD (Department of Resources 2024b), as depicted in Figure 2.1.



Figure 2.1: Upper reaches of the Laidley Creek Catchment surrounded by Little Liverpool Range (foreground) and Mistake Mountains (background) (Starkey 2023)

Overland flows generated from the steep hillslopes are collected within a distinct valley containing Laidley Creek. Low volume, channelised flows pass through the rural localities of Townson, Thornton and Mulgowie, where minor bridge crossings are located, as exemplified in Figure 2.2. When flow volumes increase substantially during peak flood events, these crossings are overtopped, as observed in Figure 2.3. A second DRDMW operated streamgauge (143209B) is located at Mulgowie which captures an upstream subcatchment area of 167 km² (Department of Regional Development, Manufacturing & Water 2024).

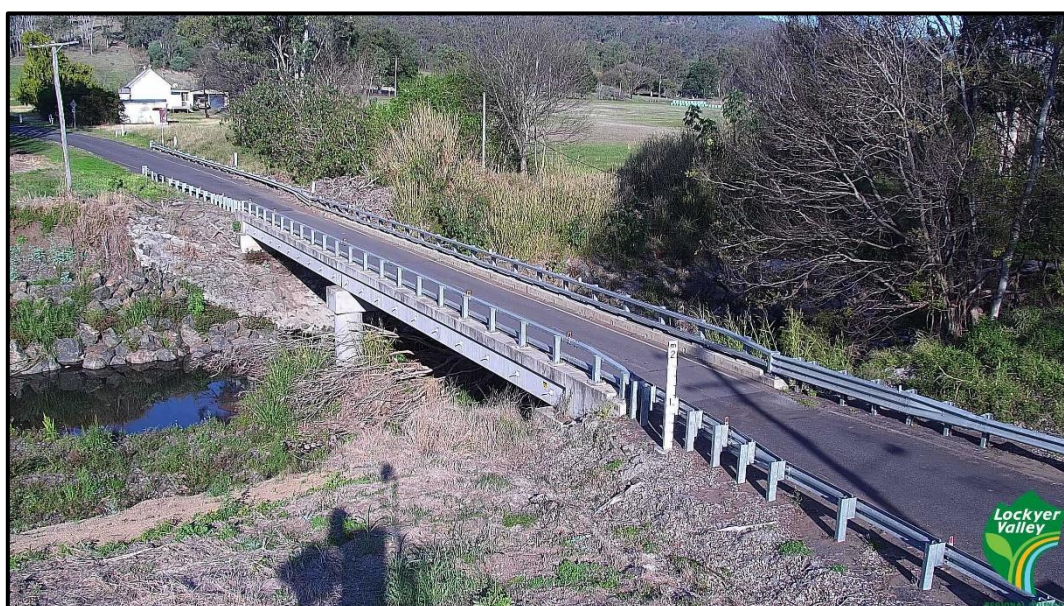


Figure 2.2: Laidley Creek crossing at Thornton (Lockyer Valley Regional Council 2024a)



Figure 2.3: Thornton crossing overtopped during May 2022 flood event (Lockyer Valley Regional Council 2022b)

Laidley Creek continues north past the outer edges of the townships of Laidley and Forest Hill, where the landscape is dominated by expansive, low-lying floodplains and rolling hills, as characterised by Figure 2.4 below. The 6.9 GL capacity off stream reservoir named Lake Dyer is situated in this portion of the catchment (SEQWater 2024). Flowing parallel to Laidley Creek is its major tributary, Sandy Creek, which originates from the slopes of Mount Berryman and flows north until its confluence with Laidley Creek downstream of Forest Hill. Laidley Creek continues north until the 143229A gauge located at the Warrego Highway crossing. Flows through the streamgauge outlet continue 4.5 kilometres downstream until the confluence of Laidley Creek and Lockyer Creek at Glenore Grove. Lockyer Creek then flows into the Brisbane River at Lowood, just downstream from the Wivenhoe Dam spillway.



Figure 2.4: Sandy Creek floodplain at Forest Hill (Lockyer Valley Regional Council 2024b)

2.2.2 Catchment land uses

The dominant land uses within the catchment are conservation, rural agricultural and rural residential zones according to the LVRC Flood Information Portal (FIP) (Lockyer Valley Regional Council 2022a), as shown in Figure 2.5. The predominantly rural nature of the catchment means the proportion of impervious surface area is negligible in the context of a regional hydrology analysis. The high proportion of natural, pervious surfaces and narrow road corridors depicted in Figures 2.1 – 2.4 support this concept.

The FIP provides detailed flood information, including flow depth, velocity, level and hazard for a range of flood events at an individual property level for the entire LVRC LGA. The information serves as a useful validation source for the modelling within this dissertation.

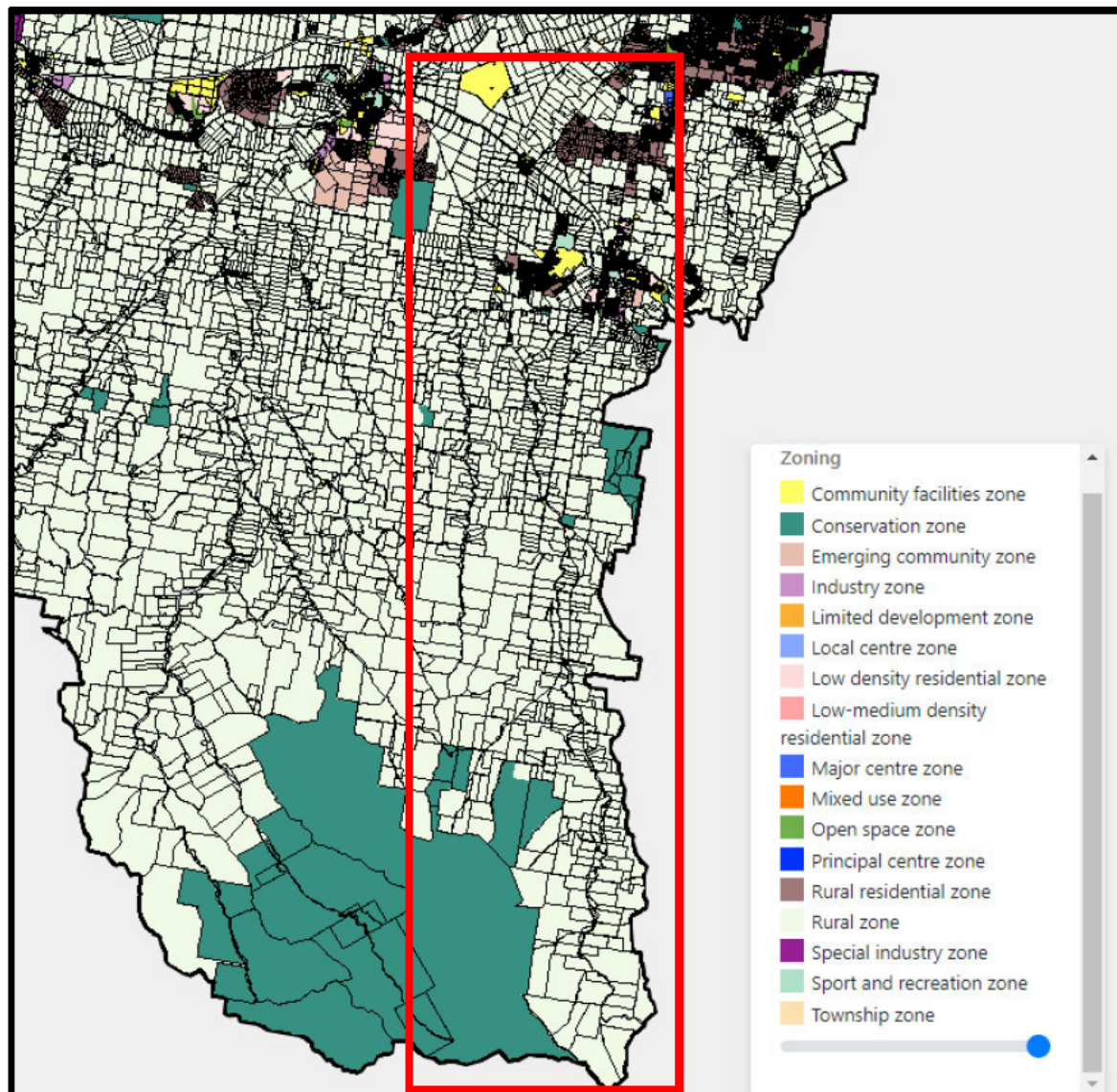


Figure 2.5: LVRC FIP land use zoning within the Laidley Creek catchment - approximate extent annotated (Lockyer Valley Regional Council 2022a).

The agricultural industry has a significant presence in the Lockyer Valley region, which in the 2020-21 financial year generated \$375 million of produce for both domestic supply and international exportation (Australian Bureau of Statistics 2021). Commodities produced in the region include vegetables, representing 86% of the regional agricultural output, as well as hay, grains and nursery flowers; and beef and poultry farming (Australian Bureau of Statistics 2021). These commodities require practices such as irrigated broadacre cropping, dryland cropping and livestock grazing, which are heavily reliant on water resource availability and distribution throughout the catchment.

During periods of drought with insufficient water availability for irrigation; crop propagation, growth and survival is continually threatened until harvest. Conversely, periods of intense rainfall and extensive flooding lead to inundation of the typically low lying, flat cropping fields, causing widespread losses of produce. Both climatic extremes threaten employment opportunities and the viability of businesses in the agricultural industry, which impacts the supply of produce into communities.

2.2.3 Warrego Highway crossing of Laidley Creek

The Warrego Highway between Ipswich and Toowoomba is referred as section 18A of the state-controlled road network managed by DTMR. This section of the network is the primary connection for communities and freight between metropolitan Southeast Queensland and regional Southern Queensland, as well as western and interstate destinations.

The Warrego Highway is classified as a national highway route and forms a critical component of the National Land Transport Network, supporting B-Double and Higher Mass Limits vehicular movements (Department of Transport and Main Roads 2019). The average annual daily traffic (AADT) on this section of the highway is 26534 vehicles per day including 21.5% heavy vehicles (Department of Transport and Main Roads 2023). 18A facilitates the transportation of \$19 billion worth of freight annually (Infrastructure Australia 2023) as a vital connection between regional primary industries and producers; and the Port of Brisbane (Department of Transport and Main Roads 2012). Freight transported along the route includes seasonal harvest produce, livestock, mining plant and equipment, fuels, building supplies and machinery, and general consumer supplies for western communities (Department of Transport and Main Roads 2012). The route also serves “as a strategic military ... link between key military installations in southern Queensland, including Amberley RAAF base, Oakey Army Aviation Centre and Borneo Barracks” (Department of Transport and Main Roads 2012).

The Laidley Creek catchment outlet coincides with the DRDMW gauging station 143229A, which is situated adjacent to the Warrego Highway at the Forest Hill – Fernvale Road intersection (between Plainland and Crowley Vale at an approximate chainage of 48.0 km), see Figure 2.6. Laidley Creek passes under the Warrego Highway at the Jack Martin Bridge.



Figure 2.6: Laidley Creek catchment outlet at 143229A gauging station adjacent to Warrego Highway (Department of Resources 2024a)

2.2.4 Flood history of Laidley Creek at the Warrego Highway

Social accessibility and economic productivity characteristics of the region are dependent on the connectivity of the Warrego Highway between Toowoomba and Ipswich, which is compromised by insufficient flood immunity above stream crossings and low lying floodplains. As identified by DTMR, the area surrounding the Laidley Creek outlet is subject to repeated major flooding which causes closures of the Warrego Highway (Department of Transport and Main Roads 2012). The road corridor between chainages 47.8 km and 48.2 km is prone to flooding, especially at both the eastbound and westbound approaches to the Jack Martin Bridge. As pictured in Figure 2.7, the existing surface vertical depression at chainage 47.9 km (at the

intersection of Forest-Hill Fernvale Road) is the lowest level of the Warrego Highway within the immediate vicinity of Laidley Creek and is most vulnerable to inundation.



Figure 2.7: Warrego Highway westbound approach towards Laidley Creek crossing (Department of Transport and Main Roads 2024b)

During peak flow events, transverse flows from Laidley Creek overtop the road surface and cannot be sufficiently dissipated by the existing minor box culvert drainage. Therefore, traffic is prohibited from passing through the crossing. Flooding was recurrent enough to warrant the installation of a monitoring camera, from which imagery from previous flooding events has featured in mainstream media and DTMR publications, see Figures 2.8 and 2.9 below.



Figure 2.8: Laidley Creek flows extensively overtopping Warrego Highway on 26/02/2022 (Department of Transport and Main Roads 2022b)



Figure 2.9: Laidley Creek flows overtopping Warrego Highway on 13/05/2022 (Department of Transport and Main Roads 2022a)

The extent of inundation and hence the length of roadway closed inherently varies between flood events due to the naturally unique rainfall distribution patterns and catchment conditions of each event. The more widespread floods, exemplified by Figure 2.8, have a longer roadway closure duration causing greater social and economic disruptions compared to less significant events. Aerial imagery captured during the January 2011 flood event, shown in Figure 2.10, demonstrates the extent of floodplain inundation from Laidley Creek (situated in the foreground along the tree line) during a peak event. The extent of flooding is consistent with the event characteristics modelled in the FIP (Lockyer Valley Regional Council 2022a).



Figure 2.10: Widespread inundation of the Laidley Creek floodplain adjacent to the Warrego Highway during the January 2011 flood event (Lacey 2011)

Listed in Table 2.1 are the previous events when the Warrego Highway has been inundated by transverse flows of Laidley Creek. The source that confirms the roadway was overtopped during each event, consisting of archival flood records for historic events, and photographic evidence in more recent times, are referenced.

Table 2.1: Observed Laidley Creek overtopping events of Warrego Highway

Start date	End date	Peak discharge at 143229A (m ³ /s)	Source of record to verify roadway inundation/overtopping
3/05/1996	6/05/1996	496.6	(Bureau of Meteorology 2010a)
10/01/2011	12/01/2011	1387.1	(Lacey 2011)
27/01/2013	29/01/2013	1041.5	(Wordsworth 2013)
25/02/2022	28/02/2022	1097.7	(Department of Transport and Main Roads 2022b)
12/05/2022	14/05/2022	521.1	(Department of Transport and Main Roads 2022a)
30/01/2024	30/01/2024	366.7	(Transport and Main Roads Queensland 2024)

2.3 Regional hydrologic modelling

2.3.1 Overview

Regional hydrologic modelling is a numeric representation of the distribution of water within the natural environment throughout the water cycle. Modelling simulates complex physical processes including rainfall, evaporation and infiltration losses to statistically estimate hydrologic processes of surface runoff, stream flow and groundwater flow (Singh & Woolhiser 2002). Modelling allows engineers and policymakers to understand catchment hydrology and implement measures to optimise resource distribution, particularly during flood or drought.

A catchment is an area bounded by a natural topographic rise which causes all surface flow to drain to a common outlet, often through at least one channel (Department of Environment & Innovation 2021). Larger regional catchments are comprised of smaller areas known as subcatchments. A rural catchment is characterised as a predominantly naturally discharging basin with a high proportion of pervious surfaces allowing infiltration of rainfall into the ground (Ladson 2014).

A hydrologic model is classified by its period of simulation as either a single event method or a continuous simulation method. Event methods simulate a singular flood event by simplifying the physical processes behind the conversion of rainfall to runoff as a set of numeric parameters (Babister, Retallick & Testoni 2019). Generally, a loss model is utilised to simulate rainfall excess from a singular storm event, while a hydrograph routing model simulates the conversion of rainfall excess to streamflow considering the spatial characteristics of a catchment (Nathan et al. 2019). With this approach, the prevailing catchment boundary conditions are specified by calibrating the model against previously observed data. Continuous simulation methods convert extended duration, continuous climatic datasets into a output streamflow dataset for the corresponding time series, from which the frequency and extent of flooding is extracted by statistical analysis (Nathan et al. 2019).

2.3.2 Introduction to Australian Rainfall and Runoff 2019 (ARR 2019)

Hydrologic modelling in Australia is standardised by design guidelines published by Engineer's Australia in Australian Rainfall and Runoff: A Guide to Flood Estimation (ARR) 2019. ARR 2019 is comprised of nine separate books. The technical guidelines presented in Books 1-5 and 7 (Ball et al. 2019; Ball, Weinmann & Boyd 2019; Bates et al. 2019; Jordan, Seed & Nathan 2019; Nathan et al. 2019; Babister, Retallick & Testoni 2019) document a variety of modelling approaches to estimate regional hydrologic characteristics. The development of each model from first principles concepts is discussed in detail and contextualised with respect to its intended purpose, required data preparation and model performance limitations.

ARR 2019 provides specific technical guidance about the requirements any catchment hydrologic assessment. ARR 2019 defines the parameters used to establish a flood hydrograph model representative of an event within a catchment, which are discussed throughout this review of literature. The modelling approaches presented within ARR 2019 are developed from the following considerations:

- Catchment geography and spatial characteristics.
- Event rainfall depth; in the form of both historic observed rainfall and design inputs.
- Event characteristics regarding the time and spatial distributions of rainfall.
- The processes which influence the conversion of rainfall to runoff.
- Observed streamflow data, if the catchment is gauged.

ARR 2019 also provides guidance for engineers to incorporate climate change projections into design flood estimation techniques. In addition, DTMR has published its own technical guidelines to standardise the adoption of these projections within modelling for a variety of different departmental projects. This guidance is examined in subsequent sections of this review.

2.3.3 Design floods and rainfalls

The objectives of catchment management and engineering design projects usually adopt risk-based failure or exceedance criteria. The hydrology field utilises hypothetical scenarios known as design flood and/or rainfall events with a specified frequency of occurrence to stipulate flood size characteristics (Bates et al. 2019). Because typical event characteristics, which consist of peak discharge, level and volume, are dependent on variable channel properties such as cross section and surface roughness, probability exceedance criteria provides a common mode of analysis for catchment scale modelling. The principles and methodologies presented in ARR 2019 were predominantly formulated from the concept of design events (Bates et al. 2019).

The probability relationship between design flood and rainfall events is not entirely direct. Flood frequency methods of discharge analysis directly estimate flood characteristics when the probability of a certain event magnitude is exceeded (Bates et al. 2019). However, the exceedance probability associated with a design rainfall event does not necessarily correlate to the corresponding exceedance probability for a flood event. In every modelling scenario, the representation of all processes that contribute to the conversion of rainfall to runoff introduces some joint uncertainty. The prevailing causes and effects associated with this conversion are directly related to the event conditions at the time of occurrence and are usually unique in space and time. Consequently, the “true probability of the derived flood characteristic may be ... biased with respect to the true flood magnitude with the same probability as the design rainfall, especially at low (exceedance) probabilities” (Bates et al. 2019). For example, a rainfall event within a saturated catchment may result in a large volume of runoff and cause significant flooding, however the same rainfall event could occur in a dry catchment may and yield minimal runoff. The process of preserving an event exceedance probability from a design rainfall and transforming it to a design flood is known as AEP neutrality (Bates et al. 2019). ARR 2019 stipulates in Book 3, Section 2.3.6.2 that caution should be exercised when utilising transformative methods of probabilistic-exceedance modelling between rainfall and discharge to avoid large margins of error (Ball et al. 2019).

2.3.4 Event terminology

The frequency of design flood and rainfall events are expressed in terms of descriptor classifications. The utilisation of each classification is dependent on the intended application of the model, as well as the frequency of occurrence of the flood or rainfall characteristic, which is, categorised from very frequent to extreme (Bates et al. 2019). Average recurrence interval (ARI), annual exceedance probability (AEP) and average number of exceedances per year (EY) are the frequency descriptors used in ARR 2019. ARI is defined as “a statistical estimate of the average period in years between the occurrence of a flood of a given size or larger” (Ladson 2014) and is expressed in years. Alternatively, AEP is defined as “the likelihood of a flood of given size or larger (occurring) in any year” (Ladson 2014) and is expressed in either percentage or 1 in X years. Frequencies higher than 50% AEP are expressed as Z EY to avoid confusion around successive seasonal events (Bates et al. 2019). Outlined in Figure 2.11 is the preferred industry terminology from ARR 2019.

Frequency Descriptor	EY	AEP (%)	AEP	ARI
			(1 in x)	
Very Frequent	12			
	6	99.75	1.002	0.17
	4	98.17	1.02	0.25
	3	95.02	1.05	0.33
	2	86.47	1.16	0.5
Frequent	1	63.21	1.58	1
	0.69	50	2	1.44
	0.5	39.35	2.54	2
	0.22	20	5	4.48
	0.2	18.13	5.52	5
Rare	0.11	10	10	9.49
	0.05	5	20	19.5
	0.02	2	50	49.5
	0.01	1	100	99.5
Very Rare	0.005	0.5	200	199.5
	0.002	0.2	500	499.5
	0.001	0.1	1000	999.5
	0.0005	0.05	2000	1999.5
	0.0002	0.02	5000	4999.5
Extreme			↓	
			PMP/ PMP Flood	

Figure 2.11: ARR 2019 Preferred Terminology (Bates et al. 2019)

2.3.5 Flood event criteria for the state-controlled road network

Several flood event metrics are used to assess the resilience of road infrastructure against inundation, which also assist the design of infrastructure upgrades and future corridor planning.

The flood immunity of a roadway is one such metric and is defined as the event probability of the flow level “that just reaches the height of the upstream shoulder of the road, or where the road is kerbed, the top of the inlet pit” (Weeks, Babister & Retallick 2023). In these scenarios, the trafficked pavement surface is above the flood level and remains dry. An allowance for model uncertainty, blockage effects and extremely rare flood magnitudes, known as freeboard, is usually prescribed between the design flood level and the structure level of interest (Weeks, Babister & Retallick 2023), as illustrated in Figure 2.12.

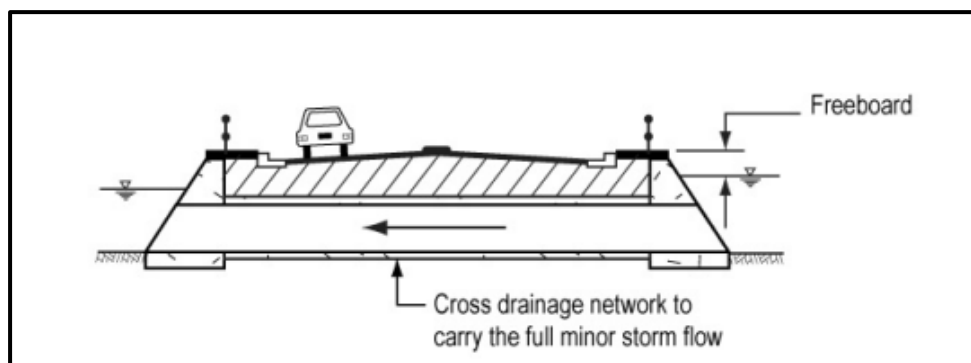


Figure 2.12: Illustration of freeboard between roadway surface and cross drainage flows (Institute of Public Works Engineering Australasia 2017)

The level of flood immunity stipulated for a specific element of road network infrastructure is dependent on many considerations, as detailed by Weeks, Babister & Retallick (2023) in Austroads Guide to Road Design Part 5: Drainage – General and Hydrology Considerations. Such considerations include:

- The strategic function of the road link within the broader network, including funding priorities.
- The availability of suitable, alternate routes during an overtopping flood event.
- Any requirements to maintain emergency access along the road link.
- Any adverse flood impacts on surrounding properties from development within and surrounding the road corridor. For example, a lower level of immunity would facilitate transverse flows across the road surface reducing upstream afflux.

Similar considerations dictate the magnitude of freeboard required for new road designs. Generally, road designs that avoid overtopping flows during a flood event provide 300 mm of

freeboard between the water surface level and the pavement subgrade or bridge soffit (Weeks, Babister & Retallick 2023).

The recommended event frequencies for flood immunity against transverse flows for the design of new road infrastructure, including bridge decks, are specified by Weeks, Babister & Retallick (2023) and adopted by DTMR (Department of Transport and Main Roads 2024e). An extract of the recommendations is provided in Figure 2.13 below.

Element	Austroads road classification	AEP
Cross drainage (culverts & bridges)	Controlled Access Highways Includes: Motorways & Freeways (National/State/Territory)	1%
	Arterial Roads Classes 1 & 2 Includes: National/State/Territory Highways, Urban Arterial Roads	2 – 1%
	Arterial Road Class 3 Includes: State/Territory main roads	2%
	Local Roads Classes 4 & 5	10 – 5%
	Urban Collector/Distributor Roads	10 – 2%
	Urban Local Roads	10%

Figure 2.13: Recommended design event AEPs for cross drainage road flood immunity (Weeks, Babister & Retallick 2023)

In this instance, the Warrego Highway is a National Highway and future flood immunity is recommended to be modelled for the 2 and 1% AEP events. To facilitate infrastructure management and future design projects, this research will determine the design discharges at the Laidley Creek outlet for the current and future climate scenarios, with an emphasis on ensuring the 2% and 1% events are accurately simulated.

Another flood event metric used by DTMR is the average annual time of submergence (AATOS), which is defined as the expected average duration per year the roadway is submerged by flood flows of any depth (Weeks, Babister & Retallick 2023). The frequency of overtopping flow events as well as the duration of each event are factors that contribute to AATOS (Weeks, Babister & Retallick 2023). The AATOS of a section of road is an alternate assessment of flood immunity that correlates flood characteristics to disruptions to traffic and incurred damage to infrastructure. Therefore, this metric is calculated by DTMR to evaluate the economic impact of disruptions caused by flooding when developing a business case for infrastructure upgrade projects (Department of Transport and Main Roads 2024e). AATOS is dependent on the catchment response to intense rainfall events which is affected by catchment area, shape, baseflow conditions and soil properties (Weeks, Babister & Retallick 2023).

2.4 Input data for hydrologic modelling

The types of accessible input data for catchment hydrologic modelling are explored in this section. The applicability of the data for different modelling approaches is examined and limitations of use are discussed.

2.4.1 Observed stream discharge data

Flood analysis requires routine collection of real flood data parameters at locations along defined flow paths, including water level stage above a datum (typically the channel base or ground surface), and subsequently discharge, the volume of water passed per unit time. Observed streamflow measurements are taken by instruments known as streamgauges. In Queensland, streamgauge monitoring is operated by the Department of Regional Development, Manufacturing & Water (DRDMW) and observations are recorded via remote electronic water level sensors and collated on the Water Monitoring Information Portal (WMIP). Hydraulic control devices such as a weir or sluice gate regulate flow in open channels to facilitate gauge measurement (Ladson 2014). Rectangular, v-notch and crump weirs are most commonly used in Queensland (Department of Regional Development, Manufacturing & Water 2024) and are typically either artificial concrete masonry structures or formations of natural channel sediment acting as a constriction (Ladson 2014). Empirical equations calibrate the observed flow depth to the equivalent discharge through the control device with known sectional properties (Caroline & Afshar 2014):

$$\text{Discharge through a rectangular weir:} \quad Q = C_d \frac{2}{3} b \sqrt{2gh}^{3/2} \quad (2.1)$$

$$\text{Discharge through a V notch weir:} \quad Q = C_d \frac{8}{15} \sqrt{2g} \tan(a/2) h^{5/2} \quad (2.2)$$

$$\text{Discharge through a crump weir:} \quad Q = \left(\frac{2}{3}\right)^{3/2} C_d C_v b \sqrt{gh}^{3/2} \quad (2.3)$$

Where Q is the weir discharge (m^3/s), h is the water depth above weir (m), C_d is the coefficient of discharge, g is the constant acceleration due to gravity ($9.81 \text{ m}^2/\text{s}$), b is the weir width (m), a is the notch weir angle (deg) and C_v is the coefficient of velocity for modular or non-modular flow, depending on the submerged condition of weir (Caroline & Afshar 2014).

In practice, empirical equations facilitate the development of discharge rating relationships. However, modern technological advancements have simplified this process. Measurements of discharge velocity in a channel by current meters are correlated to discharge at various times with associated river stage heights (Ladson 2014). A rating curve is generated by plotting stage-discharge data points and subsequently applying a best-fit curve to estimate discharge at a given

stage for a certain channel cross section (Bates et al. 2019). An example rating curve developed from a set of gauged data is shown in Figure 2.14.

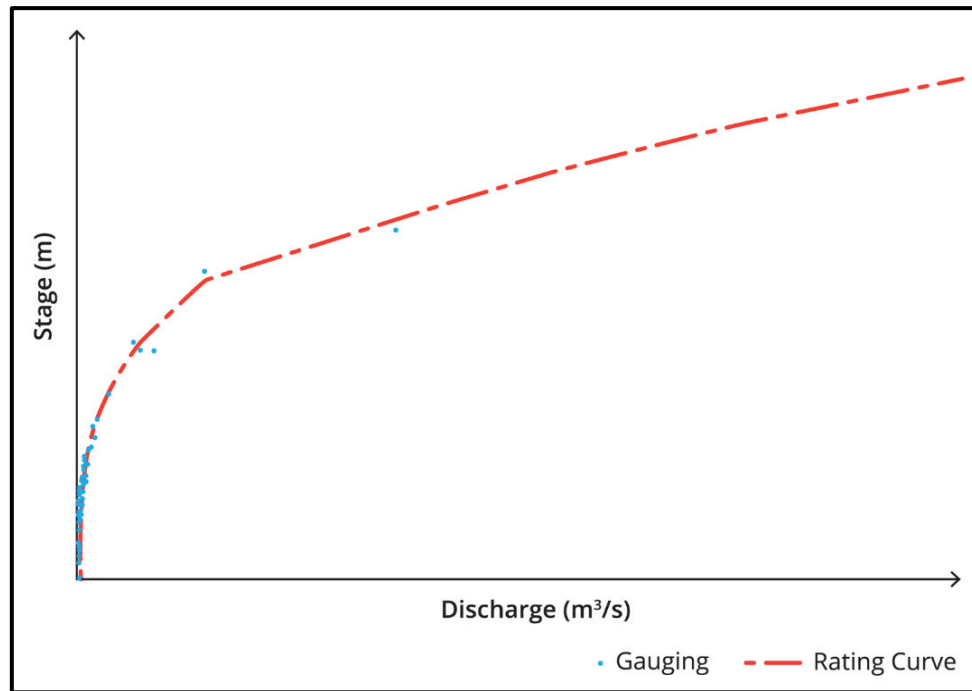


Figure 2.14: Example rating curve generated from gauged data (Bates et al. 2019)

A reliable rating curve is one that is defined thoroughly by a widespread range of flow gaugings but features densely grouped gaugings for similar flow magnitudes. A rating curve is typically well defined for low, frequently occurring flows, provided a constant control is maintained and a sufficient number of gaugings are taken. Vegetation growth, sedimentation and erosion; construction, dredging and damming; as well as downstream backwater effects significantly impact flows through a gauge (Bates et al. 2019) and modify the true site rating. Measurements of higher flows are typically less accurate for two reasons: the infrequency of rare events prohibits sufficient gauge recordings, and water level unsteadiness during intense flooding results in rapid fluctuations of flow slope, leading to variations in discharge from the steady flow condition (Bates et al. 2019). Estimating the discharge of peak flow and hypothetical design events larger than the maximum gauged level at a site requires extrapolation of the rating curve. However, extrapolating the defined curve beyond the range of gauged measurements is subject to error (Ladson 2014). This error is dependent on the nature of the true rating curve compared to the extrapolated estimate, as illustrated in Figure 2.15.

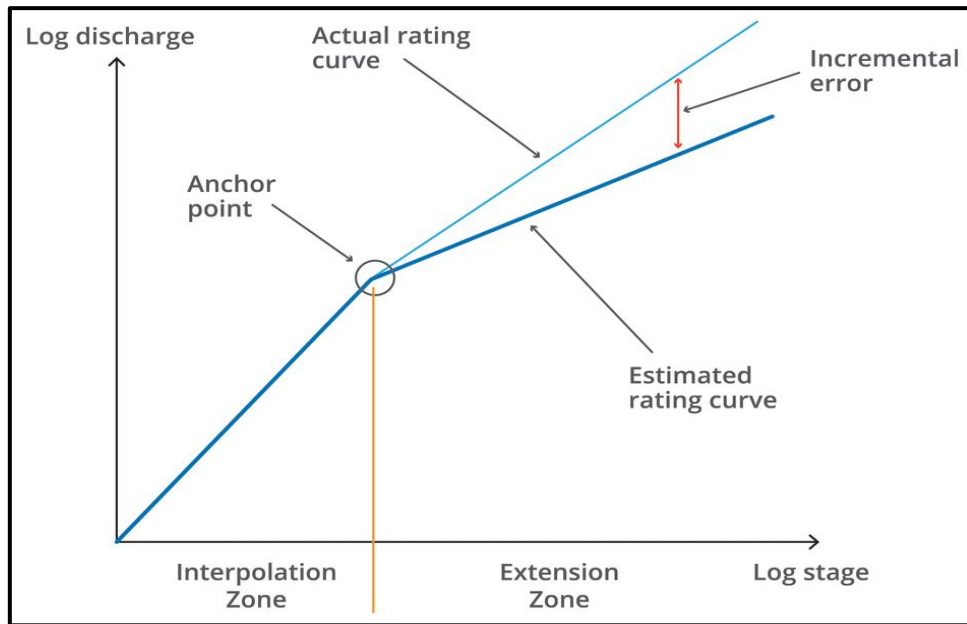


Figure 2.15: Source of incremental error through rating curve extrapolation at high discharges (Bates et al. 2019)

Streamflow data is required to be obtained and managed within various time scales for different hydrologic models, which are discussed in subsequent sections of this report. For example, flood frequency analysis computes flow quantiles from either the annual or daily maximum recorded flow, a continuous catchment simulation utilises daily total runoff volumes, while an hourly or sub-hourly increment is used for event based models which require an enhanced time resolution to generate a short duration hydrograph.

2.4.2 Observed rainfall data

The depth of precipitation that reaches the surface is recorded by an instrument known as a rain gauge. In Australia, observational data for 8000 current rainfall gauging stations is managed by the Bureau of Meteorology (BOM) Climate Data Services branch (Bureau of Meteorology 2010b, 2024b). Rainfall is also recorded at a limited number of DRDMW streamgauges. Historical rainfall data is available for an additional 11000 closed stations, including records that date back to the 1800s (Bureau of Meteorology 2010b).

Two standardised gauging instruments are used at sites across Australia. The oldest instrument is the eight inch rain gauge, which collects 25 mm of rainfall within an internal measuring cylinder while excess precipitation is captured by an outer container (Bureau of Meteorology 2007). Each gauge is placed 300 mm above the surface level to minimise the effects of wind on the accuracy of gauging (Bureau of Meteorology 2007). Observations of the rainfall

received in the preceding 24 hours to 9am are made by local volunteer personnel, who report the rainfall depths to BOM at the end of each month.

More recently, many of these stations have been replaced by contemporary automatic weather stations, which use an eight inch tipping bucket rain gauge. This instrument is capable of providing automatic readings on the depth and rate of rainfall to a precision of 0.2 mm and is self-emptying (Bureau of Meteorology 2007). This approach is more accurate and allows for more frequent rainfall observations to be recorded compared to the traditional manually documented gauging system. These advancements in gauging technology has allowed the introduction of rainfall observations at a minute, sub-hourly and hourly scale, as well as rainfall intensity measurements in the form of a pluviograph (Bureau of Meteorology 2024b).

It is rare that a station with a long operational history has maintained an entirely complete rainfall record. Common explanations provided by the Bureau of Meteorology (2010b) about the gaps in observed data sequences include:

- Closure of a station.
- Upgrade of station capacity.
- Damage sustained to an instrument which requires repair works.
- Absence of observer to take rainfall measurement.
- Automatic weather station failure.

The singular nature of a rainfall station means the observation is a point rainfall reading rather than a spatial rainfall measurement. A network of rainfall gauges is typically required to estimate the actual rainfall volume received in a regional-sized catchment over a specified interval with a sufficient degree of confidence (US National Weather Service n.d.). Various areal rainfall averaging techniques have been developed to compute catchment rainfall volumes, including the numeric and graphical methods used by the US National Weather Service (n.d.):

- Numeric methods; including arithmetic mean and distance-weighted methods.
- Graphical methods; including isohyetal (contour) and Thiessen polygon (area-weighted) methods.

Each method has its own associated advantages and disadvantages. However, the accuracy of catchment rainfall estimation is primarily dependent on the capability of each rain gauge to accurately record each rainfall event as well as ensuring sufficient coverage of gauge stations throughout the catchment (US National Weather Service n.d.). Sharp et al. (2021) noted that

many remote parts of Australia, including rural and mountainous areas in Queensland, had poor rain gauge coverage over an extended period of time due to the inherent geographic isolation and difficulties associated with access to these areas.

2.4.3 Design rainfall data

Design rainfall data is a fundamental component of many flood modelling approaches used in Australia. Observed rainfall recordings were processed to perform rainfall frequency analysis to relate the rainfall characteristics of intensity, the depth of rainfall in a certain time; frequency, the AEP of the rainfall event; and the duration of the rainfall event (Ladson, 2014). Intensity-frequency-duration (IFD) relationships are also referred to as design rainfall bursts between 1 EY and 1% AEP (Jordan, Seed & Nathan 2019) and have a similar purpose as design discharges for probabilistic hydrologic modelling. Design rainfall is expressed in the form $Y I_D$, where Y is the AEP and D is the duration of the event (Ladson 2014). Statistical exceedance design rainfalls are useful at overcoming the effects of short-term seasonality and climatic variability (Bates et al. 2019). Because numerous factors have an influence on peak flood events, the AEP of a design rainfall may not correspond to the equivalent design discharge.

Location-specific IFD relationships are retrievable from the Design Rainfall Data System (2016), managed by BOM. The database features IFD raster data at a grid cell size of 0.025° latitude and longitude (Bureau of Meteorology 2016a). The system uses cell interpolation to translate point rainfall observations into IFD relationships covering the entire Australian continent, including locations where gauged point data is unavailable or limited (Johnson et al. 2016). Such locations are geographically isolated, often due to high elevation, which prevents access to install and monitor rainfall gauges. These locations typically receive higher rainfalls than low-lying areas which contain the majority of gauge stations. (The et al. 2012), Consequently, most data is sourced from locations at lower elevations, meaning “at high elevations, rainfall is likely to be underestimated when it is spatially interpolated without reference to elevation” (The et al. 2012). The BOM IFD system used thin-plate spline smoothing of a digital elevation model (DEM) to incorporate topography into the design rainfall grid (Johnson et al. 2016), yielding more accurate IFD relationships.

IFD charts provide design rainfall depth in mm or intensity in mm/hr for events ranging from 1 minute to 7 days in duration and are available in either a tabular or chart format (Bureau of Meteorology 2016a; Jordan, Seed & Nathan 2019). Presented as Figure 2.16 is an example BOM IFD rainfall intensity chart, which illustrates that the IFD curves for different frequencies

are approximately parallel when plotted in a log-log scale. Ladson (2014) describes the two relationships that exist between IFD parameters:

- For a certain event duration, the intensity increases as the frequency reduces.
- For a certain event frequency, the intensity decreases as the duration increases.

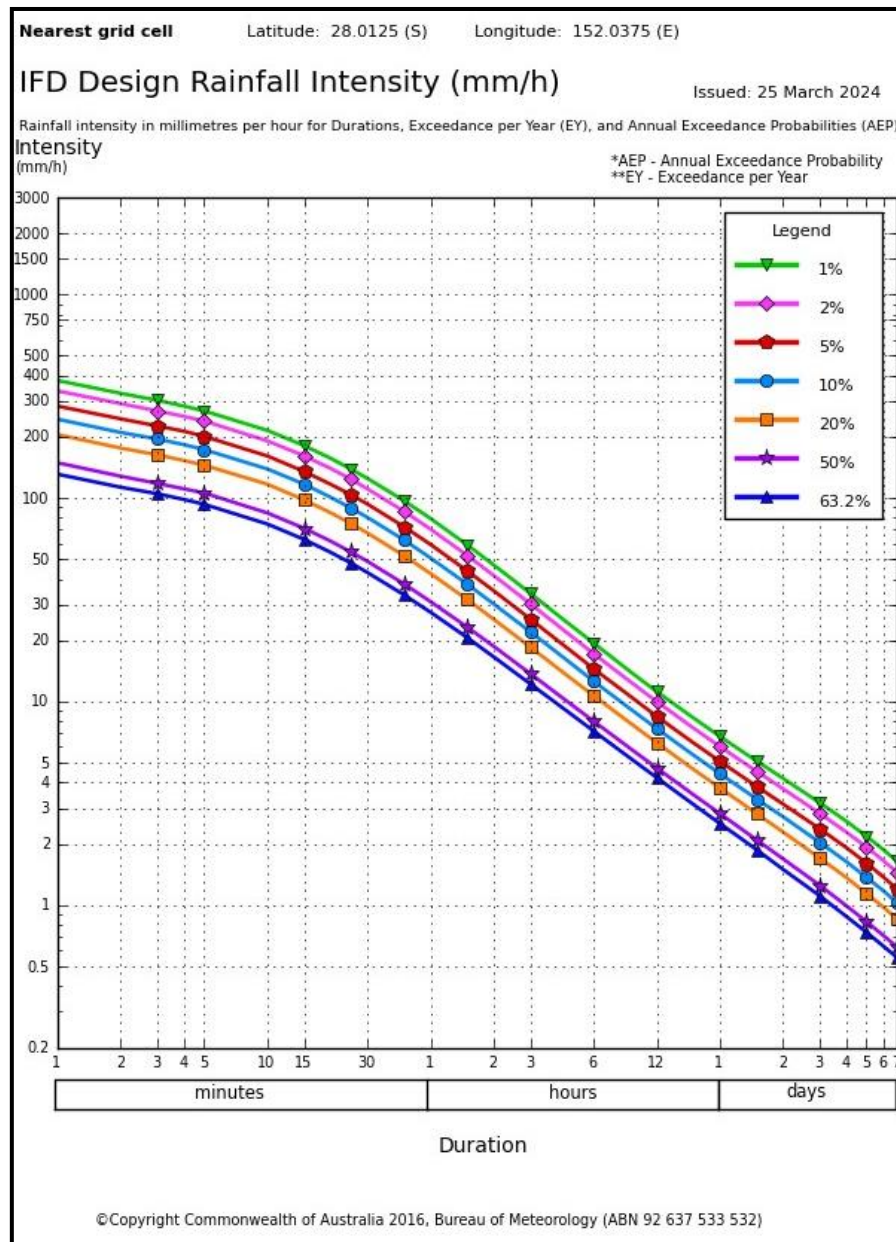


Figure 2.16: Design Rainfall Intensity IFD chart (example) (Bureau of Meteorology 2016b)

2.4.3.1 Revised LIMB 2020 IFDs

A revised set of gridded IFD relationships, known as the Lockyer-Ipswich-Moreton Bay (LIMB) 2020 IFDs, were computed for four LGAs within South-East Queensland including the LVRC after considerable differences were discovered between council rain gaugings and the BOM 2016 IFDs (Babister 2021). The methods used to derive the 2020 LIMB IFDs

prioritised localised rainfall data at a sub-daily time step to achieve “a reduction in local biases across all AEPs, durations and areas, compared to the ARR 2016 IFDs” (Babister 2021). Two alternate recommendations were provided for design flood modelling with the study region: either the revised LIMB 2020 IFDs should be adopted, or for conservative design of high rainfall events, an envelope consisting of the maximum IFDs between the LIMB 2020 and the existing BOM 2016 datasets would also be an acceptable approach (Babister 2021).

2.5 Conversion of rainfall to runoff in regional catchments

The following section introduces the fundamental hydrologic considerations for modelling the conversion process of rainfall to runoff within Australian catchments. Such processes are only applicable to non-urbanised catchments where the vast proportion of surfaces are pervious.

2.5.1 Catchment rainfall and streamflow relationships

Gauged streamflow is the combination of continual groundwater discharge into a stream, known as baseflow, and quickflow. From the commencement of a storm, stream discharge is increased from direct rainfall capture and overland surface drainage. These additions are known as quickflow, often referred to as runoff. Ladson defines quickflow as “the rapid component of catchment runoff that occurs in response to rainfall” (2014). The runoff depth generated is considered as rainfall excess, the total event rainfall depth minus any losses during the conversion process (Ball, Weinmann & Boyd 2019). The subsequent peak discharge yielded from a design rainfall event is computed in two different approaches:

- The development of a time-step discharge hydrograph from a rainfall excess hyetograph at a singular point of interest, or
- Catchment runoff routing through the combination and translation of flood hydrographs, requiring specialised software.

The underlying assumption of the singular discharge hydrograph method is that the runoff originating from the entire catchment area is instantaneously and concurrently contributing to discharge, measured at a point location (Ball, Weinmann & Boyd 2019). The resultant discharge from an excess rainfall intensity during a time-step is defined by equation 2.4 as:

$$Q_i = 0.278 I_{e_i} A \quad (2.4)$$

Where Q_i is the discharge (m^3/s) generated during a time-step i , I_{e_i} is the excess rainfall intensity (mm/hr) in the correspond time-step and A is catchment area (km^2) (Ladson 2014).

Equation 2.4 is derived from a similar approach to the time of concentration rational method (Department of Transport and Main Roads 2024a), which considers the time of drainage for runoff originating from the most distant location of a small catchment to reach outlet for peak discharge estimation. For large catchment scale analysis with flow regimes that are complex, multifaceted networks of surface and channel discharges, the time of concentration is unable to be easily determined (Ladson 2014). Instead, the critical event duration is determined through a comparison of the generated peak discharges from a range of trial durations for a specified AEP (Ball, Weinmann & Boyd 2019). The duration length with the maximum discharge provides an insight into the catchment response. The factors that predominantly affect the conversion of rainfall to runoff are:

- Inconsistent spatial distributions of rainfall.
- Temporal distribution patterns of rainfall.
- Catchment losses.

These considerations are elaborated upon below.

2.5.2 Design rainfall Areal Reduction Factor

The IFD design rainfalls are specific only to a certain point location and are generally not reflective of the average rainfall intensity across a significantly large catchment. The average areal rainfall accounts for the assumption that “larger catchments are less likely than smaller catchments to experience high intensity storms simultaneously over the whole of the catchment area” (Jordan, Seed & Nathan 2019). The ratio between catchment average and point rainfall is represented by the Areal Reduction Factor (ARF). ARR 2019 stipulates that the ARF shall be applied to reduce upstream rainfall data for catchment discharge estimation (Jordan, Seed & Nathan 2019).

ARF is dependent on AEP, event duration and to a lesser extent, catchment size. Longer duration events also consider regionalised impacts (Jordan, Seed & Nathan 2019) through variable equation coefficients. The ARR Datahub (Babister et al. 2016) generates outputs to determine the ARF of any design scenario considering a maximum event duration of 7 days and a catchment size less than 30,000 km² (Jordan, Seed & Nathan 2019)

For short duration events less than 12 hours in duration, ARF is determined by a singular equation for all locations in Australia. The short duration ARF equation, as reproduced from the ARR Data Hub in Figure 2.17, is dependent on the catchment area, as well as the event AEP and duration in minutes.

Short Duration ARF

$$ARF = \text{Min} \left[1, 1 - 0.287 \left(\text{Area}^{0.265} - 0.439 \log_{10}(\text{Duration}) \right) \cdot \text{Duration}^{-0.36} \right. \\ \left. + 2.26 \times 10^{-3} \times \text{Area}^{0.226} \cdot \text{Duration}^{0.125} (0.3 + \log_{10}(AEP)) \right. \\ \left. + 0.0141 \times \text{Area}^{0.213} \times 10^{-0.021 \frac{(\text{Duration}-180)^2}{1440}} (0.3 + \log_{10}(AEP)) \right]$$

Figure 2.17: Short duration ARF equation for all locations in Australia (Babister et al. 2016)

Events lasting over 24 hours are classified as long duration and the ARF is governed by regionalised parameters in conjunction with catchment area, design AEP and event duration. Laidley Creek is situated within the ‘Semi-arid inland QLD’ ARF classification region. The long duration ARF parameters and equation from the ARR Data Hub are shown in Figure 2.18.

$$ARF = \text{Min} \left\{ 1, \left[1 - a \left(\text{Area}^b - c \log_{10} \text{Duration} \right) \text{Duration}^{-d} \right. \right. \\ \left. \left. + e \text{Area}^f \text{Duration}^g (0.3 + \log_{10} AEP) \right. \right. \\ \left. \left. + h 10^{i \text{Area} \frac{\text{Duration}}{1440}} (0.3 + \log_{10} AEP) \right] \right\}$$

Zone	a	b	c	d	e	f	g	h	i
East Coast North	0.327	0.241	0.448	0.36	0.00096	0.48	-0.21	0.012	-0.0013

Figure 2.18: Long duration ARF parametric equation for Laidley Creek (Babister et al. 2016)

For a design scenario with a duration between 12 and 24 hours, the interpolation methods described in Chapter 4.3 of ARR 2019 Book 2 by Jordan, Seed and Nathan (2019) are used to determine ARF.

2.5.3 Rainfall temporal patterns

The temporal pattern of a rainfall event represents the distribution of rainfall intensity over a design duration, which can significantly vary between events of similar magnitude (Jordan, Seed & Nathan 2019). Previous approaches to modelling adopted a simple uniform distribution of constant rainfall intensity, however more recent literature has demonstrated temporal pattern selection has a significant impact on the catchment response, specifically the magnitude of peak discharge and shape of a flood hydrograph (Loy 1990; Ball 1994; Ladson 2014). Ball (1994) established that generated hydrographs attributed to variable rainfall rates had higher peak discharges than those of constant intensity. Further, Loy (1990) detailed that the peak discharge generated from runoff routing models featuring different temporal patterns for design

events differed by over 50%. Temporal pattern selection is a crucial consideration to preserve model probability neutrality between rainfall and discharge.

Temporal ‘loading’ characterises the nature of a temporal pattern, depending on when the majority of rainfall is received during the event. Specifically, loading is classified by the proportion of the event duration at which 50% of the cumulative event rainfall total has been received (Visser et al. 2023). Book 2 of ARR 2019 (Jordan, Seed & Nathan 2019) classifies loading into three categories, as exemplified in Figure 2.19:

- Front loaded – Minimum of 50% rainfall received in the first 40% of event duration.
- Centrally loaded – 50% of rainfall received between 40% and 60% of event duration.
- Back loaded – Minimum of 50% rainfall received from 60% of event duration onwards.

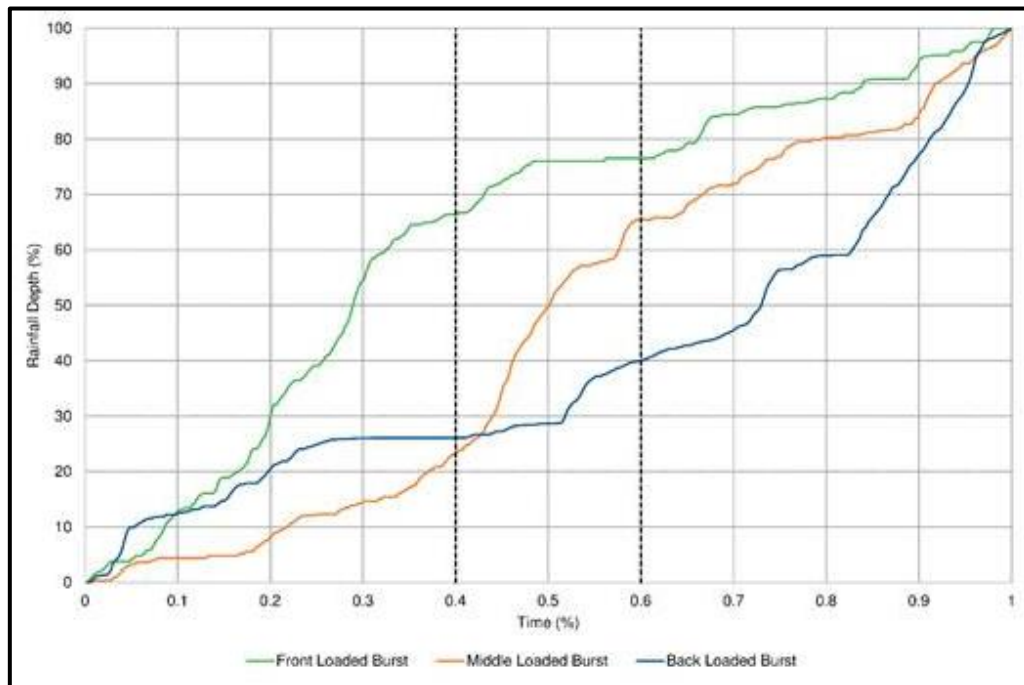


Figure 2.19: Example event cumulative burst distributions (Jordan, Seed & Nathan 2019)

The third ARR 2016 revision project focussed on the development of an ensemble of temporal patterns for design durations and AEPs representative of variable conditions experienced at any location (Loveridge, Babister & Retallick 2015). This project was a progression from the outdated practices of ARR 1987, which utilised a singular temporal pattern for each design rainfall to represent a typical storm event (Loveridge, Babister & Retallick 2015). The ARR 2019 ensemble of temporal patterns are regionalised into 12 subareas of the Australian continent. Laidley Creek is situated within the ‘East Coast North’ region. Each regional set of ten temporal patterns encompass durations from 15 minutes to 7 days across 4 burst AEP

categories ‘very rare’ to ‘frequent’ (Jordan, Seed & Nathan 2019). Patterns are retrievable from the ARR Data Hub (Babister et al. 2016). The current proportion of design pattern loadings in the Central Slopes region is detailed in Table 2.2. Centrally loaded patterns are most frequent for events both greater and less 6 hours in duration.

Table 2.2: East Coast North burst loading proportion by duration (Jordan, Seed & Nathan 2019)

Region	Duration	Front Loaded (%)	Middle Loaded (%)	Back Loaded (%)
East Coast North	≤ 6 hours	28.9	56.5	14.6
	≥ 6 hours	23.4	48.5	28.1

2.5.4 Catchment losses

Catchment loss processes are responsible for the proportion of rainfall that is not directly converted to runoff during an event. These processes include:

- Vegetation interception
- Atmospheric evapotranspiration
- Ground surface infiltration
- Surface depression and channel storage

Empirical loss models represent the effects of losses in yielding runoff discharge. Event-specific loss analysis is complex in nature, is time consuming, and requires substantial resources to obtain sufficient site data about the loss processes. Therefore, current practice advises loss values for rural catchments should be inferred from regional information as investigated by Hill, Zhang and Nathan (2016).

ARR 2019 recommends the Initial Loss (IL)-Continuing Loss (CL) model as most suitable for rural catchment design flood modelling (Ball, Weinmann & Boyd 2019). The IL-CL model assigns constant depth values to both the IL and CL for an event. IL is considered as the beginning storm losses (as listed above) that occur prior to the infiltration capacity of the ground being exceeded (Ball, Weinmann & Boyd 2019). Once the surface is saturated and surface runoff begins, a CL is adopted across the remaining storm event duration. The IL-CL model is applied directly to the time-stepped rainfall hyetograph to produce a rainfall excess hydrograph, refer to Figure 2.20. Ball, Weinmann and Boyd noted that IL and CL “do not vary systematically with the severity of the event (therefore) ... loss is independent of AEP” (2019).

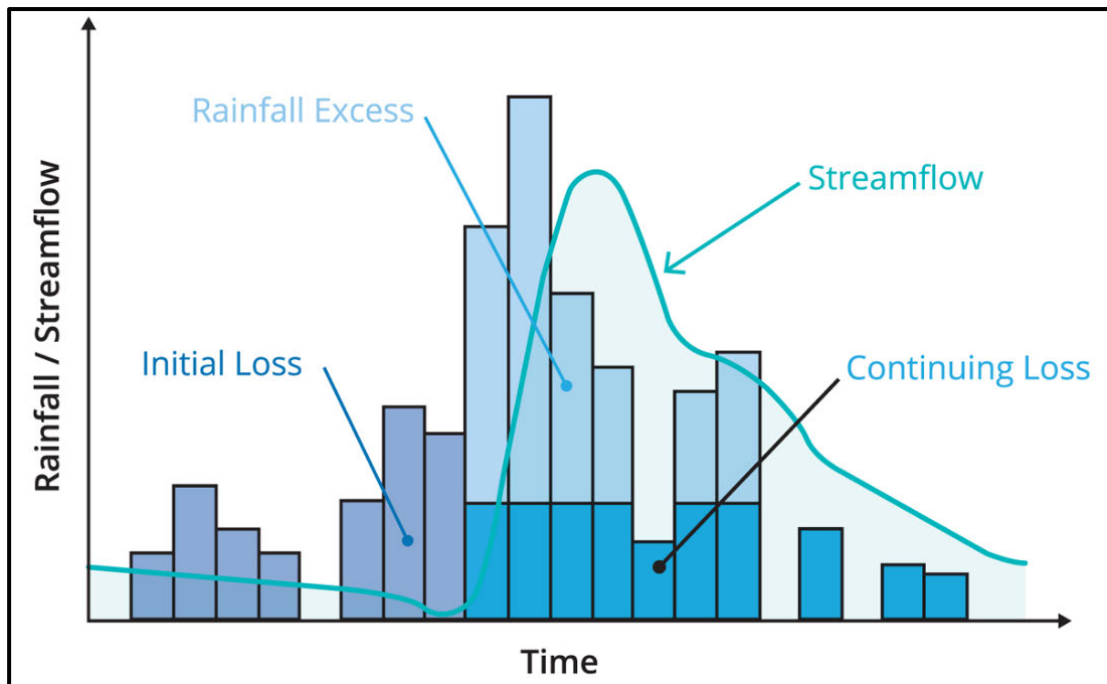


Figure 2.20: IL/CL model application to hyetograph (Ball, Weinmann & Boyd 2019)

Figures 2.21 and 2.22, both extracted from ARR 2019 Book 5 by Ball, Weinmann and Boyd (2019), illustrate the spatial distribution of regionalised losses within non-arid rural catchments, at a discrete incremental scale across Australia. Median initial loss is displayed in Figure 2.21, while continuing loss depth is shown in Figure 2.22.

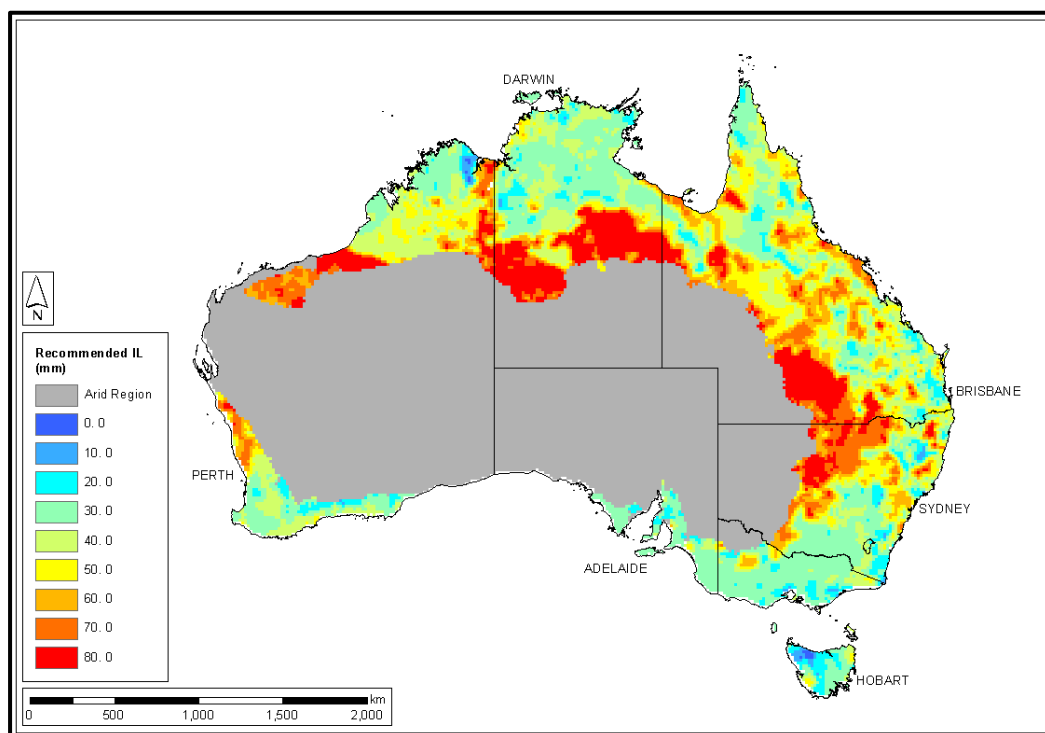


Figure 2.21: Median initial loss distribution for Australia (Ball, Weinmann & Boyd 2019)

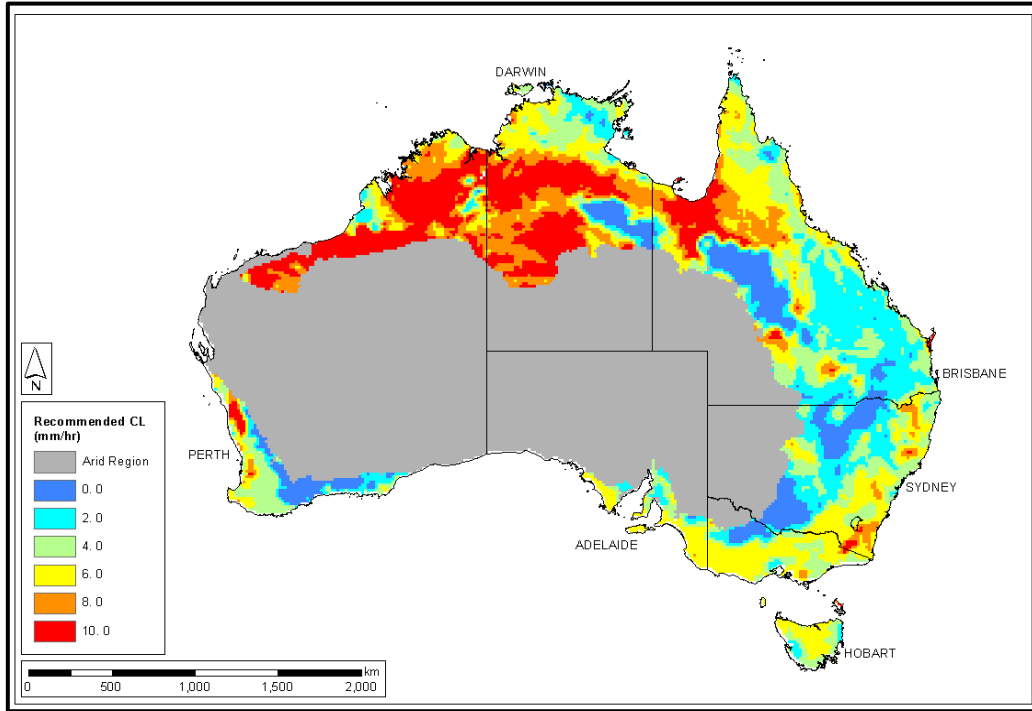


Figure 2.22: Continuous loss distribution in Australia (Ball, Weinmann & Boyd 2019)

Considerations for burst and storm differences are required for event-based modelling. The BOM design IFDs are considered as critical ‘bursts’ while the ARR 2019 IL depths are for an entire ‘storm’ event (Ladson 2016). The burst component represents the most intense period with the lowest probability occurrence in the entire event, and generally reflects the whole storm event in larger catchments (Ball, Weinmann & Boyd 2019). The pre-burst component occurs prior to the burst and provides an indication of pre-event conditions including surface saturation and storage, which impacts initial loss characteristics (Ladson 2016). Pre-burst rainfall depths are also retrievable from the ARR Data Hub (Babister et al. 2016). For modelling with BOM IFDs, an initial storm loss IL_s from ARR Datahub require conversion to an initial burst loss IL_b by subtracting the pre-burst rainfall depth PB per equation 2.5.

$$IL_b = IL_s - PB \quad (2.5)$$

(Jordan, Seed & Nathan 2019) noted that for non-urban, non-coastal catchments, the pre-burst rainfall typically only represents a small proportion of the total storm event and had minimal contribution to catchment runoff response. Figure 2.23 illustrates the components of a relatively short duration rainfall event with a high proportion of pre-burst rainfall. The ability to distinguish the individual components of calibration storm events is a crucial preparatory phase to ensure the accuracy of subsequent design event analysis.

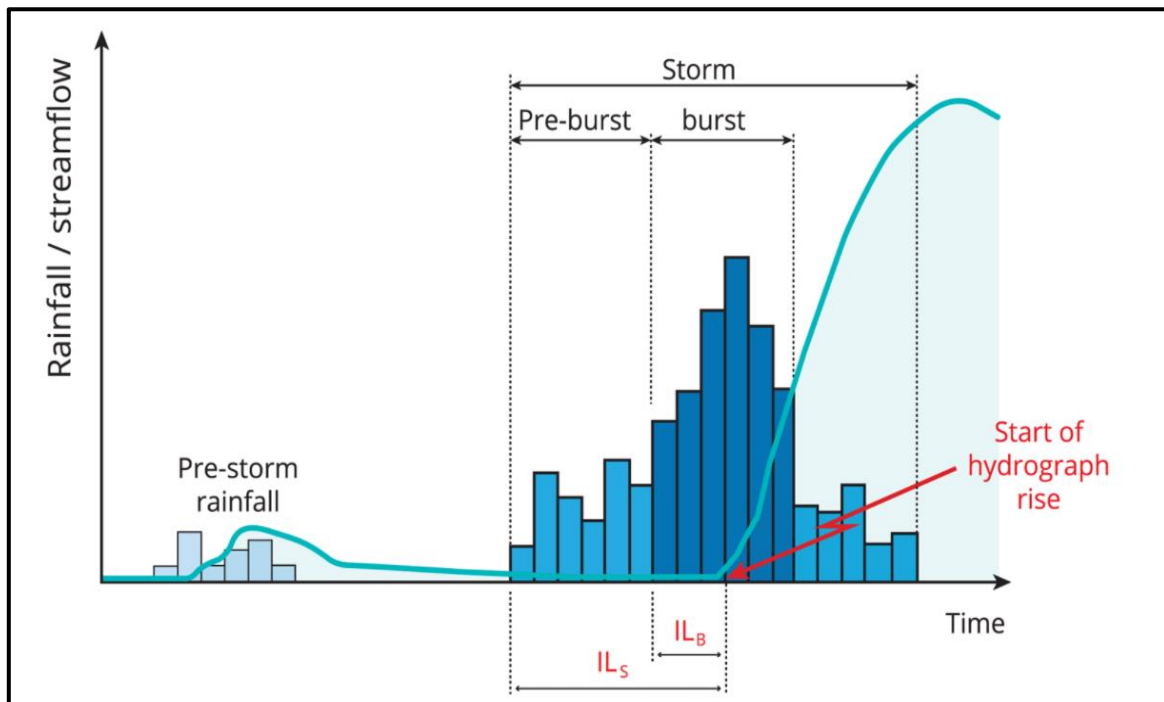


Figure 2.23: Burst and storm initial losses (Ball, Weinmann & Boyd 2019)

2.6 Hydrologic modelling techniques

Discussed in this section are the different hydrologic modelling techniques recommended by ARR 2019 and DTMR to undertake a catchment analysis. The theory and applications of each approach are introduced and the required data inputs are referenced to the previous section. The advantages and limitations of each approach are also discussed in detail.

2.6.1 At-site Flood Frequency Analysis

At-site Flood frequency analysis (FFA) correlates flood frequency and recorded discharge by fitting a probability distribution to a continuous time series of recorded streamflow discharge. Ladson describes FFA as a “statistical analysis of data (to form) useful inferences ... on the magnitude and frequency of future flood events” (2014), while Rima et al. describes FFA as “a widely used statistical technique for estimating design floods” (2022). FFA can only be undertaken within gauged catchments.

Flood peaks are considered as independent random variables in time. From a time-series plot, such as the example presented in Figure 2.24, peak flood discharge data can be classified in two series. These namely are the Annual Maximum (AM) series and Peak-Over-Threshold (POT) series. An AM series is comprised of the highest single flood discharge in each yearly period on record (Ball et al. 2019), capital Q only in Figure 2.6. A POT series consists of all flood discharge peaks that exceed a stipulated threshold discharge (Ladson 2014), capital Q

and lowercase q in Figure 2.24 provided Q also exceeds the threshold. A POT series typically includes K events for N years on record, where $N < K < 3N$ (Ladson 2014).

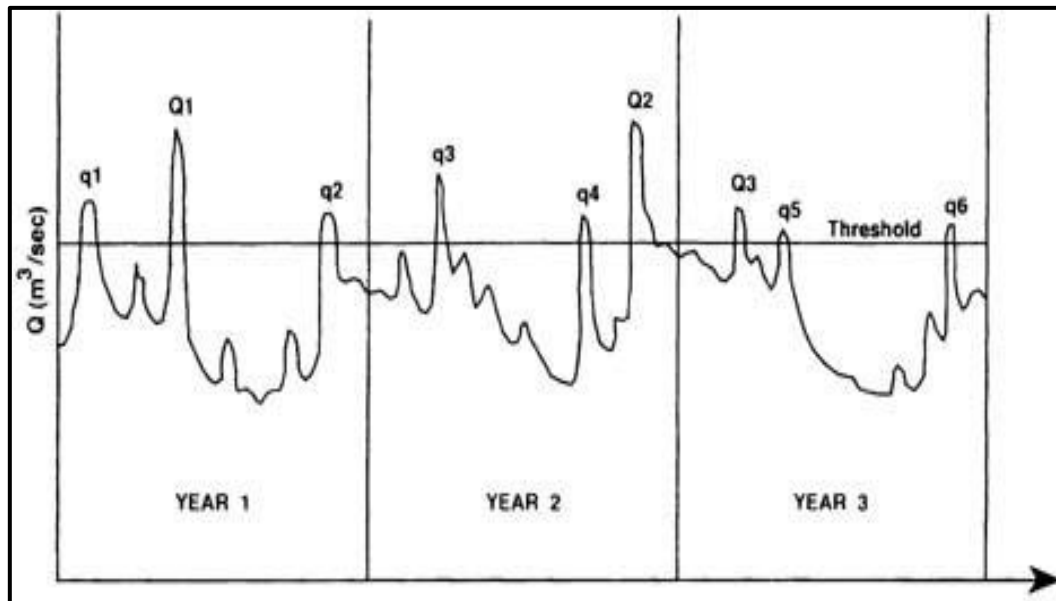


Figure 2.24: Time series plot of discharge data (Holland, Herschy & Archer 1998)

ARR 2019 recommends using the AM series for FFA when considering design events with an AEP rarer than 10% as the modelling associated with this approach is much simpler yet still generates almost identical estimates to the POT series (Ball et al. 2019). Additionally, estimations of the rarest events using POT “may be compromised in order to obtain a good fit to the smaller peaks where the bulk of the data lies” (Ball et al. 2019). The POT series is typically only preferred for common floods for urban stormwater and structure design.

2.6.1.1 Annual Maximum Series

An AM series consists of the peak discharge in each water year, considered in Queensland as the 12-month period spanning from October to September, as these months when lowest average flow is typically experienced and flooding is unlikely (Ladson 2014). All other flood peaks, regardless of their magnitude compared to the maximum peak in another water year, are omitted. Typically, the AM series will contain an equivalent number of data points to record duration in years, however this may not occur in situations with missing data in the gauged records. Ball et al. describes the correlation between adopted data from nearby catchments to produce an estimate of the magnitude of a unrecorded significant flood, and the actual discharge, as “often insufficient” (2019). In instances where the largest discharge definitely occurred outside the period of missing data, the peak discharge for that water year is still usable in the AM series. However, when the unrecorded flood “cannot be estimated with reasonable

certainty” (Ball et al. 2019), the entire water year should be omitted from the FFA. This is because FFA projections assume that the causes and effects of past flood events remain current for future conditions. Consequently, many instances of data omission will impact the accuracy of the fitted probability distribution.

The annual maximum discharges are considered as individual events, provided events where concurrent discharges in short succession were experienced have adopted a singular peak discharge. Event flood probability is described through the application of a probability distribution function to a probability plot of AM gauged discharge data against initial estimates of associated AEP. The probability notation $P(Q \leq q|\theta)$ expresses the exceedance probability of a flood q being greater than or equal to a magnitude Q , conditional on input parameters θ (Ball et al. 2019). By ranking the peak annual discharges in descending order, the estimated AEPs are derived from the plotting position method (Ladson 2014; Ball et al. 2019). ARR 2019 recommends usage of the Cunnane AEP plotting position equation for modelling consistency (Ball et al. 2019):

$$P(i) = \frac{i-0.4}{n+0.2} \quad (2.6)$$

Where P is the Cunnane plotting AEP in decimal form, i is the gauged flood rank and n is the total number of flood events gauged (Ladson 2014).

Several probability distributions have been previously adopted for FFA. The best distribution is dependent on the complex, often uninterpretable arrangement of the true discharge data.

Consequently, several valid probability distributions have been previously fitted to FFA studies, as noted by Ladson (2014). These distributions include:

- Normal
- Exponential
- Log Pearson III (LP3)
- Generalised Extreme Value (GEV)
- Generalised Pareto (GP)
- Gumbel

The adoption of some models is location dependent, for example LP3 is commonly used in the United States (Singh 1998). In Australia, ARR 2019 recommends either the LP3 or GEV distributions (Ball et al. 2019; Jordan, Seed & Nathan 2019). However, this recommendation is only an informed suggestion, as a selection of the most appropriate distribution function is arbitrary in nature, given any “rigorous analytical proof that any particular probability

distribution for floods is the correct theoretical distribution (does not exist)” (Ball et al. 2019). While the true distribution of flood frequency is indeterminable, Rahman et al. (2013) conducted analyses of 15 distributions with recorded AM series data from Australian catchments, which determined LP3, GEV and GP were the most appropriate. Ladson (2014) and Ball et al. (2019) argued that the results of such empirical studies cannot correlate to conclusive evidence towards the universal adoption of a certain distribution model, because of sample variability effects arising from the short duration of available gauge records.

The 2013 study conducted by Rahman et al. identified that within Queensland, LP3 with method of moments was the best-fitting distribution across 56 gauging sites.

2.6.1.2 Log Pearson III Distribution

The LP3 distribution is characterised by three parameters, namely scale, shape and location (Desvina et al. 2019). These parameters are determined by using the indirect method of moments to calculate the statistical moments of the dataset containing the logarithms of the Cunnane discharges (Ladson, 2014). The statistical moments considered are:

- mean, representative of the central axis of the data,
- skew, a measure of data symmetry, whether the data is mostly large or small, and
- standard deviation, a measure of data spread or separation (Singh 1998).

From the statistical moments, the LP3 distribution is represented by the general equation:

$$\log(Q_Y) = M + K_Y(g) \times S \quad (2.7)$$

Where Q_Y is the discharge of a 1 in Y AEP event, M , g and S are the mean, skew and standard deviation respectively of the $\log(Q)$ series, and K_Y is the frequency factor of the 1 in Y AEP (Ball et al. 2019). Equations for the moments of mean, skew and standard deviation for sample data x_i are:

$$\bar{x} = \frac{1}{n} \sum_{i=1}^n x_i \quad (2.8)$$

$$s = \left[\frac{\sum_{i=1}^N (x_i - \bar{x})^2}{n-1} \right]^{0.5} \quad (2.9)$$

$$g = \frac{n \sum_{i=1}^N (x_i - \bar{x})^3}{(n-1)(n-2)s^3} \quad (2.10)$$

Where $x_i = \log q_i$, the logarithm of the Cunnane discharges (Ladson, 2014).

K_Y is approximated by the Wilson-Hilferty transformation:

$$K_Y(g) = \begin{cases} \frac{2}{g} \left[\left\{ \frac{g}{6} \left(Z_Y - \frac{g}{6} \right) + 1 \right\}^3 - 1 \right] & \text{if } g \neq 0 \\ 0 & \text{if } g = 0 \end{cases} \quad (2.11)$$

Where Z_Y is the frequency factor for the standard normal distribution, given in ARR 2019 Book 3 Table 3.2.2 (Ball et al. 2019). Approximations of $K_Y(g)$ are provided in Table 7.7 of Haan (1977).

2.6.2 Runoff routing

Runoff routing is a rainfall event-based method of runoff hydrograph estimation. The approach simulates the flow characteristics during a flood event through a “series of conceptualised ... storages (to) represent the attenuation and translation effects of a catchment on the rainfall-excess hyetograph” (Laurenson, Mein & Nathan 2010). The translation and attenuation between the peaks of an inflow hyetograph and an outflow hydrograph, as shown in Figure 2.25, is indicative of the impacts of catchment spatial characteristics located between the rainfall inputs and the downstream location of analysis. Translation is representative of the lag time of flows along a stream or channel, which is directly proportional to the reach length (Ball, Weinmann & Boyd 2019). Attenuation considers the reduction in the magnitude of the flood hydrograph peak caused by concentrated and distributed storages located within a catchment, as well as transmission losses (Ball, Weinmann & Boyd 2019). Routing through additional storages diffuses the hydrograph, causing a further reduction in the peak flow while extending the duration of the discharge event (Laurenson, Mein & Nathan 2010), as evident in Figure 2.25. Forms of temporary flood storage spread throughout a catchment include:

- Depressions within overland hillsides
- Stream channels and banks
- Floodplains

Contemporary flood hydrograph modelling conceptualises these distributed storage elements as a combined network (Laurenson, Mein & Nathan 2010; Ball, Weinmann & Boyd 2019). Additionally, lakes, basins, reservoirs and dams contained within a catchment are considered concentrated storage elements as the relationship between these storages and inflow-outflow characteristics are usually more direct (Ball, Weinmann & Boyd 2019).

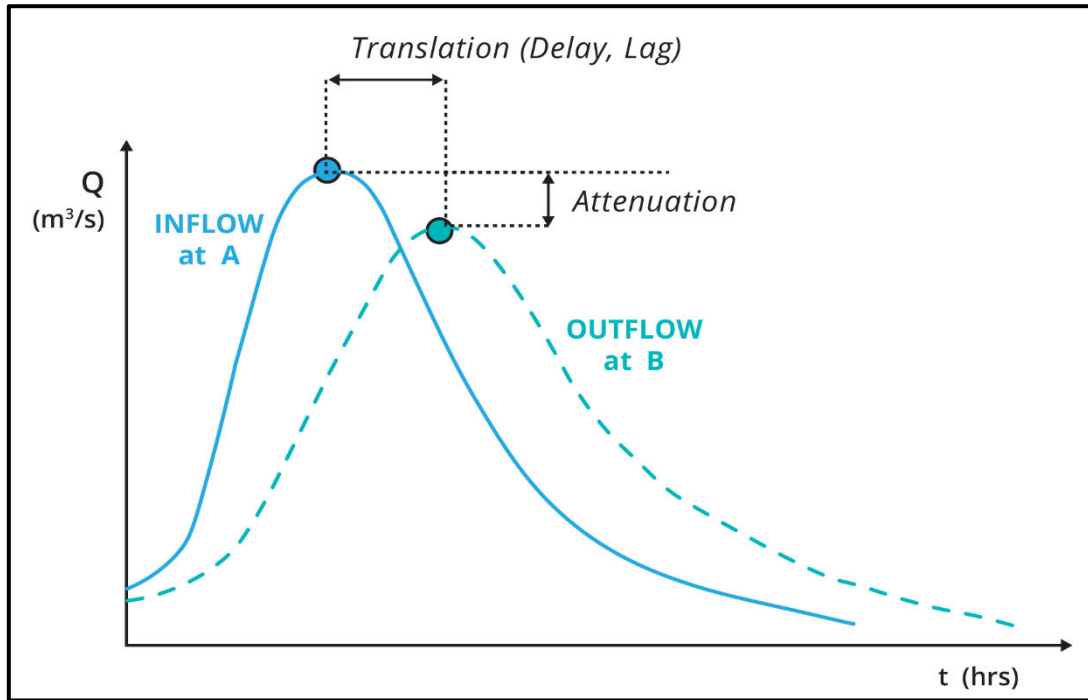


Figure 2.25: Storage and travel impacts between inflow and outflow hydrographs (Ball, Weinmann & Boyd 2019)

The spatial representations of a catchment are classified by the form and level of detail that the temporary flood storage and associated hydrologic phenomena is conceptualised. Homogenous lumped models use the time-area or unit hydrograph approaches to determine flows from small catchment or individual subcatchments within a larger catchment area (Ball, Weinmann & Boyd 2019). These approaches consider spatially uniform rainfall depths and patterns; baseflow and loss characteristics.

Semi-distributed routing methods account for the variability of these factors by partitioning the larger catchment into homogenous subcatchments. The runoff generated by each subcatchment is routed downstream through a quantified reach storage (Laurenson, Mein & Nathan 2010). The nature of semi-distributed methods complex hydrologic phenomena that influence the timing and magnitude of runoff during a flood event to be modelled. For example, non-linear catchment responses through branched networks and significant storages are conceptualised by such methods (Ball, Weinmann & Boyd 2019).

Node-reach models are the most adopted form of semi-distributed models due to their relative ease of establishment whilst being sufficiently representative of catchment configurations of varying size and complexity. In a typical node-reach model, a rainfall input is applied across each subcatchment which is converted from an excess hyetograph to an inflow hydrograph. These hydrographs are routed through reaches within the catchment, where the runoff

production is determined at critical nodes (Ball, Weinmann & Boyd 2019) ultimately concluding at the outlet where the total magnitude and timing of the runoff hydrograph is computed from all contributory flows (Laurenson, Mein & Nathan 2010; Ball, Weinmann & Boyd 2019), as demonstrated by the conceptualised model diagram in Figure 2.26 below.

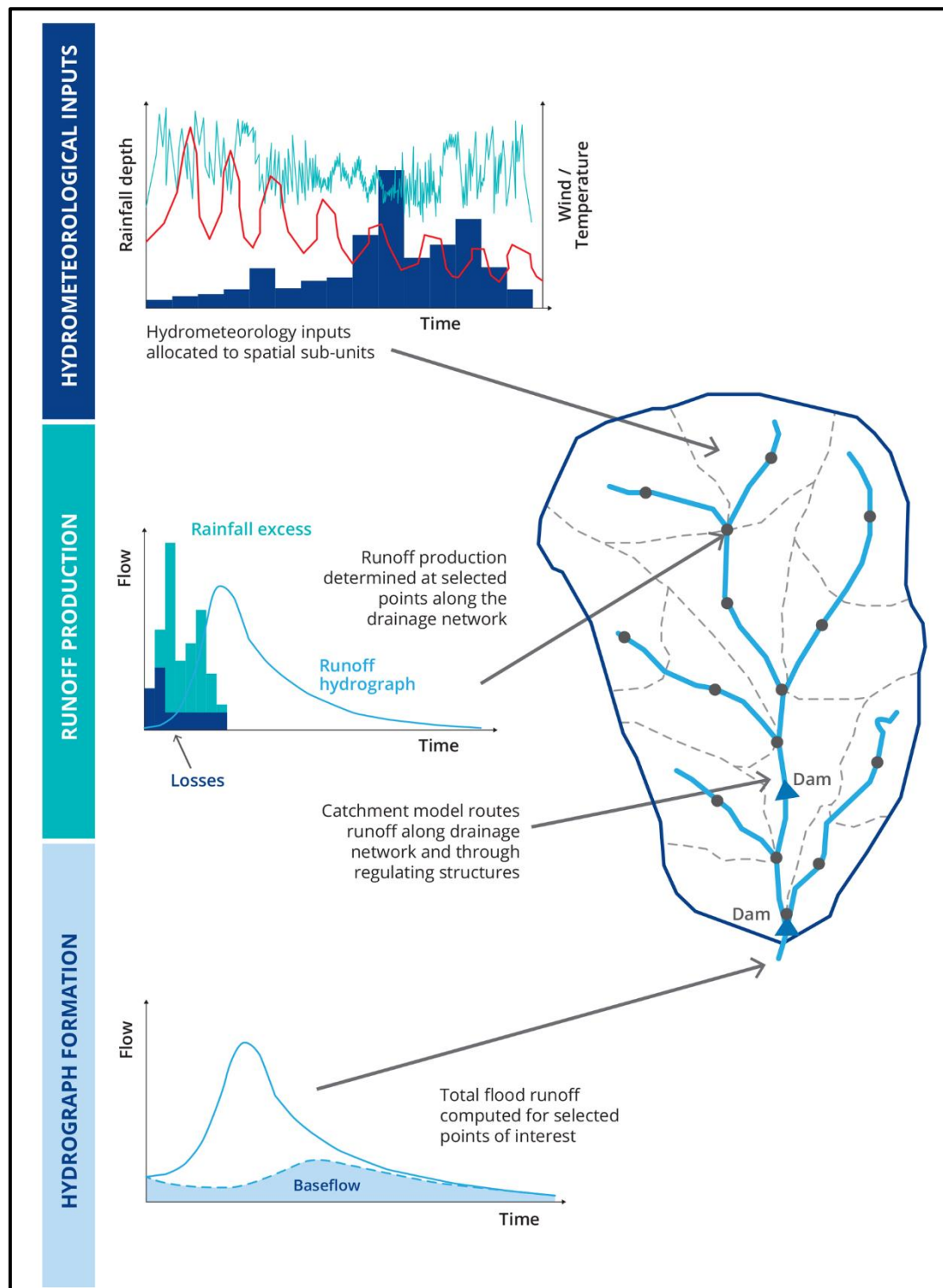


Figure 2.26: Node-reach runoff routing model processes (Ball, Weinmann & Boyd 2019)

2.6.2.1 Node-reach model features

Laurenson, Mein and Nathan (2010) outline the types of nodal features within semi-distributed models, including:

- Input nodes for excess hyetographs/inflow hydrographs at subcatchment centroids.
- Input nodes for inflow hydrographs from upstream subcatchments entering another subcatchment.
- Junction nodes between reaches.
- Reservoir storage bodies.
- Output nodes at gauging stations and locations of computed runoff hydrographs.

Linear reaches represent the stream routing links between node features.

2.6.2.2 Subcatchment area delineation

The subcatchment delineation method is a simplification of the spatial composition of a broader catchment. In a similar approach to catchment delineation, subcatchments should be defined by significant topographic features that bound sub-areas with homogenous flood characteristics (Ball, Weinmann & Boyd 2019). The number of subcatchments used was first demonstrated by Weeks (1980) to affect the model, specifically that as the number of subcatchments increased, the hydrograph peak increased and was postponed. Ball, Weinmann and Boyd (2019) suggested delineating between 10 and 100 subcatchments was common contemporary practice, depending on the total catchment area. Laurenson, Mein and Nathan (2010) recommended a minimum of five subcatchments be delineated upstream of a node where a runoff hydrograph was to be computed.

2.6.2.3 Non-linear storage routing

The general form of a storage discharge relationship correlating inflow and outflow through a routed reach is expressed by Ball, Weinmann and Boyd (2019) as:

$$S = KQ \quad (2.12)$$

Where S is the storage volume of a routed reach, Q is the discharge through the reach and K is the lag parameter between inflow into and outflow from the reach. However, the relationship between storage and discharge in routed features is typically non-linear (Ball, Weinmann & Boyd 2019), best represented by a power function first proposed by (Laurenson 1986):

$$S = kQ^m \quad (2.13)$$

Where k is a dimensionless coefficient deduced from K and m is a dimensionless exponent indicative of the relative efficiency of storage and discharge with respect to flow magnitude.

Considering equations 2.12 and 2.13, the lag parameter K can be expressed in the form:

$$K = \frac{S}{Q} = kQ^{m-1} \quad (2.14)$$

Equation 2.14 indicates three scenarios that dictate how lag time is affected by changes in the m parameter value. For the scenario $m = 1$, the relationship between storage and discharge is linear, meaning increases in storage and discharge occur at an identical rate and the lag time is constant for all storage-discharge combinations (Laurenson, Mein & Nathan 2010). Where $m < 1$, the lag time decreases with increasing magnitude of discharge, meaning the flow is characterised as efficient. Conversely, where $m > 1$, the lag time increases as storage increases, indicating flow is inefficient. Typical values of m for natural catchment streams were determined to be between 0.6 and 1.0, with 0.8 being widely adopted as an average value for modelling (Laurenson, Mein & Nathan 2010; Ball, Weinmann & Boyd 2019).

2.6.3 Continuous catchment simulation models

Continuous catchment simulation models, such as AWBM, Sacramento and Simhyd (Podger 2004), convert a complete series of climatic data inputs, usually spanning many years, into a set of runoff flows for the corresponding period as a reflection of “the full spectrum of flood and drought conditions (experienced)” (Nathan et al. 2019). Continuous simulation models use parametric values to represent catchment hydrologic characteristics including surface storage capacities and distributions of baseflow recharge and streamflow (Nathan et al. 2019).

Rainfall, potential evapotranspiration and gauged stream discharge datasets at a daily interval are required to develop a continuous simulation of a catchment. The input datasets must be complete for the entire simulation period, meaning that gap filling and stochastic approaches (Nathan et al. 2019) are usually required to address incomplete (missing data) or inadequate (short duration) data records.

A calibration of the provided climate inputs against the observed runoff data is undertaken by using a selected data optimisation technique. Then, a selected objective function assesses the calibration measure of fit and governs the criteria of which the optimal set of model parameters is determined from (Podger 2004). Once the simulated streamflows are generated, the frequency and magnitude attributes of previous flood events are determined using similar methods to FFA (Nathan et al. 2019).

An analysis of continuous simulation models performed by Ling et al. (2015) demonstrated that the method was unable to concurrently replicate a long term hydrograph in conjunction

with rare flood event characteristics to a sufficient level of accuracy. When calibrated against a comprehensive flow record, “the highest flow peaks were under estimated and the flood frequency curve calculated from simulated annual maximum series provided a very poor fit to the observed flood frequency curve” (Ling et al. 2015). Conversely, calibration against rare flood peaks reduced the model fit against the objective function criteria, while only yielding “slight improvements in matching the observed flood frequency curves” (Ling et al. 2015).

2.6.4 Regression methods of analysis

Regression based methods are simple techniques to estimate peak flow at the outlet of a catchment. Two such Australian regression methods are discussed below.

2.6.4.1 Parametric regression

Regional Flood Frequency Estimation (RFFE) is an alternate method of peak discharge estimation in both gauged and ungauged catchments. RFFE uses a regionalised least squares regression of the LP3 distribution parameters attributed to data obtained from 853 gauged catchments (Ball et al. 2019). The method transfers readily accessible flood characteristics, listed below, from a regional set of gauged catchments to any location through regional estimation equations. These equations provide consistent results with gauged records and are dependent on five variables available from BOM, WMIP and ARR Datahub:

- Area of the catchment
- $50\% I_{6h}$ and $2\% I_{6h}$ design intensities
- Ratio of $2\% I_{6h} / 50\% I_{6h}$
- Shape factor, the “shortest distance between catchment outlet and centroid divided by the square root of catchment area” (Ball et al. 2019).

In a similar nature to the development of IFDs from a finite number of data stations, uncertainty exists in the RFFE method in discrete gauged data extrapolation to ungauged catchments. RFFE is not suitable for urban catchments or areas greater than 1000 km^2 , because the technique was developed from data gauged in rural catchments with areas less than this threshold (Ball et al. 2019).

2.6.4.2 Quantile regression

The Palmen and Weeks (P&W) quantile regression technique is similar to RFFE, however regression equations were directly fitted to Queensland gauged data characterised by catchment area and $2\% I_{72h}$, rather than the distribution parameters. The regression equations yielded “reasonable results (against) independent streamflow data (and were) superior (to) the Main

Roads Rational Method” (Palmen & Weeks 2011). P&W is only appropriate for rural catchment areas less than 1000 km² (Palmen & Weeks 2011) and is typically less adopted compared to RFFE (Ball et al. 2019).

2.7 Future Climate Considerations

2.7.1 Overview of climate change

Climate change has drastically affected catchment hydrologic processes in regions globally. Current Queensland climate variability is experienced across seasonal, yearly and decadal oscillations, which are correlated to the patterned occurrence of rainfall events (Mora et al. 2013). In the upcoming 20 to 50 years (Mora et al. 2013), the effects of climate change are expected to become “increasingly pronounced (and) potentially significant” (Alluvium 2019). Long-term water resources planning must consider the projected climatic conditions and provide adaptations to mitigate adverse impacts on human populations and natural ecosystems, as well as the agricultural and industrial sectors.

Since recordkeeping began in 1910, the Australian surface temperature has risen by approximately 1.5°C (Bureau of Meteorology & CSIRO 2022). This increase is attributable to industrial greenhouse gas emissions from the energy, transportation, manufacturing and agricultural sectors (United Nations Sustainable Development Goals Summit 2023). The extent of further change is dependent on the magnitude of future emissions and the subsequent climatic response. Representative Concentration Pathways (RCPs) were developed by the Intergovernmental Panel on Climate Change (IPCC) as a projection of four characterised scenarios of greenhouse gas atmospheric concentrations and total emissions mass until 2100 (Van Vuuren et al. 2011), as indicated in Figure 2.27. Each scenario is classified as RCP X, where X is the global radiative forcing energy causing warming in 2100, relative to pre-industrial levels, in units of watts per square metre (IPCC 2018).

RCP 8.5 is the most extreme scenario, representing a future with minimal changes to current emission rates, causing CO₂ concentrations to continually rise. The intermediate scenarios, RCP 4.5 and RCP 6.0 depict scenarios featuring a short-term moderate rise, followed by a decline and eventual stabilisation in emissions by 2100. RCP 2.6 is the most ambitious scenario, where a decline in total CO₂ concentration is forecast in the near future due to rapid reductions in industrial greenhouse gas emissions (Alluvium 2019). The RCPs 4.5 and 8.5 are recommended for Queensland climate projections to provide a realistic envelope of future potential emissions (Alluvium 2019; Bates et al. 2019).

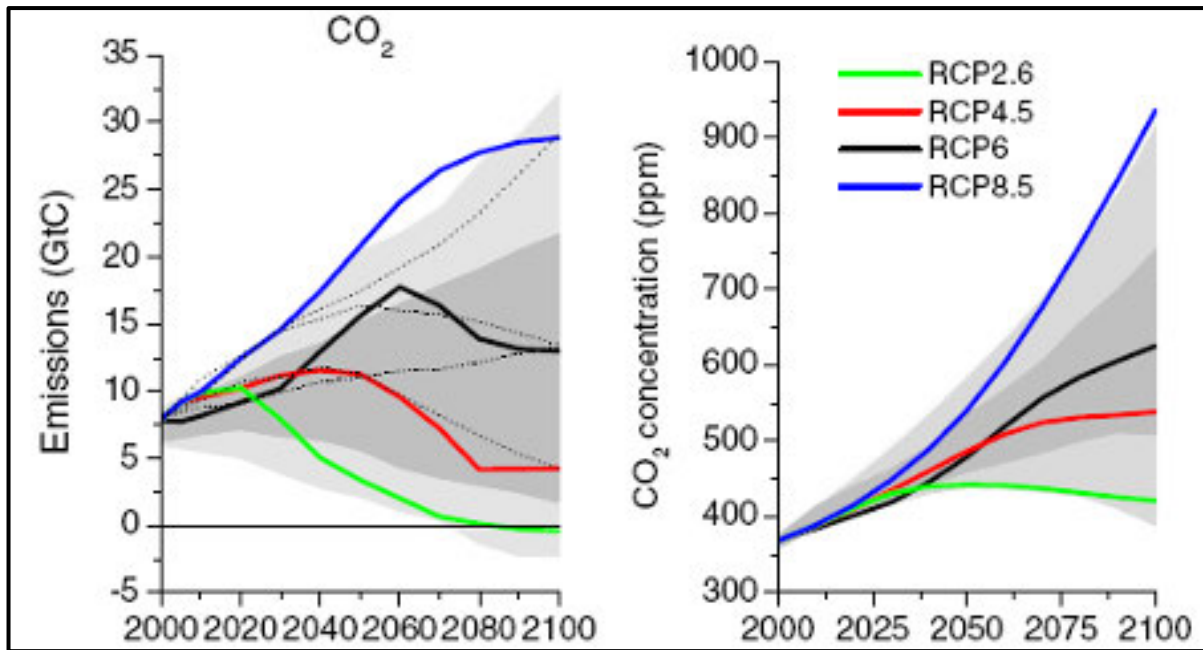


Figure 2.27: Projected CO₂ emissions (mass, left) and CO₂ atmospheric concentration (ppm, right) for RCPs until 2100 (Van Vuuren et al. 2011).

From the RCPs, three dimensional grids were used to develop representations of the physical processes that occur on and between the land and ocean surfaces as well as the atmosphere. These models are known as General Circulation Models (GCMs) and are simplifications of physics concepts such as the conservation of mass, energy and momentum within a closed system (Alluvium 2019). The GCMs were developed at a global scale, having a horizontal resolution of 200 to 300 km and 20 to 50 vertical layers distributed from the atmosphere to the surface level (CSIRO and Bureau of Meteorology 2020).

Illustrated in Figure 2.28 are the projected global mean temperature rises associated with the four RCP scenarios relative to a thirty year baseline from 1961 to 1990. Alluvium (2019) specified that for the two design emission scenarios, the increase in global average surface temperature by 2100 is predicted to range between:

- RCP 4.5: 1.1 – 2.6°C
- RCP 8.5: 2.6 – 4.8°C

The variation in predicted surface temperature increases for each RCP is caused by differences and uncertainties associated with the parameters of the unique GCMs. The period used to establish a relative baseline temperature can vary between models. The 2015 projections released by the Australian Government were derived from 47 individual GCMs (CSIRO and Bureau of Meteorology 2020). GCMs are continually refined and are seen as a motive for the global community to commence measures to mitigate climate change.

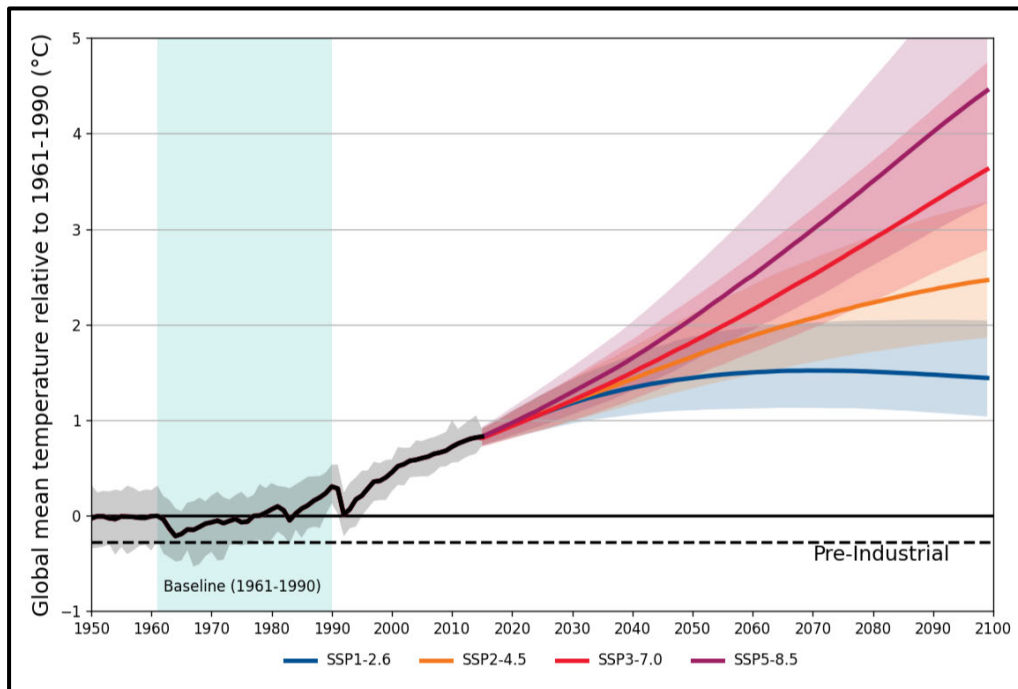


Figure 2.28: Project global temperature rises associated with the RCP climate scenarios relative to the 1961-1990 baseline (Wasko et al. 2024)

The margin of error associated with each global temperature change as presented in Figure 2.28 (and even the predictions by Alluvium (2019)) characterises the uncertainty of the individual GCMs as well as the nature of such forward-forecasting modelling, which is based upon continual revision with up-to-date climate observations and inputs.

GCMs are continually refined and are seen as a motive for the global community to commence measures to mitigate climate change. Contextualising the coarse atmospheric simulations of the GCMs for the geographic conditions of Queensland is achieved through detailed statistical downscaling. Downscaling translates the 200 km resolution GCMs to finer scale 10 to 50 km grids known as Regional Climate Models (RCMs) (CSIRO and Bureau of Meteorology 2020). The finer resolutions provides “greater detail and more accurate representation of localised extreme events” (Alluvium 2019). The GCMs and RCMs are capable of modelling components of hydrology including rainfall, pan-evaporation, runoff and channel flows (Alluvium 2019). However, the models are typically too coarse and are not calibrated to topographic runoff models and streamflow data (Alluvium 2019), making their direct hydrologic outputs unreliable. An opportunity exists for hydrologic modelling to be undertaken based on future climate projections obtained from the GCMs and RCMs.

2.7.2 Future climate influence on hydrologic components

Temperature rise is projected to modify the occurrence and extent of extreme rainfall events in Australia. The flood estimation aspects of IFD relationships and rainfall temporal patterns are most likely to be impacted (Bates et al. 2019) as discussed in the following subsections.

2.7.2.1 Intensity and frequency

Due to increased surface and atmospheric temperatures in the future, an increase in the intensity of extreme rainfall events is projected. The Bureau of Meteorology and CSIRO (2022) has already observed an increase in the intensity of extreme one hour events by approximately 10%, because for every degree of temperature warming observed, the atmospheric moisture content has risen by 7%, thus increasing the available energy to generate intense rainfall events (Dowdy 2020). Conversely, total annual rainfall and continuous steady rainfall patterns are occurring less frequently, which was attributed to “a trend towards higher surface atmospheric pressure ... and a reduction in the number of cold fronts that produce rainfall” (Bureau of Meteorology & CSIRO 2022). Bates et al. (2019) emphasised that national trends are highly variable and regionally sensitive.

2.7.2.2 Temporal patterns

Visser et al. (2023) investigated the relationships between temperature, intensity and duration on the temporal distribution patterns of Australian rainfall events. The research identified that a rise in storm temperature coincided with an increased proportion of front-loaded events (Visser et al. 2023). Additionally, the study found that a “majority of high-average intensity precipitation events are associated with front-loaded storms” (Visser et al. 2023). It was observed that events with a duration spanning less than 6 hours were more commonly front-loaded events compared to events that exceeded 6 hours (Visser et al. 2023).

The following sections outline the direct climatic impacts on the Laidley Creek catchment and guidance provided in state and federal literature for engineers and designs to incorporate climate change scenarios into flood estimation.

2.7.3 Direct climate impacts within the Lockyer Valley region

The mean annual temperature anomaly for Queensland has consistently been above the 30 year average between 1961 and 1990 of 23.2°C since 1985 (Bureau of Meteorology 2024a), as illustrated by Figure 2.29. This trend has even more prevalent in recent years as temperatures continue to rise, as indicated by the highest recorded five year running average of temperature anomaly (Bureau of Meteorology 2024a).

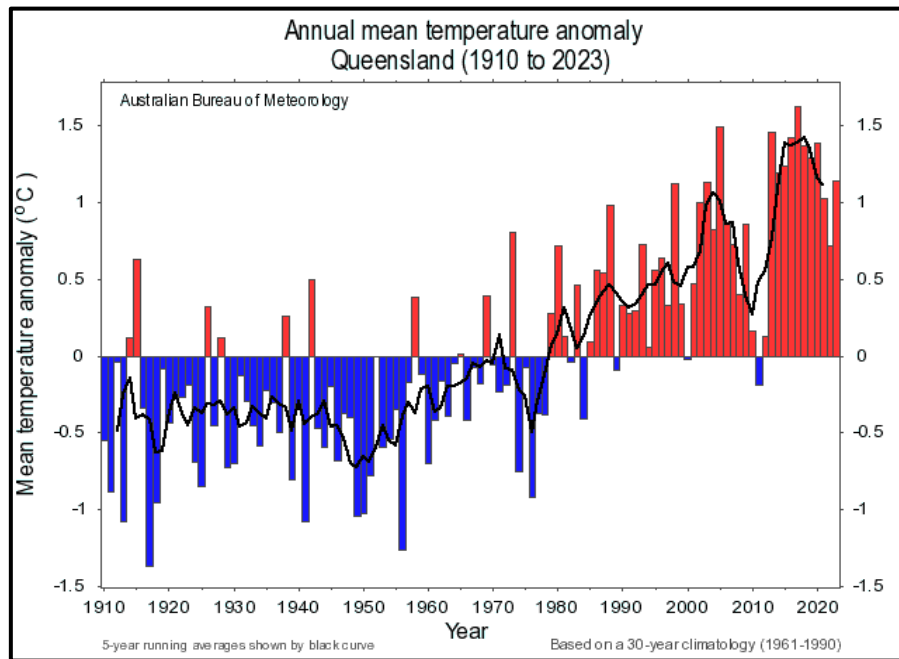


Figure 2.29: Annual mean temperature anomaly in Queensland between 1910 and 2023 based on 30 year average from 1961 to 1990 (Bureau of Meteorology 2024a)

In addition to increasing surface temperature observations, the Bureau of Meteorology and CSIRO (2022) has observed a reduction in the frequency of low-pressure system development responsible for delivering continuous rainfall to the Lockyer Valley region. Consequently, a reduction in the total annual rainfall between the period 1970 to 2022 has been observed for the entire Southern Queensland region, including the LVRC LGA (Bureau of Meteorology 2023). However, while the Bureau of Meteorology and CSIRO (2022) project the total number of rainfall events will decrease, the proportion of rainfall received from intense events in the region will increase. The resulting change in runoff for equivalent AEP events within Laidley Creek under future climate conditions has not been examined at present.

The changes to climate conditions are anticipated to significantly vary between different regions in Australia. The Queensland Future Climate Dashboard (QFCD) is an interactive, gridded database of average climate projections for four upcoming 20 year periods centred around 2030, 2050, 2070 and 2090 (Queensland Government 2024). Factors impacted by climate change, including surface temperature and total rainfall are classified by LGA or major river basin for both design RCPs (Queensland Government 2024). From the dataset, projections for the Lockyer Valley region are expecting increased surface temperatures, less total rainfall and increased concentrations of higher intensity rainfall (Queensland Government 2019).

2.7.4 Design recommendations for future flood estimation

The widespread impact of climate change on climatic components and hydrologic processes is complex in nature and is regionally specific. Consequently, ARR 2019 provides a uniform national approach to future flood estimation methodologies for engineering design purposes in Book 1, Chapter 6. This section of ARR 2019 acknowledges that ongoing research is required to “reduce key uncertainties” (Bates et al. 2019) in the design flood factors from climate change. Current understanding is predominantly concentrated around changes in rainfall intensity from climate change, while other factors are relatively unevaluated at present (Bates et al. 2019). Therefore, Book 3 of ARR 2019 recommends that long-term flood risk is considered exclusively from an increase in rainfall intensity over the project service duration. This recommendation is adopted by DTMR in its Hydrologic and Hydraulic Modelling Technical Guideline (Department of Transport and Main Roads 2024c). Book 2 of ARR 2019 supports this notion, as Jordan, Seed and Nathan emphasised that the AEP probabilistic design rainfall terminology is “equally applicable to both stationary and non-stationary climatic environments” (2019).

The temperature outputs obtained from the GCMs and RCMs are considered more reliable than the rainfall outputs. Therefore ARR 2019 has formulated the process that an adjustment factor is applied to design IFDs proportional to surface temperature projections (Bates et al. 2019). This approach ensures the predictions are representative of temperature rises as the primary cause of extreme rainfall increase and are consistent with the IPCC projections.

The expected rise in extreme rainfall intensity ranges between 2 and 28% per degree of warming (Guerreiro et al. 2018; Bates et al. 2019; Bureau of Meteorology & CSIRO 2022), however ARR 2019 has adopted median recommended rates of change per degree of temperature change depending on the storm event duration.

The IFD adjustment factor p is expressed by equation 2.15 (Wasko et al. 2024) and applies to events between 1 EY and the probable maximum precipitation (PMP) flood in Australia.

$$p = \left(1 + \frac{\alpha}{100}\right)^{\Delta T} \quad (2.15)$$

Where α is the median rate of change estimate in rainfall intensity per degree of temperature rise (%/°C) for a given event duration, per Table 2.3, and ΔT is the mean projected increase in surface temperature relative to the 1961 – 1990 baseline (°C) for a given emissions scenario and projection period, per Table 2.4.

Table 2.3: Rate of change α in rainfall intensity per degree of temperature rise (%/°C) and 66% certainty range in the value (Wasko et al. 2024)

Event duration (hours)	Median estimate α (%/°C)	Likely range [~66%] (%/°C)
≤ 1	15	7.0 – 28.0
1.5	13.7	6.1 – 25.6
2	12.8	5.5 – 24.0
3	11.8	4.7 – 22.0
4.5	10.8	4.0 – 20.3
6	10.2	3.6 – 19.2
9	9.5	3.1 – 17.8
12	9.0	2.7 – 16.9
18	8.4	2.3 – 15.7
≥ 24	8	2.0 – 15.0

Table 2.4: Mean surface temperature increase projections ΔT for design RCP scenarios relative to 1961-1990 baseline (Wasko et al. 2024)

Climate Scenario	RCP 4.5	RCP 8.5
2030 (near-term)	1.2	1.3
2050 (medium-term)	1.7	2.1
2090 (long-term)	2.4	4.1

The existing design rainfall intensity I is multiplied by the adjustment factor p to yield the projected future design rainfall intensity I_p per equation 2.16 (Wasko et al. 2024):

$$I_p = I \times p \quad (2.16)$$

Alternate surface temperature projections were published as localised gridded datasets within the QFCD (Queensland Government 2024) as listed in Table 2.5. These localised projections generated from downscaled RCMs are potentially more reflective of future conditions in the Laidley Creek catchment than globally averaged increases. However, the approach adopted by ARR 2019 as summarised relies on a common reference baseline period. The difference reference period used between Tables 2.4 and 2.5 is likely responsible for some extent of the differences between corresponding temperature rise values.

Table 2.5: Mean annual temperature rise (°C) relative to reference period 1986 – 2005 for Lockyer Valley (Queensland Government 2024).

Year	RCP 4.5 scenario	RCP 8.5 scenario
2030	0.92	0.93
2050	1.4	1.8
2090	2.1	4.1

2.7.4.1 DTMR climate change risk assessment framework

In June 2024, DTMR released the Climate Change and Natural Hazards Risk Assessment (CCNHRA) Guideline, followed by Engineering Policy (EP) 170 – CCNHRA in July 2024. Together, these documents provide “policy direction, context and background information for considering and responding to climate change and natural hazards risks on (departmental) infrastructure projects” (Department of Transport and Main Roads 2024d).

The CCNHRA framework requires at least two climate projections be incorporated into the management and planning of state controlled infrastructure (Department of Transport and Main Roads 2024f). This approach allows for both short, medium and long term impacts associated with climate change to be assessed. The selection of specific climate projection dates (2030, 2050 and 2090 typically) is dependent on the forecasted design life of the component or asset (Department of Transport and Main Roads 2024d). One projection must consider climate conditions beyond the operational lifespan of the asset (Department of Transport and Main Roads 2024f).

The stipulated minimum design life for asset components within the state controlled road network varies depending on the component purpose and criticality. Pavements have a general design life of 30 years, bridge drainage structures are designed for 50 years of operation while abutments are prescribed the longest design lifespan of 100 years (Department of Transport and Main Roads 2024f, 2024a).

2.8 Summary

From an extensive study of current literature, it has been established that the impacts of climate change at a localised scale in the Laidley Creek catchment are not yet understood. This presents an evident research gap appropriate for this dissertation to address. This literature review identified the unique characteristics of the Laidley Creek catchment that contribute to the

occurrence of complex regional hydrologic processes. The relationship between natural stream hydrology and the Warrego Highway were introduced, including flood immunity requirements for the state controlled road corridor. Standardised modelling techniques to comprehend and model rainfall and discharge processes were outlined. The development of future global emissions models and the corresponding expected temperature increases was discussed at length, including the necessary downscaling process to contextualise the projections to Australian conditions. This theory backgrounded the expected impacts on hydrologic processes within the Lockyer Valley. Recommendations provided by ARR 2019 and DTMR explain how infrastructure design and management should consider future climate scenarios, including anticipated increases in rainfall intensity. This guidance will assist the development of the methodology for this dissertation. However, the specific effects of this projected rise in rainfall intensity across the Laidley Creek catchment are yet to be measured.

3. Methodology

3.1 Introduction

The methodology documented in this chapter describes the structured modelling approach developed from the comprehensive literature review to fulfil the objectives of this research project. The chapter begins by defining the preliminary scope of research following the literature review and contextualises the objectives of the methodology with best practice modelling principles. The data acquisition and processing works required to develop the model inputs are documented, including any limitations in the availability and quality of data. The generation and calibration phases of the RORB runoff-routing model to current climate conditions in the Laidley Creek catchment are detailed. The application of independent modelling approaches as a comparison of the results produced by the runoff-routing model is described. The procedures implemented and software applications throughout the methodology are documented for clarity and evaluated against the design objectives. Finally, the project methodology is critically evaluated against a range of alternate research techniques as a measure of its credibility and validity.

3.2 Design methodology overview

The methodology for this research project was developed from insights and industry practices gained through the literature review phase to fulfil the project objectives. The review backgrounded the translation of physical processes into numeric hydrological parameters for the development of empirical modelling techniques, and subsequently, the advanced modelling practices and software applications used currently in Australia. Finally, the impacts of climate change on catchment hydrology and methods to incorporate these impacts into hydrologic models were outlined.

As such, this methodology consolidates the broad literature review into a concise course of action to develop and evaluate hydrologic models which address the current gap in knowledge regarding the anticipated changes in peak streamflow discharge from high intensity rainfall events. All data preparatory and model development works were completed on a personal laptop with a high-performance CPU and GPU capable of running hydrologic software packages.

3.2.1 Preliminary methodology scope

The methodology of this project was designed to develop hydrologic models from accessible yet reputable data sources to simulate current and future climate peak flow characteristics.

The major practical components of the research methodology outlined in this chapter are:

1. Acquisition and processing of high quality spatial and hydrologic data into suitable formats for direct input to different model packages.
2. Generation of the routing model catchment and storm files from the processed data according to model conventions. The freely available RORB package was identified early in the project as a suitable platform to facilitate modelling.
3. Calibration of the routed model catchment parameters based on a wide range of previously observed rainfall runoff relationships.
4. Simulation of a collection of design rainfall events for the standard AEPs to define the magnitude of streamflow yielded for current climate conditions. These simulations were then repeated for revised design rainfall parameters representative of anticipated future climate conditions. Results of both iterations are presented in Chapter 4.
5. Comparison of the results (where applicable) to independent hydrologic methods, including FFA and regression methods.

Initially, it was proposed that the scope of this research project could incorporate two-dimensional hydraulic modelling at the Jack Martin Bridge and the flood-prone intersection of the Warrego Highway and Forest Hill-Fernvale Road to understand flood flow characteristics through the roadway section. However, the resolution of available aerial elevation data was insufficient to produce accurate cross sections of Laidley Creek to develop such models. Additionally, the resource requirements to survey surface elevation data at multiple channel sections were not viable for such a student research project. Hence the project scope was limited to hydrologic modelling, with the results available for future hydraulic analyses.

3.2.2 Best practice modelling considerations

The practical components of the research outlined above must be supported by best practice modelling considerations to ensure that the results produced are accurate and reliable. Ensuring the quality of modelling is high also ensures outputs are useful for future research endeavours. A range of positive modelling practices and considerations for water resources and catchment modelling were synthesised by Jakeman et al. (2018) in the *Good Modelling Practice* discussion paper published by the Queensland Water Modelling Network (QWMN). The paper describes the outcome of best practice modelling as a reduction in model uncertainties while documenting “any uncertainties and assumptions for user transparency” (Jakeman et al. 2018). Conversely, poor modelling practices have negative implications which affect the reliability of

the outputs. Many of the practices described in the QWMN paper are worthwhile adopting in a contextualised capacity to enhance the methodology of this project.

Such practices include:

- A thoroughly documented introduction of the acquired datasets and their attributes, including a critical review of the quality and reliability of the data based upon any limitations and its applicability for modelling. Data management and processing should also be explained thoroughly.
- A justified explanation of the selected modelling and calibration approach, including an evaluation of any assumptions and alternative methods, ultimately deducing why the chosen method is most appropriate to conceptualise the hydrologic and catchment characteristics with respect to the research objectives.
- An extensive model testing program to verify the model suitability across a comprehensive range of conditions.
- Sensitivity analyses of the input data and model parameters to evaluate the sensitivity and uncertainties embedded within the results.
- A sanity check of the model results against independent methods of analysis to evaluate the reasonableness of the adopted method.
- Complete and concise reporting of the model results with an emphasis on the applicability of the outputs in context of the project objectives, and any uncertainties within the data. The attachment of the input and output model files within the report appendices for clarity and repeatability is a crucial practice.

3.3 Data acquisition and preparation

The input data required to develop the hydrologic models was retrieved from official primary sources including the DRDMW operated WMIP, the BOM managed DRDS and the ARR Data Hub. Data retrieval from government and academic sources with documented quality assurance procedures, measurement recordkeeping and transparent statements about the limitations in the datasets ensures the highest possible input quality for modelling. The types of data retrieved, any associated limitations, and subsequent processing measures used in preparation for hydrologic modelling are described below.

3.3.1 Catchment geographic spatial data

As an open-source, free geographic information system package, QGIS was chosen to process catchment spatial data for this project. Primarily, the software was used to delineate the boundary and determine the flow routes of Laidley Creek and its tributaries throughout the

catchment. In addition, the locations of rainfall and streamflow stations were visualised in the software to calculate spatially averaged metrics for subsequent modelling.

A suitable digital elevation model (DEM) sourced from the Shuttle Radar Topography Mission (SRTM) 1 Arc-Second Global V3 dataset published by the Earth Resources Observation and Science Center of the United States Geological Survey (2014) was downloaded as a GeoTiff file covering an indicative outline the catchment region. The file corresponding to the S28° E152° DEM was imported into QGIS and reprojected to the World Geodetic System 1984 (WGS84) coordinate reference system. WGS84 is geographically accurate to within 2 metres which is sufficient for the scale of this catchment.

Two approaches were considered to generate the catchment boundary and stream routes. The first approach is preferred as it utilises hydrologic simulation methods available through open-source QGIS plugins (including SAGA, GRASS and PCRaster) to determine spatial flow characteristics based upon a terrain analysis of the DEM raster cells. The general procedure for this approach consists of the following stages:

1. Filling surface depressions in the DEM to maintain correct hydrologic functionality.
2. Computation of flow accumulation and direction based upon the gradient and orientation of the terrain at a rasterised cell level.
3. Calibration of flow accumulation to the existing stream features shown within satellite and mapping imagery of the catchment
4. Delineation of the catchment streams above the calibrated threshold level.
5. Delineation of the catchment boundary upstream of an identified outlet based upon the DEM cell elevations within the catchment.

The advantage of this approach is that the automatic processing of the catchment boundary and streams is a relatively quick procedure to execute, and provided the input DEM is of sufficient vertical resolution, the results are usually more accurate than manual delineation. However, the main disadvantage of the flow accumulation method is that modelling expansive floodplains with very flat terrain or artificial storages often results in misaligned flow routes (Al-Muqdadi & Merkel 2011; van der Kwast 2018). When the automatic stream delineation method was applied for the Laidley Creek catchment, the outlet was displaced 1.3 kilometres north-west of its known location and the general flow path did not align with the existing route of Laidley Creek, as illustrated in Figure 3.1. The catchment area was computed as 450.6 km², which represented a 2.5% underestimation of the 462 km² area stated within the WMIP details for station 143229A (Department of Regional Development, Manufacturing & Water 2024).

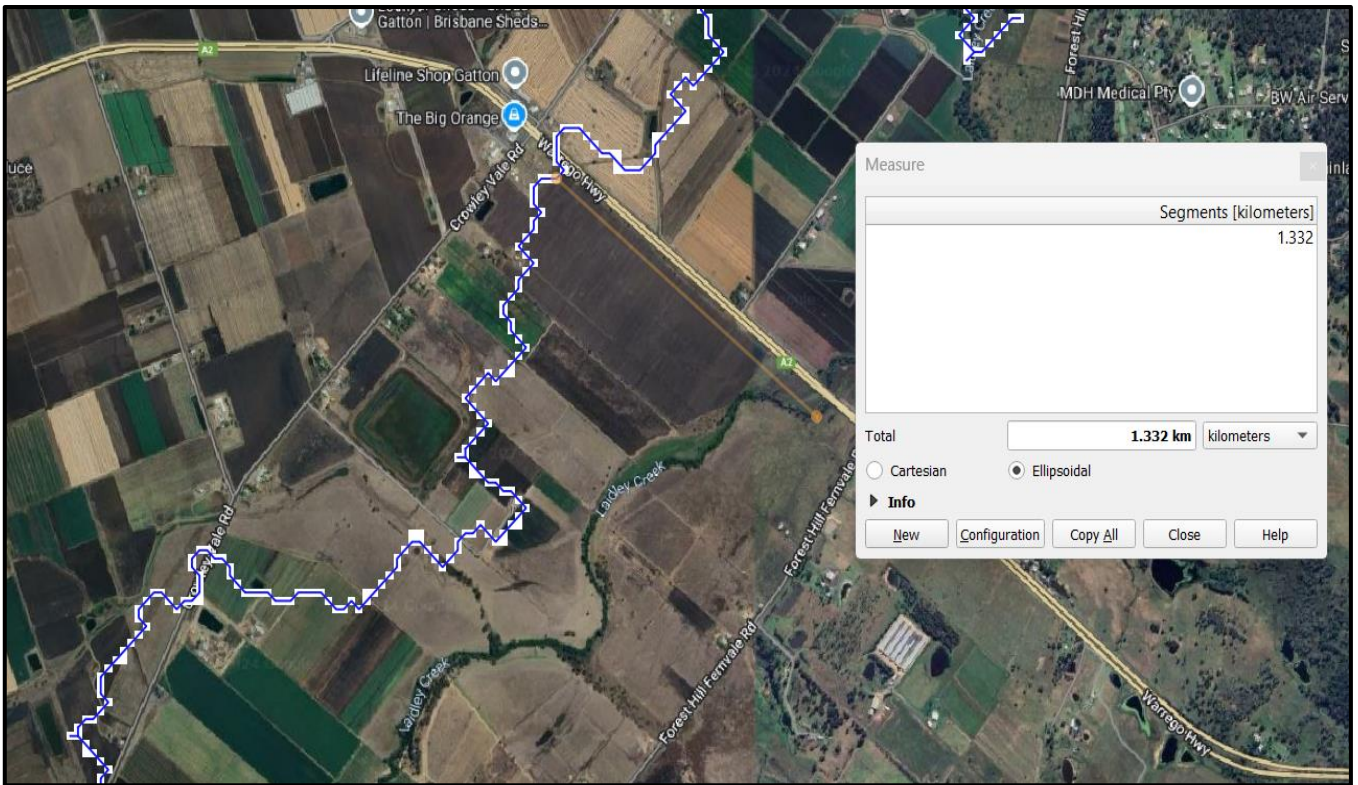


Figure 3.1: Poor alignment of Laidley Creek using the rasterised threshold flow accumulation method

The results obtained by this method were deemed unsuitable for further modelling given the misaligned Laidley Creek flow path, considering the proximity of the actual outlet site to the Warrego Highway crossing. Hence, the second, manual catchment delineation method was adopted to reduce the irrationality of the delineated catchment features. A 25 metre interval contour layer was generated from the DEM cell elevation attribute and peaks in the terrain were identified by a set of spatial point features. A second 10 metre contour layer clarified the positioning of any ridgelines and peak elevation where the terrain was difficult to interpret. The catchment boundary was then established by connecting the identified high elevation locations with the outline of a polygon shapefile feature, as illustrated in Figure 3.2.

The area of the Laidley Creek catchment upstream of the 143229A station was computed as 452.3 km². This represented a minor improvement on the automatically generated catchment area. The landmass situated between the northern catchment boundary and Lockyer Creek was identified as largest contributing explanation of the difference between the manually delineated method and WMIP catchment areas of 452.3 km² and 462 km² respectively. The terrain within this section is very flat and bounded to the south by the raised corridor of the Warrego Highway. Surface levels and flow patterns have been modified by closed system irrigation and artificial storage networks used by agricultural operators. Therefore, this section was deemed to have

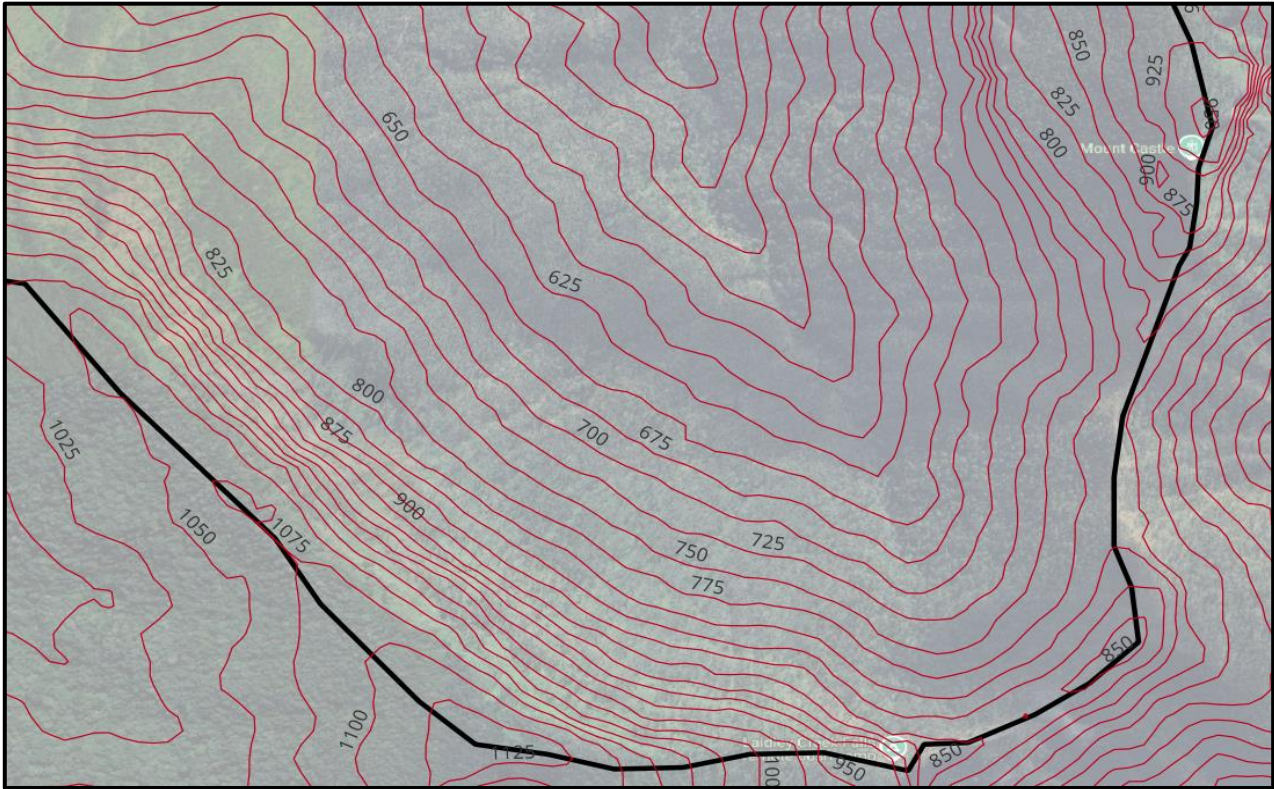


Figure 3.2: Laidley Creek catchment boundary manually delineated from ridgelines identified in the 25 metre contour overlay.

negligible impact on flood conditions at the 143229A station, such that the manually computed catchment area of 452.3 km² was representative of the contributory upstream catchment and its flow characteristics during peak flood events. Any minor boundary errors could hence be considered as having negligible impact on the catchment definition.

The catchment centroid position was determined by executing the QGIS centroid function with the catchment polygon feature as an input layer. The centroid was located at the coordinates 27.727°S 152.355°E, which almost identically correlated with the catchment centroid coordinates of 27.7266 °S 152.357 °E identified by Rahman et al. (2015) in the RFFE method.

To resolve the irrational stream delineation of the flow accumulation method, major stream flow paths were identified from the Open Street Map (OSM) spatial extent query operation using the catchment polygon as an overlay boundary. This approach yielded a series of line features that were accurately aligned to the defined flow paths observed from satellite imagery.

The delineated catchment boundary, centroid and internal stream features are identified in Figure 3.3, with the locations of the two DRDMW operated gauging stations along Laidley Creek shown for reference.

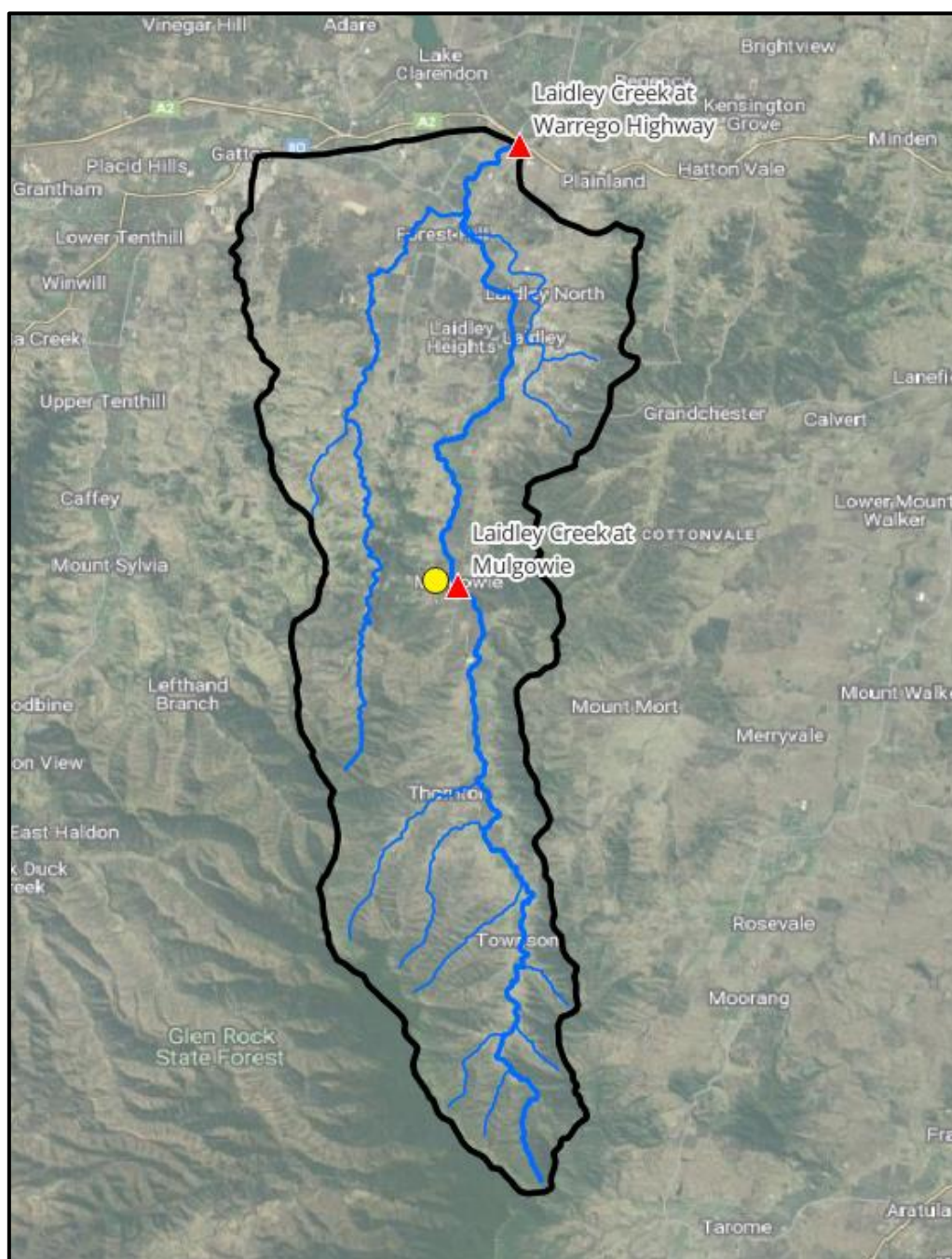


Figure 3.3: Laidley Creek catchment with centroid location, major stream network and gauging stations shown.

3.3.2 Gauged streamflow data

Historical streamgauge data was retrieved for the two Laidley Creek gauges from the WMIP website. The portal provided basic site-specific information essential for developing subsequent models. As listed in Figure 3.4, such details included the latitudinal and longitudinal coordinates, the base elevation relative to the Australian Height Datum (AHD), as well as the upstream catchment area, among other technical characteristics for each gauge.

Site no.	143229A	143209B
Zone	56	56
Easting/Northing	439678.023/6952145.579	437333.126/6932548.553
Latitude	27°33'11.4"S	27°43'47.9"S
Longitude	152°23'20.4"E	152°21'51.2"E
Site commence	31/10/1990	06/03/1967
Site ceased		
Zero gauge	76.313	132.620
Datum	AHD	AHD
Control	Two Metre Crump	Control Weir
Cease to flow level	0.505	1.000
Maximum gauged level	7.654	6.220
Maximum gauge date	28/01/2013	11/01/1968
Distance from stream mouth	5.000 km	31.000 km
Catchment area	462 sq.kms	167 sq.kms
Gaugings	59 gaugings between 01/11/1990 and 04/10/2023	224 gaugings between 06/03/1967 and 05/06/2024

Figure 3.4: Site details for the 143229A and 143209B streamgauges extracted from the WMIP (Department of Regional Development, Manufacturing & Water 2024)

Monthly, daily and hourly datasets of stream discharge and level from each gauged site were extracted from the WMIP in spreadsheet form. Data at varying time intervals was obtained to facilitate the development of different model inputs. The monthly maximum streamflow record of for the primary station at 143229A is shown in Figure 3.5, which importantly, shows that the four highest flow peaks correspond with the four largest events listed in Table 2.1. The baseflow component of runoff was zero or near-zero flow.

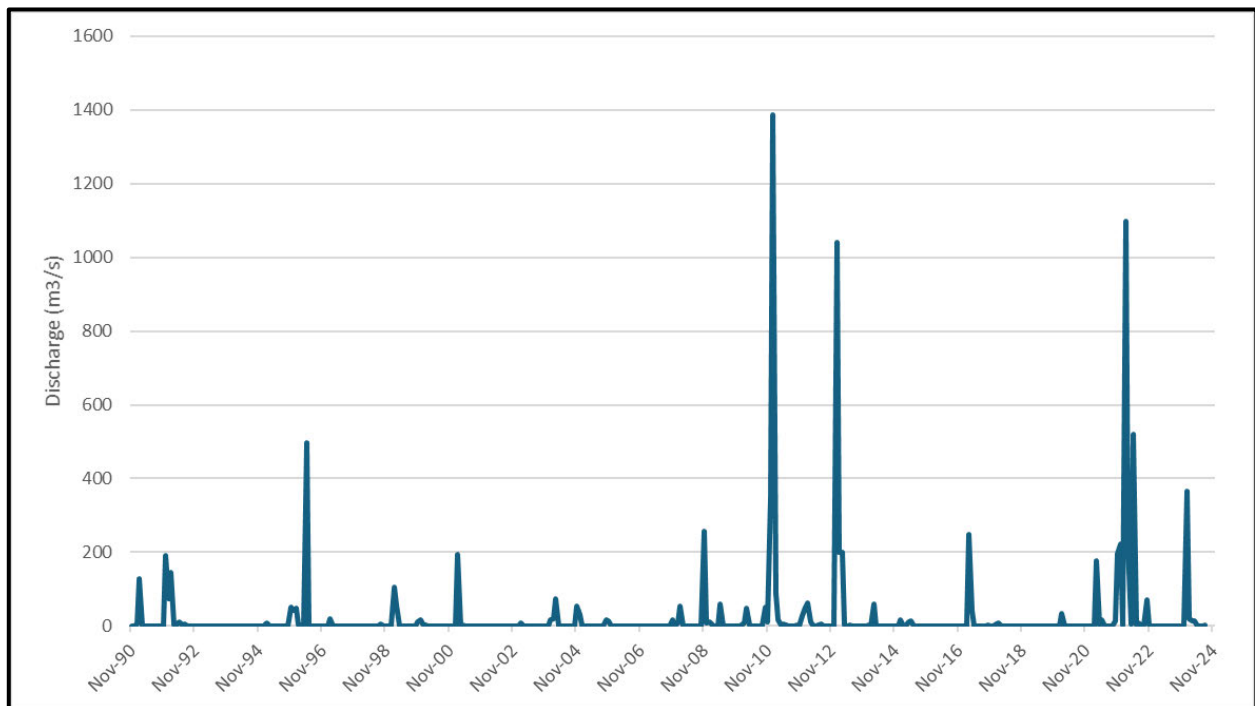


Figure 3.5: Monthly maximum streamflow record for 143229A gauge [generated from data produced by (Department of Regional Development, Manufacturing & Water 2024)]

Data quality codes assigned by DRDMW signify the quality and reliability of the individual data readings. The majority of historical data has been audited and validated by DRDMW and is considered sufficiently reliable for modelling. The most recent data recordings (typically within the last 12 to 24 months) are typically unverified, indicated as a code 40 or 130 (DRDMW 2023). A review of these dates against observed rainfall data confirmed the readings were accurate. Code 15 is used to differentiate flows less than minimum threshold of the gauge from regular flow recordings (DRDMW 2023). However, as this research is not concerned with the estimation of very frequent flood events, the precision of low flow data is not crucial, hence the quality of this data was considered sufficient. Estimated data readings are signified by code 60, which typically is observed for extrapolated high flow events beyond the limit of the gauged rating (DRDMW 2023). Similarly, the code 255 is used to signify unreported or missing data, including inaccurate data removed through an audit (DRDMW 2023). Aside from equipment faults, instances of estimated and unreported data records have occurred more frequently during extreme, high flow events (DRDMW 2023) and require considered judgment about their inclusion within input data sets for peak flow modelling.

The proportion of each data quality classification over the operational period of the primary station of interest, 143229A, were computed and listed in Table 3.1. The majority of data was considered normal, good, fair or below threshold. 4.6% of the data was considered unverified or not coded while 2.6% was estimated. No recording gaps in the data sequence were observed.

Table 3.1: Distribution of data quality by classification at 143229A station

Quality code	Definition	Occurrence (days)	Occurrence (%)
9	CITEC Normal	5343	43.3
10	Good	3323	26.9
15	Below threshold	2433	19.7
20	Fair	358	2.9
40	Unverified	245	2.0
60	Estimate	323	2.6
130	Not coded	318	2.6
255	No reading	0	0

3.3.2.1 Rating curve and control evaluation for 143229A (Warrego Highway)

Flows through the 143229A gauging station are regulated by a two metre concrete crump weir as pictured in Figure 3.6. Low to moderate flow depth readings through the section are reliable

because the fixed concrete hydraulic control section has remained constant during its period of operation. During higher flow events, the water level rises above the weir and the section incorporates the surrounding earth banks, which have a non-uniform soil profile and feature varying levels of vegetation. These areas are more susceptible to change over time from processes such as erosion and sediment deposition. However, the surrounding vegetation would offer some protection of the stream banks, meaning the section has likely remained similar over time. Regardless, the limitation that the section characteristics may not necessarily be maintained between high flow events is worth consideration.



Figure 3.6: 143229A Warrego Highway hydraulic control and surrounding stream section
(Department of Regional Development, Manufacturing & Water 2024)

The accuracy of the rating curve at 143229A is crucial towards obtaining useful results from this research given its proximity to the Warrego Highway. The site rating curve, as pictured in Figure 3.7, is well defined by 59 gaugings across an adequate range of flows. The maximum recorded flow has only exceeded the maximum gauging of approximately $980 \text{ m}^3/\text{s}$ on four separate days, with flows of this magnitude still considered fairly reliable by DRDMW Department of Regional Development, Manufacturing and Water (2024). The main limitation with the streamflow record of 143229A is its relatively short operational period, having only opened in November 1991. However, the record obtained is very reliable, as supported by Barton et al. (2015). The streamflow record from 143229A is fundamental to the modelling undertaken in this report.

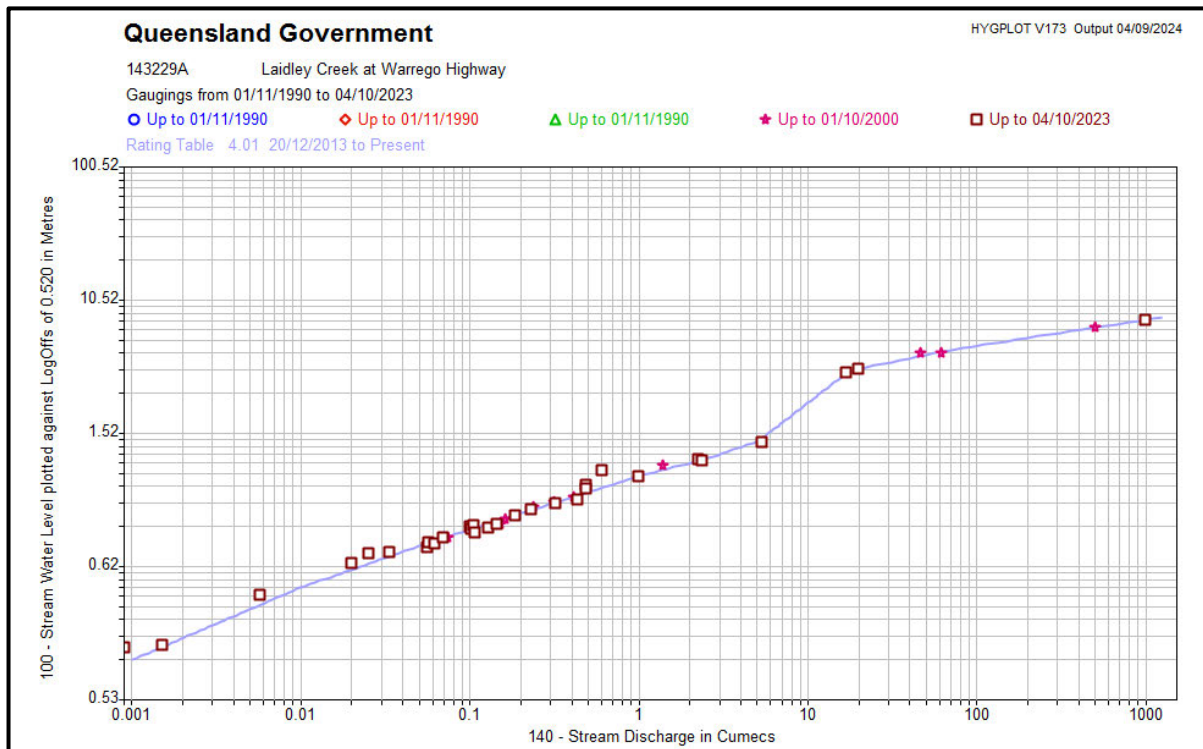


Figure 3.7: Well defined site rating curve from individual gaugings for 143229A station (Department of Regional Development, Manufacturing & Water 2024)

3.3.2.2 Rating curve and control evaluation for 143209B Laidley Creek at Mulgowie

The second gauging station along Laidley Creek is located at Mulgowie and is the outlet of an upper catchment area of 167 km². An earth-rock mound is used to regulate flows through the 143209B gauging station, as pictured in Figure 3.8.



Figure 3.8: 143209B Mulgowie hydraulic control and surrounding stream section (Department of Regional Development, Manufacturing & Water 2024)

The reliability of the streamflow data is compromised by this type of hydraulic control, as the section is vulnerable to movement over time. Cross section instability likely explains the significant variance (scatter) observed between flow gaugings of similar magnitude, as illustrated in Figure 3.9.

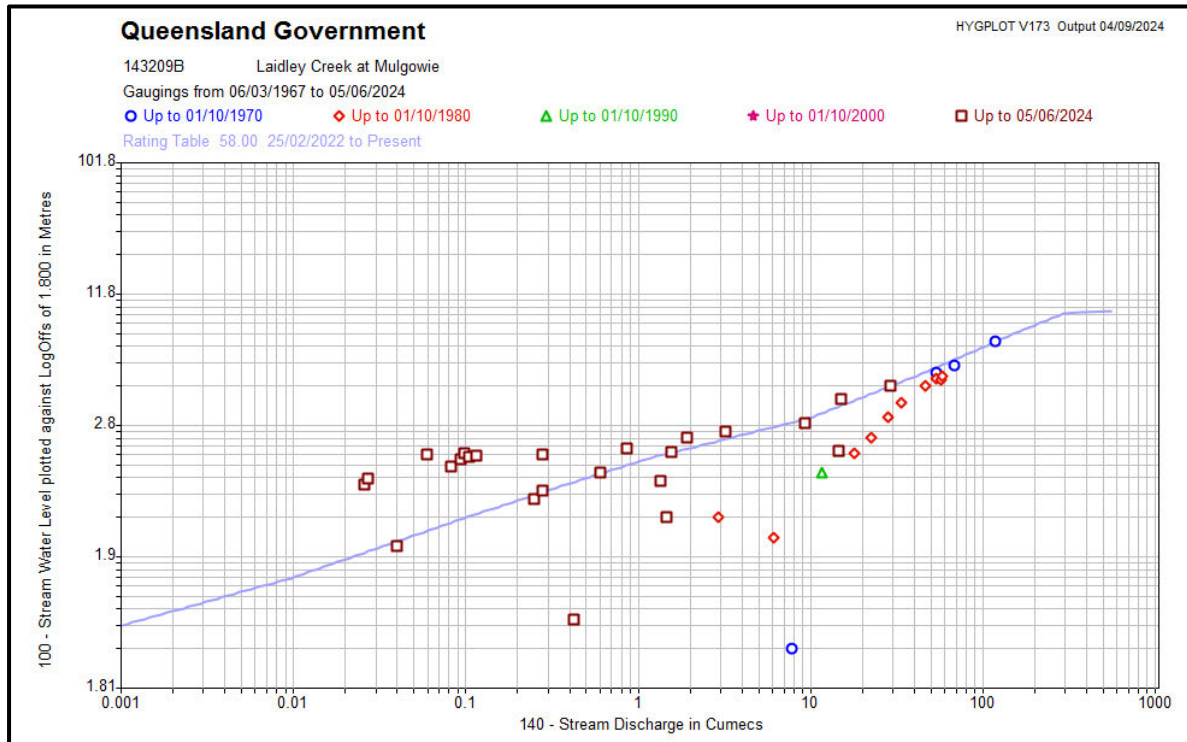


Figure 3.9: Site rating curve with significantly varied gaugings for 143209B station (Department of Regional Development, Manufacturing & Water 2024)

Since the site was opened in January 1968, 224 gaugings have been undertaken, yet the maximum gauged discharge of approximately 121 m³/s is significantly less than the maximum recorded flow of 348.9 m³/s (Department of Regional Development, Manufacturing & Water 2024). The site rating curve is poorly defined, with flows above 10.9 m³/s considered an estimate by DRDMW (2024). Peak recorded flow levels above 9.0 metres are considered ‘suspect’, indicating the readings are very unreliable. Flows levels of similar magnitude have very different discharges, as illustrated in Figure 3.9. Several limitations associated with the quality of the rating curve at the 143209B gauge, especially at high flows experienced during peak flood events, mean the streamflow datasets from this station are too compromised to be useful for any modelling in this report. All modelling will instead utilise reliable data from the 143229A station, which was the preferred station regardless because of its proximity to the Warrego Highway.

3.3.3 Observed rainfall station data

Recorded rainfall data is required to calibrate the catchment parameters of a runoff routing model against the characteristics of previously observed events. The two identified DRDMW operated streamflow gauging stations situated within the Laidley Creek catchment have an insufficient rainfall record to of any use, having only been upgraded to capture rainfall data in 2024. Therefore, alternative sources of rainfall data at daily and hourly intervals were required.

3.3.3.1 Daily observed rainfall totals

Daily observed rainfall data was sourced from 22 stations operated by BOM through its Climate Data Online portal (2024). Eleven of these stations were located within the delineated Laidley Creek catchment while the remaining eleven were located less than ten kilometres outside of the catchment. Rainfall data observed within the ten kilometre external buffer external was still considered potentially useful because of the rainfall decorrelation distance introduced in the literature review of ten kilometres as described by Podger (2004).

The BOM rainfall station provide a reasonable level of spatial and time coverage across the catchment. An initial viability assessment of the usefulness of each station was undertaken by determining which station datasets contained records during the peak flow events listed in Table 2.1. As shown in Figure 3.10, eight stations had full recorded coverage of the peak flow events while another five had a partial record. The remaining nine were not operational during any of the events of interest. Only three of the thirteen sites were situated within the catchment, however, these stations were well distributed along its north-south axis. The majority of the stations were located within the northern extent of the region and are closely clustered around the population centres of Gatton and Plainland. The recorded rainfall data in this area was able to be corroborated between stations to determine the reliability of each dataset. Additionally, where gaps existed in a station record during an event of interest, a secondary backup site was easily adopted with an adjustment correction factor applied to relate the datasets. In the more remote sections of the catchment, rainfall station coverage was much more limited. Three stations provided some level coverage of the peak flow events listed in Table 2.1 in the central catchment region, while a singular station at Townson offered coverage of the upper-most reaches. Catchment coverage was considered suboptimal through the 20 kilometre section between Mulgowie and Townson. However, in the absence of alternative rainfall data, the maximum isolation distance between any location and a rainfall dataset of approximately ten kilometres meant coverage was deemed sufficient, with limitations about the poor coverage and potential data decorrelation in certain portions of the catchment noted.

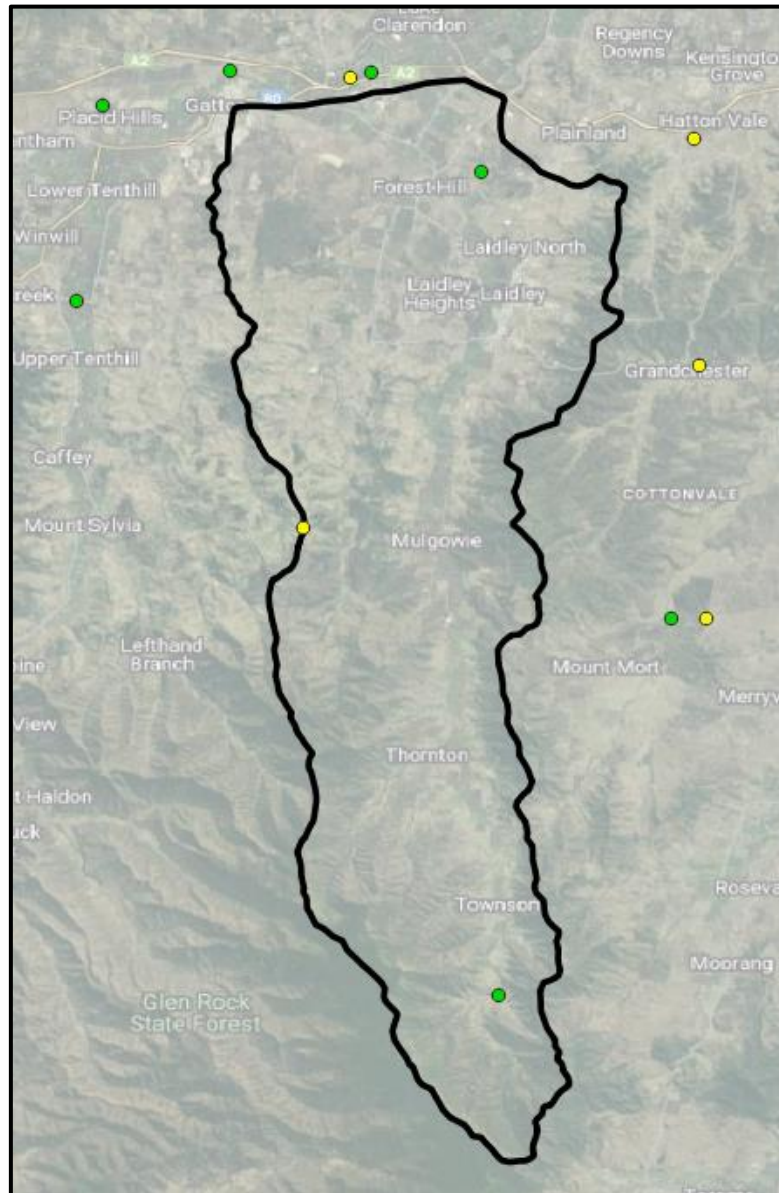


Figure 3.10: Full (green) and partial (yellow) rainfall station event record status

The reliability of the data recorded at each station was evaluated against a baseline average computed for the Forest Hill station. This station was adopted because of its location within the Laidley Creek catchment and its 130 year ongoing record to 30 April 2024. As detailed in Appendix B, the average daily rainfall at the stations in close proximity to Forest Hill conformed closely when averaged over a common operational period. This confirmed the Forest Hill station, with an average daily rainfall depth of 2.13 mm/day provided an ideal representation of the lower catchment area. Higher common period average rainfall depths were observed in the upper catchment reaches, which were not considered unreliable station readings, rather an indication of the spatial variability of rainfall through the mountainous terrain surrounding Laidley Creek.

3.3.3.2 Hourly observed rainfall

Hourly rainfall recordings were required to define the specific temporal distribution patterns of previously observed events. However, none of the rainfall stations within the catchment contained a sub-daily rainfall dataset. Two DRDMW operated streamflow gauging stations in adjacent catchments, namely Tenthill Creek and Adams Bridge (Bremer River), each had an ongoing hourly rainfall record spanning over 30 years (Department of Regional Development, Manufacturing & Water 2024). A third 30 minute rainfall depth dataset at the UQ Gatton station was sourced from BOM (2024c) however did attract a student-use retrieval and licensing fee. This dataset was reformatted at an hourly interval to correspond with the resolution of the other two datasets. The details of each hourly dataset are included in Table B2, refer to Appendix B.

The UQ Gatton and Tenthill Creek stations provide a reasonable level of sub-daily record coverage for the northern portion of the catchment. The relevancy of coverage provided by Adam's Bridge site over the eastern and southern reaches is limited as the station is located further than 10 kilometres from the catchment boundary. However, because no viable alternative dataset exists, the Adams Bridge record will be utilised with caution, noting potential limitations regarding relevancy and event decorrelation.

3.3.4 Design rainfall event parameters

Design rainfall parameters are required for discharge estimation following calibration of the runoff routing model.

3.3.4.1 LIMB-BOM IFD enveloped dataset

To support an accurate and conservative modelling approach, the LIMB-BOM IFD envelope was selected as the design rainfall dataset. The LIMB-BOM dataset was extracted from the ARR Datahub using the input catchment centroid coordinates 27.727 °S 152.355 °E. Compared to the BOM IFDs, the design rainfalls which increased in the LIMB set were less than one hour in duration. All design rainfalls of a duration of more than one hour originated from the BOM IFD set. The full enveloped IFD dataset is presented in Table C1, attached to Appendix C.

3.4.4.2 Projected future climate IFD datasets

The LIMB enveloped design rainfalls were revised to reflect the localised impacts of climate change. The projected rainfall depths for both the RCP 4.5 and 8.5 emissions scenarios by 2030, 2050 and 2090 were calculated according to Equations 2.15 and 2.16, and the values of α and ΔT according to Tables 2.3 and 2.4 respectively, as well as the ARR Datahub. The complete scaled IFD datasets are presented in Tables C4 to C9, attached to Appendix C.

3.3.4.3 ARR Datahub parameters

Design event parameters including storm losses, ARF, areal temporal patterns and preburst depths were extracted from the ARR Datahub in a text file, which is attached in Appendix D.

3.3.5 Finalisation of the design methodology scope

Considering the limited availability of some data as described above, the design methodology scope was finalised. The streamgauge record of Laidley Creek at the Warrego Highway was deemed too short to utilise FFA as the preferred method of peak flow estimation, while the limitations of regression methods were deemed too significant. Hence a runoff routing approach using the RORB package was selected and other methods including FFA, RFFE and P&W were utilised for comparative purposes, as recommended by Jakeman et al. (2018). The streamgauge rating at Mulgowie was considered too unreliable for use as a secondary gauge within the model, therefore catchment calibration and design flow simulations were based solely on the Warrego Highway site. The limitations associated with the daily rainfall record coverage in the upper Laidley Creek catchment, and hourly rainfall record coverage across the entire catchment, were recognised. However, in the absence of alternate data, the BOM and DRDMW sourced datasets were used, knowing that some uncertainty would be introduced to the model. The scaled IFD envelopes encompass three design periods: short, medium and long-term; two potential emissions scenarios: moderate and high. This arrangement provides adequate coverage of plausible future climate conditions, however utilising the median rate of change α instead of a range of values also contributes to the uncertainty of the results.

3.4 Semi-distributed runoff routing model development

Processing and management of the collected spatial, rainfall and gauged runoff data is required to develop the standard format RORB files. Firstly, the catchment spatial features were converted to the equivalent semi-distributed catchment representation for efficient file development in the RORB graphical editor. Then the recorded rainfall and runoff data was analysed to determine the RORB storm file inputs. The catchment and storm files were analysed within the RORB package to calibrate and verify the model parameter values against previously observed events of varying magnitude. Finally, the design event simulation procedure was described in preparation for the detailed results presented within Chapter 4.

3.4.1 Catchment model generation from spatial data

Preparatory spatial modelling within QGIS was required to convert the identified catchment and stream network into a format compatible with a node-reach runoff routing catchment file.

Therefore, the Laidley Creek catchment shapefile was partitioned into 20 subcatchments corresponding to the identified major flow paths and non-uniform sections of terrain. Subcatchments within the southern, mountainous sections were typically smaller than those delineated for the expansive, open downstream sections. This was because defined creek streams form between the steep ridgelines separating the upper subcatchments, while the lower subcatchments generally only contribute overland flows to either Laidley or Sandy Creek as upstream flows are conveyed towards the outlet. As determined from the subcatchment layer attribute table, the maximum subcatchment area was 56.59 km² while minimum was 3.83 km².

As introduced in the literature review, a semi-distributed model assumes uniform rainfall-excess is produced within a subcatchment and enters the network at or adjacent to the centroid of each subcatchment (Laurenson, Mein & Nathan 2010). Therefore, the subcatchment centroid positions were computed in QGIS, represented by the black nodal layer in Figure 3.11. These points were then snapped to the surrounding stream geometry, represented by the orange nodal layer, to represent the network entrance assumptions of Laurenson, Mein and Nathan (2010).

The displacement between the two point layers at 18 of the 20 subcatchments was 500 metres or less, while subcatchment 13 and 19 required additional flow reaches to connect isolated centroids to the stream network. The nature of a semi-distributed model also rendered the stream networks redundant upstream of the snapped centroid of each subcatchment. Therefore, the streams were trimmed at the subcatchment centroids as also shown in Figure 3.11.

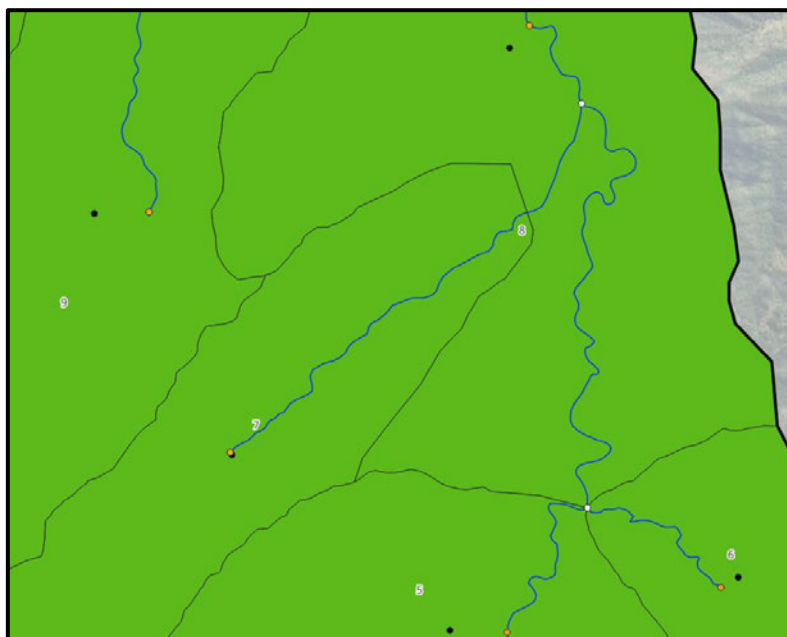


Figure 3.11: Suitable displacement between actual subcatchment centroids (black) and snapped centroid nodes to adjacent stream network (orange)

The reach length of each stream section between the centroidal and junction nodes was extracted from the shapefile attribute table. The partitioned subcatchments, configured centroids and adjusted stream network features are illustrated in Figure 3.12.

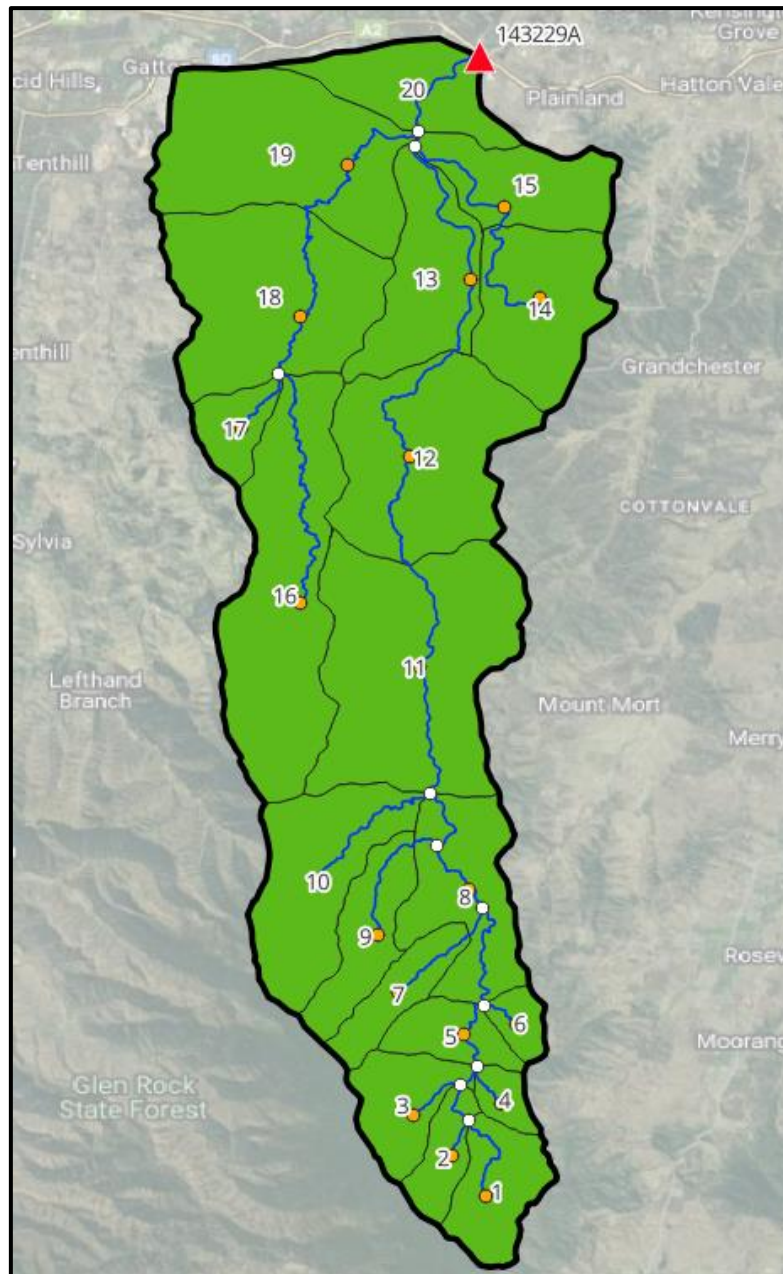


Figure 3.12: Partitioned subcatchments and adjusted stream reaches for RORB catchment file development.

The node-reach configuration of Figure 3.12 was formatted such that a RORB catchment file could be easily developed in the graphical editor package. This approach facilitated the graphical generation of a semi-distributed catchment file compatible with the RORB runoff routing modelling program. The network configuration, consisting of subcatchment areas,

reach lengths and junctions, was replicated in the graphical editor. The slope of each reach was considered as the average gradient between the bounding upper and lower node elevations.

The 6.9 GL capacity Lake Dyer is situated within subcatchment 13. While RORB has functionalities to represent special storage reservoirs as nodes, the upstream catchment that supplies Lake Dyer is only 3 km² (SEQWater 2024). Hence, the reservoir capacity itself and the tributary area were both considered insignificant when compared to Laidley Creek catchment area of 462 km². Similarly, the proportion of impervious land coverage, concentrated about the towns of Laidley and Forest Hill, as well as road surfaces located within the catchment, was deemed insignificant such that all subcatchments were considered to be entirely pervious. It is acknowledged that these simplifications have the potential to introduce some minor uncertainty to the model outputs.

A singular nodal outlet was established downstream of subcatchment 20 to represent the 143229A gauge. For the calibration phase of modelling, the print hydrograph code 7.1 was utilised to compare gauged flows. However, during the design simulation phase, the code 7 was used to generate the simulated ensemble of design discharges. Once imported to the RORB modelling package, the graphical catchment file was converted to a regular catchment file, attached to Appendix E.

3.4.2 Generation of calibration storm files from previously observed events

Rainfall and streamflow data was collected to develop the storm event files for calibration of the RORB model parameters. Storm files were developed for eight peak flow events, including the events listed in Table 2.1 where inundation of the Warrego Highway was confirmed. To ensure the calibration accurately represented as many flow scenarios as possible, events of various magnitude and timing were analysed.

The collected hourly rainfall data had two purposes, firstly, to define the event temporal distributions. Each subcatchment temporal pattern was defined by the nearest available hourly rainfall station during an event. In some instances, when the hourly rainfall station was non-operational, the second closest site was adopted. Secondly, storm event timings were dictated from the hourly rainfall distributions, including components which were considered pre-bursts and hence excluded from the events per Ladson (2016).

Similarly, the gauged streamflow record had two purposes. The event hydrographs would ultimately function as the calibration reference, while the recession timing indicated the event

conclusion. In all circumstances, the event duration was extended beyond rainfall ceasing to account for catchment transmission delays. The eight modelled extreme rainfall events are listed in Table 3.2. The number of rainfall datasets data available for analysis and the type of rainfall burst experienced are specified. The desired spread in peak flow magnitude between events is also demonstrated.

Table 3.2: Extreme rainfall events used to calibrate RORB model parameters

Start date and time of rainfall event	Rainfall duration (hours)	Active rainfall station datasets (daily/hourly)	Rainfall burst classification	Maximum discharge at 143229A
30 April 1996 17:00	138	10 / 2	Dual	496.6
18 November 2008 10:00	48	13 / 3	Single	255.9
5 January 2011 0:00	168	9 / 3	Dual	1387.1
25 January 2013 20:00	62	10 / 2	Single	1041.5
30 March 2017 0:00	23	10 / 3	Single	248.7
24 February 2022 09:00	96	6 / 2	Single	1097.7
11 May 2022 09:00	76	8 / 2	Single	521.1
28 January 2024 0:00	65	8 / 3	Single	366.7

The total rainfall received at the centroid of each subcatchment during the individual events listed in Table 3.2 was approximated by developing an event-specific isohyetal distribution. From the total point rainfall recorded at each available daily rainfall station, a raster distribution was generated in QGIS by the inverse distance weighted (IDW) interpolation operation, as illustrated in Figure 3.13 for the May 2022 event. Then, the total rainfall at each of the 20 subcatchment centroids was assigned from the identify raster attribute function in QGIS. This process was undertaken for each burst of the dual-burst events.

This method of areal rainfall approximation has several associated strengths and limitations. The influence of a singular point rainfall observation when compared to another station reduces with distance using the IDW interpolation. Therefore, a potentially inaccurate and undetected event rainfall measurement is contained within a localised proximity to the questionable station. The dominant (and assumed more accurate) range of measurements sourced from surrounding stations then are interpolated through the remaining majority of the catchment.

Additional rainfall datasets originating from locations just outside the catchment decorrelation distance of 10 kilometres (but within the extent of the definitive mountain ranges illustrated in

Figure 2.1) were unable to be sourced. Consequently, the IDW interpolation produced unrealistic circular isohyets, predominantly centred about the Townson station. However, the difference between isohyets overlaid on the southern catchment reaches was minimal, especially within the catchment boundary itself. The largest misrepresentation of rainfall distribution was observed to the south of the catchment (beneath the catchment boundary in Figure 3.13). Additionally, considering the centroidal rainfall depth as the subcatchment average is prone to some uncertainty, especially in the larger subcatchment areas where rainfall varies significantly within the singular subcatchment.

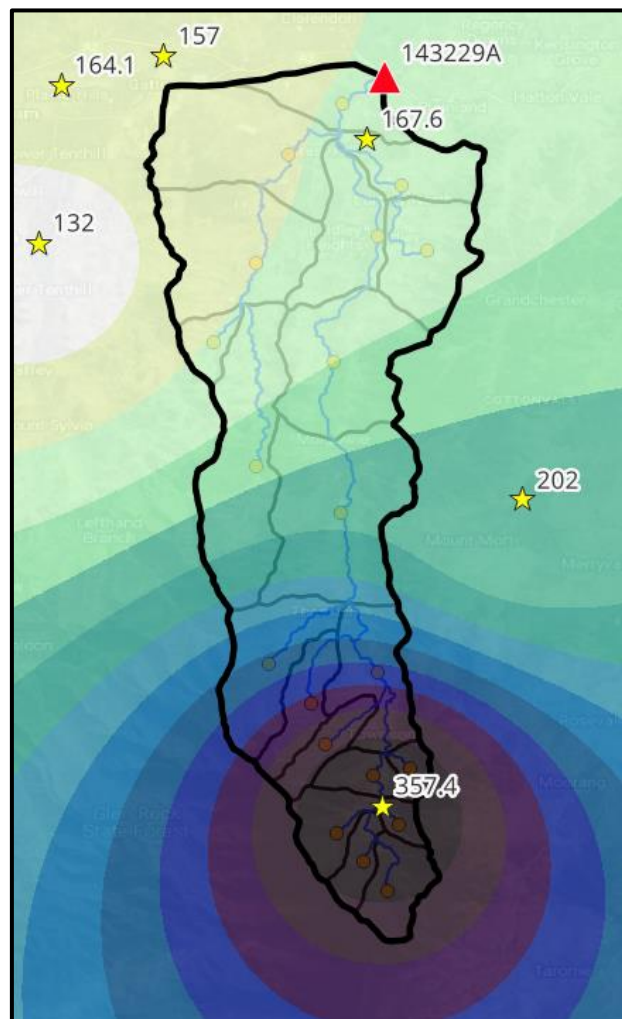


Figure 3.13: May 2022 event rainfall (mm) isohyetal distribution from active station datasets (stars)

The formatted storm event files for calibration of the RORB parameters contained hourly rainfall and runoff observations from available stations; timing definitions of these observations; and event total subcatchment rainfall depths. The storm files and associated graphical isohyetal distributions are attached within Appendix F.

3.4.3 Calibration of the RORB model parameters

The eight storm event files were separately loaded into RORB to calibrate the model parameter k_c for the Laidley Creek catchment file. Calibration of each event was based upon comparing the model calculated runoff at the catchment file outlet against the observed streamflow record from 143229A. The values of k_c and IL depth were adjusted using a trial and error approach until the calculated and observed runoff hydrographs were as aligned as possible. The m parameter value was fixed as 0.8 per the recommendations of Laurenson, Mein and Nathan (2010). The RORB FIT specification was used for calibration, such that CL values were automatically computed by the program for a given IL to produce a flow volume as equal as possible to the observed data. The IL depth considered for each event varied to represent the spread of diverse antecedent conditions captured. For events consisting of two separate bursts, two IL depths were assigned, generally the second was minimal given the preceding burst.

The suitability of the correlation achieved by the calculated hydrograph was evaluated against a set of qualitative and quantitative criteria. Aspects of the hydrograph shape were evaluated for alignment, including:

- The slope and curvature of rising and falling limbs
- The number of discrete local maxima (peaks)
- The initial commencement timing of runoff generation
- The lateral displacement between the observed and calculated hydrographs curves

Quantitative measures of correlation were determined directly within the RORB statistics panel, including the percentage difference in:

- Peak discharge
- Duration of time to peak discharge
- Duration of time to flow volume centroid

Considering multiple events during calibration of the model was necessary to ensure the selected parameters, especially k_c , were an as viably accurate representation of the physical processes that occur in the Laidley Creek catchment as possible. For a singular event modelled in the RORB environment, many different combinations of k_c and IL produce hydrographs with similar attributes and appearances. However, modelling additional events typically demonstrates which parameters are suitably applicable to a variety of events with different attributes including flow duration, peak magnitude and number of flow peaks. Then the singular value corresponding to a model parameter was determined as the measure of central

tendency of the spread of all events, excluding any notable outliers. In this instance, the mean and median values of k_c were considered.

Calibration commenced for each event by adopting the regionalised value of $k_c = 22.48$ as automatically calculated by RORB for a Queensland catchment with an area of 452 km². Then the IL depth was adjusted as much as possible for each event in an attempt to closely align the calculated and actual hydrographs. However, it was evident that the regionalised value of k_c was too low because the upper limit of IL (based upon the total rainfall received) was reached and the flood hydrograph peak was significantly greater than observed, as illustrated in Figure 3.14 for the February 2022 event and Figure 3.15 for the May 2022 event.

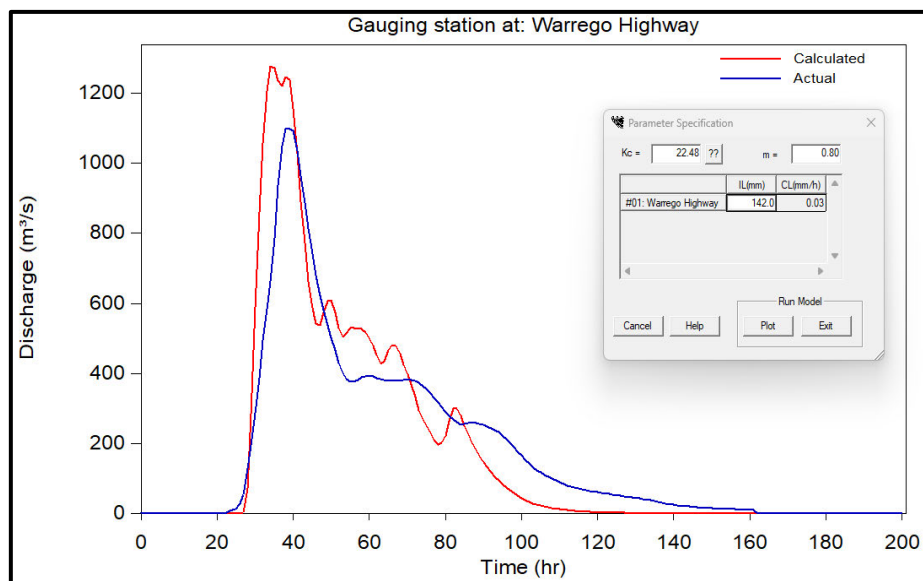


Figure 3.14: Calculated hydrograph (red) for February 2022 event using regionalised $k_c = 22.48$

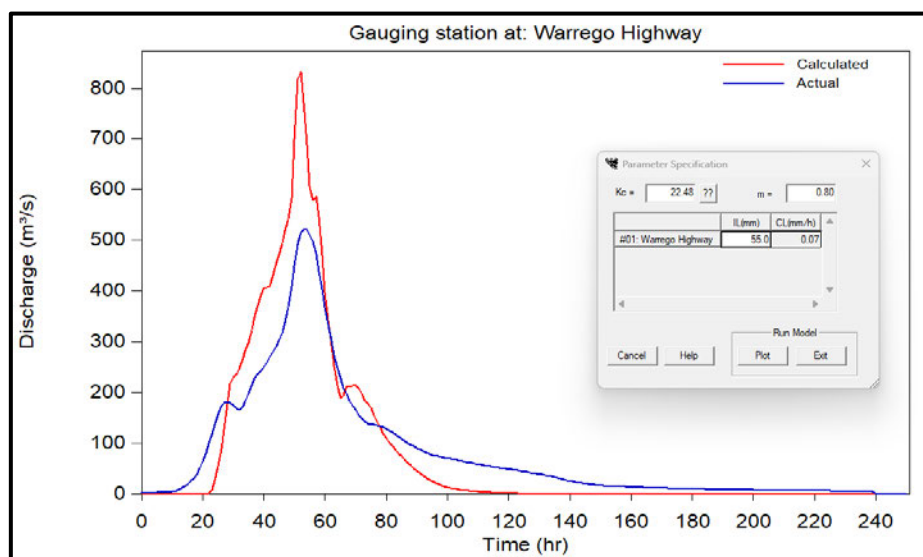


Figure 3.15: Calculated hydrograph (red) for May 2022 event using regionalised $k_c = 22.48$

Therefore, the value of k_c was adjusted as required for each event, as documented in Appendix F and is further discussed below. To ensure adjustments were not completely ‘random’, the maximum IL such that the CL remained zero or greater was identified. While not the defining parameter for every event, it was a useful indicator to narrow the range suitable k_c values.

It is recognised that the order the events were considered had the potential to somewhat affect the calibration outcomes. This is an accepted limitation of the manual calibration method provided in RORB, which does not have the capacity to automatically compute optimal parameter values for a single event, let alone across multiple events considered simultaneously.

The lateral displacement between the calculated and observed hydrographs was another notable aspect of the calibration. In some instances, the observed hydrograph shape was closely replicated by the calculated hydrograph, but the timing difference between them was significant, as exemplified in Figure 3.16 for the January 2013 event.

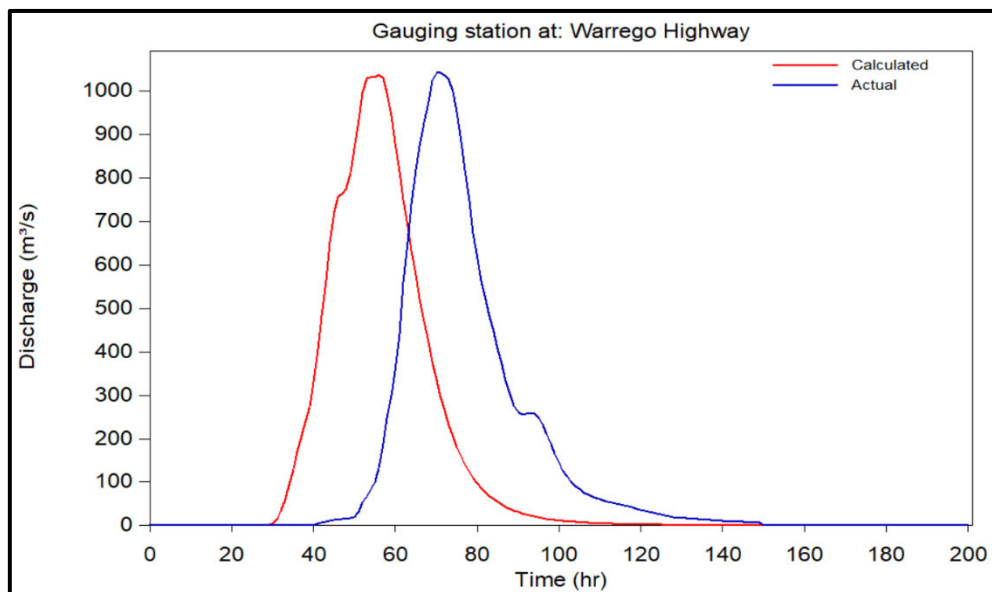


Figure 3.16: Lateral separation between calculated and observed hydrographs for January 2013 event

The potential for timing issues in catchments with very flat lower reaches was addressed in section 7.2.6 of the RORB User Manual by Laurenson, Mein and Nathan (2010), who recommended the insertion of event specific translations into the model to resolve such issues. For the events that experienced timing issues, a specified time delay was incorporated along a final arbitrary stream reach of zero length in the catchment file, which resulted in minimal separation between the hydrographs.

The majority of the events analysed for calibration were deemed suitable and the spread of parameter values was narrow. The calibration obtained for each event is expanded on below.

3.4.3.1 Calibrated events with closely replicated peak flows

a) November 2008: $k_c = 34$ & IL = 77 mm (with 4 hour delay translation)

The singular discharge peak magnitude, shape and timing was closely correlated to observed data. The peak discharge was the second lowest analysed, potential for event k_c to be less representative of higher magnitude flows (rainfall was atypically low in upper catchment).

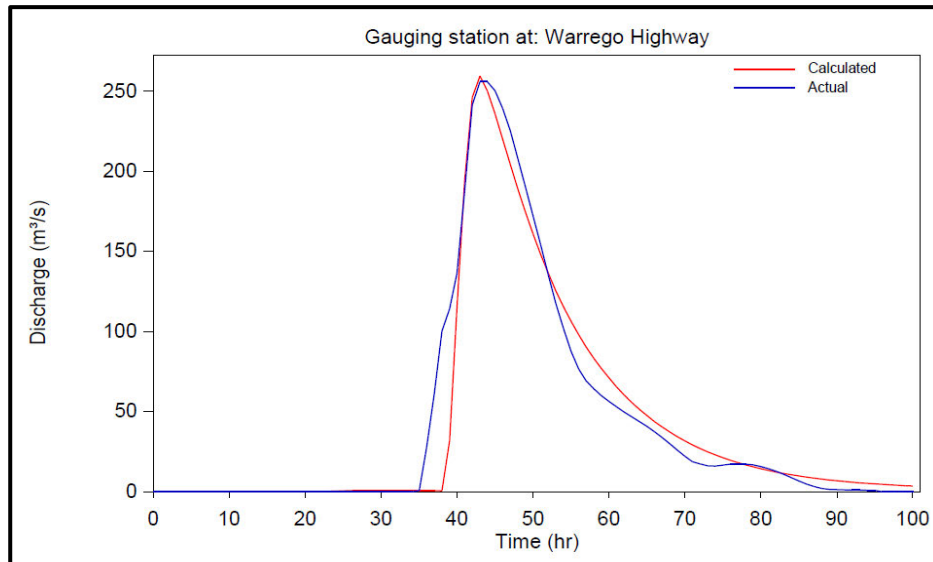


Figure 3.17: Calibrated hydrograph for November 2008 event

b) January 2011: $k_c = 26$ & IL = 9 mm

The final runoff peak closely aligned with the observed data. The magnitude and shape of the preceding peaks was generally replicated (except the peak immediately prior to the event maxima) however timing was approximately 10 hours earlier than observed.

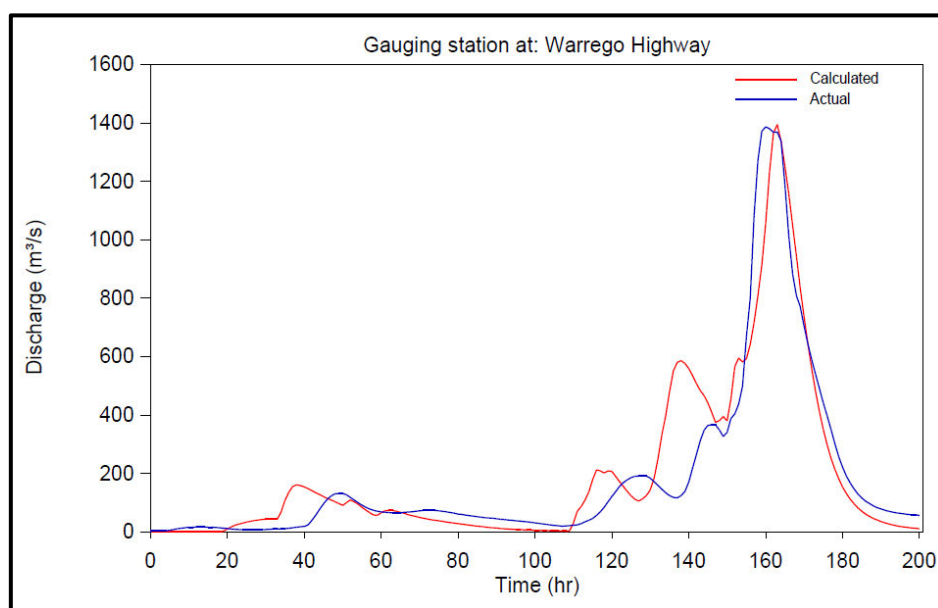


Figure 3.18: Calibrated hydrograph for January 2011 event

c) January 2013: $k_c = 30$ & IL = 60 mm (with 20 hour delay translation)

The calibration achieved for the January 2013 event was the closest of the three significant events (peak flows greater than 1000 m³/s). The hydrograph shape, especially the slopes of the rising and falling limbs, corresponded very closely to the observed data, however the timing of the singular peak was slightly delayed.

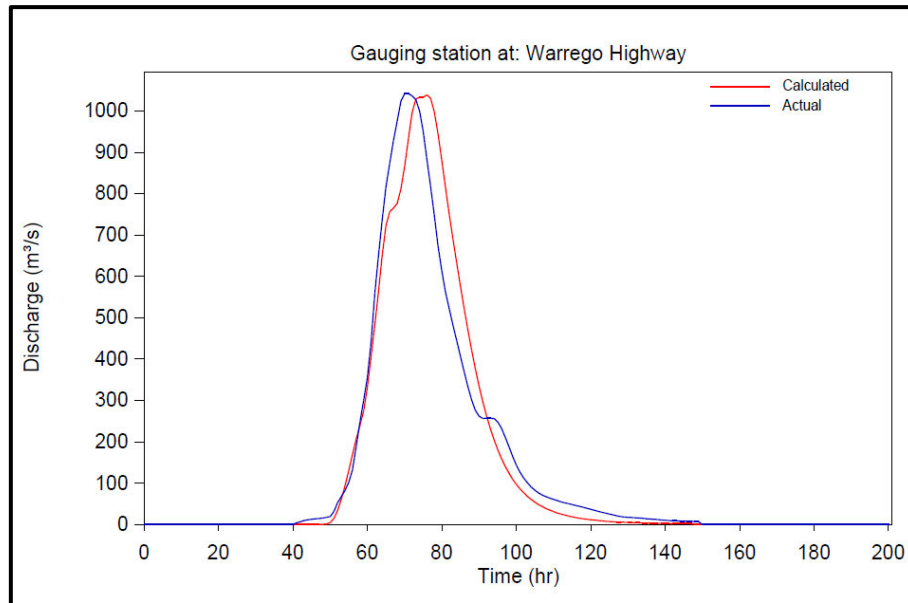


Figure 3.19: Calibrated hydrograph for January 2013 event

d) March 2017: $k_c = 23$ & IL = 107 mm (with 4 hour delay translation)

This event had a very similar magnitude to the November 2008 peak, and the hydrograph peak magnitude, shape and timing was also very closely correlated to the observed data. Rainfall in the lower subcatchments was low. Potentially k_c is also less representative of higher flows.

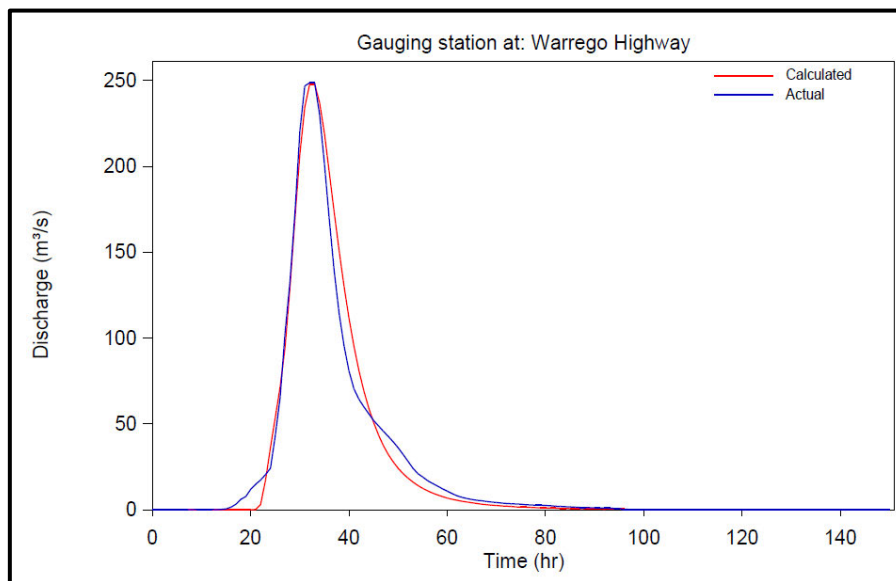


Figure 3.20: Calibrated hydrograph for March 2017 event

e) February 2022: $k_c = 29$ & IL = 142 mm

The timing and magnitude of the peak discharge was well calibrated. The shape of the 100 hour recession curve was somewhat replicated. The calculated hydrograph overestimated several observed local maxima followed by an underestimation of the final falling limb.

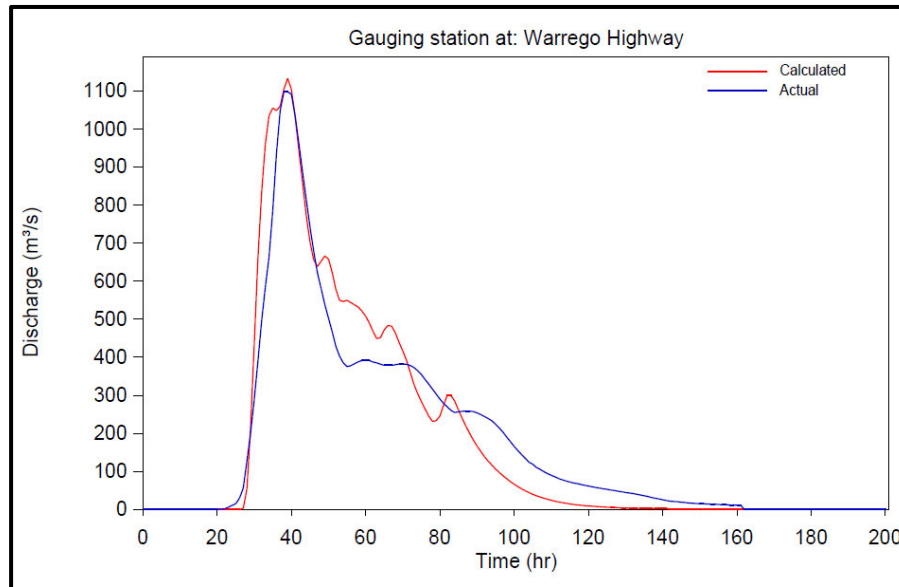


Figure 3.21: Calibrated hydrograph for February 2022 event

f) January 2024: $k_c = 28$ & IL = 39 mm (with 12 hour delay translation)

The magnitude and shape of the larger hydrograph peak was suitably approximated by the calculated hydrograph. The timing of both distinct peaks was also replicated. The smaller peak was slightly overestimated while the first recession curve was subsequently delayed. A dual burst rainfall model may have improved the calibration, however it was satisfactory regardless.

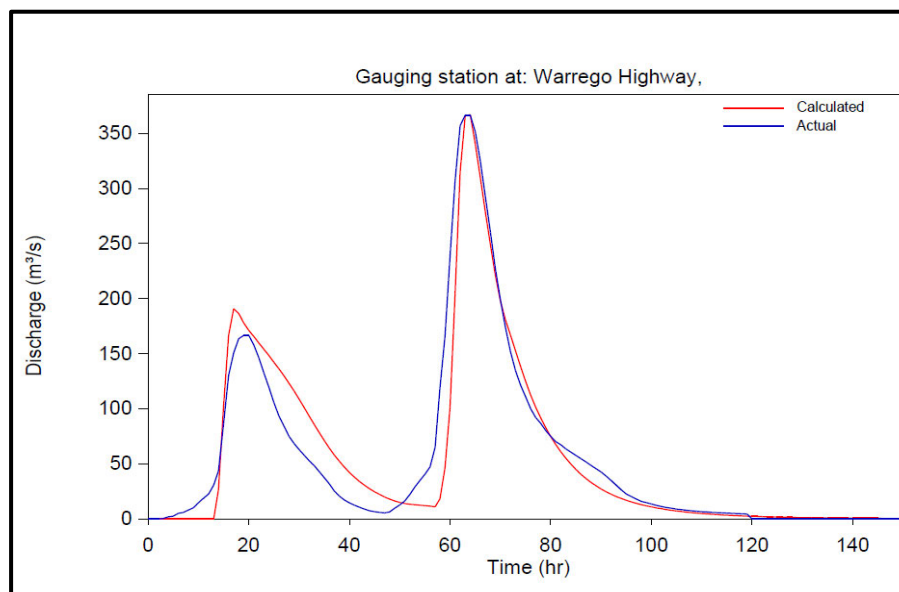


Figure 3.22: Calibrated hydrograph for January 2024 event

3.4.3.2 Problematic or uncertain calibration events

a) May 1996: $k_c = 26$ & IL = 100 mm (with 15 hour delay translation)

The oldest event analysed had two distinct flood peaks of similar magnitude that remained effectively stable for 16 to 18 hours each as a result of two separate rainfall bursts. The extent of the observed peaks were unable to be replicated by any combination of k_c and IL. While the magnitude of the first peak was somewhat similar, the second calculated peak was significantly higher when the remainder of the hydrograph was relatively well calibrated. The error between the calculated and observed peak discharge resulting from the second rainfall burst was 26.5%.

Upon inspection of the hourly streamgauge record, the peak flow readings were graded as code 60 'estimates' which indicated the readings were unreliable. This explanation is reasonable given the flows experienced during the May 1996 event were the highest observed since the site had opened in 1991. Hence no previous gaugings existed of the maximum flows experienced in May 1996 and the rating curve was poorly defined. It is plausible the actual streamflow hydrograph replicated the calculated hydrograph however this cannot be proven or demonstrated.

Otherwise, the complex hydrograph shape and timing encompassing two significant peaks and multiple local maxima was rather well replicated and the k_c value of 26 will be considered as reasonable with caution.

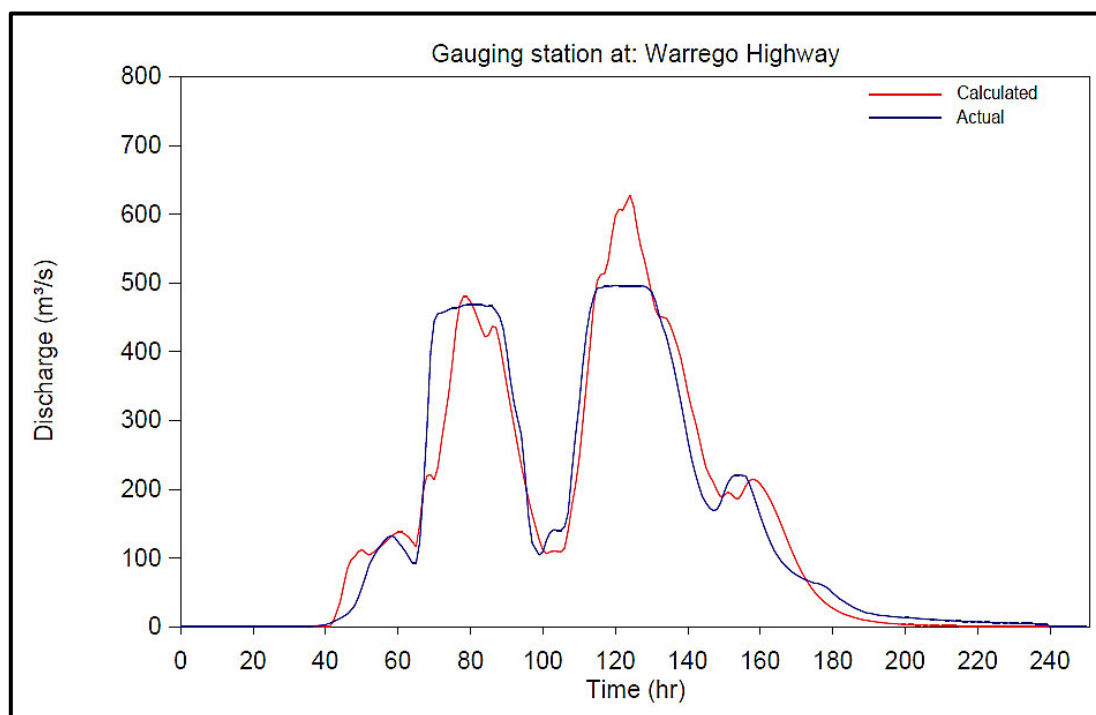


Figure 3.23: Calibrated hydrograph for May 1996 event

b) May 2022: $k_c = 41$ & IL = 0 mm

Compared to every other event, the May 2022 event required a significantly higher value of k_c to obtain a satisfactory calibration. A lengthy recessional tail period was observed in the hydrograph as continuous yet insignificant rainfall was experienced in the days following the maximum recorded discharge.

For a constant k_c value, as the IL depth was reduced, the calculated hydrograph peak also reduced and was more closely aligned towards the observed data. However, for k_c values considered for other events (between 25-35), the calculated maximum discharge still significantly exceeded the observed record when IL was minimised (set to zero) and the hydrograph shape was inaccurate. Therefore, the value of k_c was increased until both the maximum discharge and hydrograph shape were closely aligned to the observed data. This meant a k_c value of 41 was adopted for this event, which when applied to the remaining seven events, resulted in multiple unsatisfactory calibrations.

Hence this event was considered unrepresentative of the general catchment response to extreme rainfall, and the value of $k_c = 41$ was deemed an outlier.

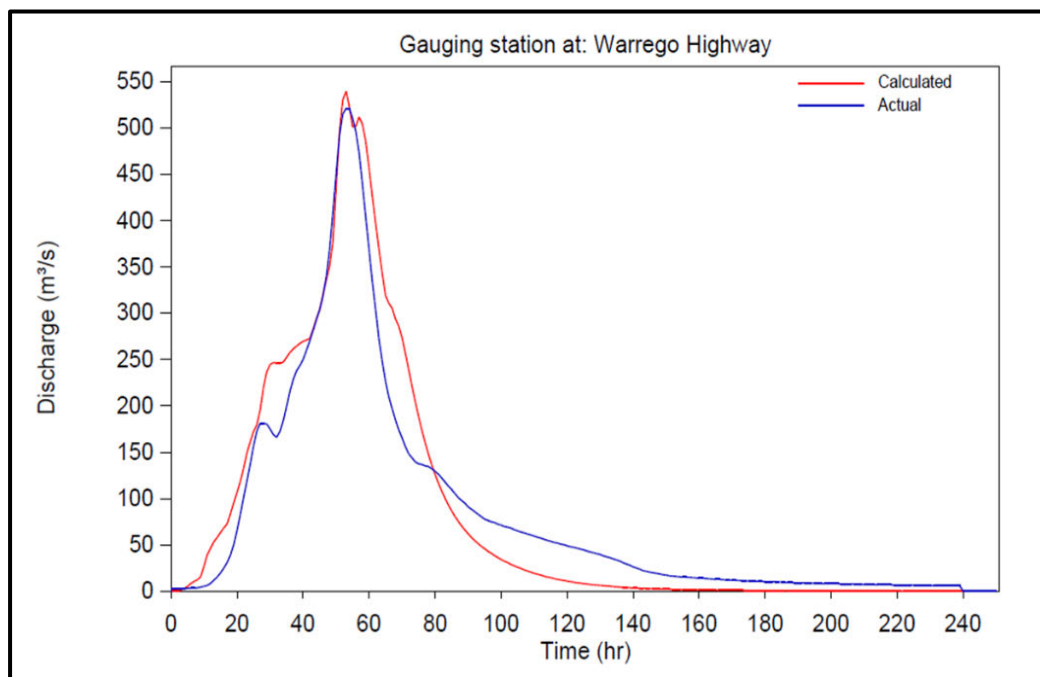


Figure 3.24: Calibrated hydrograph for May 2022 event

Because eight events covering an adequate range of durations and flow magnitudes were analysed, if one or two events were deemed unsuitable, a sufficient number of events were still calibrated to verify the accuracy of the chosen parameter values.

The selected event parameter values are summarised in Table 3.3. The mean and median value of k_c was calculated as 27. Because the same value was obtained for both measures of central tendency, $k_c = 27$ was settled upon as the calibrated value for the Laidley Creek catchment.

Table 3.3: Best-fit and average parameters for RORB calibration events

Event	k_c	IL (mm)	CL (mm/h) [computed]
April - May 1996	26	100	2.66
November 2008	34	77	9.78
January 2011	26	9	3.18
January 2013	30	60	0.94
March 2017	23	107	0.65
February 2022	29	142	0.03
May 2022 *	41	0	1.09
January 2024	34	39	5.52
Mean	27	* Indicates omitted outlier	
Median	27		

3.4.4 Design discharge simulations for current and future climate conditions

Following successful calibration of the catchment k_c parameter, the design discharge estimates were obtained using the runoff routing simulation method. The RORB DESIGN specification was used to estimate design event discharge quantities in conjunction with several design storm files. These files consisted of the ARR Datahub .txt file, the areal temporal pattern .csv file and an IFD .csv file for each climate scenario, as attached in Appendix D, E and C respectively.

Another limitation of the RORB package was that a singular set of IL and CL values had to be specified for the design simulation, despite Table 3.3 demonstrating a wide range of values were used to calibrate the catchment response to different antecedent conditions. Although a stochastic distribution about an assigned IL value can be enabled using the Monte Carlo simulation method, a singular known IL depth is still required to begin this process. The regionalised median IL and CL depths of 25 mm and 1.40 mm/hr respectively, as specified in the ARR Datahub file, were automatically assigned as the RORB simulation losses.

As the catchment area was larger than 75 km², an areal temporal pattern file was specified in the RORB input. The patterns were sorted by catchment area at discrete intervals. In this instance, RORB considered the 500 km² areal temporal patterns as closest to the catchment area of 452 km². Because areal patterns were used, the number of modelled events for each AEP was reduced from 25 IFD durations to ten events between 12 and 168 hours. Two alternate simulation methods of design discharge estimation were evaluated: Ensemble simulation and Monte Carlo (MC) simulation. The advantages and limitations of each approach are discussed below:

3.4.4.1 Ensemble simulation method

The Ensemble simulation method separately routed catchment runoff from ten temporal distribution patterns for each design event AEP between 50% and 1%, and duration between 12 and 168 hours. The set of ten simulations for the 5% AEP, 48 hour event are presented as an example in Figure 3.25. The median peak discharge from the set of ten is considered the peak flow estimate. Once repeated for all event durations, the maximum-median peak flow across all durations was considered the critical discharge estimate for a specific AEP.

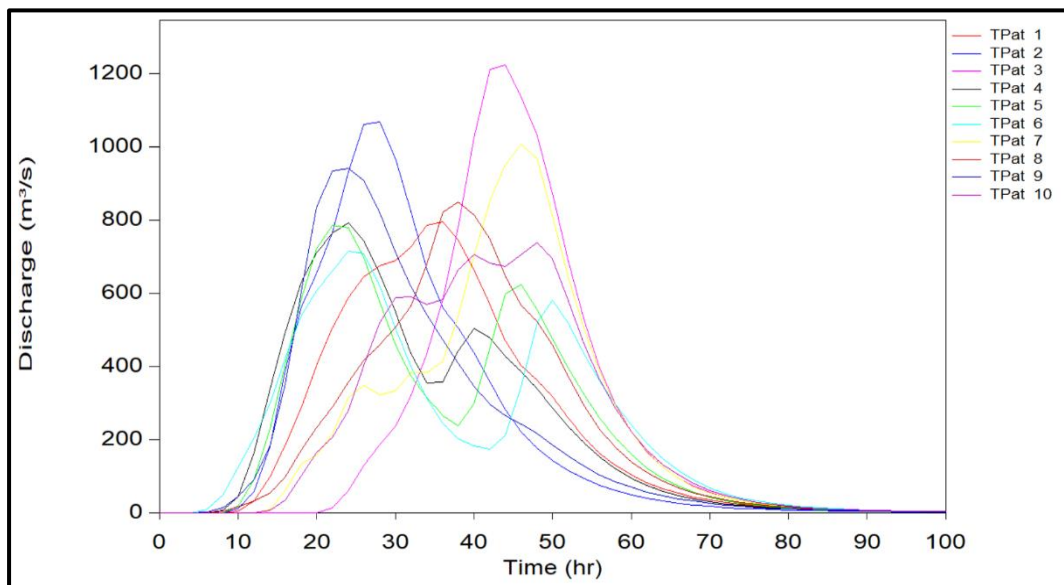


Figure 3.25: 5% AEP, 48 hour Ensemble simulation event hydrographs

The main advantage of the Ensemble method is the ability to easily demonstrate the range and extent of uncertainty in the results (through a quartile box and whisker plot). Operationally, the method had near-instantaneous simulation processing times and the generated results were able to be reproduced on separate occasions. However, the ensemble method is restricted to considering only the ten current temporal patterns and a singular IL depth.

3.4.4.2 MC simulation method

The RORB MC simulation method uses stratified sampling to derive a runoff frequency curve across a defined range of probabilities for each storm duration. Compared to the Ensemble method, the MC method maintains probability neutrality of the inputs by considering a stochastic distribution of the naturally variable processes that influence runoff generation. Therefore, the MC method was selected as the preferred simulation method for this project.

The frequency range was uniformly divided into intervals from which stochastically sampled rainfall depths were routed through the catchment file to generate a set of peak discharge values (Laurenson, Mein & Nathan 2010). The simulated results of each interval were statistically analysed to estimate the probabilistic runoff frequency curve. This procedure was repeated for each specified event duration to constitute one simulation, as illustrated in Figure 3.26. The event corresponding to the maximum discharge for a given AEP was considered the critical duration event.

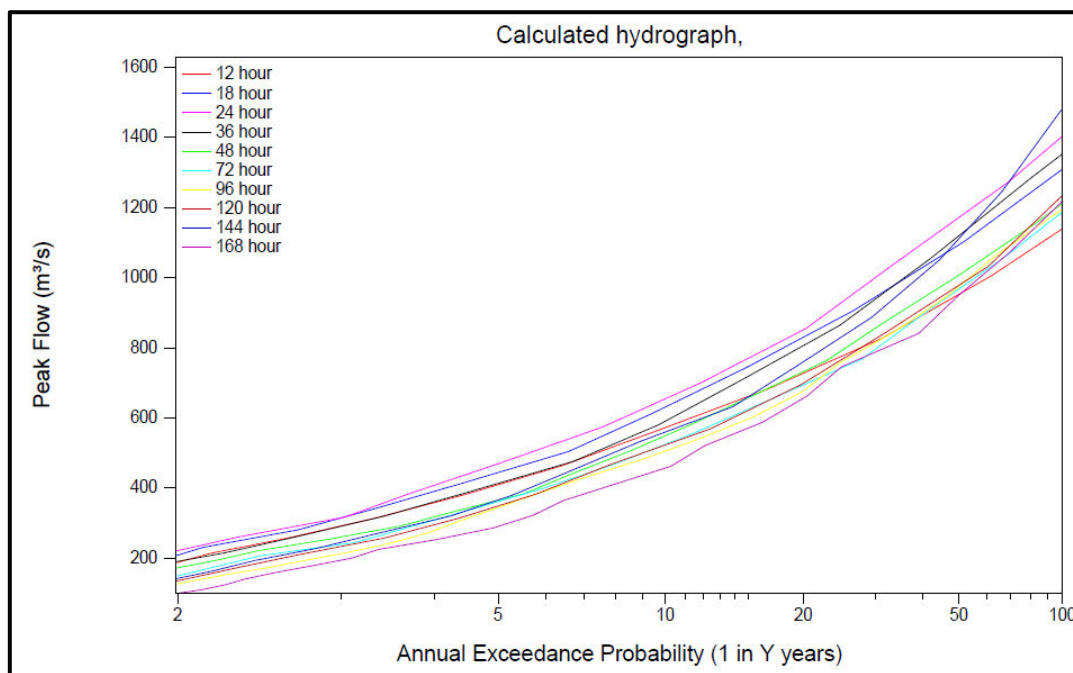


Figure 3.26: Sample set of runoff frequency curves generated from MC simulation

The model default settings of 20 stochastically sampled rainfall and IL depths simulated across 50 event frequency intervals to produce 20 flows per interval were retained as recommended in section 8.5 of the RORB User Manual by Laurenson, Mein and Nathan (2010). The nature of an MC simulation means that the results of each execution are unique. Therefore, to assess the variability of the outputs, 10 trial simulations were executed for each of the 7 climate scenarios (current and 6 future) to determine the median peak flow associated with the design

AEPs. Each simulation took between 30 and 60 seconds to execute, so modelling was restricted to 70 simulations as a balance between output result accuracy and available resources. The results are presented in chapter 4 of this report.

3.5 Bayesian Flood Frequency Analysis

Technical guidelines published by DTMR stipulate that where a streamgauge is situated in close proximity to state controlled road infrastructure, “design discharges should be calibrated (with) FFA at the gauge location if sufficient recorded data exists” (2024c). The Laidley Creek at Warrego Highway (143229A) gauge has a 33 year streamflow record, of which the AM discharge series is plotted in Figure 3.27. The relatively short gauge operating period was identified as a significant limitation of the results of an FFA.

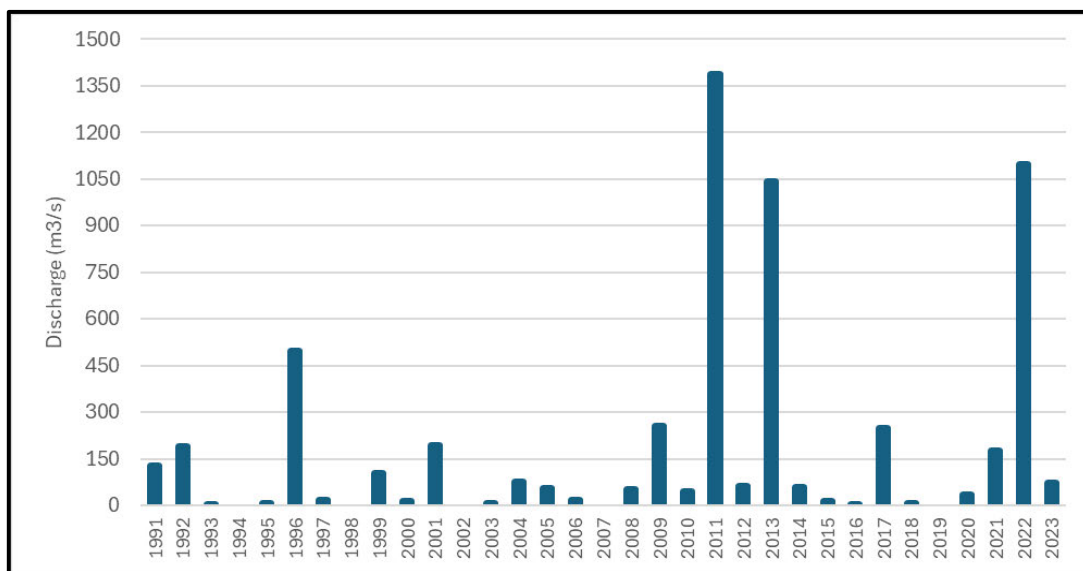


Figure 3.27: 143229A annual maximum discharge series 1991 – 2023.

The RMC-BestFit (RMC) Bayesian estimation and distribution fitting software package developed by the US Army Corps of Engineers and Institute for Water Resources (2024) was used to undertake an FFA at 143229A. While the TUFLOW FLIKE package is more commonly used to determine flood frequencies from historic data, including throughout Book 3 of ARR 2019, Ball et al. (2019) clarified that alternative software packages were acceptable for use, if applied appropriately to the modelling scenario. An annual licensing fee is associated with the TUFLOW package, therefore RMC was chosen for this study as a free option while still possessing sufficient modelling capabilities. The RMC package utilises an interactive platform to conduct a three-stage modelling approach. The software quickly processes large quantities of input data to produce both graphical and tabulated outputs. RMC is an ideal approach to efficiently undertake a FFA for this research project.

3.5.1 Initial plotting position from annual maximum series

The maximum discharge for each water year was required for analysis. The commencement of a water year corresponds to the calendar month with the lowest average flow across the 33 year record. For the 143229A gauge, August had the lowest average monthly flow of 0.1985 m³/s. Therefore, the preceding August to the current July was considered one water year. For example, the period spanning August 2008 to July 2009 was considered the 2009 water year.

Once the AM series was inputted to the RMC package, the Cunnane plotting position of each discharge was automatically computed. Alternative plotting position parameters can also be adopted. The Multiple Grubbs-Beck low outlier test is an optional measure to identify and exclude potentially influential low flows (PILFs), as recommended in Book 3, Section 2.8.6 of ARR 2019 (Ball et al. 2019). The test is required to enable the selection of some distributions that are not compatible with PILF gaugings. The rationality of this results yielded by executing this test will be evaluated given the relatively low operational period of the streamgauge.

The RMC input data interface and the subsequently generated plotting position graph of discharge against AEP for gauge 143229A are shown in Figure 3.28.

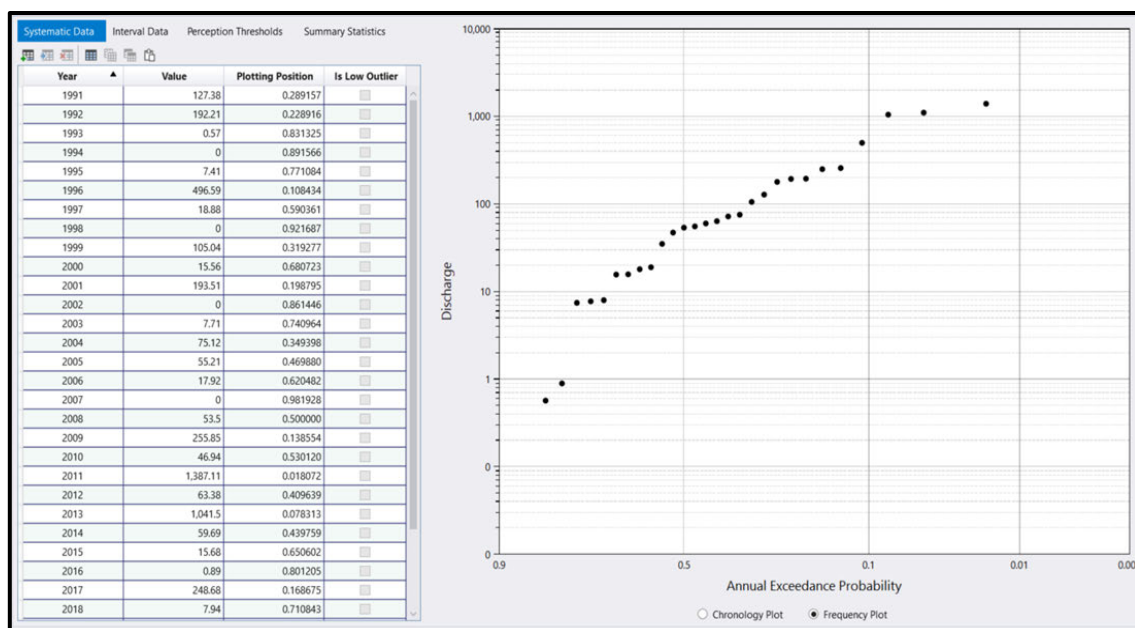


Figure 3.28: 143229A Laidley Creek at Warrego Highway AM series input and plotting position graph generated in RMC-BestFit

3.5.2 Fitted distribution functions

The second component of the RMC analysis procedure involves fitting up to 13 distribution functions to the plotted input data by the maximum likelihood estimation (MLE) method. The location, shape and scale factors, the statistical moments, and the yield value for various AEPs

corresponding to each function are presented in an output results table. The closeness of each function along the AEP domain was qualitatively inspected through a visual comparison of the plotted distributions against the input data. RMC computed three objective functions as a quantitative measurement of fit for each distribution, namely:

- Akaike Information Criteria (AIC)
- Bayesian Information Criteria (BIC)
- Root-Mean Squared Error (RMSE)

The lowest value for each objective function represents the distribution with the best fit to the input data (US Army Corps of Engineers & Institute for Water Resources 2024). Considering these metrics, in combination with a qualitative judgement of the closeness of the fit, the most suitable distribution function is identifiable. In this instance, the LP3 distribution produced the lowest RMSE of 109.40, the fifth lowest AIC and BIC ratings, and by visual inspection, appeared to effectively represent the full spread of gaugings. As such, the findings of Rahman et al. (2013) regarding the performance of the LP3 distribution are validated for the Laidley Creek catchment. The Weibull and Gamma distributions also perform well, ranking highly in terms of AIC and BIC rating; and second and third respectively in terms of RSME. Other distributions failed to perform as highly against all metrics. Because the Weibull and Gamma distributions have comparable performance to the LP3 distribution, as illustrated in Figure 3.29, all three distributions will be individually modelled using Bayesian parameter estimation.

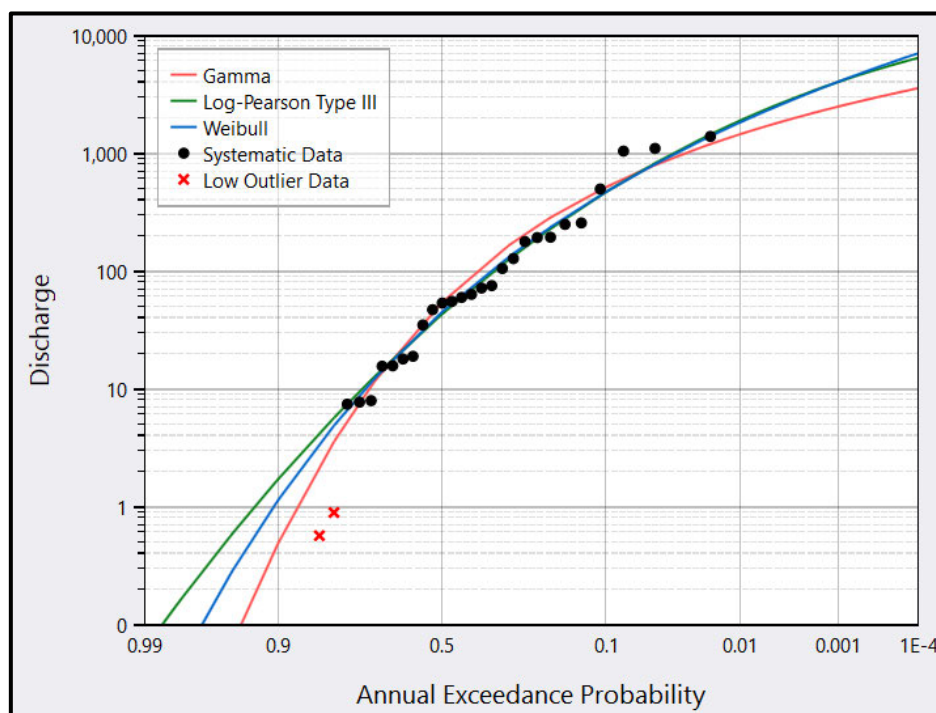


Figure 3.29: LP3, Gamma and Weibull distributions fitted to AM series with outlier flows identified

3.5.3 Bayesian parameter estimation

The final phase in the RMC modelling procedure is the Bayesian parameter estimation analysis, which is undertaken through a reiterative Markov Chain MC simulation (US Army Corps of Engineers & Institute for Water Resources 2024). The input data from step one, the three distributions from step two (once-at-a-time), and the desired parameter distribution were considered by RMC to generate 10,000 distribution parameter sets in approximately eight seconds, which converge to parametric distributions for mean, skew and standard deviation instead of a singular value of each in step two. The parametric and quantile distributions can be refined based on regionalised flood data (Smith & Doughty 2020), however, in the absence of such data, these options were kept within the default domains of the software package.

The parameters with the most frequent recurrence were identified by RMC as the posterior mode parameters, which form the posterior mode function (in the same arrangement as the parent distribution function). The uncertainty in the generated parameter sets is characterised by the 95% confidence intervals about the posterior function, as shown in Figure 3.30. It was observed that as AEP increased beyond the interpolated zone of gauged data, the confidence intervals increased significantly, emphasising the uncertainty of the estimations.

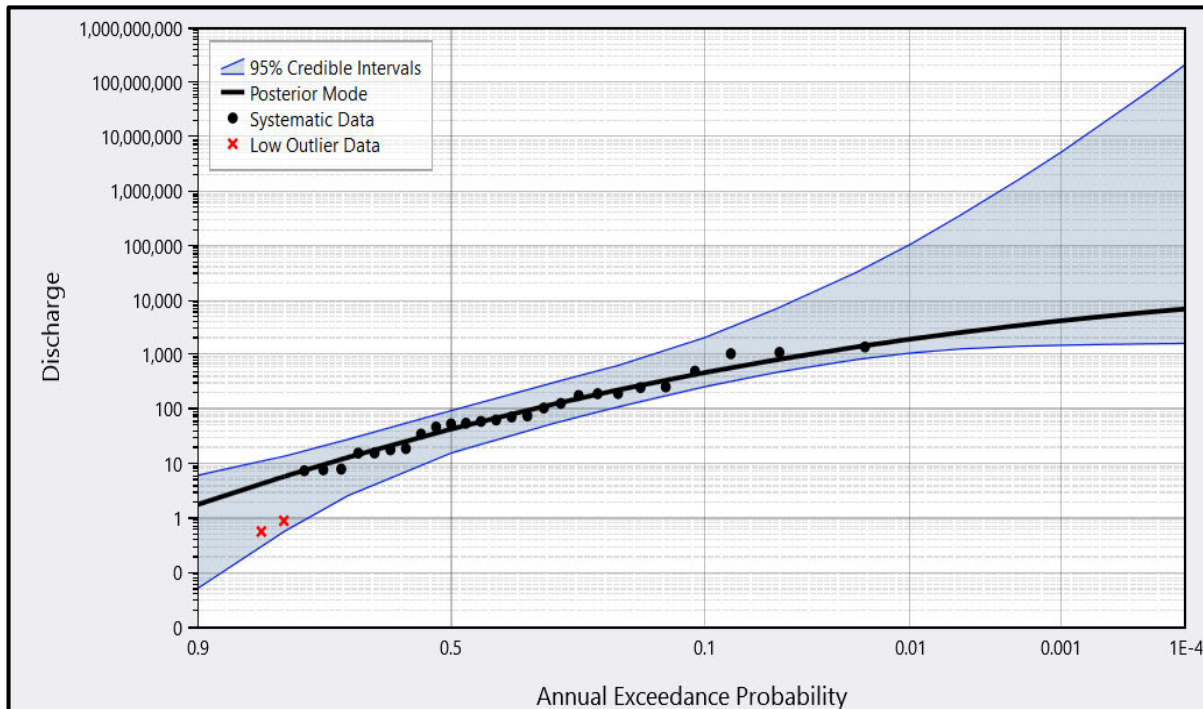


Figure 3.30: Posterior mode and confidence intervals of the Bayesian parametric estimation method for the LP3 distribution

3.5.4 FFA design discharge results

The discharges corresponding to the posterior mode frequency curve for each fitted distribution are presented in Table 3.4, while full outputs from RMC are included in Appendix I. It is intended that the simulated runoff routed discharges for the current climate scenario will be compared to the FFA results.

Table 3.4: Posterior mode FFA discharges (m³/s) for suitable distributions

AEP (%)	LP3	Gamma	Weibull
50	42.91	54.40	45.04
20	223.55	282.02	233.65
10	465.77	514.93	470.48
5	802.04	775.95	786.87
2	1386.27	1147.58	1325.57
1	1925.76	1442.20	1823.29

It is likely the Gamma function estimates are most representative of the true catchment characteristics, however this prediction will be assessed in the simulation sanity verification. It was intended for the FFA discharges to be compared to the current climate discharges estimated from the RORB simulations. However, the accuracy of the FFA method is limited by the 33 year streamgauge record, which inherently is reflective of recent events rather than the extended site flood history. A longer spanning AM series record would provide a more accurate representation of likely flood quantiles – a 33 year record has limited accuracy when considering a 1 in 100 year event. These inaccuracies are demonstrated by the significant discrepancies between the design discharges of the three functions.

3.6 Regression methods of peak flow estimation

The RFFE and P&W methods introduced in the literature review are simple peak flow estimation techniques which provide comparisons to the simulated routed discharges. The application of these methods to the Laidley Creek catchment are described below.

3.6.1 RFFE method

The RFFE method is incorporated into an online modelling tool titled RFFE Model – 2016 Release Version (Rahman et al. 2015). The RFFE model was used to generate discharge estimates for the 50%, 20%, 10%, 5%, 2% and 1% AEPs. The following user stipulated catchment attributes were required for the model to generate the estimates:

- Site name or ID
- Outlet latitude and longitude (in decimal degrees)
- Centroid latitude and longitude (in decimal degrees)
- Area (in km²)

An initial RFFE computation was executed using the corresponding catchment parameters previously determined. The centroid location was determined in QGIS from the polygon centroid execution. RFFE approximated the catchment shape as an ellipse configured about the centroid and outlet locations, as shown on an interactive map reproduced in Figure 3.31. The blue shading indicated that the shape factor of the catchment is appropriate (rather than being too narrow or irregularly shaped) such that the method is within its limits of accuracy.

The model generated discharge estimates for the six design AEPs based upon regionalised LP3 distribution parameters (Rahman et al. 2015). However, the regionalised parameters are likely unrepresentative of the Laidley Creek catchment because of its atypical topographical attributes (compared to the surrounding East Coast region) that cause significant variance in the distribution and quantity of rainfall received. To overcome this issue, the RFFE ‘Nearby’ spreadsheet containing details of surrounding gauged catchments was downloaded and inspected. The distances between the user inputted catchment (Figure 3.31) and surrounding gauged catchments used to originally formulate the RFFE method are included in this spreadsheet. The Laidley Creek catchment at the 431229A station was one such catchment used as indicated by the nearest gauge distance of 0.21 km.

Input Data

Basic Advanced

Catchment Name
Laidley Creek

Catchment Outlet Latitude
-27.555

Catchment Outlet Longitude
152.3883

Catchment Centroid Latitude
-27.7266

Catchment Centroid Longitude
152.357

Catchment Area (km²)
462

Submit

Zoom to Catchment

Map labels: Cabarah, Highfields, Toowoomba, Gatton, Laidley, Marburg, Rosewood, Ipswich, Harrisville, Boonah, Clifton, Main Range National Park, D'Aguilar National Park, Lockyer Valley Regional, Lowood, Fernvale, Marburg, Rosewood, Ipswich City, AS, Bk, Leaflet | © OpenStreetMap contributors

Figure 3.31: RFFE input tool for 143229A catchment characteristics

Discharge data sourced from a gauged catchment and adopted for the development of the RFFE method was subjected to multiple-stage processing and validation measures (Rahman et al. 2015). Therefore, this data is considered significantly more reliable than the equivalent regionalised model output. On the basis of these considerations, the estimated design discharges for the catchment were extracted directly from the existing gauged dataset and are listed in Table 3.5

Table 3.5: 143229A discharges estimates from RFFE method

AEP (%)	Discharge (m ³ /s)
50	47.15
20	209.72
10	402.95
5	661.58
2	1110.63
1	1535.72

3.6.2 P&W method

The P&W method of discharge estimation for rural Queensland catchments reduced the number of input parameters required (in comparison to RFFE) to only the catchment area and the 2% AEP, 72-hour duration design rainfall intensity at the catchment centroid. The peak discharge estimates for six ARIs ranging from 2 to 100 years at the 143229A gauge for the current climate scenario were calculated from the P&W equations listed as Equation 3.1-3.6:

$$Q_2 = 0.122 \times A^{0.757} \times i72h50y^{1.588} \quad (3.1)$$

$$Q_5 = 0.664 \times A^{0.709} \times i72h50y^{1.301} \quad (3.2)$$

$$Q_{10} = 1.419 \times A^{0.682} \times i72h50y^{1.174} \quad (3.3)$$

$$Q_{20} = 2.547 \times A^{0.673} \times i72h50y^{1.074} \quad (3.4)$$

$$Q_{50} = 4.731 \times A^{0.656} \times i72h50y^{0.968} \quad (3.5)$$

$$Q_{100} = 7.031 \times A^{0.644} \times i72h50y^{0.899} \quad (3.6)$$

Where the catchment area $A = 462 \text{ km}^2$ and the current 72 hour, 2% AEP design rainfall intensity $i72h50y$ at the Laidley Creek catchment centroid = 4.733 mm/hr (equivalent event rainfall depth from BOM-LIMB IFD envelope of 340.8 mm).

Table 3.6: 143229A discharge estimates from P&W method for current climate

ARI (years)	AEP (%)	Discharge (m³/s)
2	39.25	149.83
5	18.13	388.82
10	10	577.93
20	5	840.29
50	2	1192.59
100	1	1479.09

The numeric form of Equations 3.1-3.6 meant that the increased rainfall intensities for the future climate scenarios could be directly substituted to predict the future design discharges. The updated i72h50y intensities ranged between 5.207 and 6.485 mm/hr. This approach assumed that the distributions and relationships on which the P&W were originally derived from remain applicable for the increased rainfall intensities of future scenarios, however, this assumption has yet to be validated. Therefore, the results obtained were considered as limited provisional indications. The future climate scenario discharge estimates from the P&W equations are listed in Tables 3.7 and 3.8, and as projected, reflected significant increases.

Table 3.7: 143229A discharge estimates (m³/s) from P&W equations - RCP 4.5 scenarios

AEP (%)	2030	2050	2090
39.25	174.35	184.50	200.20
18.13	440.22	461.11	493.02
10	646.45	674.07	716.02
5	930.99	967.31	1022.23
2	1308.01	1353.91	1423.01
1	1611.59	1664.05	1742.79

Table 3.8: 143229A discharge estimates (m³/s) from P&W equations - RCP 8.5 scenarios

AEP (%)	2030	2050	2090
39.25	176.87	194.86	247.05
18.13	445.43	482.22	585.69
10	653.34	701.86	836.43
5	940.06	1003.72	1178.43
2	1319.49	1399.77	1617.59
1	1624.72	1716.33	1963.07

3.7 Research methodology evaluation

The finalised research methodology represents a culmination of several refinements as each modelling aspect was developed, whilst ensuring the scope remained viable despite time and resource constraints. The availability and applicability of sourced data was delicately evaluated against modelling recommendations introduced in the literature review, including ARR 2019, DTMR guidelines and the RORB User Manual, to ensure the finalised model represented the physical hydrologic properties of the Laidley Creek catchment as accurately as possible. Any necessary assumptions and simplifications of these complex characteristics were justified. Alternative modelling approaches were investigated at several stages throughout the methodology, including the automatic catchment delineation method, the continuous catchment simulation method of runoff estimation, and the Ensemble event-based method. In each instance, justifications to support the selection of the finalised method were provided.

Many aspects of the methodology are typical of best practices currently used in industry. This project considered the most recent climate change projections and guidance for hydrologic modelling provided by ARR 2019 and DTMR. Specifically, the IFD adjustment factors for the different RCP scenarios (Appendix C) and median surface temperature projections were released on the ARR Datahub on 27 August 2024 to coincide with the significantly revised ARR 2019 Book 1: Chapter 6 titled *Climate Change Considerations*. Similarly, the CCNHRA and associated engineering policies were published by DTMR in June 2024. With continuing advancements in research and understand, it is practically certain these methods, guidelines and projections will be revised again in the future.

3.8 Summary

This research methodology presented a five-stage approach to quantify the implications of climate change scenarios on peak discharge hydrology within the Laidley Creek catchment. The reviewed background literature was synthesised to correspond with the project objectives and industry best-modelling practices to guide model development. Input data was obtained from relevant sources to formulate the catchment and storm event files. Eight historic peak rainfall runoff events were analysed to calibrate the RORB routing model parameter $k_c = 27$ for the Laidley Creek catchment. Discharge estimation methods were documented, including independent analytical and statistical methods, while the Ensemble and MC simulation methods were compared. The MC method was selected to generate the median design discharge estimates for the current and future climate scenarios, as presented in Chapter 4.

4. Results

The design simulation results for the current and future climate IFDs are discussed in this chapter. A sensitivity analysis of the simulated model parameter values was also completed.

4.1 Design discharge simulation for current climate conditions

The design routing simulation outlined in the previous chapter was first undertaken for current climate conditions by specifying the LIMB-BOM IFD envelope as the input design rainfall set. The calibrated catchment parameters $k_c = 27$, $m = 0.8$ (assumed fixed) and regionalised losses $IL = 25$ mm and $CL = 1.4$ mm/hr were specified. 10 sample simulations were executed, of which the median, minimum and maximum peak discharges for the six design AEPs between 50% and 1% are listed in Table 4.1. The median flows were adopted as the design discharge estimates. The full sample simulation outputs are attached in Appendix G.

Table 4.1: Simulated design discharges for current climate scenario (2020 envelope)

AEP (%)	Discharge (m ³ /s)		
	<u>Median</u>	Minimum	Maximum
50	223.0	210.4	233.7
20	467.1	457.6	482.2
10	661.9	649.4	676.5
5	868.4	833.7	888.0
2	1164.5	1149.4	1178.0
1	1411.4	1381.3	1479.9

The critical duration of each design AEP across the ten samples was the 24 hour event, except the 1% AEP, where for one sample simulation, the 144 hour event corresponded with the critical flow. In most sample instances the 144 hour event produced the second highest peak discharges.

As an indication of the uncertainty of the results, the inter-quartile and full ranges of simulated peak discharges for each AEP were represented as a proportion of the median flow. The full range varied between 2.4% for the 2% AEP event and 10.4% for the 50% AEP event. Similarly, the inter-quartile range varied between 1.3% for the 2% AEP event and 3.1% for the 50% AEP event. The extent of uncertainty associated with the 10 sample simulations for each design AEP is illustrated in Figure 4.1.

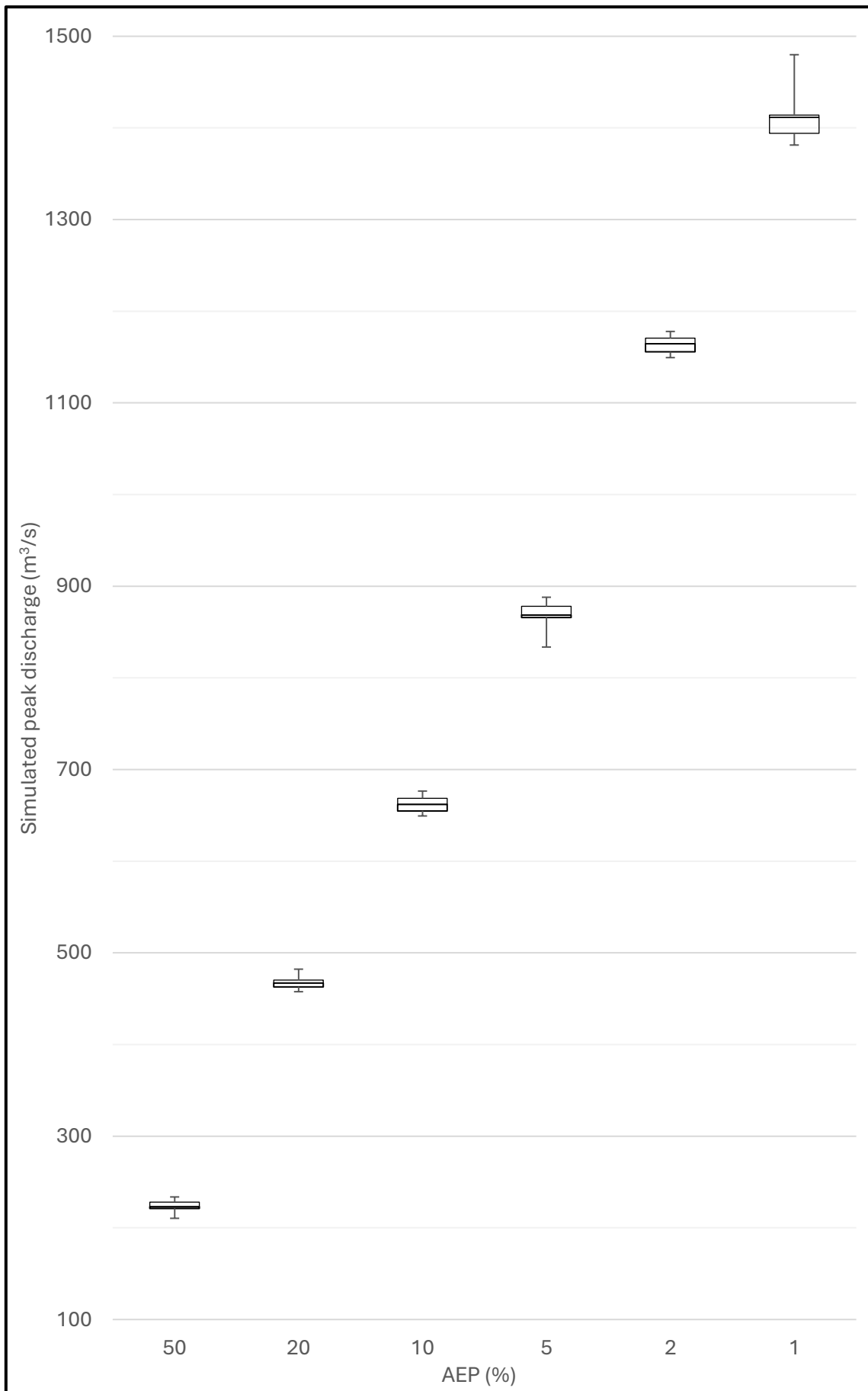


Figure 4.1: Distribution of MC simulated peak discharges for current climate scenario

4.2 Design discharge simulation for future climate scenarios

The design routing simulations were repeated for the six future climate projections each corresponding to a revised IFD file. The median peak discharges estimates for the RCP 4.5 scenarios are listed in Table 4.2 while estimates for the RCP 8.5 scenarios are listed in Table 4.3. Full simulation outputs are attached in Appendix G. The percentage increase compared to the corresponding median discharge for current conditions per Table 4.1 is also indicated.

Table 4.2: Simulated median discharge estimates for RCP 4.5 scenarios and percentage increase compared to current climate simulated median

AEP (%)	Discharge 2030 (m ³ /s)	Increase (%)	Discharge 2050 (m ³ /s)	Increase (%)	Discharge 2090 (m ³ /s)	Increase (%)
50	281.1	26	296.2	33	330.0	48
20	547.5	17	580.1	24	630.4	35
10	767.4	16	799.5	21	865.8	31
5	992.7	14	1044.5	20	1116.7	29
2	1315.1	13	1383.0	19	1483.7	27
1	1587.9	12	1659.5	18	1772.3	26

For the RCP 4.5 scenarios, the 24 hour event was the dominant critical duration. However, six of the 30 samples indicated that the critical duration of the 1% AEP event was 144 hours.

Table 4.3: Simulated median discharge estimates for RCP 8.5 scenarios and percentage increase compared to current climate simulated median

AEP (%)	Discharge 2030 (m ³ /s)	Increase (%)	Discharge 2050 (m ³ /s)	Increase (%)	Discharge 2090 (m ³ /s)	Increase (%)
50	280.3	26	320.0	43	431.5	94
20	555.5	19	614.9	32	780.9	67
10	779.5	18	842.5	27	1056.5	60
5	1010.4	16	1086.9	25	1341.2	54
2	1340.7	15	1446.6	24	1762.8	51
1	1612.4	14	1736.0	23	2096.3	49

For the RCP 8.5 scenarios, the 24 hour event was also the dominant critical duration. However, the critical duration of two of the 30 samples for the 1% AEP event was 144 hours. The 18 hour event was deemed critical for 16 of the 90 sample discharges across the 50%, 20% and 10% AEP events, which was progressively more prevalent by 2090.

Several trends were observed in the percentage increase in the median peak discharge of the Laidley Creek catchment compared to the current (2020 envelope) simulations. This percentage increase was larger across the RCP 8.5 events, which ranged between 14% and 94%, compared to the RCP 4.5 events, which ranged between 12% and 48%.

Rarer events (lower AEP) were observed to have a reduced percentage increase compared to more frequent events. The 50% AEP events experienced a significantly larger percentage increase compared to all other design events. Events of an earlier projection year had a reduced percentage increase compared to the longer term projections. In summary, the observed trends generally align with the relationships between the individual IFD adjustment factors included in Appendix B.

The uncertainty in the results was also considered at the design event level across the current and future climate simulations. The increased simulated peak discharge for the 1% AEP event until 2090 as a result of the RCP 8.5 emissions scenario is illustrated in Figure 4.2. The inter-quartile and full ranges about the median discharge of each year are also shown to demonstrate the uncertainty of the sample outputs. Similar figures for each design AEP and RCP scenario were produced and are attached in Appendix G.

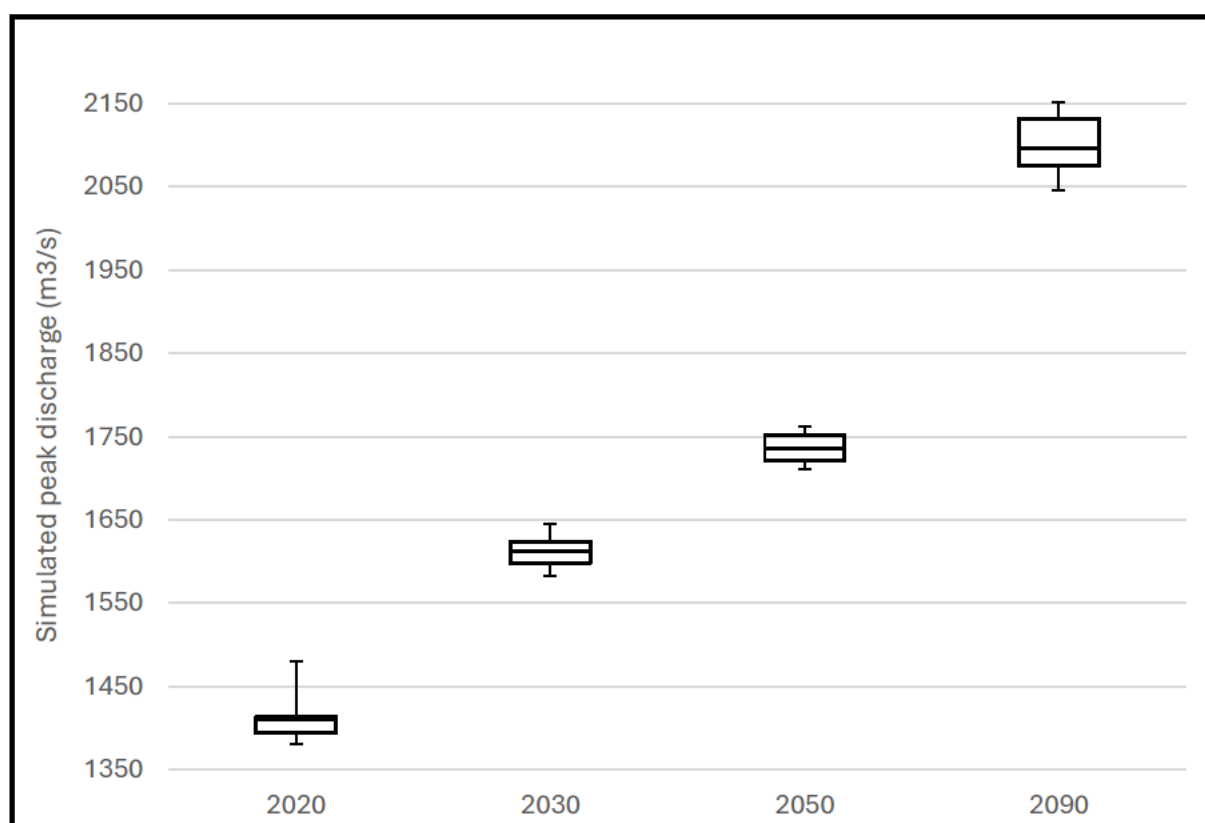


Figure 4.2: Distribution of sample 1% AEP event discharges for current IFDs and RCP 8.5 scenarios

A comparison of the RCP 4.5 and 8.5 emissions scenarios was also undertaken for each design event frequency. The increased peak discharges for the 1% AEP event until 2090 from both the RCP 4.5 and 8.5 scenarios (assuming a linear rate of change between simulated years) are shown in Figure 4.3. The full range of each sample set of outputs constituting a simulation is also shown. Similar figures for each design AEP were also produced and are attached in Appendix G.

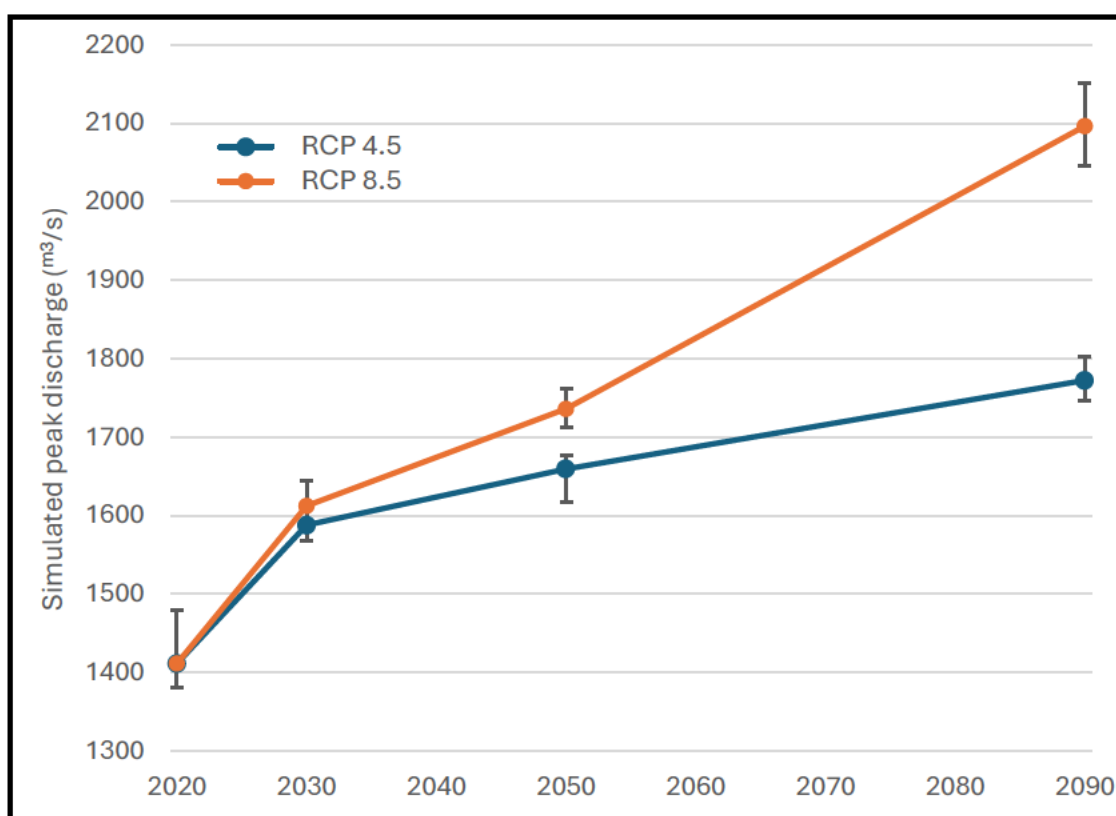


Figure 4.3: Median 1% AEP peak discharges for RCP 4.5 and 8.5 scenarios to 2090

Figure 4.3 shows that a similar rate of increase is projected until 2030 for the 1% AEP event under both emissions scenarios. However, following 2030, peak discharges simulated for the RCP 8.5 scenario increased significantly more than those of the RCP 4.5 scenario. A similar trend was observed for the 2% AEP event.

No apparent trend was noted in the extent of sample uncertainty across Figures 4.1, 4.2 or 4.3.

4.3 Sensitivity analysis of the model parameters

An analysis of the model sensitivity was performed through a once-at-a-time adjustment of the input parameters. A parameter value was separately increased or decreased while the original values of the remaining parameters were preserved. The m parameter was assumed a fixed value of 0.8, therefore six separate adjustments were made. Five sample simulations were

executed for each adjustment, resulting in a total of 30 additional sample simulations being completed. The resultant changes in the median peak discharge of the design AEPs for the current climate model (Table 4.1) were evaluated in Table 4.4. The full outputs of the sensitivity analysis are included in Appendix H.

Table 4.4: Sensitivity analysis of model parameters – current climate simulation

RORB input parameter	Value for simulation	Once-at-a-time adjustment	Evaluation of model response to individual parameter adjustment
k_c	27	± 2.7 [10%]	<p>+10%: Average median discharge decreased by 7.4%. 1% AEP critical duration increased to 144 hours in four samples, 36 hrs in one sample. 24 hours for other AEPs.</p> <p>- 10%: Average median discharge increased by 7.9%. 50% AEP critical duration decreased to 18 hours in one sample. 24 hours for all other AEPs.</p>
m	0.8	Assumed fixed value for modelling of natural streams and channels per Laurenson, Mein and Nathan (2010).	
IL	25 mm	± 5 mm [20%]	<p>+20%: Average median discharge decreased by 5.8%. 1% AEP critical duration increased to 144 hours in one sample, 24 hours for all other AEPs.</p> <p>- 20%: Average median discharge increased by 3.8%. 20% AEP critical duration decreased to 18 hours in one sample. 24 hours for all other AEPs.</p>
CL	1.4 mm/hr	± 0.28 mm [20%]	<p>+20%: Average median discharge decreased by 4.6%. 1% AEP critical duration increased to 144 hours in one sample, 24 hours for all other AEPs.</p> <p>- 20%: Average median discharge increased by 5.1%. 1% AEP critical duration increased to 144 hours in one sample, 24 hours for all other AEPs.</p>

The sensitivity analysis demonstrated that the catchment storage parameter k_c was the most influential parameter on the results simulated, with the largest changes in output median discharge experienced when k_c was adjusted. The IL and CL depths had less impact on the model output despite being adjusted by a greater proportion of the originally simulated value. Adjustments of the parameters also varied the critical duration of some samples however the 24 hour event remained the dominant duration.

5. Discussion

This chapter examines the simulated design discharges in greater detail and considers the outputs in terms of the physical hydrologic processes of the Laidley Creek catchment. The validity of the simulated results was evaluated through comparisons to independent estimation techniques. The limitations associated with the model inputs, assumptions and capabilities were referenced to discuss the output limitations. Finally, potential improvements are suggested before the outputs are incorporated within a future 2D hydraulic investigation of the Warrego Highway bridge crossing of Laidley Creek.

5.1 Independent sanity validation of the results

The independent methods of discharge estimation introduced in the literature review and applied to the Laidley Creek catchment in the methodology were used as a comparison for the current and future simulated design discharges. It was recognised that results obtained from these methods are simply estimates, and only provide an indicative representation of catchment hydrologic characteristics.

5.1.1 Comparison of current design discharge simulation

FFA, RFFE and P&W methods were three independent approaches used to compare the simulation results of Table 4.1 for the current climate IFDs. The corresponding estimates obtained by each independent method and the percentage difference compared to the median simulated design discharges are listed in Table 5.1.

Table 5.1: Comparison of current climate simulation with independent estimates (m³/s)

AEP (%)	Median Discharge (Table 4.1)	FFA method		RFFE method		P&W method	
		Discharge	% Diff.	Discharge	% Diff.	Discharge	% Diff.
50	223.0	54.4	75.6	47.2	-78.9	Estimates not provided by method	
20	467.1	282.0	-39.6	209.7	-55.1		
10	661.9	514.9	-22.2	403.0	-39.1	577.9	-12.7
5	868.4	776.0	-10.6	661.6	-23.8	840.3	-3.2
2	1164.5	1147.6	-1.5	1110.6	-4.6	1192.6	2.4
1	1411.4	1442.2	2.2	1535.7	8.8	1479.1	4.8

The comparisons of Table 5.1 indicated that the less frequent events were aligned closer to the independent methods, improving the confidence in these simulations. In particular, the 2% and

1% AEP simulated discharges were within 5% of all three independent method estimates except for the 1% RFFE estimate, which differed by 8.8%. Confidence in the results of these events was identified as the most crucial aspect of the simulation, because the 2% and 1% AEP design discharges are the recommended flood immunity threshold flows for the Warrego Highway crossing of Laidley Creek, as introduced in the literature review.

For the more frequent events, the difference between the simulations and estimates increased significantly, especially for the 50%, 20%, and to a lesser extent, the 10% AEP events. Generally, the simulated discharges had the closest alignment to the P&W estimates, followed by the FFA gamma distribution estimates, which also yielded the closest correlation to the 2% and 1% AEP events. The RFFE estimates had the largest difference for all design events.

5.1.2 Comparison of design discharges for future climate scenarios

Of the three independent techniques, only the P&W method had the capability to estimate future discharges from the revised IFD sets. The primary limitation of this approach is that the P&W method cannot estimate the 50% and 20% AEP event discharges, which had the highest percentage differences identified in Table 5.1. These discharges cannot be estimated because the P&W equations were developed for the 1 in 2 and 1 in 5 ARIs, which do not correspond to the aforementioned AEPs per Figure 2.11. Therefore the 50% and 20% AEP discharges for future climate scenarios cannot be validated and should be treated with extreme caution.

The remaining simulated discharge events were compared with the estimates obtained from the P&W equations for the two RCP scenarios in 2030, 2050 and 2090 (per Tables 3.7 and 3.8) by calculating the corresponding percentage difference, as listed in Tables 5.2 and 5.3.

Table 5.2: Comparison of RCP 4.5 scenario simulations with P&W estimates (m³/s)

AEP (%)	Median Discharge (Table 4.2)			P&W method revised for RCP 4.5 scenario (Table 3.7)					
				2030	% Diff.	2050	% Diff.	2090	% Diff.
50	281.1	296.2	330.0	Estimates not provided by method					
20	547.5	580.1	630.4						
10	767.4	799.5	865.8	646.5	-15.8	674.1	-15.7	716.0	-17.3
5	992.7	1044.5	1116.7	931.0	-6.2	967.3	-7.4	1022.2	-8.5
2	1315.1	1383.0	1483.7	1308.0	-0.5	1353.9	-2.1	1423.0	-4.1
1	1587.9	1659.5	1772.3	1611.6	1.5	1664.1	0.3	1742.8	-1.7

Table 5.3: Comparison of RCP 8.5 scenario simulations with P&W estimates (m³/s)

AEP (%)	Median Discharge (Table 4.3)			P&W method revised for RCP 8.5 scenario (Table 3.8)					
				2030	% Diff.	2050	% Diff.	2090	% Diff.
50	280.3	320.0	431.5	Estimates not provided by method					
20	555.5	614.9	780.9						
10	779.5	842.5	1056.5	653.3	-16.2	701.9	-16.7	836.4	-20.8
5	1010.4	1086.9	1341.2	940.1	-7.0	1003.7	-7.7	1178.4	-12.1
2	1340.7	1446.6	1762.8	1319.5	-1.6	1399.8	-3.2	1617.6	-8.2
1	1612.4	1736.0	2096.3	1624.7	0.8	1716.3	-1.1	1963.1	-6.4

A similar level of alignment was observed between the RCP scenarios of Tables 5.2 and 5.3 indicating that the P&W equations were not necessarily less applicable for a particular scenario. In a similar manner to Table 5.1, the less frequent event estimations were aligned much closer to the corresponding simulated discharges for both emissions scenarios compared to the 10% and 5% AEP events. For the RCP 8.5 scenario, the estimate correlation decreased for the more distant projections however no definitive trend was observed in the RCP 4.5 projections.

The close correlation between the 2% and 1% AEP future event discharges confirmed the confidence already established in these simulations, enhancing the model suitability for future roadway immunity modelling. The magnitude of the differences between the P&W estimates and the simulated discharges is similar to the differences in the sample event distributions. However, it is reiterated that these estimates are simply a supporting validation of the model, which itself forms the most detailed representation of the Laidley Creek catchment hydrology.

5.2 Limitations of the results

The output validation indicated that the RORB simulation model was suitably calibrated for the less frequent 2% and 1% AEP events across current and future climate projection scenarios. This attribute was crucial in ensuring the results could support highway immunity modelling, as the primary intention of this project. However, the model performance worsened for the higher frequency events. The limitations of the results ultimately originated from the limitations associated with the input data as well as the modelling techniques used.

5.2.1 Data limitations

Several limitations were noted with the various forms of input data used to formulate the model. The limiting factors with the highest impact on the model outputs are discussed below.

5.2.1.1 Uncertainty in the climate projections

The uncertainty of the climate projections is best characterised by the extremely wide range of likely rates of change in increases to extreme rainfall per degree of surface temperature warming, as presented in Table 2.3. The median rates of change value were adopted for this project, rather than a distribution of potential rates of change.

The limitations in the climate projections originate from the uncertainties embedded within the GCMs to accurately forecast anticipated future climate conditions. This uncertainty is represented by the wide range of results obtained between the individual GCMs for different climate metrics, including rises in surface temperature, wind, humidity and evaporation.

In addition, the climate projections are simply that – forecasts of potential future conditions – and can only be verified after the occurrence through observation. These projections are continually revised with updated observations and advancements in literature.

5.2.1.2 Inadequate catchment coverage from rainfall stations

The spatial coverage of the catchment by the rainfall stations varied between calibrated events, but especially at an hourly level, was limited. The two streamflow gauging stations only began recording rainfall measurements in July 2024 while the majority of the BOM operated sites were located to the north of the catchment around the populated areas of Gatton and Plainland.

The rainfall interpolation was significantly influenced by the singular Townson daily rainfall station in the central and southern subcatchments. It was difficult to distinguish between naturally occurring, long-term increased average rainfall at the site or an unreliable rainfall gauge. Other influential sites for these subcatchments were situated outside the catchment boundary, often amongst separate mountain ranges with highly variable and potentially unrepresentative rainfall patterns. The central subcatchments were poorly covered during the most recent events, as illustrated in Figure 5.1 following the closure of the Thornton gauge in 2008 and the Mount Berryman gauge in 2020. The coverage of older events, such as May 1996, was far superior.

These limitations were exacerbated when the hourly rainfall data was used to define the temporal patterns of the calibration events. Only three stations were identified and all three stations were located outside the catchment boundary, resulting in a questionable level of coverage. The UQ Gatton and Upper Tenthill stations are positioned close together with minimal unique coverage while the Bremer River site is located over 10 kilometres to the east of the catchment. The available hourly rainfall data was potentially unrepresentative of the

rainfall distributions within the central subcatchments, increasing the uncertainty of the results including magnitude and timing aspects.

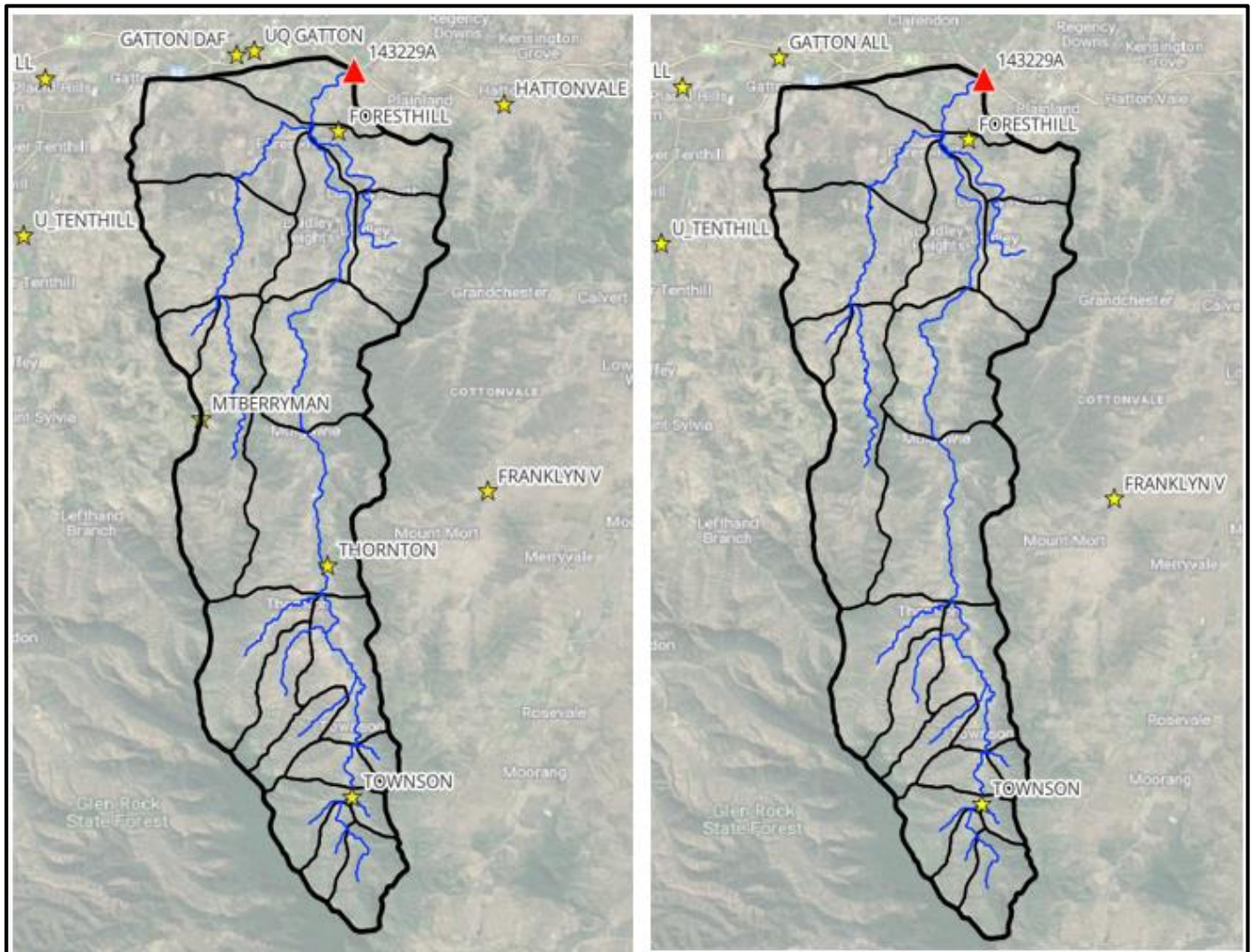


Figure 5.1: Reduction of central catchment daily rainfall station coverage from May 1996 (left) to February 2022 (right)

5.2.1.3 Duration of the gauged streamflow record

Despite the well-defined rating curve of the 143229A gauging station, the 33 gauged streamflow gauged record was considered relatively short ultimately limiting two critical aspects of the model development. The restricted duration significantly affected the reliability of the FFA as a broad range of dry and wet conditions prior to 1991 were not captured in the analysis. Within the most recent 13 years of the entire 33 year period, all three maximum flow events exceeding $1000 \text{ m}^3/\text{s}$ at 143229A occurred. These recorded events had a significant impact on increasing the discharge estimates for all AEPs, which may have resulted in an uncertain or inaccurate representation of the extended site history. This uncertainty is demonstrated by both the large variance between discharge estimates from the three fitted

distribution functions, as well as the large margin of error about the Bayesian posterior mode distribution. Secondly, notable high flow events which occurred prior to the gauge opening 1991 were not captured, hence reducing the number of available events to consider for calibration of the model parameters.

5.2.1.4 Simplification of catchment spatial features

The incorporation of catchment spatial features and attributes into a semi-distributed node-reach model required several simplifications. As previously discussed, the manually delineated catchment had an area of 452 km² while the WMIP 143229A station details page noted the catchment area as 462 km². This difference has the ability to impact the results to some extent.

The stream reach configuration and the subcatchment centroidal flow path arrangement has an impact on the results. The length of each reach was approximated by the vectorized stream path segments. These lengths were altered slightly where the subcatchment centroids did not closely align with the delineated streams. The reach slopes were averaged by considering the change in elevation between the centroid and junction nodes. A sufficient level of accuracy was difficult to obtain from the supplied DEM within the very flat lower reaches, potentially explaining the necessity for event specific translations during the calibration event modelling.

The entire catchment area was assumed as both rural and pervious to simplify modelling. In reality, a portion of the ground surface area consists of impervious surfaces, especially around the communities of Laidley, Forest Hill, and the eastern edges of Gatton. Computing the proportion of pervious land coverings was deemed outside the scope of work for this project. Similarly, the characteristics of urban runoff and storage in these locations were not considered, but would also impact the catchment response during an extreme rainfall event.

5.2.2 Modelling limitations

Limitations associated with the adopted modelling methodology facilitated the uncertainty in the results, especially for the higher frequency events. The basis of this report assumed that the relatively certain relationships, calibrations and simulations of the model remain an accurate representation of future hydrologic conditions following revisions to the input rainfall datasets. The most notable considerations are discussed below.

5.2.2.1 Calibration uncertainty

Limitations attributed to the calibration of the RORB model parameters originated from the flood immunity modelling objectives of this project. The 2% and 1% AEP recommended

design flow thresholds meant an emphasis was placed on ensuring maximum flow characteristics were as precisely calibrated as possible, compared to the lower flow components of the event hydrographs. This emphasis is illustrated in Figure 5.2 for the January 2011 event, where an accurate representation of timing, shape and magnitude was obtained for the final flood peak, however the preceding fluctuations were less precisely calibrated.

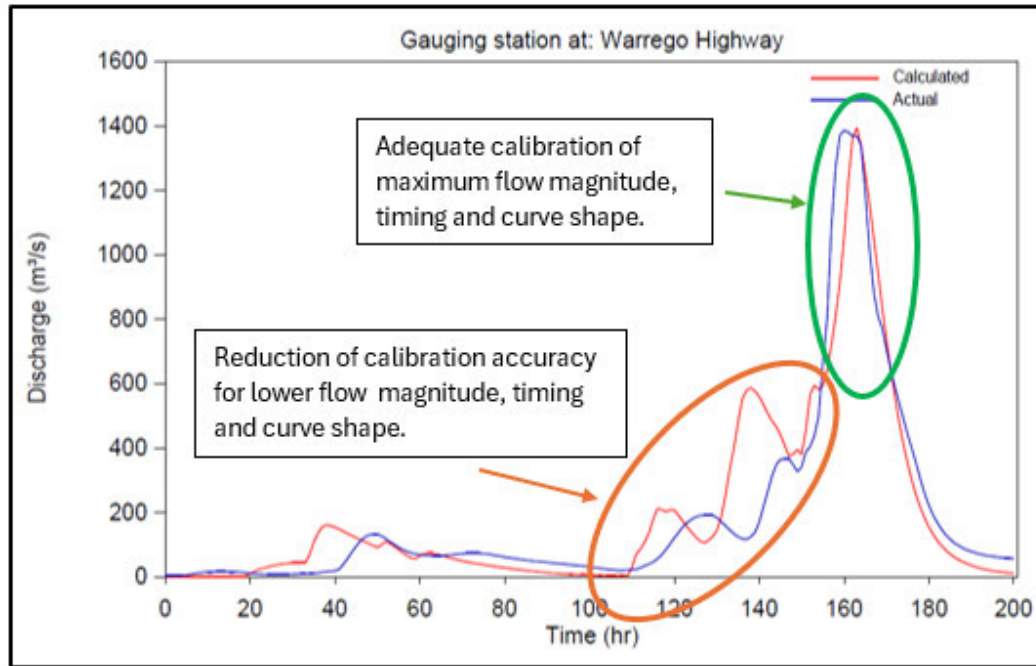


Figure 5.2: Level of calibration accuracy for various flow magnitudes during January 2011 event

Several technical components of the calibration also introduced uncertainties to the model. Foremost, many combinations of different k_c and IL values produced calculated hydrographs of similar appearance, meaning it was difficult to calibrate the most suitable set of parameters for each event. This limitation was overcome by considering the median value of k_c across eight unique peak flow events, however this approach also introduced uncertainties to the results. The median $k_c = 27$ simply represented the most appropriate representation for most events, however, this value was not identified as the best fit value for any individual event. The calibrated events were not re-evaluated using the median $k_c = 27$ to adjust the fitted IL depth due to time constraints.

The number of events considered for calibration indicated multiple aspects associated with the uncertainty of the results. One identified outlier event from eight modelled events demonstrated the calibrated catchment parameters may not necessarily be applicable to all past events. Considering only 8 events during the calibration limited the variety of rainfall-runoff characteristics evaluated. Additional event modelling would confirm or disassociate the

calibrated parameter values. The requirement to introduce event specific translations during calibration also indicated a limited ability for the model to represent past peak flow events in the very flat, lower subcatchment reaches.

5.2.2.2 Simulation uncertainty

Limitations of the design simulations originated from the calibration limitations in conjunction with components of the simulation method. The nature of the correlation between the simulated and independent estimates for varying event frequencies was unsurprising, given the calibration was based upon eight extreme rainfall events with an emphasis on the accuracy of the alignment against maximum flow characteristics. However, the differences observed for the 50% and 20% AEP events for the current enveloped IFDs was significant enough to indicate the model had limited capability to accurately represent frequent flow events.

Limiting the simulation of each climate scenario to a set of ten sample simulations limited the accuracy of the results. The margin of error about each set of simulations represented up to 10.4% of the median event discharge (for current conditions) but this varied drastically between AEPs with no apparent trend. Additional samples would facilitate the convergence of results allowing for a more certain median discharge to be extracted.

The critical event duration was a particularly uncertain aspect of the simulation. Despite seven of the eight historic events used to calibrate the model exceeding 48 hours in duration, the critical duration throughout the simulation of current and future climate scenarios was predominantly the 24 hour design event, followed by the 144 hour event. Therefore, the accuracy of the design simulations, especially for current conditions, was limited. Two potential causes of this uncertainty were identified:

- The RORB simulation specification considered a uniform spatial distribution of design rainfall across the 20 subcatchment centroidal inputs. However, the rainfall interpolations undertake for each of the eight calibrated events demonstrated that the distribution of rainfall is spatially variable across the catchment. The extent of the variability of rainfall across the calibrated events was observed to a variable factor itself. Therefore, the assumption that the design storm specification was spatially uniform is inaccurate. However, due to the insufficient coverage of long-term rainfall observation throughout several regions of the Laidley Creek catchment, it was impossible to ascertain an average rainfall spatial distribution pattern.

- Secondly, the highest IFD adjustment factors for future climate projections corresponded to the shortest duration events, increasing the likelihood these events would dominate in future years.

5.2.2.3 Validation uncertainty

The independent validation methods and the generic comparative approach to evaluate the simulated results have some degree of uncertainty. As discussed, the streamgauge duration considered for FFA was inadequate while the regionalised parameters of the RFFE and P&W methods represent major simplifications of the catchment hydrologic characteristics.

Minimal verification of the discharges corresponding to future climate scenarios was attained. While FFA methods typically provide the most localised representation of the three estimation techniques, the method is fundamentally an analysis of historically gauged data which cannot be applied to forecast evolving hydrologic characteristics.

Only the singular P&W method was able to produce some revised estimates, however, the high frequency 50% and 20% AEP events were unable to be validated by any method. The necessary assumption that the numeric P&W relationships were maintained for future climate scenarios, despite being developed from historically gauged data, further limited the certainty of the verification.

5.2.2.4 Limited consideration of time variable components

As introduced in the literature review, regional catchment hydrology is influenced by several factors which are likely to experience changes over time but were not incorporated within the revised future scenario models. Factors not considered are both dependent and non-dependent on the level of future climate change, as noted below:

- Altered storm event characteristics including temporal distribution patterns and losses as a consequence of evolving climate conditions.
- Urbanisation and development within the Laidley Creek catchment with the potential to modify natural flow regimes and reduce the proportion of pervious surface cover.

5.3 Potential model improvements

Potential improvements were identified to reduce the limitations and uncertainties associated with the results. These improvements were unable to be implemented within the defined project scope due to overall time and resource constraints. The suggested improvements include the completion of:

- Additional model calibrations of past events to verify the suitability of the median catchment storage parameter k_c , with a focus on improving the calibration of medium and high frequency flows. The viability of continuous catchment simulation methods to improve the accuracy of frequent event discharges should be explored.
- Additional design simulations with modified loss values more representative of the wide spread of losses observed during calibration.
- Additional design simulations with an increased number of revised IFD sets incorporating a wider range of the projected surface temperature rises.
- Additional sample simulations for each climate scenario to converge about the median discharge estimates.
- An analysis of the long-term averaged spatial distribution of rainfall (potentially through gridded rainfall products) to improve the accuracy of the design event timing and critical duration.
- The acquisition of remote-sensed Light Detection and Ranging (LiDAR), ground survey, or similarly precise elevation data to improve the accuracy of the catchment spatial model, especially within the very flat lower subcatchments which resulted in the necessity for event specific translations.
- The consideration of additional time variable factors within the future climate dependent discharge models, as discussed.

6. Conclusion

The content presented in this dissertation described the extent and adequacy in which the research project addressed each of the six project objectives. Each chapter represented the progression of the project towards the definition of a set of current and future design discharges for the Laidley Creek catchment at the Warrego Highway crossing site. The set of results offers a practical indication of anticipated future flow characteristics in the short, medium and long-term horizons to inform corridor planning and infrastructure design within DTMR.

The literature review demonstrated an evident lack of knowledge surrounding the exact impacts of climate change on peak discharge hydrology within the Laidley Creek catchment. Several background aspects of the research problem were introduced in this chapter, including the physical and hydrological attributes of the case study catchment. The cross-disciplinary flood immunity design requirements for the state-controlled Warrego Highway corridor were introduced, which indicated that producing accurate design discharges for the 2% and 1% AEP events was crucial towards achieving the objectives of this project. The applications, advantages and limitations of various hydrologic modelling techniques were examined, ultimately leading to the development of an event based, semi-distributed node-reach runoff routing model within the RORB platform. The broad implications of climate change on catchment hydrology were introduced and recently released design approaches of ARR 2019 were examined.

The literature review findings were synthesised into an appropriately scoped design methodology which considered best practice modelling techniques. Spatial and hydrologic data was retrieved from relevant sources and processed to formulate the catchment model and storm event files. The RORB model parameters were calibrated against eight historic high rainfall-runoff events. The MC simulation method was chosen to estimate the design discharges for the current and six future climate scenarios from sets of sample simulations, which are analysed in the results chapter of this report. A sensitivity analysis of the model parameters was undertaken and independent estimation techniques were used to evaluate the likely accuracy and extent of uncertainty in the results. The advantages, assumptions, uncertainties and limitations of the model were discussed throughout the development and analysis of the model.

6.1 Summary of results

The results provided a useful indication of the anticipated peak flow characteristics of the Laidley Creek catchment under a range of differing climate forecasts. Most crucially, the

independent estimation techniques implied that the model was accurately calibrated for the National Highway flood immunity threshold flows corresponding to the 2% and 1% AEP events. The uncertainty in the results increased for the higher frequency events, with the alignment between the independent estimates and the simulated flows decreasing.

The results projected that for the 2% AEP design event, peak discharge from the RCP 4.5 emissions scenario will increase from its current magnitude by 13% by 2030, 19% by 2050 and 27% by 2090. For the RCP 8.5 scenario, these projections rise to 15% by 2030, 24% by 2050 and drastically to 51% by 2090.

For the 1% AEP design event, the corresponding increases to peak discharge are slightly less than the 2% AEP projections. Under the RCP 4.5 emissions scenario, the projected rise in 1% AEP discharges are 12% by 2030, 18% by 2050 and 26% by 2090. For the RCP 8.5 scenario, these projections are 14% by 2030, 23% by 2050 and 49% by 2090.

6.2 Recommended future work

Two avenues of additional work are recommended as an extension of this dissertation. These recommendations were formed by considering the broader context of the design problem, specifically flood resilience and immunity modelling of the Warrego Highway at Laidley Creek for DTMR as administrators of the state-controlled network.

Firstly, it is recommended that enhancements are made to the hydrologic model (developed in this project report) by implementing some or all of the suggested list of improvements. These enhancements would reduce the uncertainty of the simulated design discharges, particularly for the higher frequency discharges.

Secondly, undertaking a two dimension hydraulic investigation of the Warrego Highway crossing of Laidley Creek at the Jack Martin Bridge is the next logical avenue of research. The output discharges obtained from this hydrologic simulation were formatted to be directly applicable as inputs for a hydraulic flow model. A potential model could therefore consider the design discharges corresponding to both current and future climate conditions, to evaluate the impact of climate change on the flood immunity of state-controlled roadway infrastructure.

The acquisition of LiDAR and/or bridge section survey data was not viable for this project but would significantly assist the development of a two dimensional hydraulic study.

7. References

- Al-Muqdadi, SW & Merkel, BJ 2011, 'Automated watershed evaluation of flat terrain', *Journal of Water Resource and Protection*, vol. 3, no. 12, p. 892.
- Alluvium 2019, *Critical review of climate change and water modelling in Queensland – Final Report*, Prepared collaboratively with CSIRO and University of Newcastle on behalf of the Queensland Water Modelling Network, Brisbane, Queensland.
- Australian Bureau of Statistics 2021, *Lockyer Valley - Value of Agricultural Commodities Produced, Australia, Cat. No. 7503.0*, Informed Decisions, <<https://economy.id.com.au/lockyer-valley/value-of-agriculture?BMID=40>>.
- Babister, M 2021, *Updated Local Design Rainfalls for Brisbane, Ipswich, Lockyer Valley and Moreton Bay*, Sydney, viewed 20 July 2024, <https://data.arr-software.org/static/pdf/IFD_Report_Final_June2021_compressed.pdf>.
- Babister, M, Retallick, M & Testoni, I 2019, 'Book 7 - Application of Catchment Modelling Systems in Australian Rainfall and Runoff: A Guide to Flood Estimation', in J Ball, et al. (eds), Commonwealth of Australia (Geoscience Australia).
- Babister, M, Trim, A, Testoni, I & Retallick, M 2016, *The Australian Rainfall & Runoff Datahub*, 37th Hydrology and Water Resources Symposium Queenstown NZ, <<https://data.arr-software.org/>>.
- Ball, J, Weinmann, E & Boyd, M 2019, 'Book 5 - Flood Hydrograph Estimation in Australian Rainfall and Runoff: A Guide to Flood Estimation ', in J Ball, et al. (eds), Commonwealth of Australia (Geoscience Australia).
- Ball, J, Kuczera, G, Franks, S, Rahman, A, Haddad, K & Weinmann, E 2019, 'Book 3 - Estimating Peak Discharges in Australian Rainfall and Runoff: A Guide to Flood Estimation ', in J Ball, et al. (eds), Commonwealth of Australia (Geoscience Australia).
- Ball, JE 1994, 'The influence of storm temporal patterns on catchment response', *Journal of Hydrology*, vol. 158, no. 3-4, pp. 285-303.
- Barton, C, Wallace, S, Syme, B, Wong, WT & Onta, P 2015, 'Brisbane River catchment flood study: comprehensive hydraulic assessment overview', *Floodplain Management Association National Conference, Brisbane Convention & Exhibition Centre, Brisbane*, pp. 19-22.
- Bates, B, McLuckie, D, Westra, S, Johnson, F, Green, J, Mummery, J & Abbs, D 2019, 'Book 1 - Scope and Philosophy in Australian Rainfall and Runoff: A Guide to Flood Estimation ', in J Ball, et al. (eds), Commonwealth of Australia (Geoscience Australia).
- Bureau of Meteorology 2007, *Observation of rainfall*, Melbourne, viewed June 8, <<http://www.bom.gov.au/climate/cdo/about/rain-measure.shtml>>.
- Bureau of Meteorology 2010a, *Queensland Flood Summary 1990-1999*, <http://www.bom.gov.au/qld/flood/fld_history/floodsum_1990.shtml>.

Bureau of Meteorology 2010b, *About rainfall data*, Melbourne, viewed 10 April, <<http://www.bom.gov.au/climate/data/>>.

Bureau of Meteorology 2016a, *Design Rainfall Data System (2016)*, Commonwealth of Australia, Canberra, <<http://www.bom.gov.au/water/designRainfalls/revised-ifd/>>.

Bureau of Meteorology 2016b, *IFD Design Rainfall Intensity (mm/h)*, Intensities_-28.009_152.029_ifds, Commonwealth of Australia, Canberra.

Bureau of Meteorology 2023, *Trend in total rainfall annual 1970-2022*

Bureau of Meteorology 2024a, *Annual mean temperature anomaly - Queensland - 1910 to 2023*, tmean.qld.0112.20439.

Bureau of Meteorology 2024b, *Climate Data Online*, 10 May 2024, <<http://www.bom.gov.au/climate/data/>>.

Bureau of Meteorology 2024c, *Cumulative half hourly rainfall since 9am daily - Station 040082 University of Queensland Gatton* 2 September 2024.

Bureau of Meteorology & CSIRO 2022, *State of the Climate 2022 - Australia's changing climate*, <http://www.bom.gov.au/state-of-the-climate/australias-changing-climate.shtml#:~:text=The%20intensity%20of%20short%2Dduration,the%20north%20of%20the%20country.>>.

Caroline, L & Afshar, NR 2014, 'Effect of types of weir on discharge', *Journal of Civil Engineering, Science and Technology*, vol. 5, no. 2, pp. 35-40.

CSIRO and Bureau of Meteorology 2020, *Climate Change in Australia - Overview*, <https://www.climatechangeinaustralia.gov.au/en/overview/>>.

Department of Agriculture, Water & the Environment (Geological & Bioregional Assessments) 2019, *Figure 28 Floodplains in the upper Condamine River*, (Geological & Bioregional Assessments), Canberra.

Department of Environment, Science, & Innovation 2021, *Hydrology – Catchment and subcatchment*, viewed 28 March 2024, <<https://wetlandinfo.des.qld.gov.au/wetlands/ecology/processes-systems/water/hydrology/landscape.html>>.

Department of Regional Development, Manufacturing & Water 2024, *Water Monitoring Information Portal*, <<https://water-monitoring.information.qld.gov.au/>>.

Department of Resources 2024a, *Queensland Globe*.

Department of Resources 2024b, *QTopo*, Queensland.

Department of Transport and Main Roads 2012, *Warrego Highway Upgrade Strategy: Brisbane to Charleville*, Brisbane, https://www.tmr.qld.gov.au/_/media/d96861ede2d44769833585a8a0dee46d.pdf?rev=8c171acefc454be9a6101fe554fd935d>.

Department of Transport and Main Roads 2019, *Heavy Vehicle Routes - Queensland*, National Heavy Vehicle Regulator National Network Map, <<https://qldspatial.information.qld.gov.au/catalogue/custom/detail.page?fid={2757F8EA-5B2F-4F03-902F-F9D7D038BF1B}>>.

Department of Transport and Main Roads 2022a, *13/05/2022 Glenore Grove traffic camera*.

Department of Transport and Main Roads 2022b, *26/02/2022 Warrego/Fernvale traffic camera*.

Department of Transport and Main Roads 2023, *18A Warrego Highway traffic statistics*, TMR Chartview application.

Department of Transport and Main Roads 2024a, *Manual: Design Criteria for Bridges and Other Structures*, Queensland.

Department of Transport and Main Roads 2024b, *18A Warrego Highway Ch 47.849*, Front view.

Department of Transport and Main Roads 2024c, *Hydrologic and Hydraulic Modelling Guideline*, Brisbane, viewed 10 March 2024, <https://www.tmr.qld.gov.au/_media/95713822caab4d85a514d815503a45dc.pdf?rev=3a9fb c2fd9ff43abb5a4bee429034fb1&sc_lang=en&hash=E2FBDAD9A0D93CBE3173AA297911912B>.

Department of Transport and Main Roads 2024d, *Engineering Policy 170 Climate Change and Natural Hazards Risk Assessment* Brisbane, viewed 2 August 2024, <https://www.tmr.qld.gov.au/_media/0d9f27f02be448f59e1dfc59c141b301.pdf?rev=9e4049 cff414486d94eb0dd765a76af1&sc_lang=en&hash=409E51A1F8A1ECB8746E3810F6ADE D7A>.

Department of Transport and Main Roads 2024e, *Supplement to Austroads Guide to Road Design Part 5: Drainage – General and Hydrology Considerations*, Brisbane, <https://www.tmr.qld.gov.au/_media/busind/techstdpubs/road-planning-and-design/road-planning-and-design-2nd-edition/rpdmsupvol3part5.pdf>.

Department of Transport and Main Roads 2024f, *Climate Change and Natural Hazards Risk Assessment Guideline*, Brisbane, viewed 28 August 2024, <https://www.tmr.qld.gov.au/_media/f62d991e97a74ba1b34fe019c16c3d60.pdf?rev=62c3fd 9b1fed47a18dd0a14309b8b651&sc_lang=en&hash=ED114DB6A463A6F24DBF143DF2BD 329E>.

Desvina, AP, Novia, SA, Yendra, R, Hendri, M & Fudholi, A 2019, 'Log Pearson III Distribution and Gumbel Distribution Model for Rainfall Data in Pekanbaru', *International Journal of Engineering and Advanced Technology (IJEAT)*, vol. 9, no. 1, pp. 803-7.

Dowdy, AJ 2020, 'Climatology of thunderstorms, convective rainfall and dry lightning environments in Australia', *Climate Dynamics*, vol. 54, no. 5, pp. 3041-52.

DRDMW 2023, *Water Monitoring Information Portal Glossary & Metadata*, Queensland, <<https://water-monitoring.information.qld.gov.au/wini/documents/webglossary.pdf>>.

Guerreiro, SB, Fowler, HJ, Barbero, R, Westra, S, Lenderink, G, Blenkinsop, S, Lewis, E & Li, X-F 2018, 'Detection of continental-scale intensification of hourly rainfall extremes', *Nature Climate Change*, vol. 8, no. 9, pp. 803-7.

Hill, P, Zhang, J & Nathan, R 2016, 'Australian rainfall and runoff Revision Project 6: Loss models for catchment simulation', *Commonwealth of Australia: Canberra, Australia*.

Holland, P, Herschy, R & Archer, D 1998, *Flood frequency analysis*, Figure 4.

Infrastructure Australia 2023, *Warrego Highway east corridor improvements*, viewed 18 August, <<https://www.infrastructureaustralia.gov.au/map/warrego-highway-east-corridor-improvements>>.

Institute of Public Works Engineering Australasia, Q 2017, *Queensland Urban Drainage Manual*, Queensland.

IPCC 2018, *Global warming of 1.5° C. An IPCC Special Report on the impacts of global warming of 1.5°C above pre-industrial levels and related global greenhouse gas emission pathways, in the context of strengthening the global response to the threat of climate change, sustainable development, and efforts to eradicate poverty*.

Jakeman, AJ, El Sawah, S, Cuddy, S, Robson, B, McIntyre, N & Cook, F 2018, 'QWMN Good Modelling Practice Principles'.

Johnson, F, Hutchinson, M, The, C, Beesley, C & Green, J 2016, 'Topographic relationships for design rainfalls over Australia', *Journal of Hydrology*, vol. 533, pp. 439-51.

Jordan, P, Seed, A & Nathan, R 2019, 'Book 2 - Rainfall Estimation in Australian Rainfall and Runoff: A Guide to Flood Estimation ', in J Ball, et al. (eds), *Commonwealth of Australia* (Geoscience Australia).

Lacey, B 2011, *Lockyer Valley flood aftermath*, The Chronicle, Toowoomba.

Ladson, A 2014, *Hydrology : an Australian Introduction*, Oxford University Press, South Melbourne.

Ladson, T 2016, 'Initial loss: storm v burst', <<https://tonyladson.wordpress.com/2016/11/08/initial-loss-storm-v-burst/>>.

Laurenson, E 1986, 'Variable time-step nonlinear flood routing', *Hydrosoft 86: hydraulic engineering software*, pp. 61-72.

Laurenson, E, Mein, R & Nathan, R 2010, 'RORB version 6 Runoff Routing program', *Programmer Manual*.

Ling, F, Pokhrel, P, Cohen, W, Peterson, J, Blundy, S & Robinson, K 2015, *Revision Project 8: Use of continuous simulation models for design flood estimation, Revision Project 12: Selection of an approach. Stage 3 Report*, ARR Report.

Lockyer Valley Regional Council 2022a, *Lockyer Valley Flood Information Portal*, 2024, 18 August, <<https://floodinformationportal.lvrc.qld.gov.au/flood/>>.

Lockyer Valley Regional Council 2022b, *Thornton Flood Monitoring Camera*, Thornton School Rd: Bridge - 2022-05-13 08:11:01, The Chronicle, Toowoomba.

Lockyer Valley Regional Council 2024a, *Thornton Flood Monitoring Camera*, Thornton School Rd: Bridge - 2024-08-23 15:48:43.

Lockyer Valley Regional Council 2024b, *Forest Hill Flood Monitoring Camera*, Whiteway Rd: Overflow - 2024-08-24 15:47:48.

Loveridge, M, Babister, M & Retallick, M 2015, 'Australian Rainfall and Runoff Revision Project 3: Temporal Patterns of Rainfall', *Engineers Australia*, Barton.

Loy, A 1990, 'Effects of data errors on flood estimates using two runoff routing models', UNSW Sydney.

Mora, C, Frazier, AG, Longman, RJ, Dacks, RS, Walton, MM, Tong, EJ, Sanchez, JJ, Kaiser, LR, Stender, YO & Anderson, JM 2013, 'The projected timing of climate departure from recent variability', *Nature*, vol. 502, no. 7470, pp. 183-7.

Nathan, R, Ling, F, Ladson, A & Ball, J 2019, 'Book 4 -Catchment Simulation for Design Flood Estimation in Australian Rainfall and Runoff: A Guide to Flood Estimation ', in J Ball, et al. (eds), Commonwealth of Australia (Geoscience Australia).

Palmen, L & Weeks, W 2011, 'Regional flood frequency for Queensland using the quantile regression technique', *Australasian Journal of Water Resources*, vol. 15, no. 1, pp. 47-57.

Podger, G 2004, *Rainfall Runoff Library User Guide*, CRC for Catchment Hydrology, <<https://toolkit.ewater.org.au/Tools/DownloadDocumentation.aspx?id=1000351>>.

Queensland Government 2019, *Climate change in the South East Queensland region*, Department of Environment and Science, <https://www.qld.gov.au/data/assets/pdf_file/0023/67631/seq-climate-change-impact-summary.pdf>.

Queensland Government 2024, *Queensland Future Climate Dashboard*, The Long Paddock, <<https://longpaddock.qld.gov.au/qld-future-climate/dashboard/>>.

Rahman, A, Haddad, K, Haque, M, Kuczera, G, Weinmann, P, Stensmyr, P, Babister, M & Weeks, W 2015, 'The New Regional Flood Frequency Estimation Model for Australia: RFFE Model 2015', *36th Hydrology and Water Resources Symp.*, Hobart.

Rahman, AS, Rahman, A, Zaman, MA, Haddad, K, Ahsan, A & Imteaz, M 2013, 'A study on selection of probability distributions for at-site flood frequency analysis in Australia', *Natural hazards*, vol. 69, pp. 1803-13.

Rima, L, Rahman, A, Haddad, K & Alim, MA 2022, 'Low flows in annual maximum flood data: does it matter in flood frequency analysis?', *Proceedings of the 3rd International Conference on Water and Environmental Engineering (iCWEE-2022)*, 27-30 November 2022, Sydney, Australia, pp. 123-9.

SEQWater 2024, *Dams and weirs: Bill Gunn (Lake Dyer)*, viewed 2 September, <<https://www.seqwater.com.au/dams/bill-gunn-lake-dyer>>.

- Sharp, C, Schepen, A, Das, S & Everingham, Y 2021, 'Geostatistical merging of weather radar data with a sparse rain gauge network in Queensland'.
- Singh, VP 1998, 'Log-pearson type III distribution', *Entropy-based parameter estimation in hydrology*, pp. 252-74.
- Singh, VP & Woolhiser, DA 2002, 'Mathematical modeling of watershed hydrology', *Journal of hydrologic engineering*, vol. 7, no. 4, pp. 270-92.
- Smith, C & Doughty, M 2020, *RMC-BestFit Quick Start Guide*, US Army Corps of Engineers.
- Starkey, G 2023, *Laidley Creek Falls Remote Camp*, Alltrails.
- The, C, Johnson, F, Hutchinson, M & Green, J 2012, 'Gridding of design rainfall parameters for the IFD revision project for Australia', *Hydrology and Water Resources Symposium 2012*, Engineers Australia Barton, ACT, pp. 1425-32.
- Transport and Main Roads Queensland 2024, *Footage from today!*, Facebook, 30 January 2024.
- United Nations Sustainable Development Goals Summit 2023, *Goal 13: Take urgent action to combat climate change and its impacts*,
<https://www.un.org/sustainabledevelopment/climate-change/>>.
- United States Geological Survey 2014, *Shuttle Radar Topography Mission (SRTM) 1 Arc-Second Global S28E152 v3*.
- US Army Corps of Engineers & Institute for Water Resources, RMC 2024, *RMC-BestFit software*, 1.0.
- US National Weather Service n.d., *Precipitation Measurements*, Arkansas-Red Basin, Tulsa,
<https://www.weather.gov/abrfc/map#:~:text=The%20grid%20point%20precipitation%20value,obtain%20the%20areal%20average%20precipitation.>.>
- van der Kwast, H 2018, *QGIS and Open Data for Hydrological Applications – Exercise Manual*, OpenCourseWare,
https://courses.gisopencourseware.org/pluginfile.php/137/mod_resource/content/1/QGIS_and_Open_Data_for_Hydrological_Applications_Exercise_Manual_v3.4.1b.pdf>.
- Van Vuuren, DP, Edmonds, J, Kainuma, M, Riahi, K, Thomson, A, Hibbard, K, Hurtt, GC, Kram, T, Krey, V & Lamarque, J-F 2011, 'The representative concentration pathways: an overview', *Climatic change*, vol. 109, pp. 5-31.
- Visser, JB, Wasko, C, Sharma, A & Nathan, R 2023, 'Changing Storm Temporal Patterns with Increasing Temperatures across Australia', *Journal of Climate*, vol. 36, no. 18, pp. 6247-59.
- Wasko, C, Westra, S, Nathan, R, Pepler, A, Raupach, TH, Dowdy, A, Johnson, F, Ho, M, McInnes, KL & Jakob, D 2024, 'A systematic review of climate change science relevant to Australian design flood estimation', *Hydrology and Earth System Sciences*, vol. 28, no. 5, pp. 1251-85.

Weeks, W 1980, 'Using the Laurenson model: traps for young players', *National Conference Publication*, pp. 29-33.

Weeks, W, Babister, M & Retallick, M 2023, *Austroads Guide to Road Design Part 5: Drainage – General and Hydrology Considerations* Sydney, viewed 20 July 2024, <https://austroads.com.au/publications/road-design/agrd05/media/AGRD05-23_Guide_to_Road_Design_Part-5_Drainage_General_and_Hydrology_Considerations.pdf>.

Wordsworth, M 2013, 'Live: Flood disaster unfolds as weather wreaks havoc', <https://www.abc.net.au/news/2013-01-28/qld-flooding-alert-moves-south/4486666>>.

Appendix A: Project specification and work plan (topic later refined)

Title: Instantaneous Peak Flow Estimation Considering Climate Change Scenarios in the Upper Condamine Basin
Name: Hayden Jago
Student ID: [REDACTED]
Major: Civil Engineering
Supervisor: Dr Sreeni Chadalavada
Enrolment: ENP4111-YL1-2024

Project Specification

Introduction and Background:

Changing climates and weather patterns are having diverse impacts on regions globally. Surface temperatures have risen by approximately 1.5°C since Australian records began in 1910 (Bureau of Meteorology & CSIRO 2022). Surface temperature increases are a consequence of greenhouse gas emissions from energy, industry, transport, and agriculture sectors (United Nations Sustainable Development Goals Summit 2023). As a result, total annual rainfall in regional Queensland has declined since 1970 (Bureau of Meteorology & CSIRO 2022). Climate forecasts have predicted even greater rises in surface temperatures, particularly in Southern Queensland. Per degree of future warming, heavy rainfall intensity is predicted to increase by 2-15% (Guerreiro et al. 2018; Bates et al. 2019; Bureau of Meteorology & CSIRO 2022). Further surface warming could increase the intensity and frequency of short, heavy precipitation “bursts” causing flood events in regional catchments (Visser et al. 2023).

The Upper Condamine River Basin is located in regional southeastern Queensland and encompasses the headwaters and tributaries of the Condamine River. The basin features varied topography including the elevated western faces of the Great Dividing Range and the flat open plains of the Darling Downs and Western Downs, see Figure 1. The catchment is the main water source for many irrigation and domestic uses (Dafny & Silburn 2013). The diverse elevation of locations within the catchment contribute to dynamic rainfall distribution patterns (Dafny & Silburn 2013). Consequently, the generated hydrologic runoff systems are highly complex. This research will focus on quantifying the parameters that affect the hydrologic cycle in the Upper Condamine Basin to generate a rainfall-discharge hydrograph representative of the conditions expected in future decades.

Modelling allows engineers and policymakers to comprehend hydrologic processes and enable measures that best manage water resources distribution during periods of drought or flooding. Queensland hydrologic modelling is directed by design guidelines published in Books 1 to 5 of Engineers Australia’s *Australian Rainfall and Runoff: A Guide to Flood Estimation* (referred to as ARR 2019 (Ball et al. 2019; Ball, Weinmann & Boyd 2019; Bates et al. 2019; Jordan, Seed & Nathan 2019; Nathan et al. 2019). Book 1 Chapter 5 provides generalised technical advice for considering future climate change scenarios in a project design life. ARR 2019 uses flood hydrograph generation as a method to estimate instantaneous peak flow. This technique considers catchment runoff generation as the conversion of rainfall through losses into a downstream flood hydrograph (Bates et al. 2019).

The major sources of raw data for this project are easily accessible online. Design rainfall IFDs for locations across the Upper Condamine Basin are obtainable from the Bureau of Meteorology (2016). Additionally, streamflow discharge data is available at several Queensland Government gauge locations along the Condamine River (Department of Regional Development, Manufacturing & Water 2023).

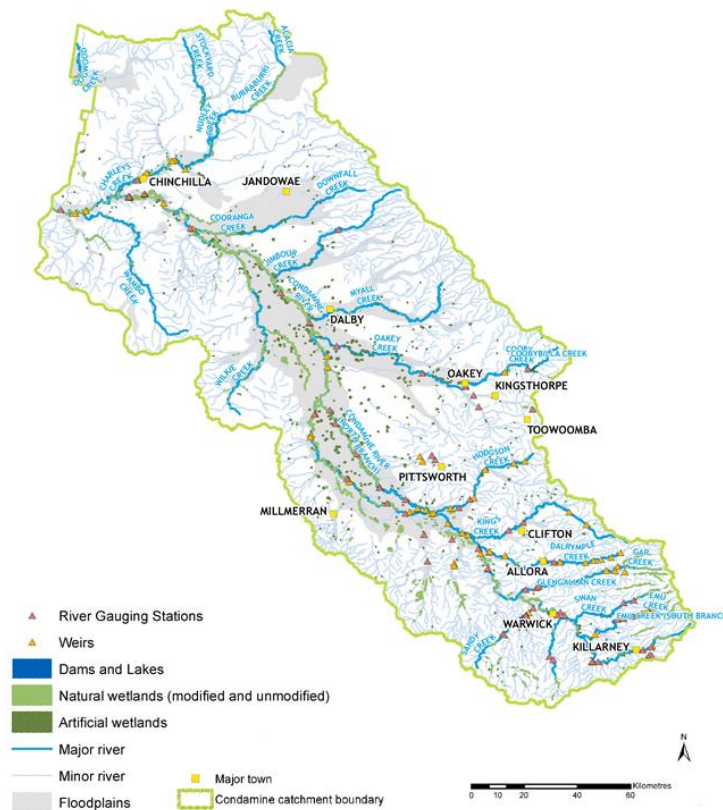


Figure 1: The Upper Condamine River Basin (Department of Agriculture, Water & the Environment (Geological & Bioregional Assessments) 2019)

Objectives and Aims:

This research project aims to fulfil gaps in knowledge about the impacts of climate change scenarios on hydrologic processes at locations of various elevation in the Upper Condamine River Basin.

○ Specific Objectives:

- Calibrate and modify existing design rainfall models to accurately represent dynamic future rainfall events impacted by climate change.
- Develop future rainfall-runoff hydrographs for a number of high- and low-elevation case study locations within the Upper Condamine Basin.
- Compare the findings of future flow hydrograph modelling with current flow characteristics.

○ Expected Outcomes:

- Clear identification of changes observed to rainfall models and discharge hydrographs in future decades to understand the quantifiable impacts of climate change scenarios on peak discharge across sites in the catchment.
- Enhanced understanding of high elevation hydrology in Queensland.
- Possible starting point for further research into integrated watershed management, catchment flood simulations, or flood damage probability assessment.

The knowledge from this research would have the potential to facilitate the development of flood management strategies and engineering solutions to mitigate the impacts of future weather events on local communities in the Upper Condamine Basin. Additionally, this research may assist sustainable water resource allocation and distribution in the region.

Work Plan

Programme: Version 2 - February 2024

- **Month 1: Project Commencement and Proposal**
 - Liaise with supervisor to refine scope of research.
 - Develop project specification and formulate detailed programme schedule for proposal submission.
- **Months 2-3: Literature Review**
 - Conduct a comprehensive literature review of future climate scenarios and their impact on fundamental hydrologic design parameters.
 - Review key model parameters including rainfall/flow data sources relevant to the case study region. Identify parameters that require further investigation.
 - Review existing hydrologic technical guidelines and publications to begin developing the research methodology.
- **Month 4: Research Methodology Development**
 - Collate findings from literature review to identify appropriate modelling processes and critical locations suitable to become case study sites for hydrologic analysis (including sites of high and low elevations)
 - Finalise the project methodology through a clearly defined hydrologic modelling procedure, step-by-step.
- **Months 5-7: Hydrologic Modelling**
 - Conduct baseline modelling for flow at existing streamgauge sites.
 - Verify current rainfall models correspond to current streamflow models.
 - Extend current rainfall models to develop rainfall-runoff hydrographs at each study location with no available streamgauge data.
 - Formulate future rainfall models by considering the calibrated rainfall models in conjunction with the identified impacts of climate change scenarios on rainfall patterns.
 - Apply future rainfall models to the study locations to develop future rainfall-runoff hydrographs.
- **Months 8-9: Hydrologic Analysis, Model Refinements and Report Writing**
 - Compare the current and future rainfall-runoff hydrographs to identify impacts of climate change factors on peak flow estimation in the case study catchment.
 - Make any model refinements to improve accuracy and usefulness of findings.
 - Compose findings into a technical discussion in the dissertation report.
- **Month 10: Project Finalisation**
 - Complete, review, proof, and submit the report.
 - Prepare a visual presentation summarising the project development, model findings and outcomes. Submit a personal reflection about the project.

See attached proposed schedule for detailed breakdown of individual project components below.

Timeline:

YEAR LONG STUDY PERIOD [ENR4111] WEEK	1	2	3	4	5	6	7	8	9	10	11	12	13	14	15	16	17	18	19	20	21	22	23	24	25	26	27	28	29	30	31	32	02-Sep-24	33	34	35	36	37	38	39	40	41	42	43	44	45	46
TASKS:																																															
Task 1: Project preparation																																															
1A Proposal & justification approval																																															
1B Report paper drafting																																															
Task 2: Literature review and methodology																																															
2A Background literature review																																															
2B Methodology - hydrologic method formulation																																															
2C Methodology - site selection																																															
Task 3: Hydrologic model development																																															
3A Existing streamgauge site modelling																																															
3B Current rainfall model calibration=																																															
3C Future (Climate impacted) rainfall modelling																																															
3D Future peak flow modelling																																															
Task 4: Hydrologic model verification																																															
4A Results analysis																																															
4B Model refinements & recommendations																																															
Task 5: Project Finalisation																																															
5A Research presentation and reflection																																															
5B Report paper completion																																															

Resources required:

- **Equipment:**
 - Personal computer with internet access.
 - Dual monitor setup for convenient, simultaneous access to different aspects of project (i.e. modelling calculations and report paper).
- **Software:**
 - Prepare dissertation paper and presentation slides using Word and PowerPoint, which are included in the university edition of the Microsoft Office suite.
 - Perform hydrologic model calculations and obtain graphical outputs in Excel.
 - Manage references using university-provided EndNote citation tool.
 - Manage dissertation storage and backup using OneDrive cloud.
- **Access:**
 - Access to university library resources and online scholarly search engines for literature review and methodology development.
 - Retrieve streamgauge observations and rainfall metrics from official government databases.

Appendix B: Rainfall station datasets coverage

Table B1: Daily rainfall stations with dated averages to Forest Hill reference baseline

Station Name	Station ID	Record start date	Record finish date	Average daily rainfall (mm/d)	F.H. time equivalent baseline (mm/d)	Difference to baseline (%)	Calibration event coverage (Table 3.2)	
							Full record	Partial record
Forest Hill	40079	1/02/1894	Open	2.132	Catchment baseline		<input checked="" type="checkbox"/>	
Mulgowie	40570	1/01/1998	8/12/2004	2.053	1.784	15.07		
Laidley	40716	27/01/2009	30/05/2011	9.782	2.556	282.75		
Laidley PO	40114	1/02/1894	31/12/1993	2.202	2.132	3.27		
Laidley Ck	40011	1/10/1964	31/12/1979	2.564	2.539	0.98		
Mulgowie TM	40835	2/06/2010	6/01/2012	0.711	2.943	-75.83		
Mt Berryman	40310	1/07/1961	26/01/2020	2.413	2.173	11.03		<input checked="" type="checkbox"/>
Grandchester	40091	12/02/1894	31/03/2014	2.406	2.122	13.37		<input checked="" type="checkbox"/>
Upper Tenthill	40388	1/01/1959	Open	2.108	2.228	-5.39	<input checked="" type="checkbox"/>	
Mt Sylvia	40384	1/07/1953	31/10/2002	2.085	2.245	-7.13		
Gatton DAFF	40436	1/07/1968	31/05/2014	2.194	2.181	0.62		<input checked="" type="checkbox"/>
UQ Gatton	40082	1/08/1897	30/04/2024	2.094	2.133	-1.85	<input checked="" type="checkbox"/>	
Thornton	40751	1/11/1993	31/03/2008	2.189	1.787	22.49		
Franklyn Vale	40374	1/02/1894	Open	2.407	2.132	12.88	<input checked="" type="checkbox"/>	
Rock View	40605	1/03/1919	31/12/1969	2.748	2.102	30.73		
Franklyn Vale Alert	40912	30/11/2000	Open	2.220	2.128	4.32		<input checked="" type="checkbox"/>
Gatton Allan St	40083	1/02/1894	Open	2.130	2.132	-0.07	<input checked="" type="checkbox"/>	
Hattonvale	40095	1/08/1909	11/03/2020	2.115	2.120	-0.22		<input checked="" type="checkbox"/>
Thornton BVRT	40202	1/08/1915	30/06/1983	2.647	2.166	22.23		
Placid Hills	40449	1/01/1970	Open	2.183	2.206	-1.07	<input checked="" type="checkbox"/>	
Townson East	40392	1/01/1958	31/08/1978	3.250	2.439	33.23		
Townson	40675	1/12/1977	9/09/2023	3.023	2.117	42.85		<input checked="" type="checkbox"/>

High priority daily rainfall stations

- Forest Hill (baseline for evaluation of poor sites)
- Upper Tenthill
- UQ Gatton
- Franklyn Vale (eastern coverage)
- Gatton Allan St
- Placid Hills
- Townson (southern coverage until 2023)
- Mt Berryman (south-western coverage until 2020)
- Grandchester (north-eastern coverage until 2014)
- Hattonvale (north-eastern coverage until 2014)
- Gatton DAFF (northern sites covered during offline periods until 2014)

Table B2: Hourly rainfall stations

Station name	Station ID	Station operator	Record start date	Record finish date	Calibration event coverage (Table 3.2)	
					Full record	Partial record
UQ Gatton	40082	BOM	16/07/2002	Open		<input checked="" type="checkbox"/>
Tenthill Creek	143212A	DRDMW	10/02/1993	Open	<input checked="" type="checkbox"/>	
Bremer River at Adams Bridge	143110A	DRDMW	13/11/1992	Open	<input checked="" type="checkbox"/>	

Appendix C: Design rainfall IFDs at Laidley Creek catchment centroid

Table C1: LIMB 2020 – BOM IFD envelope (current climate)

Coordinates	-27.727		152.355		ENVELOPED			
AEP (%) / Duration	63.23	50	20	10	5	2	1	0.5
5 min	9.5	10.5	13.7	16.1	18.5	21.9	24.7	28.3
10 min	15.5	17.3	22.5	25.9	29.4	34.8	38.9	44.6
15 min	19.5	21.9	28.5	32.5	37.3	44.1	49.4	56.5
20 min	22.4	25.2	32.9	37.5	43.1	51.2	57.3	65.5
25 min	24.6	27.7	36.4	41.3	47.8	56.7	63.6	72.8
30 min	26.4	29.8	39.2	44.5	51.6	61.3	68.8	78.7
45 min	30.2	34.2	45.2	51.5	59.9	71.4	80.2	91.8
1 hr	32.9	37.3	49.5	56.5	65.6	78.3	88.2	101
1.5 hr	36.6	41.5	55.5	63.7	73.6	88	99.3	114
2 hr	39.3	44.6	59.9	69.2	79.3	94.9	107	123
3 hr	43.3	49.2	66.6	77.6	87.8	105	119	136
4.5 hr	47.8	54.3	74.4	87.4	99.8	117	132	151
6 hr	51.3	58.5	80.6	95.4	109.7	128.3	143	163
9 hr	56.9	65.1	90.9	108.7	126.1	149.7	167.9	191.9
12 hr	61.3	70.3	99.3	119.6	139.8	167.6	189.4	217.2
18 hr	68.9	78.7	112.9	137.5	162.5	197.4	225.5	258.4
24 hr	75.9	86	123.8	151.9	181	222.1	255.6	292.1
30 hr	81.7	92.8	132.9	164.1	196.7	243.3	281.6	321.6
36 hr	86.5	98.5	140.7	174.7	210.5	261.9	304.6	349.1
48 hr	94.3	108	153.6	192.3	233.5	293.4	343.7	394.7
72 hr	105	120	173	218.5	268	340.8	403.2	464.2
96 hr	111	128	186.9	237.6	292.9	375.1	446.1	513.3
120 hr	116	133	198.3	252.5	311.9	400.8	477.9	548.4
144 hr	119	136	208	264.7	326.9	420.4	501.6	576.1
168 hr	121	141.8	216.5	275.1	338.9	435.6	519.3	599.5

Table C2: IFD adjustment factors – RCP 4.5 scenarios

Storm Duration / Year	<1 hr	1.5 hr	2 hr	3 hr	4.5 hr	6 hr	9 hr	12 hr	18 hr	>24 hr
2030	1.18	1.17	1.16	1.14	1.13	1.12	1.12	1.11	1.1	1.1
2050	1.27	1.24	1.23	1.21	1.19	1.18	1.17	1.16	1.15	1.14
2090	1.4	1.36	1.34	1.31	1.28	1.26	1.24	1.23	1.21	1.2

Table C3: IFD adjustment factors – RCP 8.5 scenarios

Storm Duration / Year	<1 hr	1.5 hr	2 hr	3 hr	4.5 hr	6 hr	9 hr	12 hr	18 hr	>24 hr
2030	1.2	1.18	1.17	1.16	1.14	1.13	1.13	1.12	1.11	1.11
2050	1.34	1.31	1.29	1.26	1.24	1.23	1.21	1.2	1.18	1.18
2090	1.77	1.69	1.64	1.58	1.52	1.49	1.45	1.42	1.39	1.37

Table C4: RCP 4.5 2030 IFDs

Coordinates	-27.727		152.355		RCP 4.5 2030			
AEP (%) / Duration	63.23	50	20	10	5	2	1	0.5
5 min	11.2	12.4	16.2	19.0	21.8	25.8	29.1	33.4
10 min	18.3	20.4	26.6	30.6	34.7	41.1	45.9	52.6
15 min	23.0	25.8	33.6	38.4	44.0	52.0	58.3	66.7
20 min	26.4	29.7	38.8	44.3	50.9	60.4	67.6	77.3
25 min	29.0	32.7	43.0	48.7	56.4	66.9	75.0	85.9
30 min	31.2	35.2	46.3	52.5	60.9	72.3	81.2	92.9
45 min	35.6	40.4	53.3	60.8	70.7	84.3	94.6	108.3
1 hr	38.8	44.0	58.4	66.7	77.4	92.4	104.1	119.2
1.5 hr	42.8	48.6	64.9	74.5	86.1	103.0	116.2	133.4
2 hr	45.6	51.7	69.5	80.3	92.0	110.1	124.1	142.7
3 hr	49.4	56.1	75.9	88.5	100.1	119.7	135.7	155.0
4.5 hr	54.0	61.4	84.1	98.8	112.8	132.2	149.2	170.6
6 hr	57.5	65.5	90.3	106.8	122.9	143.7	160.2	182.6
9 hr	63.7	72.9	101.8	121.7	141.2	167.7	188.0	214.9
12 hr	68.0	78.0	110.2	132.8	155.2	186.0	210.2	241.1
18 hr	75.8	86.6	124.2	151.3	178.8	217.1	248.1	284.2
24 hr	83.5	94.6	136.2	167.1	199.1	244.3	281.2	321.3
30 hr	89.9	102.1	146.2	180.5	216.4	267.6	309.8	353.8
36 hr	95.2	108.4	154.8	192.2	231.6	288.1	335.1	384.0
48 hr	103.7	118.8	169.0	211.5	256.9	322.7	378.1	434.2
72 hr	115.5	132.0	190.3	240.4	294.8	374.9	443.5	510.6
96 hr	122.1	140.8	205.6	261.4	322.2	412.6	490.7	564.6
120 hr	127.6	146.3	218.1	277.8	343.1	440.9	525.7	603.2
144 hr	130.9	149.6	228.8	291.2	359.6	462.4	551.8	633.7
168 hr	133.1	156.0	238.2	302.6	372.8	479.2	571.2	659.5

Table C5: RCP 4.5 2050 IFDs

Coordinates	-27.727		152.355		RCP 4.5 2050			
AEP (%) / Duration	63.23	50	20	10	5	2	1	0.5
5 min	12.1	13.3	17.4	20.4	23.5	27.8	31.4	35.9
10 min	19.7	22.0	28.6	32.9	37.3	44.2	49.4	56.6
15 min	24.8	27.8	36.2	41.3	47.4	56.0	62.7	71.8
20 min	28.4	32.0	41.8	47.6	54.7	65.0	72.8	83.2
25 min	31.2	35.2	46.2	52.5	60.7	72.0	80.8	92.5
30 min	33.5	37.8	49.8	56.5	65.5	77.9	87.4	99.9
45 min	38.4	43.4	57.4	65.4	76.1	90.7	101.9	116.6
1 hr	41.8	47.4	62.9	71.8	83.3	99.4	112.0	128.3
1.5 hr	45.4	51.5	68.8	79.0	91.3	109.1	123.1	141.4
2 hr	48.3	54.9	73.7	85.1	97.5	116.7	131.6	151.3
3 hr	52.4	59.5	80.6	93.9	106.2	127.1	144.0	164.6
4.5 hr	56.9	64.6	88.5	104.0	118.8	139.2	157.1	179.7
6 hr	60.5	69.0	95.1	112.6	129.4	151.4	168.7	192.3
9 hr	66.6	76.2	106.4	127.2	147.5	175.1	196.4	224.5
12 hr	71.1	81.5	115.2	138.7	162.2	194.4	219.7	252.0
18 hr	79.2	90.5	129.8	158.1	186.9	227.0	259.3	297.2
24 hr	86.5	98.0	141.1	173.2	206.3	253.2	291.4	333.0
30 hr	93.1	105.8	151.5	187.1	224.2	277.4	321.0	366.6
36 hr	98.6	112.3	160.4	199.2	240.0	298.6	347.2	398.0
48 hr	107.5	123.1	175.1	219.2	266.2	334.5	391.8	450.0
72 hr	119.7	136.8	197.2	249.1	305.5	388.5	459.6	529.2
96 hr	126.5	145.9	213.1	270.9	333.9	427.6	508.6	585.2
120 hr	132.2	151.6	226.1	287.9	355.6	456.9	544.8	625.2
144 hr	135.7	155.0	237.1	301.8	372.7	479.3	571.8	656.8
168 hr	137.9	161.7	246.8	313.6	386.3	496.6	592.0	683.4

Table C6: RCP 4.5 2090 IFDs

Coordinates	-27.727		152.355		RCP 4.5 2090			
AEP (%) / Duration	63.23	50	20	10	5	2	1	0.5
5 min	13.3	14.7	19.2	22.5	25.9	30.7	34.6	39.6
10 min	21.7	24.2	31.5	36.3	41.2	48.7	54.5	62.4
15 min	27.3	30.7	39.9	45.5	52.2	61.7	69.2	79.1
20 min	31.4	35.3	46.1	52.5	60.3	71.7	80.2	91.7
25 min	34.4	38.8	51.0	57.8	66.9	79.4	89.0	101.9
30 min	37.0	41.7	54.9	62.3	72.2	85.8	96.3	110.2
45 min	42.3	47.9	63.3	72.1	83.9	100.0	112.3	128.5
1 hr	46.1	52.2	69.3	79.1	91.8	109.6	123.5	141.4
1.5 hr	49.8	56.4	75.5	86.6	100.1	119.7	135.0	155.0
2 hr	52.7	59.8	80.3	92.7	106.3	127.2	143.4	164.8
3 hr	56.7	64.5	87.2	101.7	115.0	137.6	155.9	178.2
4.5 hr	61.2	69.5	95.2	111.9	127.7	149.8	169.0	193.3
6 hr	64.6	73.7	101.6	120.2	138.2	161.7	180.2	205.4
9 hr	70.6	80.7	112.7	134.8	156.4	185.6	208.2	238.0
12 hr	75.4	86.5	122.1	147.1	172.0	206.1	233.0	267.2
18 hr	83.4	95.2	136.6	166.4	196.6	238.9	272.9	312.7
24 hr	91.1	103.2	148.6	182.3	217.2	266.5	306.7	350.5
30 hr	98.0	111.4	159.5	196.9	236.0	292.0	337.9	385.9
36 hr	103.8	118.2	168.8	209.6	252.6	314.3	365.5	418.9
48 hr	113.2	129.6	184.3	230.8	280.2	352.1	412.4	473.6
72 hr	126.0	144.0	207.6	262.2	321.6	409.0	483.8	557.0
96 hr	133.2	153.6	224.3	285.1	351.5	450.1	535.3	616.0
120 hr	139.2	159.6	238.0	303.0	374.3	481.0	573.5	658.1
144 hr	142.8	163.2	249.6	317.6	392.3	504.5	601.9	691.3
168 hr	145.2	170.2	259.8	330.1	406.7	522.7	623.2	719.4

Table C7: RCP 8.5 2030 IFDs

Coordinates	-27.727		152.355		RCP 8.5 2030			
AEP (%) / Duration	63.23	50	20	10	5	2	1	0.5
5 min	11.4	12.6	16.4	19.3	22.2	26.3	29.6	34.0
10 min	18.6	20.8	27.0	31.1	35.3	41.8	46.7	53.5
15 min	23.4	26.3	34.2	39.0	44.8	52.9	59.3	67.8
20 min	26.9	30.2	39.5	45.0	51.7	61.4	68.8	78.6
25 min	29.5	33.2	43.7	49.6	57.4	68.0	76.3	87.4
30 min	31.7	35.8	47.0	53.4	61.9	73.6	82.6	94.4
45 min	36.2	41.0	54.2	61.8	71.9	85.7	96.2	110.2
1 hr	39.5	44.8	59.4	67.8	78.7	94.0	105.8	121.2
1.5 hr	43.2	49.0	65.5	75.2	86.8	103.8	117.2	134.5
2 hr	46.0	52.2	70.1	81.0	92.8	111.0	125.2	143.9
3 hr	50.2	57.1	77.3	90.0	101.8	121.8	138.0	157.8
4.5 hr	54.5	61.9	84.8	99.6	113.8	133.4	150.5	172.1
6 hr	58.0	66.1	91.1	107.8	124.0	145.0	161.6	184.2
9 hr	64.3	73.6	102.7	122.8	142.5	169.2	189.7	216.8
12 hr	68.7	78.7	111.2	134.0	156.6	187.7	212.1	243.3
18 hr	76.5	87.4	125.3	152.6	180.4	219.1	250.3	286.8
24 hr	84.2	95.5	137.4	168.6	200.9	246.5	283.7	324.2
30 hr	90.7	103.0	147.5	182.2	218.3	270.1	312.6	357.0
36 hr	96.0	109.3	156.2	193.9	233.7	290.7	338.1	387.5
48 hr	104.7	119.9	170.5	213.5	259.2	325.7	381.5	438.1
72 hr	116.6	133.2	192.0	242.5	297.5	378.3	447.6	515.3
96 hr	123.2	142.1	207.5	263.7	325.1	416.4	495.2	569.8
120 hr	128.8	147.6	220.1	280.3	346.2	444.9	530.5	608.7
144 hr	132.1	151.0	230.9	293.8	362.9	466.6	556.8	639.5
168 hr	134.3	157.4	240.3	305.4	376.2	483.5	576.4	665.4

Table C8: RCP 8.5 2050 IFDs

Coordinates	-27.727		152.355		RCP 8.5 2070			
AEP (%) / Duration	63.23	50	20	10	5	2	1	0.5
5 min	12.7	14.1	18.4	21.6	24.8	29.3	33.1	37.9
10 min	20.8	23.2	30.2	34.7	39.4	46.6	52.1	59.8
15 min	26.1	29.3	38.2	43.6	50.0	59.1	66.2	75.7
20 min	30.0	33.8	44.1	50.3	57.8	68.6	76.8	87.8
25 min	33.0	37.1	48.8	55.3	64.1	76.0	85.2	97.6
30 min	35.4	39.9	52.5	59.6	69.1	82.1	92.2	105.5
45 min	40.5	45.8	60.6	69.0	80.3	95.7	107.5	123.0
1 hr	44.1	50.0	66.3	75.7	87.9	104.9	118.2	135.3
1.5 hr	47.9	54.4	72.7	83.4	96.4	115.3	130.1	149.3
2 hr	50.7	57.5	77.3	89.3	102.3	122.4	138.0	158.7
3 hr	54.6	62.0	83.9	97.8	110.6	132.3	149.9	171.4
4.5 hr	59.3	67.3	92.3	108.4	123.8	145.1	163.7	187.2
6 hr	63.1	72.0	99.1	117.3	134.9	157.8	175.9	200.5
9 hr	68.8	78.8	110.0	131.5	152.6	181.1	203.2	232.2
12 hr	73.6	84.4	119.2	143.5	167.8	201.1	227.3	260.6
18 hr	81.3	92.9	133.2	162.3	191.8	232.9	266.1	304.9
24 hr	89.6	101.5	146.1	179.2	213.6	262.1	301.6	344.7
30 hr	96.4	109.5	156.8	193.6	232.1	287.1	332.3	379.5
36 hr	102.1	116.2	166.0	206.1	248.4	309.0	359.4	411.9
48 hr	111.3	127.4	181.2	226.9	275.5	346.2	405.6	465.7
72 hr	123.9	141.6	204.1	257.8	316.2	402.1	475.8	547.8
96 hr	131.0	151.0	220.5	280.4	345.6	442.6	526.4	605.7
120 hr	136.9	156.9	234.0	298.0	368.0	472.9	563.9	647.1
144 hr	140.4	160.5	245.4	312.3	385.7	496.1	591.9	679.8
168 hr	142.8	167.3	255.5	324.6	399.9	514.0	612.8	707.4

Table C9: RCP 8.5 2090 IFDs

Coordinates	-27.727		152.355		RCP 8.5 2090			
AEP (%) / Duration	63.23	50	20	10	5	2	1	0.5
5 min	16.8	18.6	24.2	28.5	32.7	38.8	43.7	50.1
10 min	27.4	30.6	39.8	45.8	52.0	61.6	68.9	78.9
15 min	34.5	38.8	50.4	57.5	66.0	78.1	87.4	100.0
20 min	39.6	44.6	58.2	66.4	76.3	90.6	101.4	115.9
25 min	43.5	49.0	64.4	73.1	84.6	100.4	112.6	128.9
30 min	46.7	52.7	69.4	78.8	91.3	108.5	121.8	139.3
45 min	53.5	60.5	80.0	91.2	106.0	126.4	142.0	162.5
1 hr	58.2	66.0	87.6	100.0	116.1	138.6	156.1	178.8
1.5 hr	61.9	70.1	93.8	107.7	124.4	148.7	167.8	192.7
2 hr	64.5	73.1	98.2	113.5	130.1	155.6	175.5	201.7
3 hr	68.4	77.7	105.2	122.6	138.7	165.9	188.0	214.9
4.5 hr	72.7	82.5	113.1	132.8	151.7	177.8	200.6	229.5
6 hr	76.4	87.2	120.1	142.1	163.5	191.2	213.1	242.9
9 hr	82.5	94.4	131.8	157.6	182.8	217.1	243.5	278.3
12 hr	87.0	99.8	141.0	169.8	198.5	238.0	268.9	308.4
18 hr	95.8	109.4	156.9	191.1	225.9	274.4	313.4	359.2
24 hr	104.0	117.8	169.6	208.1	248.0	304.3	350.2	400.2
30 hr	111.9	127.1	182.1	224.8	269.5	333.3	385.8	440.6
36 hr	118.5	134.9	192.8	239.3	288.4	358.8	417.3	478.3
48 hr	129.2	148.0	210.4	263.5	319.9	402.0	470.9	540.7
72 hr	143.9	164.4	237.0	299.3	367.2	466.9	552.4	636.0
96 hr	152.1	175.4	256.1	325.5	401.3	513.9	611.2	703.2
120 hr	158.9	182.2	271.7	345.9	427.3	549.1	654.7	751.3
144 hr	163.0	186.3	285.0	362.6	447.9	575.9	687.2	789.3
168 hr	165.8	194.3	296.6	376.9	464.3	596.8	711.4	821.3

Appendix D: ARR Datahub files - Laidley Creek catchment

Results - ARR Data Hub

[STARTTXT]

Input Data Information

[INPUTDATA]

Latitude -27.727

Longitude 152.355

[END_INPUTDATA]

River Region

[RIVREG]

Division North East Coast

River Number 43

River Name Brisbane River

[RIVREG_META]

Time Accessed 08 September 2024 10:12AM

Version 2016_v1

[END_RIVREG]

ARF Parameters

[LONGARF]

Zone East Coast North

a 0.327

b 0.241

c 0.448

d 0.36

e 0.00096

f 0.48
g -0.21
h 0.012
i -0.0013

[LONGARF_META]

Time Accessed 08 September 2024 10:12AM

Version 2016_v1

[END_LONGARF]

Storm Losses

[LOSSES]

ID 12400

Storm Initial Losses (mm) 25

Storm Continuing Losses (mm/h) 1.4

[LOSSES_META]

Time Accessed 08 September 2024 10:12AM

Version 2016_v1

[END_LOSSES]

Temporal Patterns

[TP]

code ECnorth

Label East Coast North

[TP_META]

Time Accessed 08 September 2024 10:12AM

Version 2016_v2

[END_TP]

Areal Temporal Patterns

[ATP]

code ECnorth

arealabel East Coast North

[ATP_META]

Time Accessed 08 September 2024 10:12AM

Version 2016_v2

[END_ATP]

Median Preburst Depths and Ratios

[PREBURST]

min (h)\AEP(%)	50	20	10	5	2	1
60 (1.0)	0.2 (0.005)		1.4 (0.031)		2.3 (0.041)	3.1 (0.047)
6.2 (0.079)	8.5 (0.097)					
90 (1.5)	0.1 (0.002)		0.7 (0.013)		1.1 (0.017)	1.4 (0.020)
6.7 (0.076)	10.6 (0.107)					
120 (2.0)	0.0 (0.000)		0.7 (0.012)		1.1 (0.016)	1.5 (0.019)
9.0 (0.095)	14.7 (0.137)					
180 (3.0)	0.0 (0.000)		0.8 (0.013)		1.3 (0.018)	1.8 (0.021)
13.5 (0.128)	22.2 (0.187)					
360 (6.0)	0.2 (0.004)		1.5 (0.020)		2.3 (0.026)	3.2 (0.030)
10.6 (0.084)	16.2 (0.114)					
720 (12.0)	0.5 (0.007)		6.3 (0.067)		10.1 (0.090)	13.8 (0.106)
18.2 (0.116)	21.4 (0.121)					
1080 (18.0)	0.0 (0.000)		7.0 (0.065)		11.6 (0.090)	16.1 (0.107)
20.5 (0.114)	23.9 (0.116)					
1440 (24.0)	0.0 (0.000)		4.0 (0.033)		6.6 (0.046)	9.1 (0.055)
13.5 (0.067)	16.8 (0.073)					
2160 (36.0)	0.0 (0.000)		1.4 (0.010)		2.4 (0.014)	3.3 (0.017)
6.7 (0.028)	9.3 (0.034)					
2880 (48.0)	0.0 (0.000)		0.5 (0.003)		0.9 (0.005)	1.2 (0.005)
3.2 (0.012)	4.7 (0.015)					
4320 (72.0)	0.0 (0.000)		0.0 (0.000)		0.0 (0.000)	0.0 (0.000)
0.9 (0.003)	1.5 (0.004)					

[PREBURST_META]

Time Accessed 08 September 2024 10:12AM

Version 2018_v1

Note Preburst interpolation methods for catchment wide preburst has been slightly altered. Point values remain unchanged.

[END_PREBURST]From preburst class

10% Preburst Depths

[PREBURST10]

min (h)\AEP(%)	50	20	10	5	2	1
60 (1.0)	0.0 (0.000)		0.0 (0.000)		0.0 (0.000)	0.0 (0.000)
0.0 (0.000)	0.0 (0.000)					
90 (1.5)	0.0 (0.000)		0.0 (0.000)		0.0 (0.000)	0.0 (0.000)
0.0 (0.000)	0.0 (0.000)					
120 (2.0)	0.0 (0.000)		0.0 (0.000)		0.0 (0.000)	0.0 (0.000)
0.0 (0.000)	0.0 (0.000)					
180 (3.0)	0.0 (0.000)		0.0 (0.000)		0.0 (0.000)	0.0 (0.000)
0.0 (0.000)	0.0 (0.000)					
360 (6.0)	0.0 (0.000)		0.0 (0.000)		0.0 (0.000)	0.0 (0.000)
0.0 (0.000)	0.0 (0.000)					
720 (12.0)	0.0 (0.000)		0.0 (0.000)		0.0 (0.000)	0.0 (0.000)
0.0 (0.000)	0.0 (0.000)					
1080 (18.0)	0.0 (0.000)		0.0 (0.000)		0.0 (0.000)	0.0 (0.000)
0.0 (0.000)	0.0 (0.000)					
1440 (24.0)	0.0 (0.000)		0.0 (0.000)		0.0 (0.000)	0.0 (0.000)
0.0 (0.000)	0.0 (0.000)					
2160 (36.0)	0.0 (0.000)		0.0 (0.000)		0.0 (0.000)	0.0 (0.000)
0.0 (0.000)	0.0 (0.000)					
2880 (48.0)	0.0 (0.000)		0.0 (0.000)		0.0 (0.000)	0.0 (0.000)
0.0 (0.000)	0.0 (0.000)					
4320 (72.0)	0.0 (0.000)		0.0 (0.000)		0.0 (0.000)	0.0 (0.000)
0.0 (0.000)	0.0 (0.000)					

[PREBURST10_META]

Time Accessed 08 September 2024 10:12AM

Version 2018_v1

Note Preburst interpolation methods for catchment wide preburst has been slightly altered. Point values remain unchanged.

[END_PREBURST10]From preburst class

25% Preburst Depths

[PREBURST25]

min (h)\AEP(%)	50	20	10	5	2	1
----------------	----	----	----	---	---	---

60 (1.0)	0.0 (0.000)	0.0 (0.000)	0.0 (0.000)	0.0 (0.000)
0.3 (0.004)	0.5 (0.006)			
90 (1.5)	0.0 (0.000)	0.0 (0.000)	0.0 (0.000)	0.0 (0.000)
0.3 (0.003)	0.5 (0.005)			
120 (2.0)	0.0 (0.000)	0.0 (0.000)	0.0 (0.000)	0.0 (0.000)
0.1 (0.001)	0.2 (0.002)			
180 (3.0)	0.0 (0.000)	0.0 (0.000)	0.0 (0.000)	0.0 (0.000)
0.2 (0.002)	0.4 (0.003)			
360 (6.0)	0.0 (0.000)	0.0 (0.000)	0.0 (0.000)	0.0 (0.000)
0.2 (0.001)	0.3 (0.002)			
720 (12.0)	0.0 (0.000)	0.0 (0.000)	0.0 (0.000)	0.0 (0.000)
1.5 (0.010)	2.7 (0.015)			
1080 (18.0)	0.0 (0.000)	0.2 (0.002)	0.3 (0.003)	0.5 (0.003)
1.9 (0.010)	2.9 (0.014)			
1440 (24.0)	0.0 (0.000)	0.0 (0.000)	0.0 (0.000)	0.0 (0.000)
0.0 (0.000)	0.0 (0.000)			
2160 (36.0)	0.0 (0.000)	0.0 (0.000)	0.0 (0.000)	0.0 (0.000)
0.0 (0.000)	0.0 (0.000)			
2880 (48.0)	0.0 (0.000)	0.0 (0.000)	0.0 (0.000)	0.0 (0.000)
0.0 (0.000)	0.0 (0.000)			
4320 (72.0)	0.0 (0.000)	0.0 (0.000)	0.0 (0.000)	0.0 (0.000)
0.0 (0.000)	0.0 (0.000)			

[PREBURST25_META]

Time Accessed 08 September 2024 10:12AM

Version 2018_v1

Note Preburst interpolation methods for catchment wide preburst has been slightly altered. Point values remain unchanged.

[END_PREBURST25]From preburst class

75% Preburst Depths

[PREBURST75]

min (h)\AEP(%)	50	20	10	5	2	1
60 (1.0)	4.8 (0.146)	18.1 (0.389)	27.0 (0.480)	35.4 (0.540)		
32.8 (0.419)	30.8 (0.349)					
90 (1.5)	3.7 (0.100)	12.7 (0.244)	18.7 (0.298)	24.5 (0.333)		
46.1 (0.524)	62.3 (0.628)					
120 (2.0)	2.5 (0.064)	11.2 (0.199)	16.9 (0.250)	22.4 (0.283)		
64.7 (0.681)	96.3 (0.899)					
180 (3.0)	3.0 (0.068)	22.4 (0.359)	35.3 (0.470)	47.6 (0.542)		
71.9 (0.684)	90.2 (0.759)					
360 (6.0)	14.8 (0.271)	29.6 (0.393)	39.5 (0.437)	48.9 (0.465)		
65.5 (0.520)	78.0 (0.547)					
720 (12.0)	15.1 (0.222)	28.7 (0.307)	37.7 (0.338)	46.4 (0.357)		
72.3 (0.463)	91.8 (0.518)					
1080 (18.0)	16.0 (0.205)	33.0 (0.307)	44.2 (0.344)	55.0 (0.367)		

65.4 (0.362)	73.3 (0.356)			
1440 (24.0)	10.5 (0.122)	21.0 (0.176)	28.0 (0.196)	34.6 (0.207)
58.7 (0.290)	76.7 (0.332)			
2160 (36.0)	10.9 (0.111)	16.4 (0.119)	20.0 (0.120)	23.4 (0.120)
31.2 (0.131)	37.0 (0.135)			
2880 (48.0)	2.1 (0.019)	8.2 (0.054)	12.2 (0.066)	16.0 (0.073)
30.5 (0.114)	41.4 (0.134)			
4320 (72.0)	0.0 (0.000)	4.9 (0.029)	8.2 (0.039)	11.3 (0.045)
20.0 (0.064)	26.5 (0.073)			

[PREBURST75_META]

Time Accessed 08 September 2024 10:12AM

Version 2018_v1

Note Preburst interpolation methods for catchment wide preburst has been slightly altered. Point values remain unchanged.

[END_PREBURST75]From preburst class

90% Preburst Depths

[PREBURST90]

min (h)\AEP(%)	50	20	10	5	2	1
60 (1.0)	15.7 (0.481)	60.0 (1.289)	89.4 (1.592)	117.5 (1.791)		
105.2 (1.343)	96.0 (1.089)					
90 (1.5)	19.9 (0.540)	60.6 (1.160)	87.5 (1.390)	113.3 (1.539)		
151.7 (1.724)	180.5 (1.818)					
120 (2.0)	27.1 (0.679)	52.3 (0.929)	69.0 (1.018)	85.1 (1.072)		
158.2 (1.667)	213.0 (1.989)					
180 (3.0)	27.2 (0.611)	73.4 (1.175)	104.0 (1.385)	133.4 (1.519)		
139.1 (1.323)	143.3 (1.207)					
360 (6.0)	39.6 (0.728)	74.0 (0.982)	96.8 (1.072)	118.6 (1.127)		
164.0 (1.301)	198.1 (1.389)					
720 (12.0)	35.7 (0.526)	65.5 (0.701)	85.3 (0.763)	104.2 (0.801)		
156.6 (1.002)	195.8 (1.105)					
1080 (18.0)	31.5 (0.404)	63.4 (0.590)	84.6 (0.658)	104.8 (0.699)		
119.0 (0.658)	129.6 (0.629)					
1440 (24.0)	34.9 (0.406)	58.8 (0.493)	74.6 (0.522)	89.7 (0.537)		
114.9 (0.568)	133.8 (0.579)					
2160 (36.0)	37.1 (0.376)	43.9 (0.318)	48.4 (0.291)	52.7 (0.270)		
90.2 (0.378)	118.2 (0.431)					
2880 (48.0)	27.1 (0.252)	38.4 (0.252)	45.8 (0.248)	53.0 (0.243)		
86.6 (0.323)	111.8 (0.361)					
4320 (72.0)	9.5 (0.079)	25.7 (0.149)	36.3 (0.172)	46.6 (0.184)		
65.1 (0.208)	79.0 (0.218)					

[PREBURST90_META]

Time Accessed 08 September 2024 10:12AM

Appendix E: RORB catchment file

```

C Laidley Creek
C
C #FILE COMMENTS
C 0
C
C #SUB-AREA AREA COMMENTS
C 0
C
C #IMPERVIOUS FRACTION COMMENTS
C 0
C
C #BACKGROUND IMAGE
C T F
C
C #NODES
C 36
C 1      95.000      95.000      1.000 1 0      3 Subcatchment
C 13.918520      0.000000 0 0 0
C
C 2      92.891      53.309      1.000 1 0      3 Subcatchment
C 7.407192      0.000000 0 0 0
C
C 3      90.484      60.233      1.000 0 0      4
C 0.000000      0.000000 0 0 0
C
C 4      88.047      60.204      1.000 0 0      6
C 0.000000      0.000000 0 0 0
C
C 5      90.239      46.882      1.000 1 0      4 Subcatchment
C 12.661318      0.000000 0 0 0
C
C 6      86.814      60.197      1.000 0 0      8
C 0.000000      0.000000 0 0 0
C
C 7      89.535      87.993      1.000 1 0      6 Subcatchment
C 3.893288      0.000000 0 0 0
C
C 8      85.356      60.283      1.000 1 0      9 Subcatchment
C 8.606579      0.000000 0 0 0
C
C 9      83.915      60.283      1.000 0 0      11
C 0.000000      0.000000 0 0 0
C
C 10     84.906      80.382      1.000 1 0      9 Subcatchment
C 4.189867      0.000000 0 0 0
C
C 11     76.262      60.167      1.000 0 0      12
C 0.000000      0.000000 0 0 0
C
C 12     73.371      60.198      1.000 1 0      14 Subcatchment
C 23.696005      0.000000 0 0 0
C
C 13     86.367      16.621      1.000 1 0      11 Subcatchment
C 9.419337      0.000000 0 0 0
C
C 14     69.635      60.284      1.000 0 0      16
C 0.000000      0.000000 0 0 0
C
C 15     77.910      23.860      1.000 1 0      14 Subcatchment
C 14.119680      0.000000 0 0 0
C
C 16     65.765      60.370      1.000 0 0      18
C 0.000000      0.000000 0 0 0
C
C 17     74.307      13.842      1.000 1 0      16 Subcatchment
C 28.255606      0.000000 0 0 0
C
C 18     57.186      60.082      1.000 1 0      19 Subcatchment
C 56.592533      0.000000 0 0 0
C
C 19     51.063      59.987      1.000 0 0      20

```

0.000000	0.000000	0	0	0					
C Mulgowie TM									
C 20	42.602		60.072	1.000	1	0	21	Subcatchment	
C 12	41.276543		0.000000	0	0	0			
C 21	31.585		60.486	1.000	0	0	22		
C 0.000000	0.000000	0	0	0					
C 22	25.249		60.385	1.000	1	0	23	Subcatchment	
C 13	23.390030		0.000000	0	0	0			
C 23	16.911		60.495	1.000	0	0	24		
C 0.000000	0.000000	0	0	0					
C 24	14.714		60.375	1.000	0	0	28		
C 0.000000	0.000000	0	0	0					
C 25	48.329		92.470	1.000	1	0	26	Subcatchment	
C 14	25.320984		0.000000	0	0	0			
C 26	33.685		92.513	1.000	0	0	27		
C 0.000000	0.000000	0	0	0					
C 27	27.167		92.641	1.000	1	0	23	Subcatchment	
C 15	18.146849		0.000000	0	0	0			
C 28	10.724		60.169	1.000	1	0	36	Subcatchment	
C 20	17.716366		0.000000	0	0	0			
C 29	70.865		5.000	1.000	1	0	31	Subcatchment	
C 16	48.529217		0.000000	0	0	0			
C 30	49.582		13.393	1.000	1	0	31	Subcatchment	
C 17	7.546566		0.000000	0	0	0			
C 31	41.564		25.328	1.000	0	0	32		
C 0.000000	0.000000	0	0	0					
C 32	32.689		25.617	1.000	1	0	33	Subcatchment	
C 18	43.470638		0.000000	0	0	0			
C 33	23.214		33.806	1.000	0	0	34		
C 0.000000	0.000000	0	0	0					
C 34	18.898		46.223	1.000	1	0	24	Subcatchment	
C 19	44.153233		0.000000	0	0	0			
C 35	3.558		60.252	1.000	0	1	0	Subcatchment	
C 19	44.153233		0.000000	70	0	0			
C 36	4.507		67.084	1.000	0	0	35		
C 0.000000	0.000000	0	0	0					
C #REACHES									
C 35									
C 1	1 0		1 3		0	1	0	4.078	
C 2.550	92.378								
C 2	75.406		2 3		0	1	0	1.064	
C 4.793	1 0								
C 3	91.490		3 4		0	1	0	1.780	
C 1.854	57.147								
C 4	1 0		5 4		0	1	0	2.243	
C 2.853	89.161								
C 89.284	60.233								

C		52.754					
C	5		4	6	0 1 0	0.950	
1.368		1 0					
C		87.452					
C		60.233					
C	6		7	6	0 1 0	2.013	
2.534		1 0					
C		88.523					
C		76.680					
C	7		6	8	0 1 0	1.563	
0.576		1 0					
C		86.194					
C		60.197					
C	8		8	9	0 1 0	1.866	
0.589		1 0					
C		84.669					
C		60.240					
C	9		10	9	0 1 0	1.305	
3.142		1 0					
C		84.542					
C		71.321					
C	10		9	11	0 1 0	5.228	
0.574		1 0					
C		81.512					
C		60.152					
C	11		11	12	0 1 0	1.050	
0.476		1 0					
C		74.259					
C		60.112					
C	12		13	11	0 1 0	4.746	
2.507		1 0					
C		80.393					
C		39.813					
C	13		12	14	0 1 0	3.385	
0.384		1 0					
C		70.959					
C		60.284					
C	14		15	14	0 1 0	5.797	
2.191		1 0					
C		74.073					
C		39.620					
C	15		14	16	0 1 0	2.890	
0.277		1 0					
C		67.256					
C		60.284					
C	16		17	16	0 1 0	6.668	
1.275		1 0					
C		70.639					
C		33.714					
C	17		16	18	0 1 0	5.480	
0.383		1 0					
C		60.353					
C		60.082					
C	18		18	19	0 1 0	4.756	
0.147		1 0					
C		54.012					
C		60.029					
C	19		19	20	0 1 0	5.150	
0.369		1 0					
C		46.456					
C		59.987					
C	20		20	21	0 1 0	6.420	
0.280		1 0					
C		35.248					
C		60.085					
C	21		21	22	0 1 0	3.160	
0.222		1 0					
C		28.097					
C		60.343					
C	22		22	23	0 1 0	6.732	
0.193		1 0					

C		20.417				
C		60.471				
C	23		23	24	0 1 0	0.364
C	0.000	1 0				
C		15.812				
C		60.334				
C	24		25	26	0 1 0	5.990
C	0.351	1 0				
C		41.201				
C		92.469				
C	25		26	27	0 1 0	0.865
C	0.578	1 0				
C		30.379				
C		92.638				
C	26		27	23	0 1 0	5.109
C	0.078	1 0				
C		22.677				
C		78.904				
C	27		24	28	0 1 0	1.622
C	0.432	1 0				
C		13.123				
C		60.210				
C	28		29	31	0 1 0	11.985
C	0.834	1 0				
C		53.782				
C		17.230				
C	29		30	31	0 1 0	3.623
C	1.021	1 0				
C		45.880				
C		18.715				
C	30		31	32	0 1 0	2.918
C	0.548	1 0				
C		36.942				
C		25.328				
C	31		32	33	0 1 0	5.685
C	0.299	1 0				
C		27.587				
C		29.371				
C	32		33	34	0 1 0	3.328
C	0.300	1 0				
C		21.296				
C		39.499				
C	33		34	24	0 1 0	4.090
C	0.147	1 0				
C		16.462				
C		54.267				
C	34		28	36	0 1 0	3.311
C	0.000	1 0				
C		7.615				
C		63.627				
C	35		36	35	0 1 0	0.000
C	0.000	1 0				
C		4.032				
C		63.668				
C						
C	#STORAGES					
C	0					
C						
C	#INFLOW/OUTFLOW					
C	0					
C						
C	END RORB_GE					
C						
1						
1, 4.078, -99						
Sub-area Subcatchment 1, Reach	- Generate rainfall	Reach 1 node 1				
downstream		excess h'graph and route				
3						
Store running hydrograph						
1, 1.064, -99						
Sub-area Subcatchment 2, Reach	- Generate rainfall	Reach 2 node 2				
		excess h'graph and route				

```

downstream
4
Add running h'graph to last stored h'graph      ,
5, 1.780, -99                                   ,Reach 3
Reach - Route running h'graph downstream
3
Store running hydrograph
1, 2.243, -99                                   ,Reach 4 node 5
Sub-area Subcatchment 3, Reach - Generate rainfall excess h'graph and route
downstream
4
Add running h'graph to last stored h'graph      ,
5, .950, -99                                    ,Reach 5
Reach - Route running h'graph downstream
3
Store running hydrograph
1, 2.013, -99                                   ,Reach 6 node 7
Sub-area Subcatchment 4, Reach - Generate rainfall excess h'graph and route
downstream
4
Add running h'graph to last stored h'graph      ,
5, 1.563, -99                                   ,Reach 7
Reach - Route running h'graph downstream
2, 1.866, -99                                   ,Reach 8 node 8
Sub-area Subcatchment 5, Reach - Generate rainfall excess h'graph, add to
running h'graph, and route downstream
3
Store running hydrograph
1, 1.305, -99                                   ,Reach 9 node 10
Sub-area Subcatchment 6, Reach - Generate rainfall excess h'graph and route
downstream
4
Add running h'graph to last stored h'graph      ,
5, 5.228, -99                                   ,Reach 10
Reach - Route running h'graph downstream
3
Store running hydrograph
1, 4.746, -99                                   ,Reach 12 node 13
Sub-area Subcatchment 7, Reach - Generate rainfall excess h'graph and route
downstream
4
Add running h'graph to last stored h'graph      ,
5, 1.050, -99                                   ,Reach 11
Reach - Route running h'graph downstream
2, 3.385, -99                                   ,Reach 13 node 12
Sub-area Subcatchment 8, Reach - Generate rainfall excess h'graph, add to
running h'graph, and route downstream
3
Store running hydrograph
1, 5.797, -99                                   ,Reach 14 node 15
Sub-area Subcatchment 9, Reach - Generate rainfall excess h'graph and route
downstream
4
Add running h'graph to last stored h'graph      ,
5, 2.890, -99                                   ,Reach 15
Reach - Route running h'graph downstream
3
Store running hydrograph
1, 6.668, -99                                   ,Reach 16 node 17
Sub-area Subcatchment 10, Reach - Generate rainfall excess h'graph and
route downstream
4
Add running h'graph to last stored h'graph      ,
5, 5.480, -99                                   ,Reach 17
Reach - Route running h'graph downstream
2, 4.756, -99                                   ,Reach 18 node 18
Sub-area Subcatchment 11, Reach - Generate rainfall excess h'graph, add to
running h'graph, and route downstream
5, 5.150, -99                                   ,Reach 19
Reach - Route running h'graph downstream
2, 6.420, -99                                   ,Reach 20 node 20

```

```

Sub-area Subcatchment 12, Reach - Generate rainfall excess h'graph, add to
running h'graph, and route downstream
5, 3.160, -99 ,Reach 21
Reach - Route running h'graph downstream
2, 6.732, -99 ,Reach 22 node 22
Sub-area Subcatchment 13, Reach - Generate rainfall excess h'graph, add to
running h'graph, and route downstream
3 ,
Store running hydrograph
1, 5.990, -99 ,Reach 24 node 25
Sub-area Subcatchment 14, Reach - Generate rainfall excess h'graph and
route downstream
5, .865, -99 ,Reach 25
Reach - Route running h'graph downstream
2, 5.109, -99 ,Reach 26 node 27
Sub-area Subcatchment 15, Reach - Generate rainfall excess h'graph, add to
running h'graph, and route downstream
4 ,
Add running h'graph to last stored h'graph
5, .364, -99 ,Reach 23
Reach - Route running h'graph downstream
3 ,
Store running hydrograph
1, 11.985, -99 ,Reach 28 node 29
Sub-area Subcatchment 16, Reach - Generate rainfall excess h'graph and
route downstream
3 ,
Store running hydrograph
1, 3.623, -99 ,Reach 29 node 30
Sub-area Subcatchment 17, Reach - Generate rainfall excess h'graph and
route downstream
4 ,
Add running h'graph to last stored h'graph
5, 2.918, -99 ,Reach 30
Reach - Route running h'graph downstream
2, 5.685, -99 ,Reach 31 node 32
Sub-area Subcatchment 18, Reach - Generate rainfall excess h'graph, add to
running h'graph, and route downstream
5, 3.328, -99 ,Reach 32
Reach - Route running h'graph downstream
2, 4.090, -99 ,Reach 33 node 34
Sub-area Subcatchment 19, Reach - Generate rainfall excess h'graph, add to
running h'graph, and route downstream
4 ,
Add running h'graph to last stored h'graph
5, 1.622, -99 ,Reach 27
Reach - Route running h'graph downstream
2, 3.311, -99 ,Reach 34 node 28
Sub-area Subcatchment 20, Reach - Generate rainfall excess h'graph, add to
running h'graph, and route downstream
5, .000, -99 ,Reach 35
Reach - Route running h'graph downstream
7 ,
PRINT

```

7.1 in FIT run

```

0
C Sub Area Data
C Areas, km**2, of subareas A,B...
13.91852, 7.40719, 12.66132, 3.89329, 8.60658,
4.18987, 9.41934, 23.69600, 14.11968, 28.25561,
56.59253, 41.27654, 23.39003, 25.32098, 18.14685,
48.52922, 7.54657, 43.47064, 44.15323, 17.71637,
-99
C Impervious Fraction Data
0, -99 ,No impervious areas in
system

```


Appendix F: Calibration storm event files

F1: May 1996 event

Calibration summary

Event ID	May 96
Start Date	30/04/1996 17:00
End Date	6/05/1996 10:00
Duration (hours)	0:00
Number of peaks	2
Maximum gauged discharge at 143229A (m3/s)	496.592
Supplementary peak discharge (m3/s)	470.6

Total event rainfall record				
Station name	Station ID	Recorded rainfall Burst 1 (mm)	Recorded rainfall Burst 2 (mm)	Notes
Forest Hill	040079	270	151.1	
Upper Tenthill	040388	195.6	174.2	
UQ Gatton	040082	287	141.7	
Franklyn Vale	040374	304.5	156	
Placid Hills	040449	265.5	154	
Townson	040675	371.4	304.8	
Gatton DAFF	040436	277.8	148.4	
Hattonvale	040095	355	143.4	
Mt Berryman	040310	231.2	137.6	
Thornton	040751	331.4	219.4	
Average proportion		0.636	0.364	

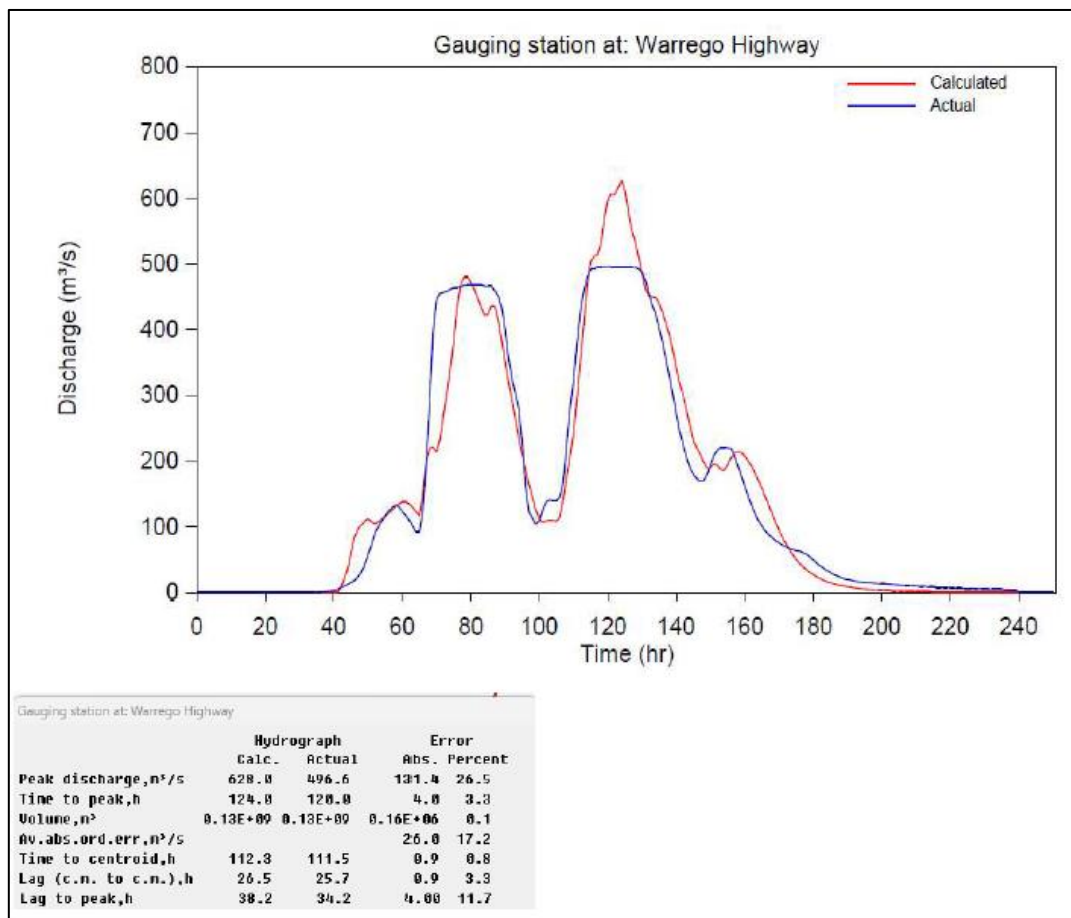
Subcatchment centroid event rainfall depths from QGIS Interpolation		
Subcatchment ID	Rainfall depth Burst 1 (mm)	Rainfall depth Burst 2 (mm)
1	405.9	232.7
2	415.7	238.4
3	416.9	239.1
4	426.4	244.5
5	423.0	242.5
6	415.4	238.1
7	390.6	224.0
8	351.8	201.7
9	360.7	206.8
10	337.1	193.2
11	325.9	186.8
12	275.8	158.1
13	277.2	159.0
14	282.7	162.1
15	274.6	157.4
16	253.0	145.0
17	256.8	147.3
18	270.9	155.4
19	274.2	157.2
20	272.3	156.1

RORS gauged data statistics			
Peak flow (m3/s)	Total flow volume (m3)	Time to peak (hrs)	Time to centroid (hrs)
496.6	1.30E+08	120	111.5

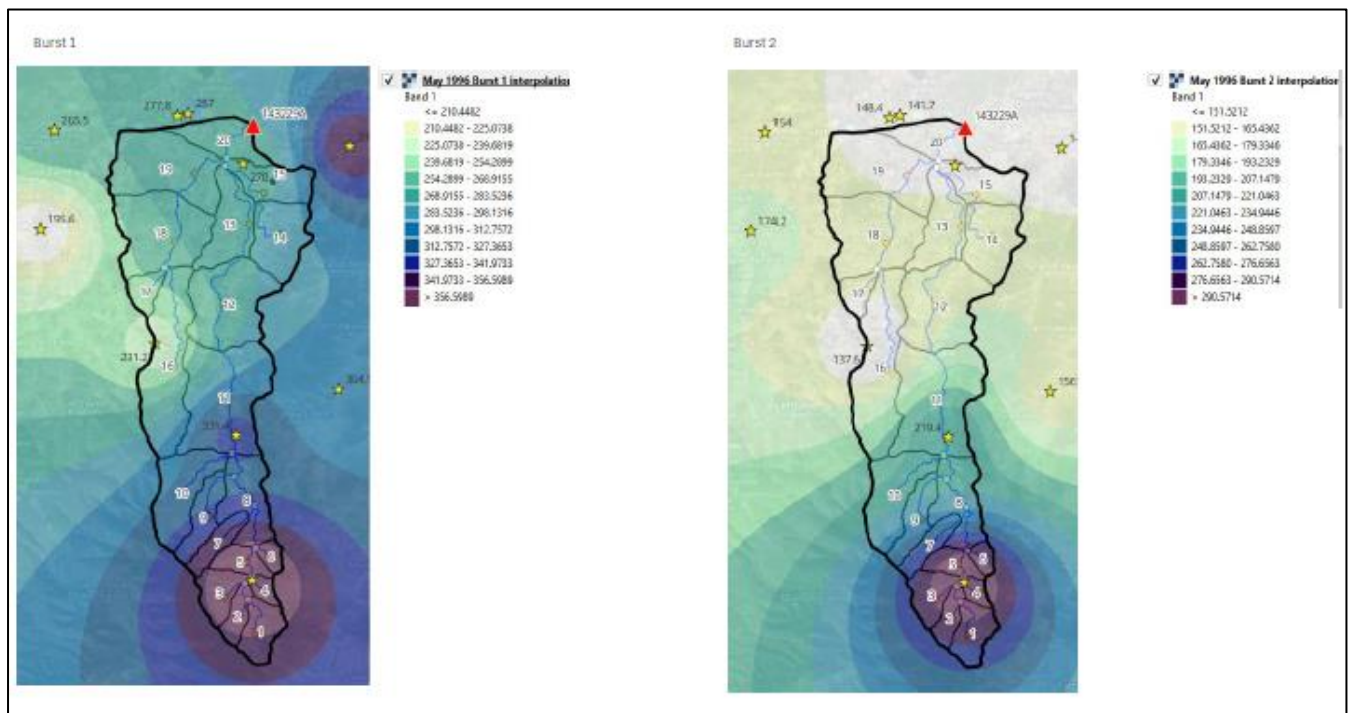
RORS calibrated parameters and statistics											
m	kc	IL 1	CL 1	IL 2	CL 2	Peak flow (m3/s)	Error (%)	Total flow volume (m3)	Error (%)	Time to peak (hrs)	Error (%)
0.8	27	100	2.66	0	0.07	618.3	24.5	1.30E+08	0.1	109	-9.2
0.8	28	100	2.66	0	0.07	609	22.6	1.30E+08	0.1	109	-9.2
0.8	26	80	2.98	0	0.07	627.7	26.4	1.30E+08	0.1	109	-9.2
0.8	26	120	2.22	0	0.07	628.4	26.5	1.30E+08	0.1	109	-9.2
0.8	26	100	2.66	2	0.02	632.2	27.3	1.30E+08	0.1	109	-9.2
0.8	26	100	2.66	0	0.07	628	26.5	1.30E+08	0.1	109	-9.2
0.8	26	100	2.66	0	0.07	628	26.5	1.60E+05	0.1	124	3.3

Best shape resemblance
15 hr translation

Calibrated hydrograph



QGIS event rainfall interpolation



RORB Storm file

[illegible]

F2: November 2008 event

Event calibration summary

Event ID Nov-08
 Start Date 18/11/2008 10:00
 End Date 20/11/2008 9:00
 Duration (hours) 48
 Number of peaks 1
 Maximum gauged
 discharge at 143229A
 (m³/s) 255.9
 Supplementary peak
 discharge (m³/s) n/a

Total event rainfall record			
Station name	Station ID	Recorded rainfall (mm)	Notes
Forest Hill	040079	129.9	
Mt Berryman	040310	177.7	
Upper Tenthill	040388	116.4	
UQ Gatton	040082	203.6	
Franklyn Vale	040374	148	
Franklyn Vale Alert	040912	171	
Gatton Allan St	040083	218.2	
Placid Hills	040449	173.2	
Townson	040675	138.6	
Bremer River	WMIP	108	
Gatton DAFF	040436	197.6	
Grandchester	040091	248.8	
Hattonvale	040095	216.4	

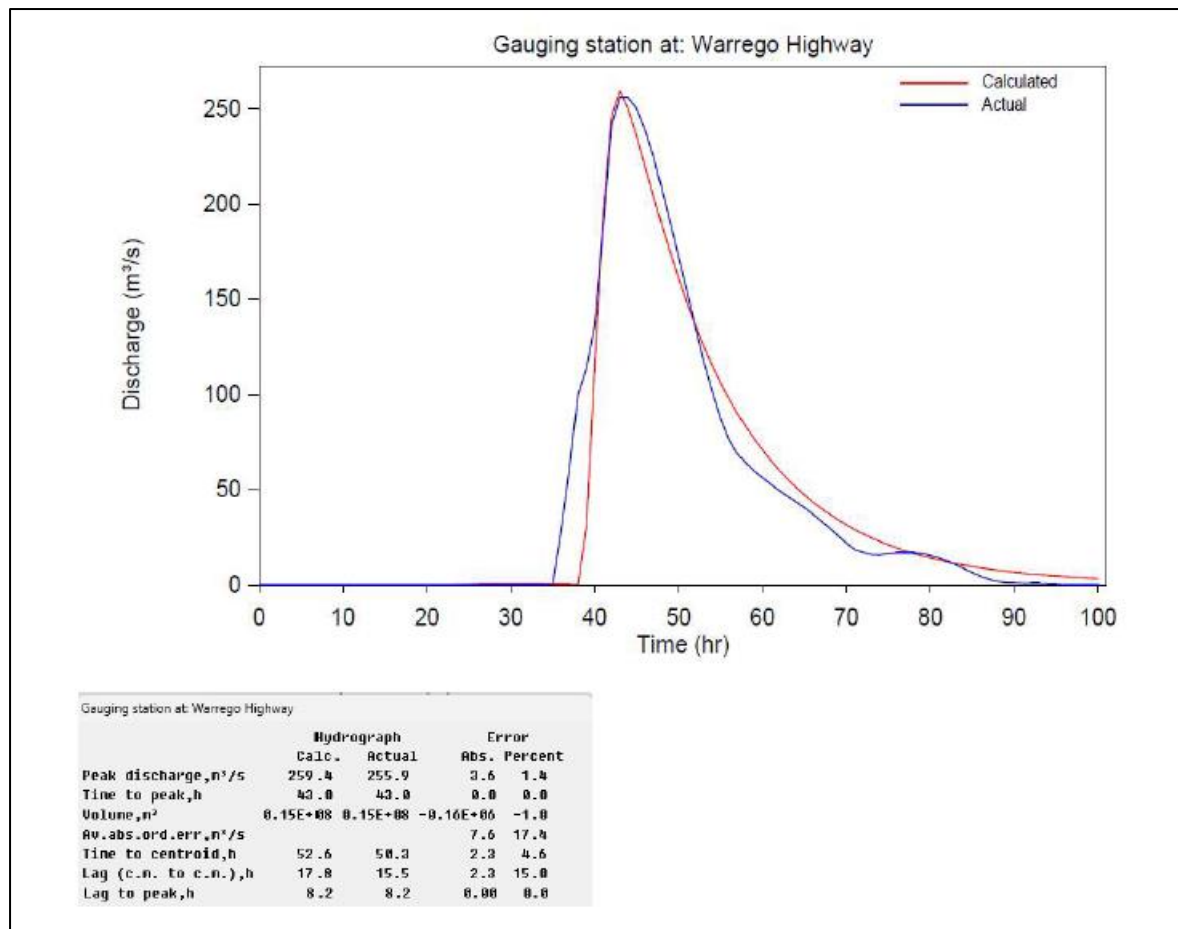
Subcatchment centroid event rainfall depths from QGIS interpolation	
Subcatchment ID	Rainfall depth (mm)
1	144.3
2	141.8
3	141.4
4	139.3
5	139.9
6	141.5
7	146.8
8	157.4
9	154.8
10	163.7
11	174.9
12	185.7
13	200.9
14	210.1
15	204.2
16	177.6
17	177.4
18	185.8
19	197.8
20	200.5

RORB gauged data statistics			
Peak flow (m ³ /s)	Total flow volume (m ³)	Time to peak (hrs)	Time to centroid (hrs)
255.9	1.50E+07	43	50.3

RORB calibrated parameters and statistics											
m	kc	IL	CL	Peak flow (m ³ /s)	Error (%)	Total flow volume (m ³)	Error (%)	Time to peak (hrs)	Error (%)	Time to centroid (hrs)	Error (%)
0.8	39	100	7.43	257	0.4	1.50E+07	-1.4	40	-7	49.1	-2.3
0.8	35	100	7.43	286.1	11.8	1.49E+07	-1.1	39	-9.3	47.8	-5
0.8	35	75	9.95	246.5	-3.7	1.49E+07	-0.9	39	-9.3	49.1	-2.2
0.8	35	77	9.78	250.8	-2	1.49E+07	-0.9	39	-9.3	49.1	-2.2
0.8	34	77	9.78	259.4	1.4	1.49E+07	-0.7	39	-9.3	48.7	-3
0.8	34	77	9.78	259.4	1.4	1.48E+07	-1	43	0	52.6	4.6

4 hr translation

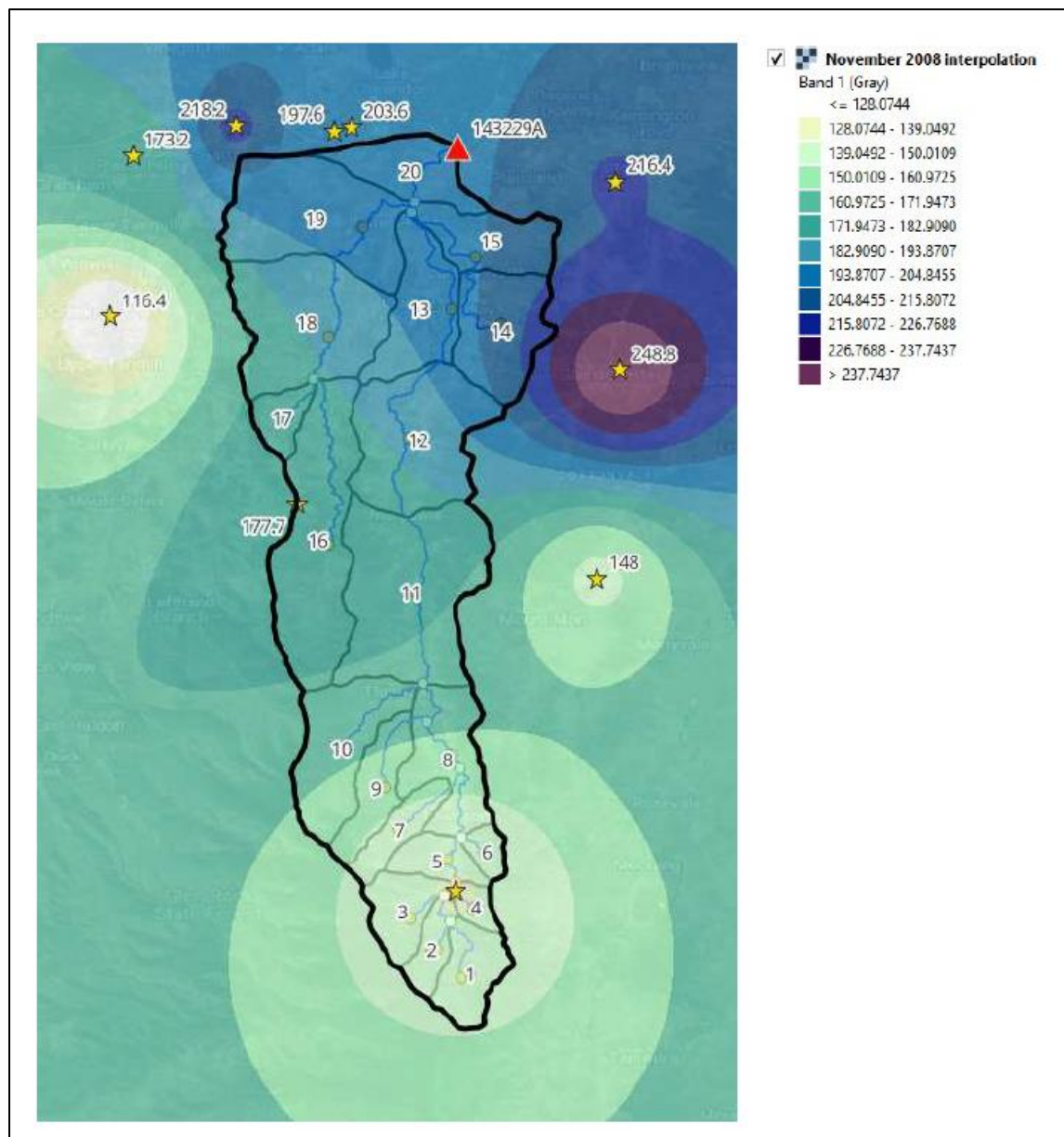
Calibrated hydrograph



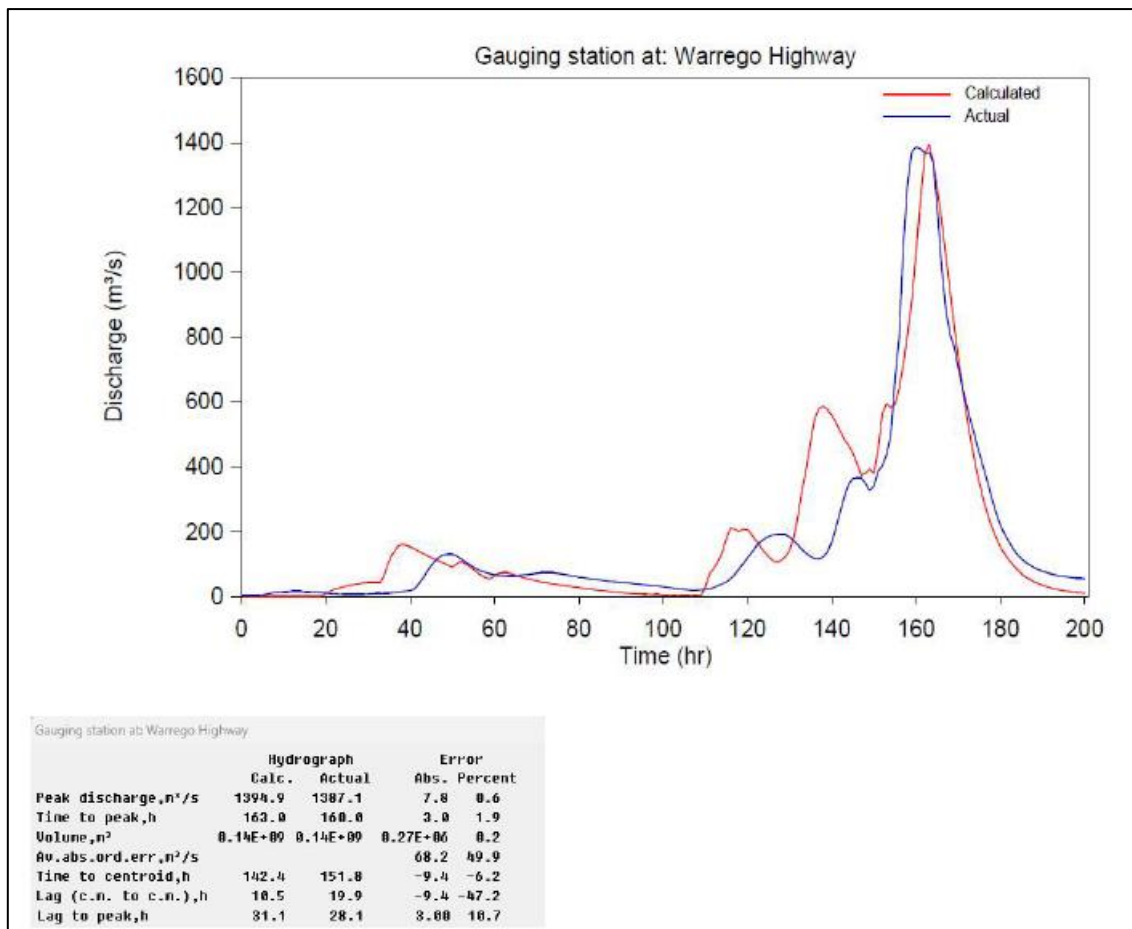
RORB Storm file

[illegible]

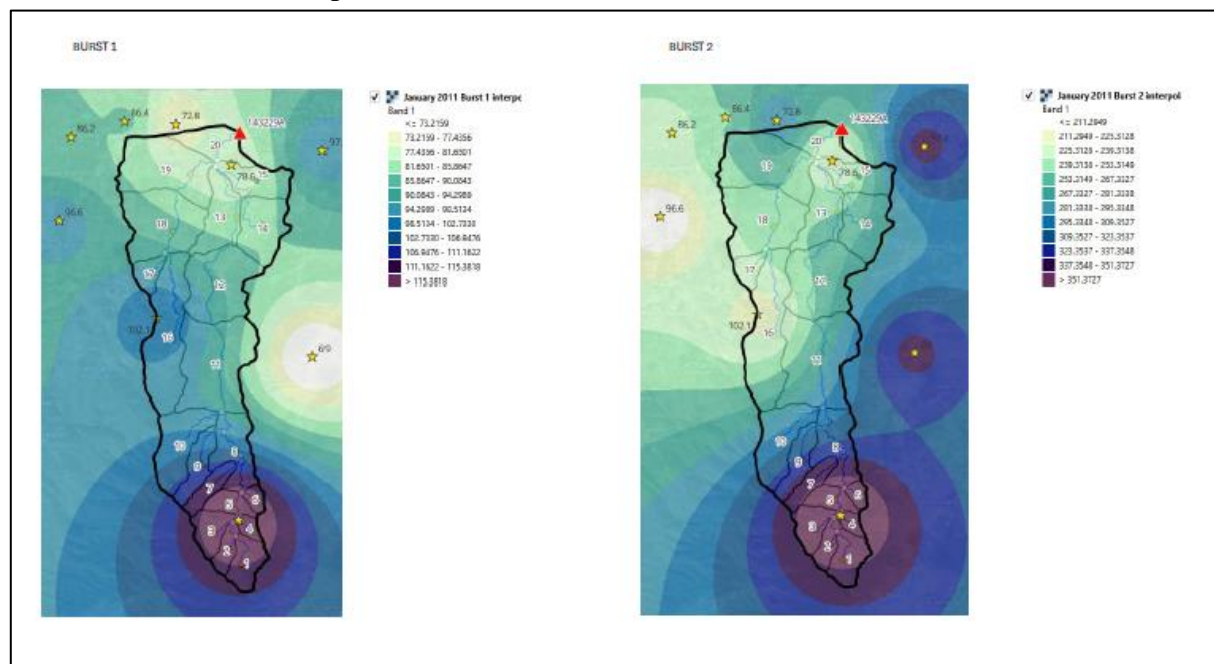
QGIS event rainfall interpolation



Calibrated hydrograph



QGIS event rainfall interpolation



RORB Storm file

```
5-12 January 2011
FIT
C      time inc = 1 hr, calcs for 250 incs, 2 bursts
C      2 pluvios, non uniform pattern
1,290,2,2,1,-99,
0,106,107,168, rain from 0 - 168 time incs
Upper Tenthill
0,0,0,0,0,0,0,0,0,0,0,0,0,0,0,1,0,1,7,1,0,1,0,0,0,1,2,1,0,0,1,2,2,19,9,1,1,1,
0,0,0,0,0,0,0,0,0,0,0,0,0,3,13,1,0,0,0,0,0,0,4,7,9,2,0,1,0,0,0,0,0,0,3,3,0,0,0,0,0,0,
0,0,0,0,0,1,0,0,0,0,0,0,0,1,0,0,0,0,0,0,0,0,0,0,0,0,0,0,0,0,0,0,0,4,17,1,0,7,5,10
,3,1,4,6,0,1,1,0,0,0,0,1,3,0,3,1,2,1,1,8,0,1,0,0,0,0,0,2,2,0,0,0,11,1,4,28,12
,2,0,2,2,9,9,10,17,14,1,1,0,1,0,0,0,-99, mm/hr
Bremer River
0,0,0,0,0,0,0,0,0,0,0,0,0,0,0,0,0,0,0,0,0,21,1,2,1,0,1,0,0,0,0,2,1,1,0,1,3,7,13,6,3,3
,2,1,0,0,0,0,0,0,0,0,0,0,0,0,0,0,0,0,0,0,0,1,6,2,7,0,0,0,0,0,0,0,0,0,0,0,0,0,0,0,0,
0,0,0,0,0,0,0,0,0,0,0,0,0,1,0,0,0,0,0,0,1,1,0,0,0,0,0,0,0,0,0,0,0,1,11,1,0,1,2,0,0,
0,1,2,0,0,1,0,0,0,0,0,0,3,5,0,14,16,9,6,8,5,1,2,1,0,2,0,3,0,4,1,0,4,1,0,0,3,2,2
0,14,20,4,8,9,11,11,32,5,2,1,0,0,0,0,-99,mm/hr
C      sub catchment rainfalls from isohyetal map
115.4,117.2,117.6,119,118.6,117.2,113.2,102.5,107,100.7,91.3,91.1,83.6,85.1,8
1.4,100.95,8,87.8,80.5,79.3,-99, Sub area event total rainfalls B1
354.4,359.3,359.9,364.2,363,360,348,326.1,329.1,302.2,273,254.2,253.6,267.1,2
43.8,228.5,234.1,248.2,253,241,-99, Sub area event total rainfalls B2
C      pluivo reference numbers
2,2,2,2,2,2,2,2,2,2,2,2,2,2,2,2,1,1,1,1,-99,
2,2,2,2,2,2,2,2,2,2,2,2,2,2,2,2,1,1,1,1,-99,
C Hydrograph data
0,287,-99,
Warrego Highway
3.919,3.875,3.864,3.831,3.809,4.938,7.674,10.422,12.656,14.259,15.462,16.102,
16.363,16.409,16.409,16.141,15.53,14.647,13.629,12.555,11.254,10.029,8.95,8.0
77,7.455,7.006,6.713,6.663,6.958,7.461,7.79,9.017,9.762,10.036,10.187,10.679,
11.922,13.791,15.538,17.315,18.77,23.58,39.874,57.183,77.245,95.644,111.501,1
22.89,130.212,131.443,131.443,126.975,118.404,109.115,99.977,91.566,84.402,78
.418,74.157,70.749,68.636,67.025,65.901,65.247,65.117,65.443,66.626,67.759,69
.043,70.749,72.097,72.95,73.207,73.207,73.207,72.608,70.416,68.365,66.164,63.
889,61.052,59.518,57.419,55.493,53.728,51.952,50.327,48.846,47.347,46.283,44.
894,43.536,42.351,40.915,39.561,38.241,36.913,35.415,33.884,32.251,30.642,28.
953,27.337,25.501,23.821,22.342,20.852,19.751,20.069,21.349,22.662,24.034,27.
879,34.162,39.874,46.033,56.479,68.839,84.691,102.764,121.337,138.023,155.239
,168.366,177.775,185.421,189.985,190.724,190.724,190.724,183.799,172.081,159.
681,146.354,133.793,124.065,117.9,116.273,123.803,138.595,171.061,218.887,265
.593,313.575,348.347,364.829,366.386,366.386,348.646,326.45,340.333,388.423,4
04.542,437.892,498.251,667.074,800.261,1083.633,1273.241,1372.328,1387.109,13
81.047,1368.531,1369.148,1338.868,1187.874,1012.437,882.031,807.598,773.223,7
06.365,644.259,589.968,539.88,491.23,441.647,397.996,351.051,302.981,257.967,
221.794,191.465,167.698,147.253,129.261,115.777,104.924,96.821,89.126,82.4,78
.509,74.244,70.582,67.894,65.508,63.25,61.924,59.945,58.372,57.656,56.188,54.
976,53.954,52.779,51.569,50.864,50.488,50.381,49.713,49.075,48.437,47.799,47.
161,46.523,45.886,45.248,44.61,44.017,43.424,42.831,42.238,41.645,41.052,39.9
63,38.772,37.582,36.391,35.372,34.79,34.207,33.624,32.883,32.021,31.159,30.29
6,29.333,28.353,27.372,26.385,25.366,24.346,23.327,22.427,21.685,20.942,20.19
9,19.708,19.316,18.924,18.532,18.301,18.07,17.839,17.611,17.389,17.167,16.945
,16.707,16.457,16.206,15.956,15.683,15.407,15.13,14.866,14.672,14.479,14.286,
14.092,13.897,13.702,13.507,13.308,13.108,12.907,12.707,12.465,12.223,11.981,
11.735,11.478,11.221,10.965,10.783,10.66,10.536,10.413,10.25,-99,m3/s
C proportional flow volumes
16309,119743,-99, any units
```


F4: January 2013 event

Calibration summary

Event ID	Jan 13
Rainfall event characteristics	
Start date & time	25/01/2013 20:00
End date & time	28/01/2013 9:00
Rainfall duration (hours)	61:00:00
Number of bursts	1
Runoff characteristics	
Hydrograph duration	153:00:00
Number of peaks	1
Maximum gauged discharge at 143229A (m ³ /s)	1041.502
Supplementary peak discharge (m ³ /s)	N/A

Total event rainfall record			
Station name	Station ID	Recorded rainfall (mm)	Notes
Forest Hill	040079	162.8	
Mt Berryman	040310	278	
Upper Tenthill	040388	200.2	
UQ Gatton	040082	227	
Franklyn Vale	040374	279	
Franklyn Vale Alert	040912	322.6	
Gatton Allan St	040083	n/a	
Placid Hills	040449	309.2	
Townson	040675	546.8	
Gatton DAFF	040436	220	
Grandchester	040091	308.8	

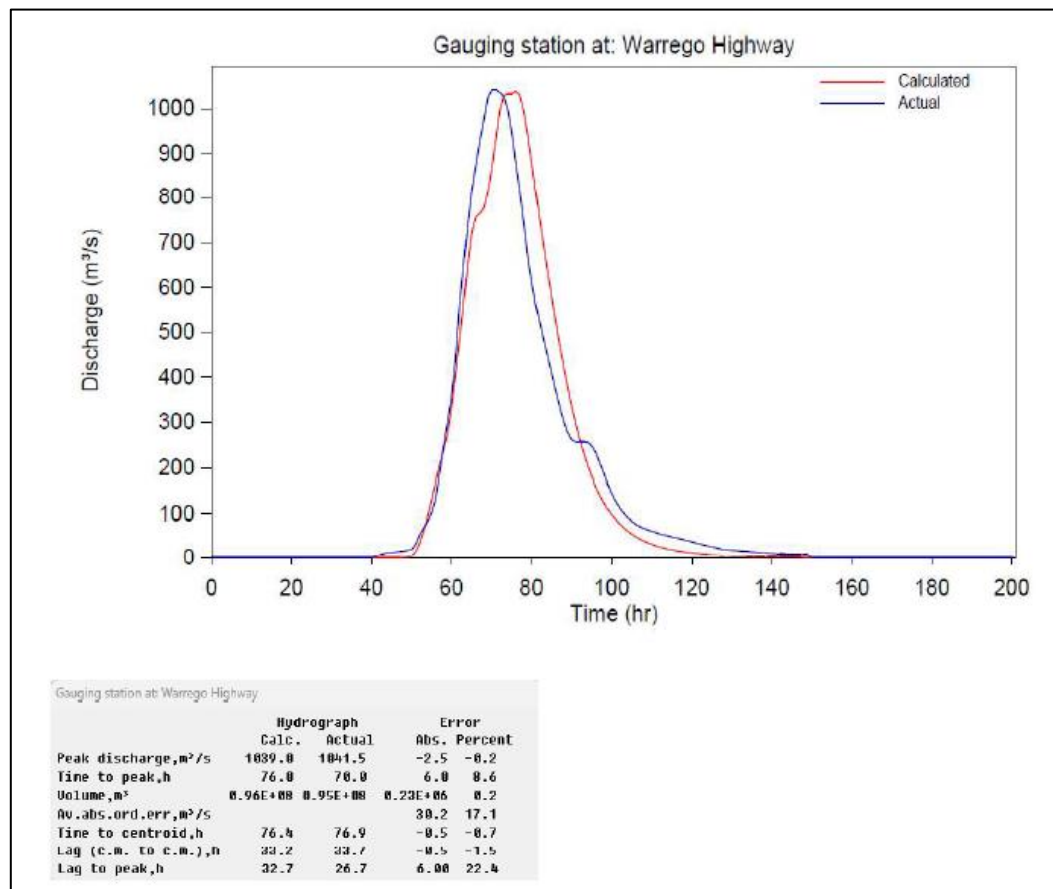
Subcatchment centroid event rainfall depths from QGIS interpolation	
Subcatchment ID	Rainfall depth (mm)
1	524.7
2	534.7
3	535.8
4	544.2
5	541.9
6	536.2
7	510.8
8	453.1
9	465.7
10	395.3
11	293.4
12	253.7
13	197.7
14	205.5
15	179.1
16	277.1
17	258.9
18	225.7
19	202.2
20	186

RORB gauged data statistics			
Peak flow (m ³ /s)	Total flow volume (m ³)	Time to peak (hrs)	Time to centroid (hrs)
1041.5	9.50E+07	70	76.9

RORB calibrated parameters and statistics											
m	kc	IL	CL	Peak flow (m ³ /s)	Error (%)	Total flow volume (m ³)	Error (%)	Time to peak (hrs)	Error (%)	Time to centroid (hrs)	Error (%)
0.8	36	80	0.45	1038.9	-0.3	9.54E+07	0.4	57	-18.6	60.2	-21.8
0.8	34	75	0.6	1045.1	0.3	9.53E+07	0.3	57	-18.6	59	-23.3
0.8	32	66	0.81	1036.6	-0.5	9.53E+07	0.3	56	-20	57.7	-25.1
0.8	32	60	0.94	1019.6	-2.1	9.53E+07	0.3	57	-18.6	57.3	-25.5
0.8	30	60	0.94	1039	-0.2	9.52E+07	0.2	56	-20	56.4	-26.6
0.8	30	60	0.94	1039	-0.2	9.52E+07	0.2	76	8.6	76.4	-0.7

20 hr translation

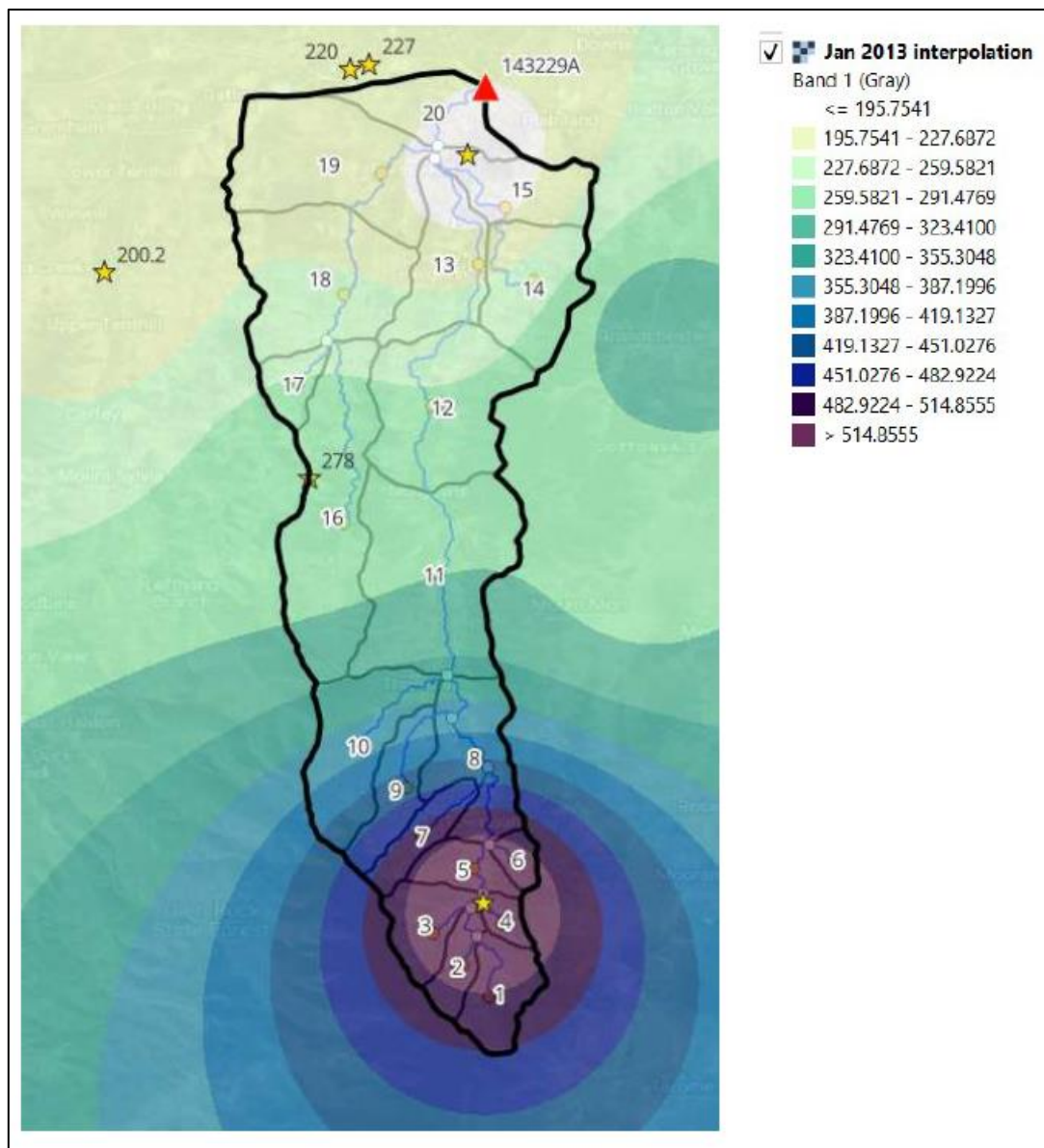
Calibrated hydrograph



RORB Storm file

[illegible]

QGIS event rainfall interpolation



F5: March 2017 event

Calibration summary

Event ID	Mar-17
Start Date	30/03/2017 0:00
End Date	30/03/2017 23:00
Duration (hours)	23:00
Number of peaks	1
Maximum gauged discharge at 143229A (m3/s)	248.682
Supplementary peak discharge (m3/s)	N/A

Total event rainfall record			
Station name	Station ID	Recorded rainfall (mm)	Notes
Forest Hill	040079	123	
Mt Berryman	040310	123.4	
Upper Tenthill	040388	81	
UQ Gatton	040082	99	
Franklyn Vale	040374	157.5	
Franklyn Vale Alert	040912	163.2	
Gatton Allan St	040083	95	
Placid Hills	040449	91.9	
Townson	040675	185	
Bremer River	WMIP	219	

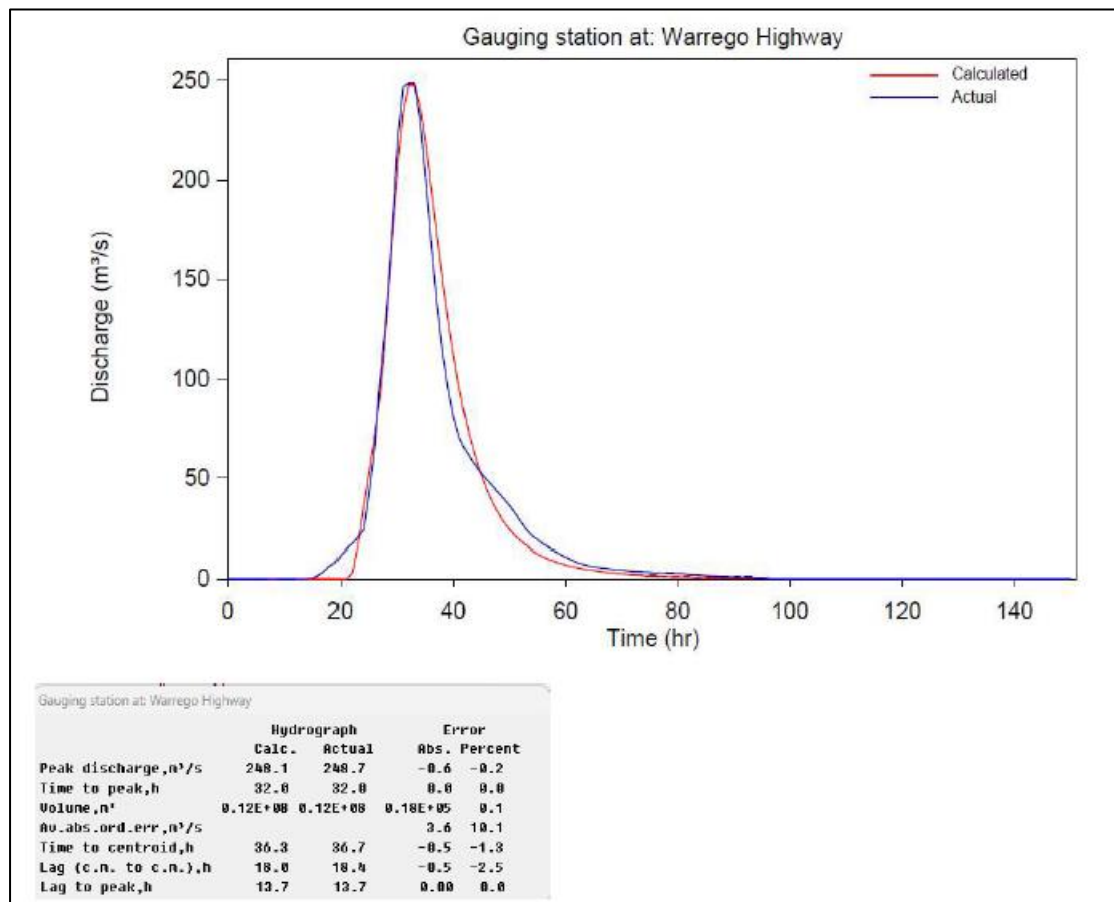
Subcatchment centroid event rainfall depths from QGIS interpolation	
Subcatchment ID	Rainfall depth (mm)
1	177.7
2	180.8
3	181.3
4	184
5	183.2
6	181.2
7	173.8
8	160.7
9	163.2
10	149.9
11	138.1
12	126.1
13	120.1
14	123.4
15	120.7
16	124.5
17	118.3
18	113
19	111.3
20	116.6

RORB gauged data statistics			
Peak flow (m3/s)	Total flow volume (m3)	Time to peak (hrs)	Time to centroid (hrs)
248.7	1.20E+07	32	36.7

RORB calibrated parameters and statistics											
m	kc	IL	CL	Peak flow (m3/s)	Error (%)	Total flow volume (m3)	Error (%)	Time to peak (hrs)	Error (%)	Time to centroid (hrs)	Error (%)
0.8	28	105	0.65	221.7	-10.8	1.21E+07	0.4	29	-9.4	33.5	-8.7
0.8	28	50	7.85	174.7	-29.8	1.20E+07	0.3	28	-12.5	30.1	-18.1
0.8	28	80	4.96	195.3	-21.5	1.20E+07	0.3	29	-9.4	31.6	-13.8
0.8	23	80	4.96	215.4	-13.4	1.20E+07	0.2	27	-15.6	30.3	-17.5
0.8	23	105	0.65	245.9	-1.1	1.20E+07	0.3	28	-12.5	32.1	-12.6
0.8	23	107	0.65	248.1	-0.2	1.20E+07	0.1	32	0	36.3	-1.3

4hr translation

Calibrated hydrograph



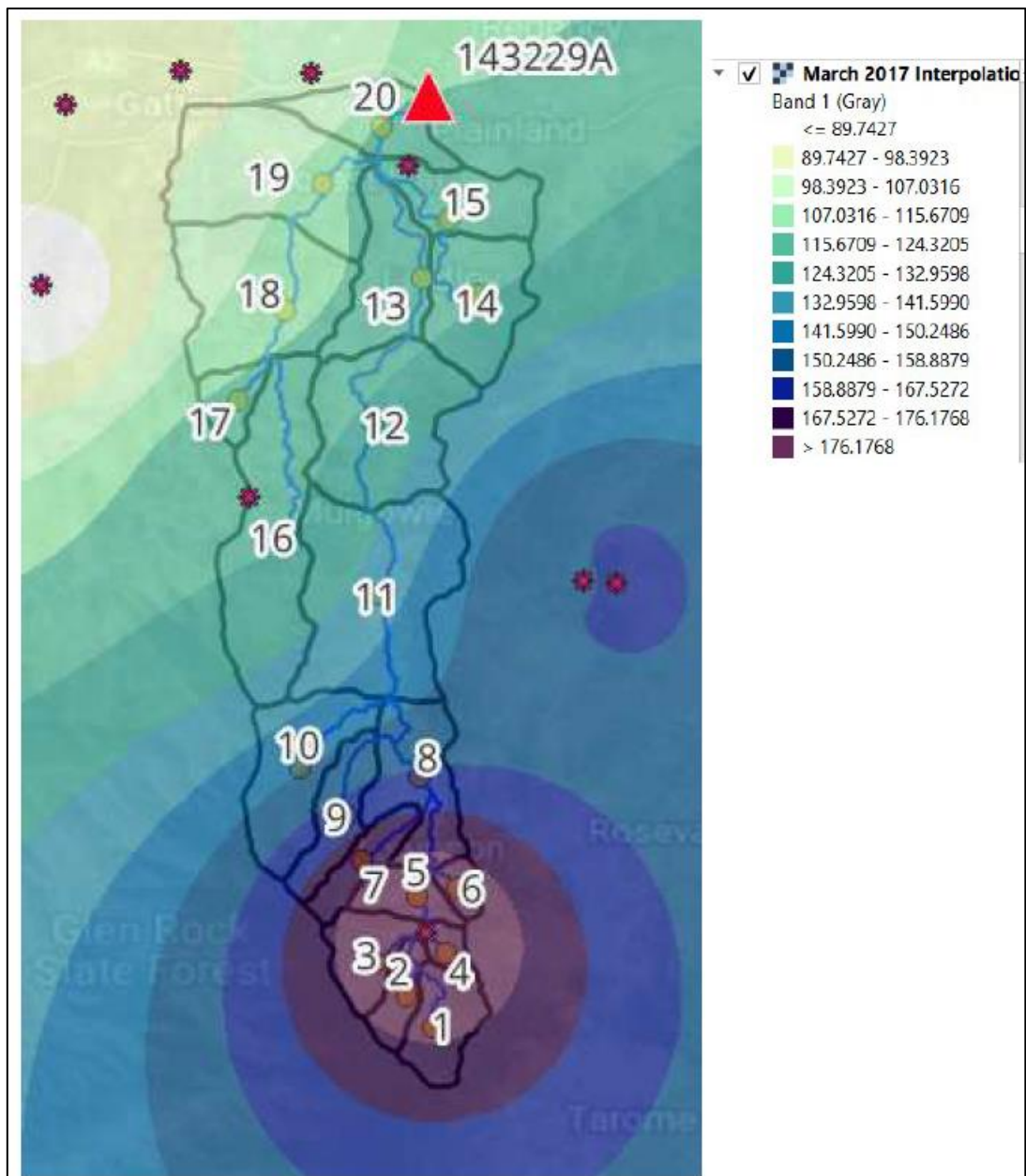
RORB Storm file

```

30-Mar-17
FIT
C      time inc = 1 hr, calcs for 150 incs, 1 bursts
C      3 pluvios, non uniform pattern
1,150,1,3,1,-99,
0,21, rain from 0 - 21 time incs
Bremer River
2,8,4,1,6,13,28,13,1,2,0,1,1,12,19,29,21,15,31,4,8,-99, mm/hr
Tenthill
1,5,10,8,6,4,7,6,3,0,2,1,3,3,3,5,3,4,1,3,3,-99,mm/hr
UQ Gatton
1,6,12,2,2,8,3,2,6,2,2,8,11,8,14,0,8,1,0,4,0,6,1,6,5,4,3,12,11,4,4,6,0,1,2,0,
6,-99,mm/hr
C      sub catchment rainfalls from isohyetal map
177.7,180.8,181.3,184,183.2,181.2,173.8,160.7,163.2,149.9,138.1,126.1,120.1,1
23.4,120.7,124.5,118.3,113,111.3,116.6,-99, Sub area event total rainfalls
C      pluivo reference numbers
1,1,1,1,1,1,1,1,1,1,1,1,3,3,3,2,2,1,1,-99
C Hydrograph data
0,95,-99
Warrego Highway
0.029,0.032,0.035,0.035,0.04,0.041,0.05,0.059,0.181,0.238,0.238,0.218,0.218,0
.208,0.249,0.523,1.608,3.349,6.119,7.712,12.106,14.943,17.402,20.526,24.258,4
2.804,65.299,102.877,132.96,172.763,220.544,246.857,248.682,248.682,230.269,2
00.923,169.541,139.312,114.542,95.538,80.899,70.582,64.509,60.088,56.059,51.9
76,48.804,45.872,42.893,39.638,36.215,32.322,28.321,24.258,21.059,19.038,16.9
32,15.312,13.924,12.407,10.851,9.414,8.231,7.265,6.54,6.018,5.585,5.26,4.942,
4.57,4.274,4.025,3.795,3.595,3.412,3.244,3.081,2.933,2.798,2.658,2.521,2.368,
2.208,2.046,1.902,1.755,1.617,1.503,1.394,1.307,1.215,1.136,1.046,0.97,0.905,
0.839,-99, m3/s

```

QGIS event rainfall interpolation



F6: February 2022 event

Calibration summary

Event ID

Feb - Mar 22

Rainfall event characteristics

Start date & time24/02/2022 10:00

End date & time28/02/2022 9:00

Rainfall duration (hours)95:00:00

Number of bursts1

Runoff characteristics

Hydrograph duration146 hrs

Number of peaks1, minor recession peaks

Maximum gauged discharge at 143229A1097.7 (m3/s)

Supplementary peak discharge (m3/s)n/a

Total event rainfall record

Station name	Station ID	Recorded rainfall (mm)	Notes
Forest Hill	040079	463	
UQ Gatton	040082	n/a	
Placid Hills	040449	506	
Gatton Allan St	040083	279	
Upper Tenthill	040388	366	
Franklyn Vale	040374	402.5	
Townson	040675	443	

Subcatchment centroid event rainfall depths from QGIS interpolation

Subcatchment ID	Rainfall depth (mm)
1	440.7
2	442.1
3	442.4
4	443.5
5	443.1
6	442.2
7	439
8	429.4
9	433.3
10	425.7
11	411.5
12	413.2
13	439.2
14	433.6
15	453
16	408.7
17	401.4
18	408.8
19	428.4
20	453

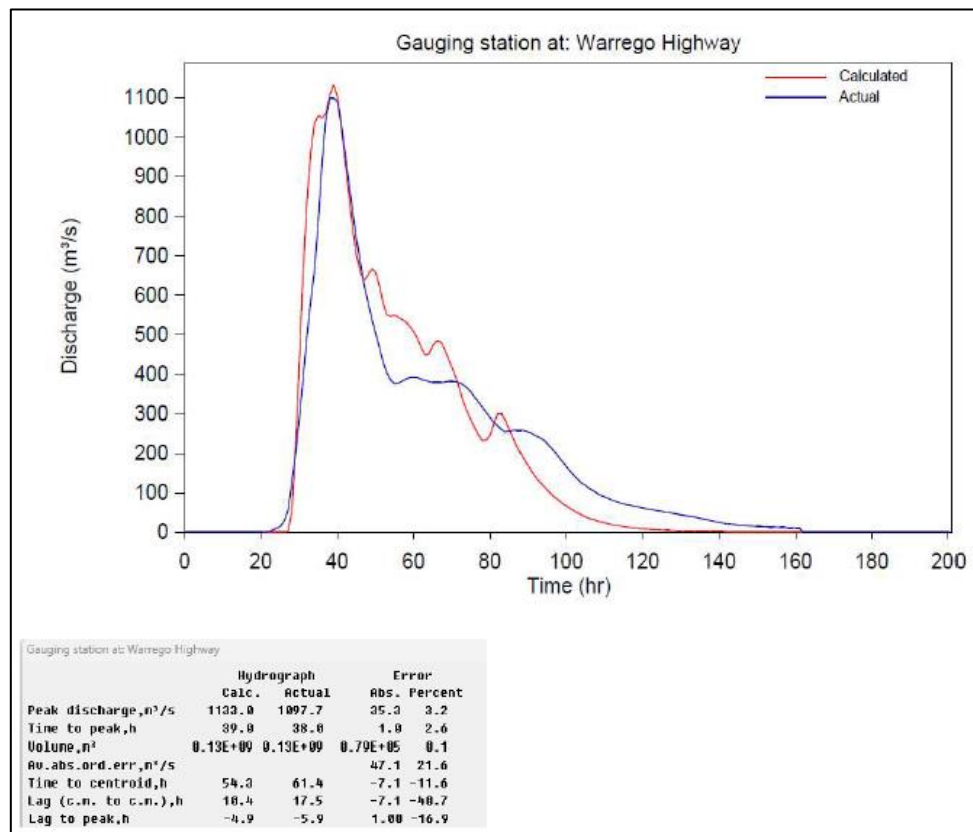
RORB gauged data statistics

Peak flow (m3/s)	Total flow volume (m3)	Time to peak (hrs)	Time to centroid (hrs)
1097.7	1.30E+08	38	61.4

RORB calibrated parameters and statistics

m	kc	IL	CL	Peak flow (m3/s)	Error (%)	Total flow volume (m3)	Error (%)	Time to peak (hrs)	Error (%)	Time to centroid (hrs)	Error (%)
0.8	29	140	0.07	1116.6	1.7	1.30E+08	0.1	39	2.6	54.5	-11.3
0.8	28	140	0.07	1140.8	3.9	1.30E+08	0.1	39	2.6	54.1	-11.9
0.8	28	142	0.03	1133	3.2	1.30E+08	0.1	39	2.6	54.3	-11.6
0.8	29	142	0.03	1108.3	1	1.30E+08	0.1	39	2.6	54.7	-11.1

Calibrated hydrograph



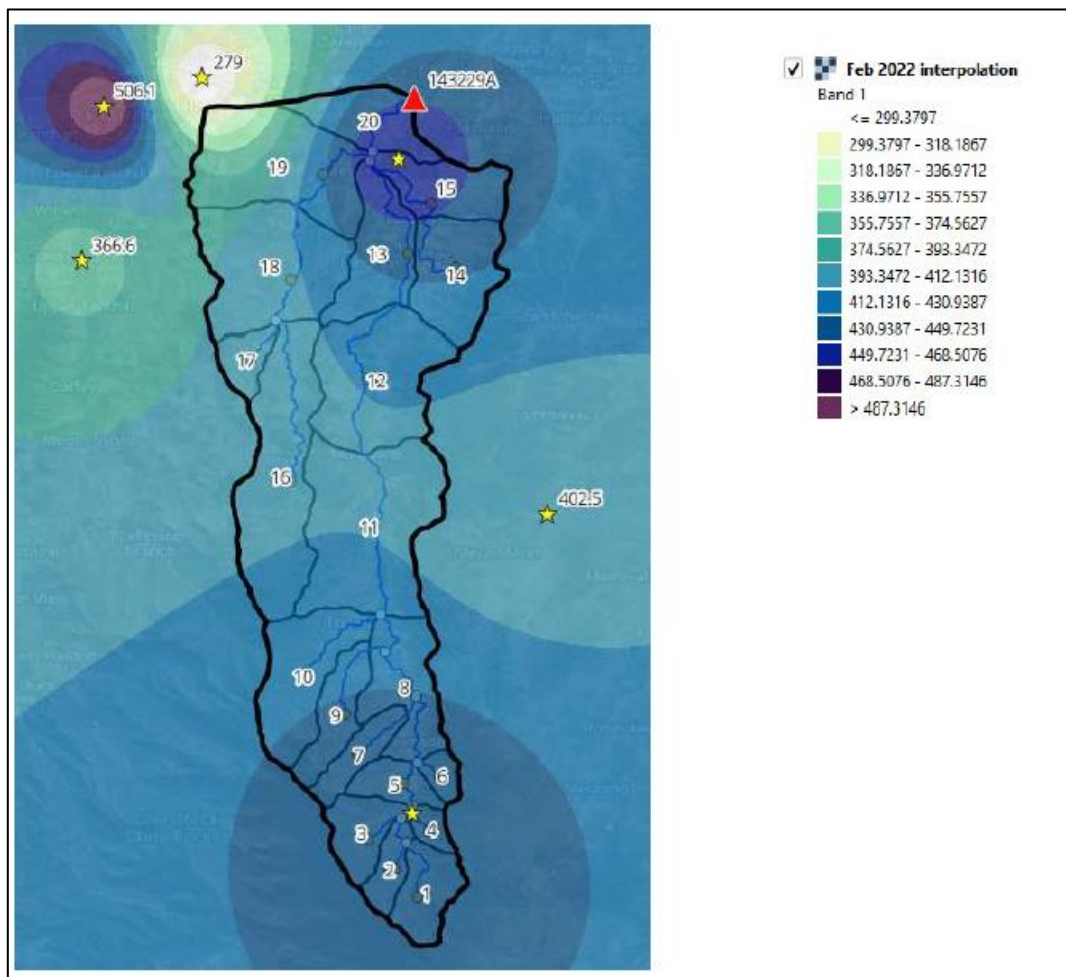
RORB Storm file

```

24-28 Feb 2022
FIT
C      time inc = 1 hr, calcs for 250 incs, 1 bursts
      2 pluvios, non uniform pattern
1,200,1,2,1,-99,
0,96, rain from 0 - 96 time incs
Upper Tenthill
1,3,1,2,0,0,0,0,1,1,0,0,1,2,1,2,5,2,5,9,10,7,6,6,20,6,24,23,22,17,15,13,9,6,3
5,8,10,3,2,0,1,1,0,4,3,8,7,5,2,1,2,4,6,3,3,4,3,2,3,1,2,2,7,4,3,2,1,1,2,0,0,0
2,0,1,0,2,4,3,7,1,0,0,0,0,0,0,0,0,0,0,0,0,0,0,-
99,mm/hr,.....
Bremer River
0,17,6,7,2,0,0,6,1,0,0,0,3,13,25,7,1,10,4,5,4,4,1,3,10,4,5,7,8,6,7,6,5,7,4,5,
7,6,2,1,0,0,2,2,2,6,8,7,6,3,1,1,2,7,3,3,7,4,5,8,4,1,3,7,5,3,3,3,4,6,4,5,7,10,
3,5,8,7,5,6,5,10,4,5,3,3,0,0,0,0,0,1,2,0,0,0,-
99,mm/hr,.....
.....
C      sub catchment rainfalls from isohyetal map
440.7,442.1,442.4,443.5,443.1,442.2,439.4,429.4,433.3,425.7,411.5,413.2,439.2,4
33.6,453,408.7,401.4,408.8,428.4,453,-99, Sub area event total rainfalls
C      pluvia reference numbers
1,1,1,1,1,1,1,1,1,1,1,1,1,1,1,1,1,1,1,1,-99,
C Hydrograph data
0,161,-99,start and end times
Warrego Highway
0.058,0.055,0.05,0.049,0.044,0.042,0.039,0.037,0.035,0.033,0.032,0.032,0.031,
0.031,0.031,0.035,0.039,0.044,0.066,0.097,0.188,0.391,1.026,5.609,10.408,14.7
92.29,251.55,678,127.376,196.337,286.218,387.443,494.112,583.805,663.401,785
747.936,045.1049,062,1097.718,1097.718,1092.223,1035.485,964.037,887.979,814.
99,742.904,678.724,622.078,580.977,538.11,502.001,465.906,429.353,403.14,385.
49,375.841,377.435,382.898,388.423,391.374,391.703,391.703,387.443,385.49,381
929,379.035,379.356,379.356,380.319,382.575,382.575,381.607,378.715,373.3,36
4.518,355.292,342.692,329.877,316.616,304.054,290.596,278.62,269.717,260.331,
254.919,256.322,257.967,258.674,258.674,257.026,254.22,249.598,244.141,238.78
233.078,224.099,213.773,203.247,190.17,178.476,166.533,154.926,144.715,134.9
11,124.59,119.291,110.422,105.498,99.647,94.374,89.933,85.856,81.179,77.875,7
4.679,72.267,69.487,67.776,65.605,63.427,61.536,59.744,57.88,56.168,54.441,52
91,51.361,49.496,47.973,46.628,44.755,43.387,41.656,39.892,38.061,36.018,34.
095,31.533,29.487,27.477,25.238,23.506,21.856,20.848,20.001,19.064,18.112,17.
185,16.308,15.74,15.203,14.786,14.322,13.882,13.448,13.027,12.635,12.25,11.88
4.11,535.11,247.10,905.-99,m3/s

```


QGIS event rainfall interpolation



F7: May 2022 event

Calibration summary

Event ID May-22
Start Date 11/05/2022 6:00
End Date 14/05/2022 9:00
Duration (hours) 0:00
Number of peaks 1
Maximum gauged discharge at 143229A (m3/s) 521.093
Supplementary peak discharge (m3/s) N/A

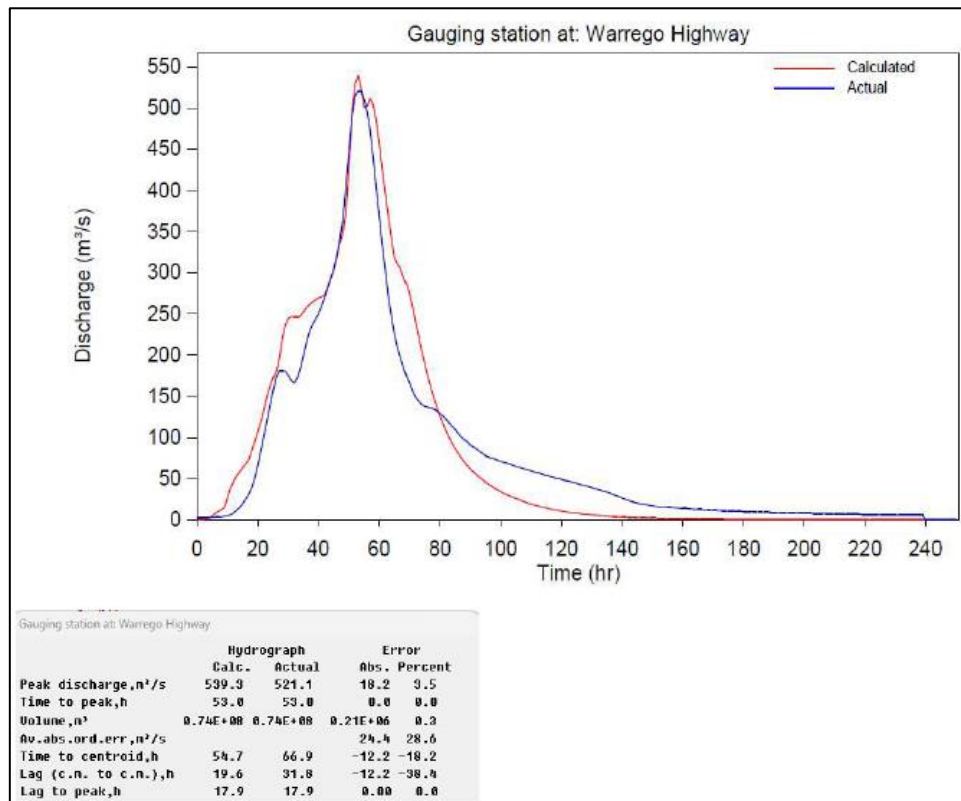
Total event rainfall record			
Station name	Station ID	Recorded rainfall (mm)	Notes
Forest Hill	040079	167.6	Offline
Upper Tenthill	040388	132	
UQ Gatton	040082	n/a	
Franklyn Vale	040374	202	
Franklyn Vale Alert	040912	200.4	
Gatton Allan St	040083	157	
Placid Hills	040449	164.1	
Townson	040675	357.4	
Bremer River	WMIP	204	

Subcatchment centroid event rainfall depths from QGIS interpolation	
Subcatchment ID	Rainfall depth (mm)
1	343
2	349.5
3	350.7
4	355.5
5	354.2
6	349.8
7	335.9
8	295.3
9	311.9
10	277.1
11	214.1
12	184.2
13	170.9
14	174.8
15	168.7
16	196.5
17	168.1
18	166.4
19	166.1
20	167.4

RORB gauged data statistics			
Peak flow (m3/s)	Total flow volume (m3)	Time to peak (hrs)	Time to centroid (hrs)
521.1	7.40E+07	53	66.9

RORB calibrated parameters and statistics											
m	kc	IL	CL	Peak flow (m3/s)	Error (%)	Total flow volume (m3)	Error (%)	Time to peak (hrs)	Error (%)	Time to centroid (hrs)	Error (%)
0.8	35	20	0.81	602	15.5	7.42E+07	0.3	52	-1.9	54.1	-19.1
0.8	38	10	0.96	561.5	7.8	7.42E+07	0.3	53	0	54.3	-18.8
0.8	40	5	1.03	539.3	3.5	7.42E+07	0.3	53	0	54.7	-18.2
0.8	40	0	1.09	532.1	2.1	7.42E+07	0.3	53	0	54.1	-19
0.8	41	0	1.09	525.4	0.8	7.42E+07	0.3	53	0	54.6	-18.3

Calibrated hydrograph



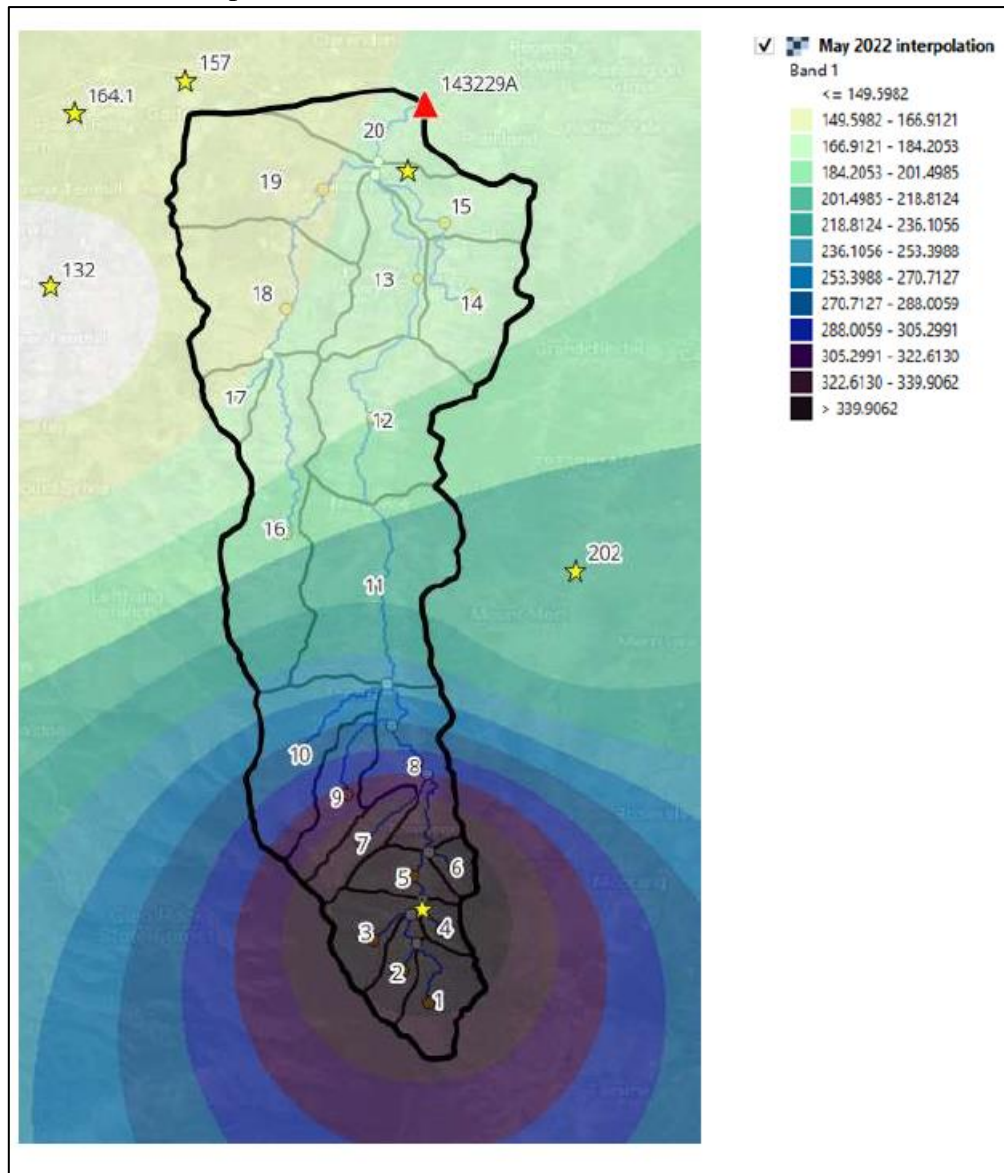
RORB Storm file

```

11 - 14 May 2022
FIT
C      time inc = 1 hr, calcs for 250 incs, 1 bursts
C      2 pluvious, non uniform pattern
1,250,1,2,1,-99,
0,76, rain from 0 - 76 time incs
Bremer River
1,0,0,3,1,5,2,5,1,11,2,1,1,2,2,5,2,6,14,2,0,0,0,0,0,0,0,4,6,13,4,4,2,3,5,13,1
,1,2,3,6,10,4,6,5,8,2,10,4,1,2,1,0,0,0,2,0,1,0,3,0,0,0,0,1,0,0,1,2,1,1,1,3,2,
0,0,-99,mm/hr
Tenthill
1,1,4,1,2,1,1,0,2,6,1,0,0,1,2,1,1,4,1,2,0,3,1,0,1,0,5,4,0,0,1,0,1,0,2,1,1,0,1
,0,1,1,4,0,2,3,2,2,6,13,3,2,1,0,0,9,2,0,0,1,0,0,0,0,1,6,0,2,3,1,1,1,1,1,0,0,-
99,mm/hr
C      sub catchment rainfalls from isohyetal map
343.349,5,350.7,355.5,354.2,349.8,335.9,295.3,311.9,277.1,214.1,184.2,170.9,1
74.8,168.7,196.5,168.1,166.4,166.1,167.4,-99, Sub area event total rainfalls
C      pluio reference numbers
1,1,1,1,1,1,1,1,1,1,1,1,2,2,2,2,2,2,2,-99,
C Hydrograph data
0,239,-99,
Warrego Highway
2.779,2.798,2.798,2.817,2.884,3.031,3.401,3.574,3.841,4.323,5.301,6.332,8.487
,11.836,15.251,19.645,24.789,30.968,39.01,50.296,65.544,82.778,101.196,119.16
4,137.026,156.814,173.105,181.299,181.299,180.413,175.168,168.869,166.201,172
.592,184.338,199.577,215.807,228.34,237.675,243.465,250.287,259.857,270.206,2
81.387,292.936,303.785,318.564,339.451,368.261,408.772,451.148,492.463,515.09
1,521.093,521.093,511.263,496.592,473.429,439.766,404.542,369.202,334.492,304
.323,272.413,248.453,226.636,209.751,197.096,184.879,174.306,165.375,156.182,
148.309,143.828,139.6,137.453,136.885,135.191,134.491,132.131,129.397,126.309
,122.111,117.774,113.44,109.589,105.383,100.863,97.9,94.902,91.053,88.524,85.
758,82.968,80.528,77.694,76.352,74.941,74.07,72.267,71.336,69.872,69.104,68.0
91,66.344,65.177,63.906,63.009,61.653,60.838,59.516,58.384,57.213,56.168,54.8
69,53.91,52.806,51.976,50.852,50.045,49.05,48.07,47.441,46.485,45.357,44.525,
43.342,42.315,41.307,40.488,39.47,38.061,37.089,36.293,35.008,33.683,32.467,3
0.584,29.251,27.994,26.277,24.878,23.707,22.191,21.413,20.694,19.946,19.347,1
8.665,17.904,17.325,16.631,16.098,15.734,15.535,15.39,15.167,14.986,14.732,14
.412,14.171,13.888,13.641,13.424,13.171,12.918,12.708,12.479,12.238,12.022,11
.866,11.692,11.511,11.337,11.175,11.013,10.875,10.767,10.653,10.485,10.408,10
.258,10.174,10.048,9.862,9.683,9.521,9.378,9.246,9.168,9.055,8.941,8.798,8.74
4,8.625,8.529,8.416,8.344,8.237,8.183,8.082,8.016,7.95,7.867,7.772,7.688,7.62
9,7.533,7.444,7.361,7.289,7.194,7.129,7.063,6.98,6.879,6.855,6.778,6.73,6.689
,6.653,6.588,6.546,6.481,6.398,6.362,6.32,6.237,6.184,6.142,6.113,6.036,5.965
,5.935,5.923,5.882,5.846,5.828,5.816,5.816,-99,mm/hr

```

QGIS event rainfall interpolation



F8: January 2024 event

Calibration summary

Event ID Jan-24
 Start Date 28/01/2024 0:00
 End Date 30/01/2024 16:00
 Duration (hours) 0:00
 Number of peaks 1
 Maximum gauged discharge at 143229A (m3/s) 366.698
 Supplementary peak discharge (m3/s) N/A

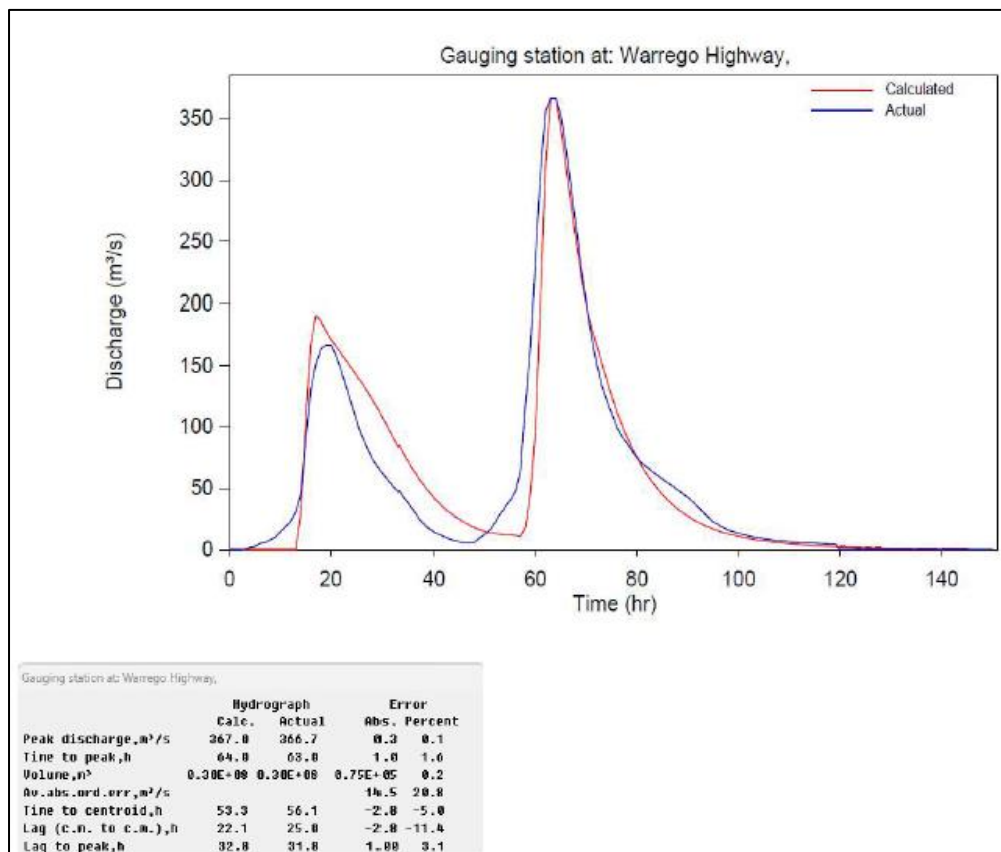
Total event rainfall record			
Station name	Station ID	Recorded rainfall (mm)	Notes
Forest Hill	040079	156.1	
Upper Tenthill	040388	151.8	
UQ Gatton	040082	163.8	
Franklyn Vale	040374	180	
Franklyn Vale Alert	040912	188.8	
Gatton Allan St	040083	138.7	
Placid Hills	040449	173.8	
Townson	040675	n/a	
Besmer River	WMIP	164	

Subcatchment centroid event rainfall depths from QGIS interpolation	
Subcatchment ID	Rainfall depth (mm)
1	174
2	174
3	173.3
4	175.1
5	175.3
6	176.3
7	174.4
8	177
9	174.3
10	172.8
11	175.6
12	168.8
13	165
14	166.8
15	164.8
16	168.9
17	162.2
18	161.9
19	162.2
20	164

RORB gauged data statistics			
Peak flow (m3/s)	Total flow volume (m3)	Time to peak (hrs)	Time to centroid (hrs)
366.7	3.00E+07	63	56.1

RORB calibrated parameters and statistics											
m	kc	IL	CL	Peak flow (m3/s)	Error (%)	Total flow volume (m3)	Error (%)	Time to peak (hrs)	Error (%)	Time to centroid (hrs)	Error (%)
0.8	27	36	5.85	364.8	-0.5	3.01E+07	0.3	54	9	42.5	-24.4
0.8	28	39	5.52	367	0.1	3.01E+07	0.2	55	-12.7	44.3	-21
0.8	27	36	5.85	364.8	-0.5	3.01E+07	0.3	63	0	51.4	-8.4
0.8	28	39	5.52	367	0.1	3.01E+07	0.2	64	1.6	53.3	-5
											12 hr translation
											12 hr translation

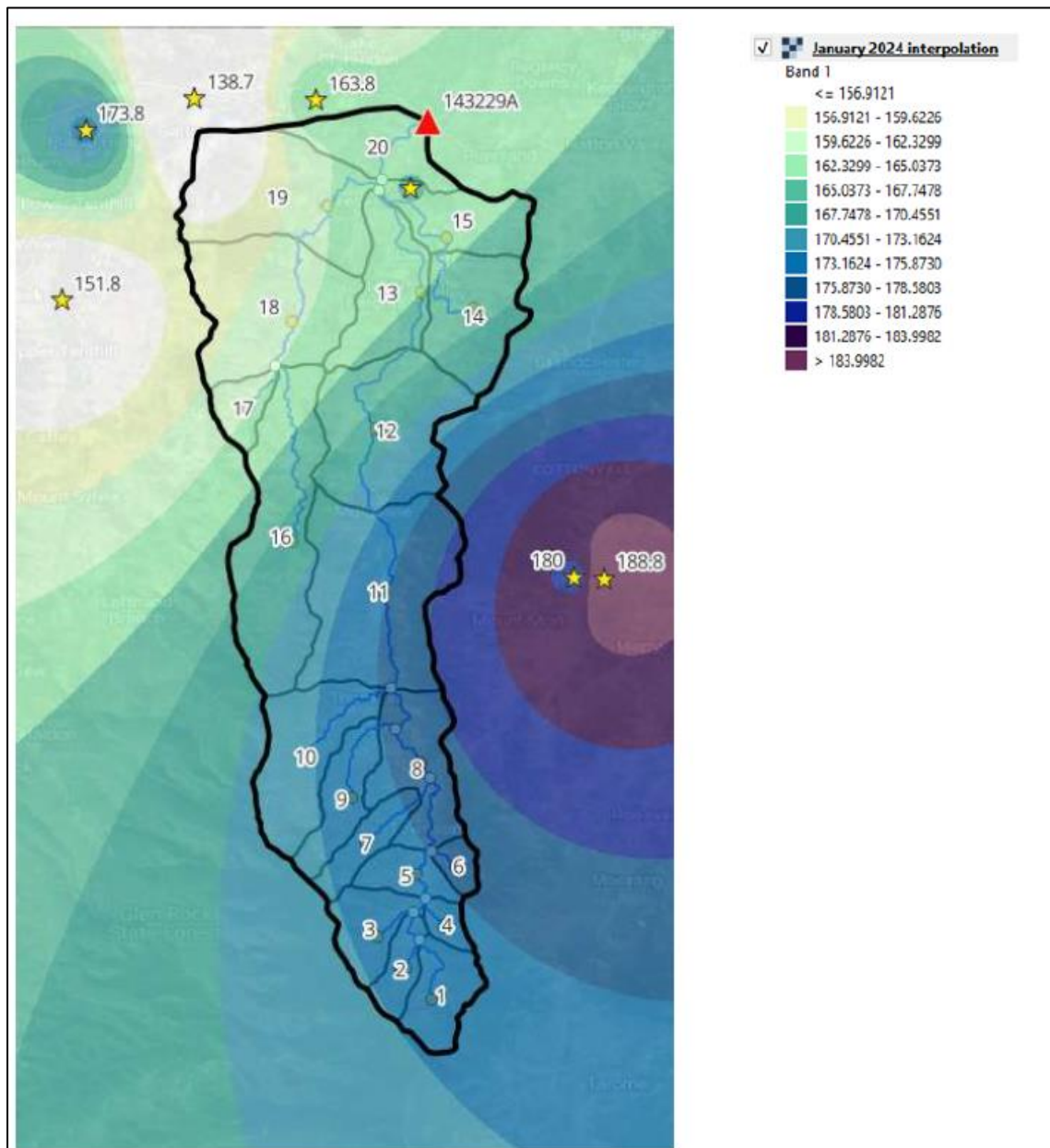
Calibrated hydrograph



RORB Storm file

[illegible]

QGIS event rainfall interpolation



Appendix G: Design discharge simulation sets

Summary of results

Current climate conditions

AEP (%)	Discharge (m ³ /s)		
	<u>Median</u>	Minimum	Maximum
50	223	210.4	233.7
20	467.1	457.6	482.2
10	661.9	649.4	676.5
5	868.4	833.7	888
2	1164.5	1149.4	1178
1	1411.4	1381.3	1479.9

RCP 4.5 Scenarios

AEP (%)	Discharge 2030 (m ³ /s)	Increase (%)	Discharge 2050 (m ³ /s)	Increase (%)	Discharge 2090 (m ³ /s)	Increase (%)
50	281.1	26	296.2	33	330	48
20	547.5	17	580.1	24	630.4	35
10	767.4	16	799.5	21	865.8	31
5	992.7	14	1044.5	20	1116.7	29
2	1315.1	13	1383	19	1483.7	27
1	1587.9	12	1659.5	18	1772.3	26

RCP 8.5 Scenarios

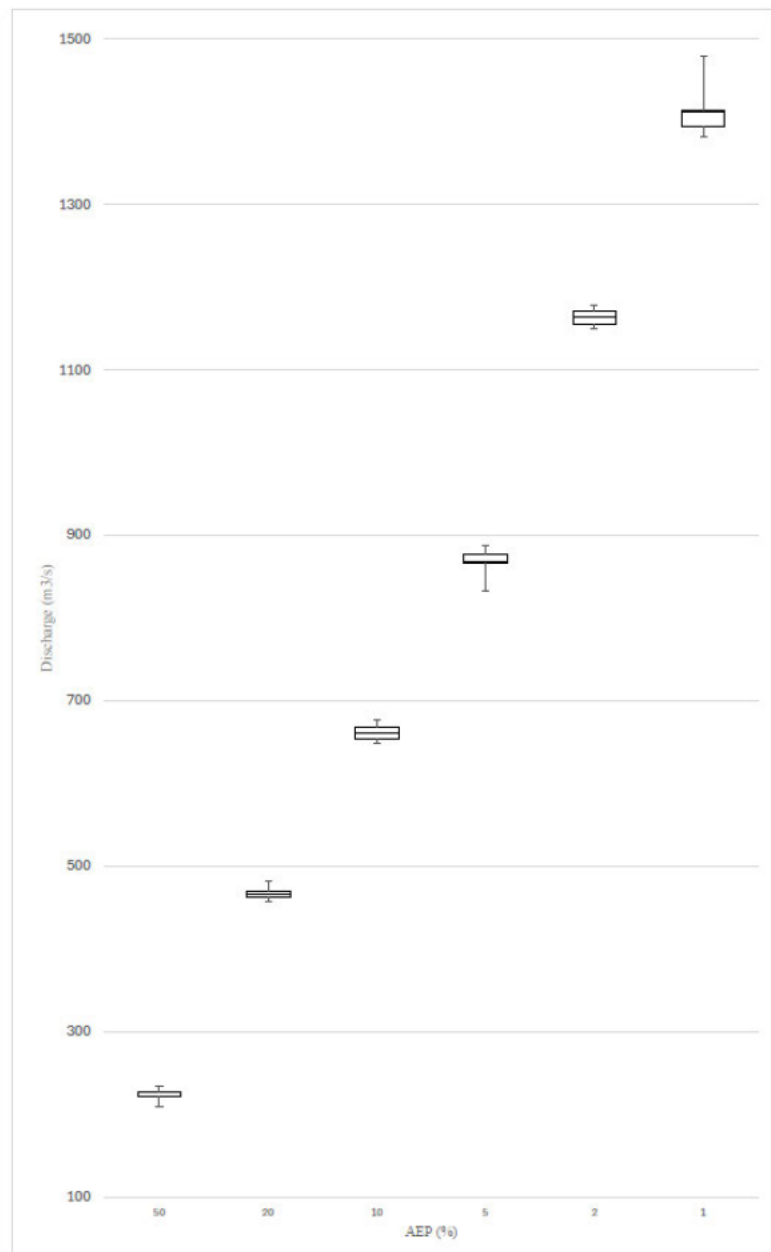
AEP (%)	Discharge 2030 (m ³ /s)	Increase (%)	Discharge 2050 (m ³ /s)	Increase (%)	Discharge 2090 (m ³ /s)	Increase (%)
50	280.3	26	320	43	431.5	94
20	555.5	19	614.9	32	780.9	67
10	779.5	18	842.5	27	1056.5	60
5	1010.4	16	1086.9	25	1341.2	54
2	1340.7	15	1446.6	24	1762.8	51
1	1612.4	14	1736	23	2096.3	49

CURRENT CLIMATE SIMULATION SET

Discharges recorded on run number											Min	Q1	Mean	Q3	Max
AEP	1	2	3	4	5	6	7	8	9	10					
50	221.236	233.731	210.416	229.172	228.795	226.195	221.947	221.387	225.044	212.086	210.416	221.2738	223.4955	228.146	233.731
20	468.506	463.759	470.936	462.639	482.217	476.184	465.054	468.993	467.637	465.218	457.637	462.919	465.136	470.3265	482.217
10	654.101	649.685	657.332	676.54	672.006	666.061	650.023	669.559	649.392	665.913	649.392	654.9088	661.968	668.6845	676.54
5	850.198	833.659	879.021	887.981	872.742	872.588	805.032	875.055	868.324	879.008	833.659	865.855	872.665	878.0295	887.981
2	1170.973	1149.414	1150.073	1162.976	1168.953	1164.528	1169.343	1177.438	1153.274	1177.968	1149.414	1155.7	1166.741	1170.566	1177.968
1	1479.891	1400.479	1410.085	1382.208	1408.98	1391.992	1442.725	1401.45	1381.316	1415.271	1381.316	1394.114	1405.215	1413.975	1479.891

AEP	Critical duration										Min	Q1	Mean	Q3	Max
50	24	24	24	24	24	24	24	24	24	24					
20	24	24	24	24	24	24	24	24	24	24	210.416	221.2738	223.0011	228.146	233.731
10	24	24	24	24	24	24	24	24	24	24	457.637	462.919	467.1143	470.3265	482.217
5	24	24	24	24	24	24	24	24	24	24	649.392	654.9088	661.8612	668.6845	676.54
2	24	24	24	24	24	24	24	24	24	24	833.659	865.855	868.4268	878.0295	887.981
1	144	24	24	24	24	24	24	24	24	24	1149.414	1155.7	1164.494	1170.566	1177.968
											1381.316	1394.114	1411.44	1413.975	1479.891

Range	IQR		
23.315	10.4%	6.87225	3.1%
24.58	5.3%	7.4095	1.6%
27.148	4.1%	13.77575	2.1%
54.322	6.2%	12.1745	1.4%
28.554	2.4%	14.866	1.3%
98.575	7.0%	19.86075	1.4%



2030 RCP 4.5 SIMULATION SET

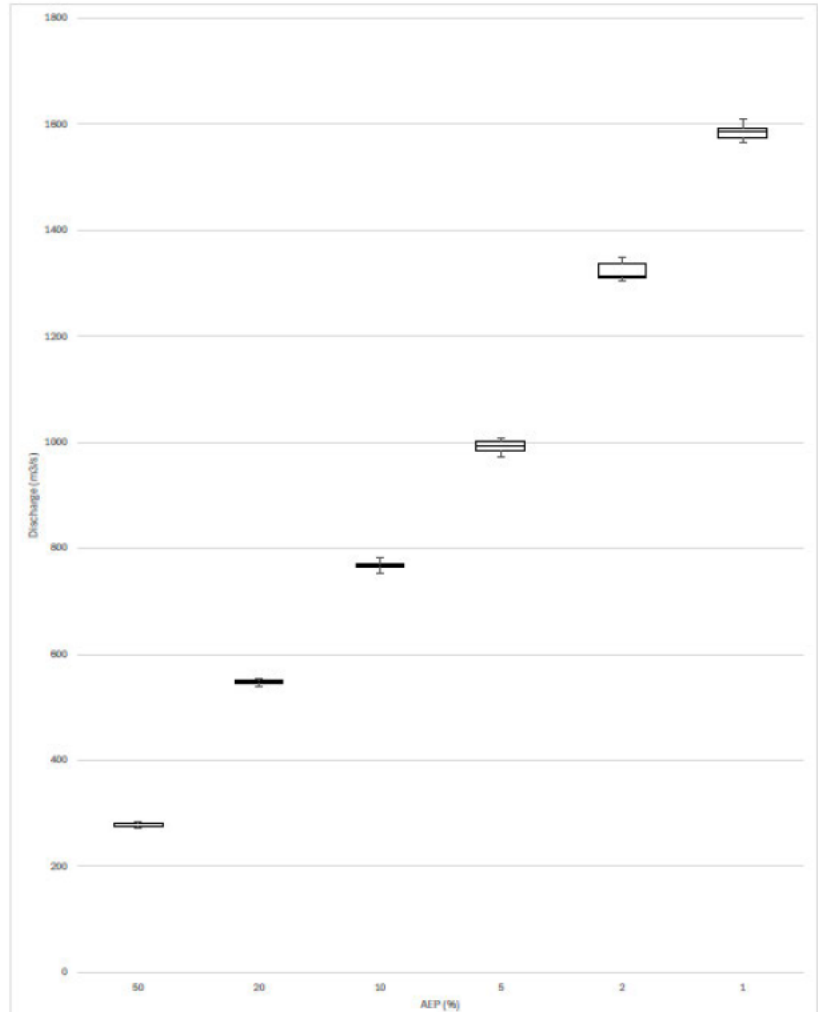
Discharges recorded on run number

AEP	1	2	3	4	5	6	7	8	9	10	Min	Q1	Mean	Q3	Max
50	279.954	273.168	286.18	282.072	274.761	271.626	280.654	282.562	281.568	285.799	271.626	276.0593	281.111	282.4395	286.18
20	550.125	547.121	540.336	549.488	553.228	546.578	544.194	551.64	543.601	547.921	540.336	544.79	547.521	549.9658	553.228
10	763.551	753.008	768.216	763.419	781.807	766.522	772.303	756.689	771.349	772.859	753.008	763.452	767.369	772.0645	781.807
5	987.807	972.66	985.349	981.914	1000.7	1008.939	1005.884	1003.294	974.95	997.664	972.66	982.7728	992.7355	1002.646	1008.939
2	1314.005	1316.191	1348.034	1339.234	1311.278	1326.685	1306.96	1313.393	1340.31	1304.488	1304.488	1311.807	1315.098	1336.097	1348.034
1	1571.109	1571.156	1590.476	1587.027	1592.483	1567.25	1611.027	1588.681	1598.856	1584.548	1567.25	1574.504	1587.854	1591.981	1611.027

AEP Critical duration

AEP	1	2	3	4	5	6	7	8	9	10	Paste only
50	24	24	24	24	24	24	24	24	24	24	271.626
20	24	24	24	24	24	24	24	24	24	24	540.336
10	24	24	24	24	24	24	24	24	24	24	753.008
5	24	24	24	24	24	24	24	24	24	24	972.66
2	24	24	24	24	24	24	24	24	24	24	1304.488
1	24	24	24	144	24	144	24	24	144	144	1567.25

Range	IQR	
14.554	5.2%	6.38025
12.892	2.4%	5.17575
28.799	3.8%	8.6125
36.279	3.7%	19.87275
43.546	3.3%	24.29
43.777	2.8%	17.47725

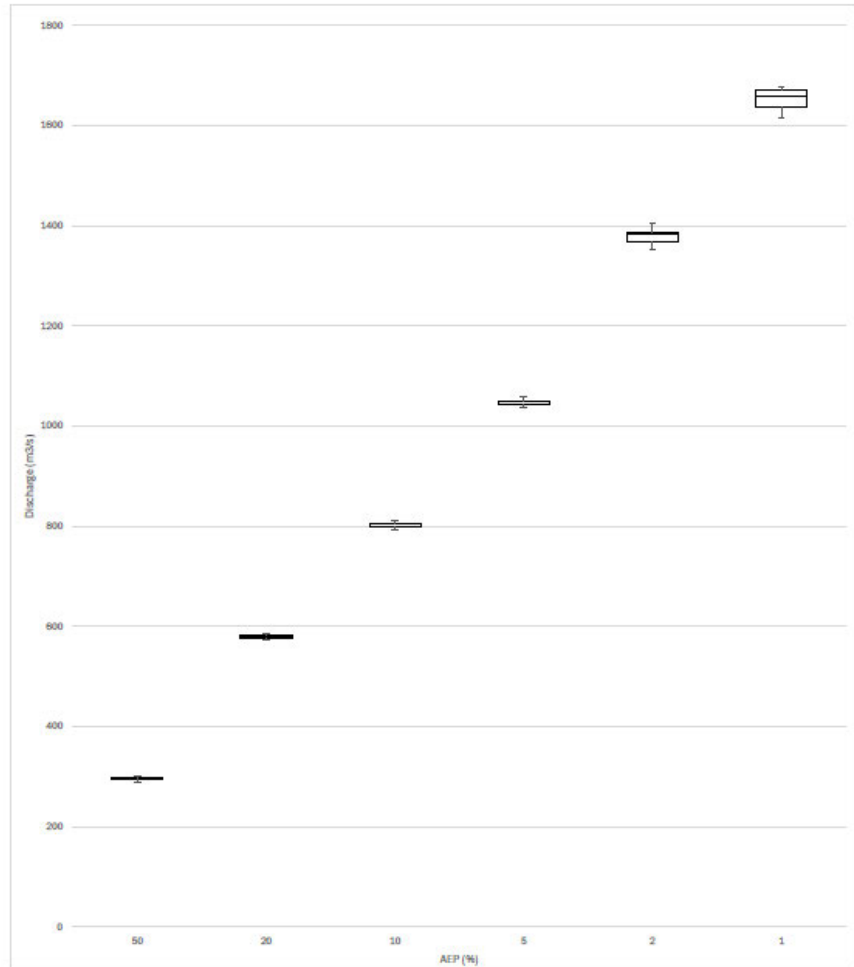


2050 RCP 4.5 SIMULATION SET

Discharges recorded on run number											Min	Q1	Mean	Q3	Max
AEP	1	2	3	4	5	6	7	8	9	10					
50	298.702	295.384	288.53	297.966	293.4	299.594	288.471	297.06	294.141	300.125	288.471	293.5853	296.222	298.518	300.125
20	580.895	577.959	571.635	583.666	575.405	581.803	581.21	585.641	574.597	579.243	571.635	576.0435	580.069	581.6548	585.641
10	810.672	797.141	798.112	806.488	797.739	791.66	798.333	808.106	804.186	800.647	791.66	797.8323	799.49	805.9125	810.672
5	1038.445	1036.323	1051.171	1057.846	1045.076	1042.906	1042.846	1047.11	1043.995	1048.337	1036.323	1042.861	1044.536	1048.03	1057.846
2	1388.628	1362.064	1364.078	1383.73	1386.113	1394.521	1382.278	1354.338	1406.098	1379.371	1354.338	1367.901	1383.004	1387.999	1406.098
1	1634.936	1620.766	1675.095	1616.497	1671.545	1671.987	1647.516	1646.001	1672.675	1677.281	1616.497	1637.702	1659.531	1672.503	1677.281

Critical duration											Paste only				
AEP	1	2	3	4	5	6	7	8	9	10					
50	24	24	24	24	24	24	24	24	24	24	288.471	293.5853	296.222	298.518	300.125
20	24	24	24	24	24	24	24	24	24	24	571.635	576.0435	580.069	581.6548	585.641
10	24	24	24	24	24	24	24	24	24	24	791.66	797.8323	799.49	805.9125	810.672
5	24	24	24	24	24	24	24	24	24	24	1036.323	1042.861	1044.536	1048.03	1057.846
2	24	24	24	24	24	24	24	24	24	24	1354.338	1367.901	1383.004	1387.999	1406.098
1	144	24	24	24	144	24	24	24	24	24	1616.497	1637.702	1659.531	1672.503	1677.281

Range	IQR		
11.654	3.9%	4.93275	1.7%
14.006	2.4%	5.61125	1.0%
19.012	2.4%	8.08025	1.0%
21.523	2.1%	5.16925	0.5%
51.76	3.7%	20.098	1.5%
60.784	3.7%	34.80075	2.1%

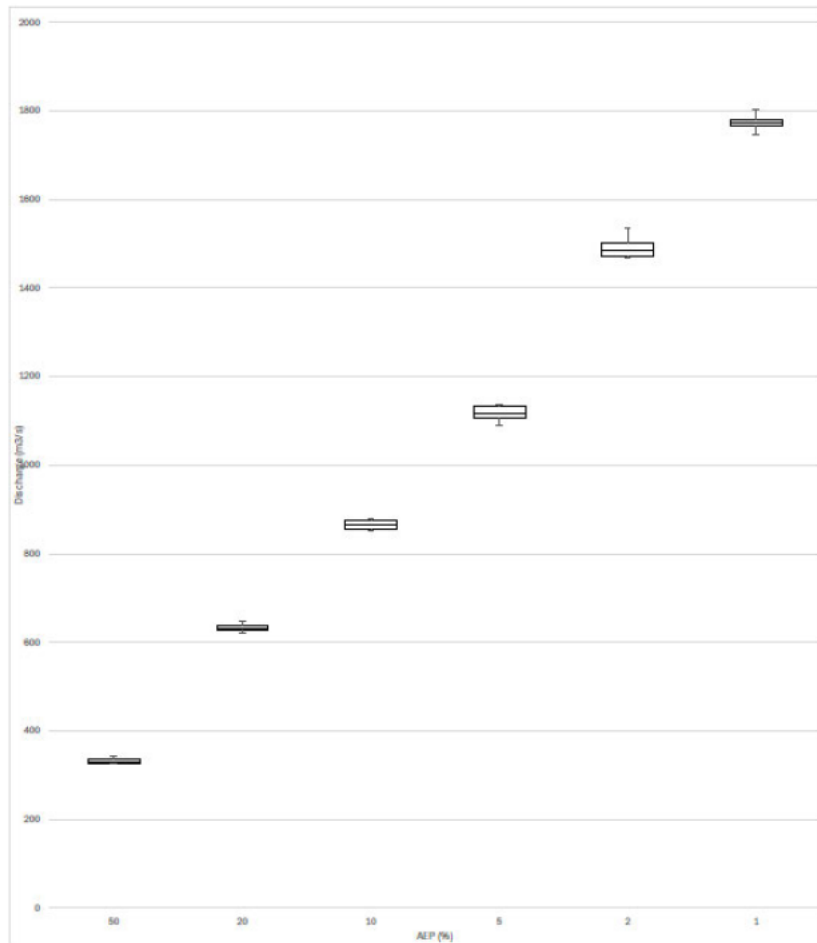


2090 RCP 4.5 SIMULATION SET

AEP	Discharges recorded on run number										Min	Q1	Mean	Q3	Max
	1	2	3	4	5	6	7	8	9	10					
50	329.836	330.232	337.908	336.792	329.005	331.294	341.708	326.444	326.494	326.276	326.276	327.1218	330.034	335.4175	341.708
20	633.788	637.38	626.963	621.66	646.923	625.83	637.481	626.046	647.15	620.185	620.185	625.884	630.3705	637.4558	647.15
10	860.397	878.226	855.143	851.021	876.856	874.917	871.195	878.867	854.701	859.933	851.021	856.3405	865.796	876.3713	878.867
5	1089.814	1113.558	1133.541	1105.796	1100.926	1116.291	1137.002	1131.97	1117.062	1134.256	1089.814	1107.363	1116.687	1133.148	1137.002
2	1506.273	1536.182	1472.063	1502.175	1472.628	1477.348	1470.669	1490.054	1468.925	1497.719	1468.925	1472.204	1483.701	1501.061	1536.182
1	1767.225	1802.894	1781.39	1777.837	1767.068	1762.076	1746.75	1792.632	1769.729	1774.879	1746.75	1767.107	1772.304	1780.502	1802.894

AEP	Critical duration										Min	Q1	Mean	Q3	Max
	24	24	24	24	24	24	24	24	24	24					
50	24	24	24	24	24	24	24	24	24	24	326.276	327.1218	330.034	335.4175	341.708
20	24	24	24	24	24	24	24	24	24	24	620.185	625.884	630.3705	637.4558	647.15
10	24	24	24	24	24	24	24	24	24	24	851.021	856.3405	865.796	876.3713	878.867
5	24	24	24	24	24	24	24	24	24	24	1089.814	1107.363	1116.687	1133.148	1137.002
2	24	24	24	24	24	24	24	24	24	24	1468.925	1472.204	1483.701	1501.061	1536.182
1	24	24	24	24	24	24	24	24	24	24	1746.75	1767.107	1772.304	1780.502	1802.894

Range	IQR		
15.432	4.7%	8.29575	2.5%
26.965	4.3%	11.57175	1.8%
27.846	3.2%	20.00075	2.3%
47.188	4.2%	25.78525	2.3%
67.257	4.5%	28.85675	1.9%
56.144	3.2%	13.3945	0.8%

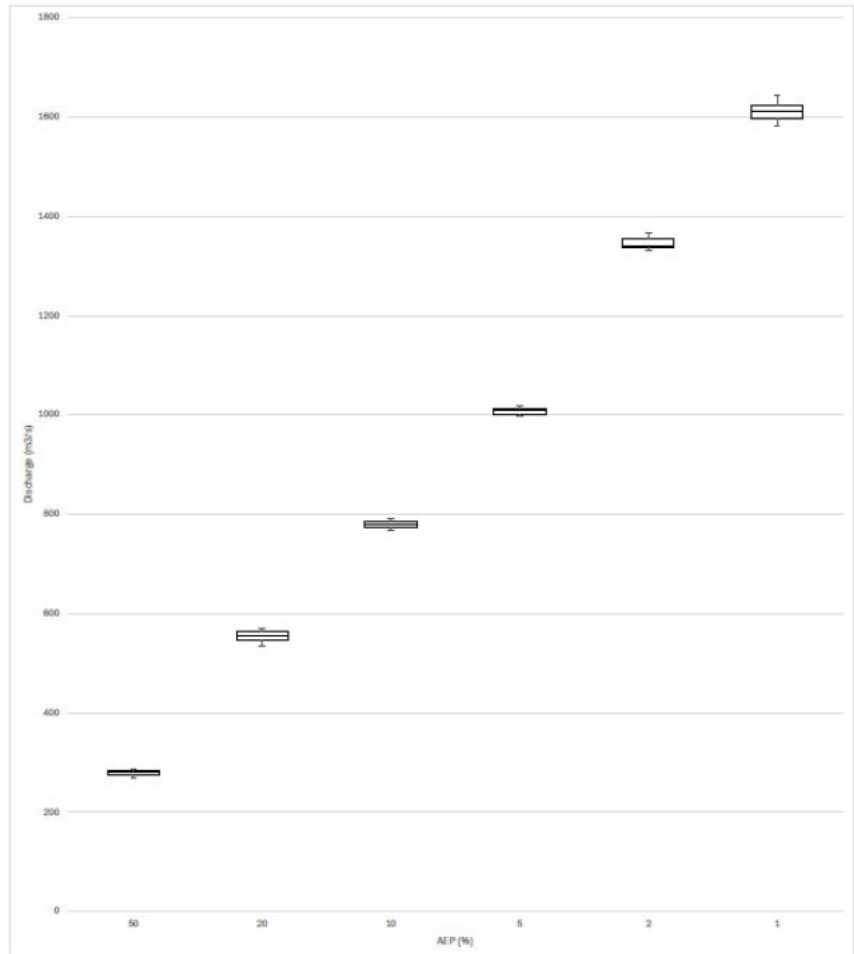


2030 RCP 8.5 SIMULATION SET

Discharges recorded on run number											Min	Q1	Mean	Q3	Max
AEP	1	2	3	4	5	6	7	8	9	10					
50	268.763	274.524	281.173	277.536	275.548	279.442	282.101	286.343	281.566	283.579	268.763	276.045	280.3075	281.9673	286.343
20	545.243	558.22	540.28	551.36	552.877	533.806	565.469	569.197	563.553	561.287	533.806	546.7698	555.5485	562.9865	569.197
10	777.978	790.378	775.04	773.836	781.078	765.999	786.242	768.319	784.705	791.854	765.999	774.137	779.528	785.8578	791.854
5	1012.555	1015.638	1010.57	998.752	1012.794	998.006	996.839	1001.433	1010.186	1017.084	996.839	999.4223	1010.378	1012.734	1017.084
2	1340.338	1341.096	1337.515	1365.906	1337.432	1331.536	1351.34	1355.956	1338.883	1359.029	1331.536	1337.857	1340.717	1354.802	1365.906
1	1615.446	1596.471	1583.388	1609.338	1625.844	1606.445	1619.589	1645.19	1592.063	1644.844	1583.388	1598.215	1612.392	1624.28	1645.19

AEP	Critical duration										Min	Q1	Mean	Q3	Max
50	24	24	24	24	24	24	24	24	24	24	268.763	276.045	280.3075	281.9673	286.343
20	24	24	24	24	24	24	24	24	24	24	533.806	546.7698	555.5485	562.9865	569.197
10	24	24	24	24	24	24	24	24	24	24	765.999	774.137	779.528	785.8578	791.854
5	24	24	24	24	24	24	24	24	24	24	996.839	999.4223	1010.378	1012.734	1017.084
2	24	24	24	24	24	24	24	24	24	24	1331.536	1337.857	1340.717	1354.802	1365.906
1	24	24	24	24	24	144	24	144	24	24	1583.388	1598.215	1612.392	1624.28	1645.19

Range	IQR		
17.58	6.3%	5.92225	2.1%
35.391	6.4%	16.21675	2.9%
25.856	3.3%	11.72075	1.5%
20.245	2.0%	13.312	1.3%
34.37	2.6%	16.945	1.3%
61.802	3.8%	26.06575	1.6%

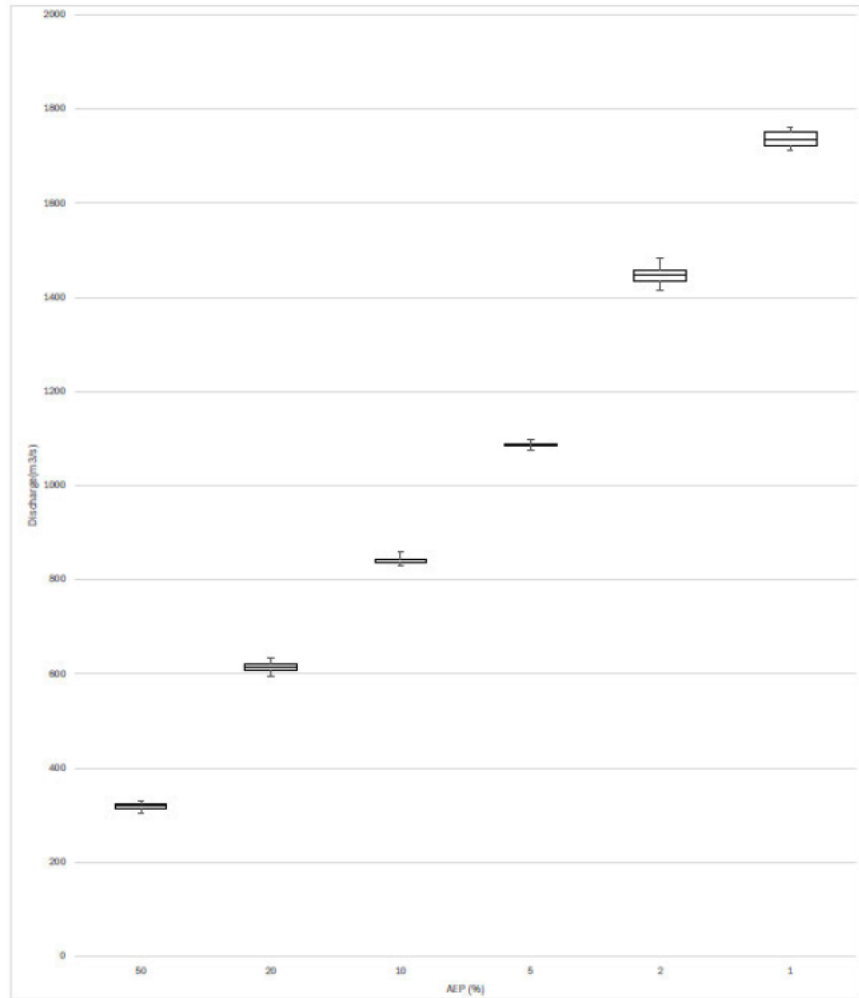


2050 RCP 8.5 SIMULATION SET

AEP	Discharges recorded on run number										Min	Q1	Mean	Q3	Max
	1	2	3	4	5	6	7	8	9	10					
50	321.665	303.939	328.794	313.948	311.59	319.953	325.16	314.835	320.013	322.843	303.939	314.1698	319.963	322.5485	328.794
20	626.156	632.77	621.009	611.152	616.821	603.413	595.582	621.844	607.056	612.96	595.582	608.08	614.8905	621.6353	632.77
10	839.854	858.456	844.09	844.171	851.815	840.991	835.238	844.419	831.839	832.752	831.839	836.392	842.5405	844.357	858.456
5	1084.787	1086.157	1085.904	1080.234	1073.83	1090.746	1087.6	1087.668	1099.031	1087.628	1073.83	1085.066	1086.879	1087.658	1099.031
2	1443.851	1427.49	1470.873	1458.534	1482.577	1449.31	1414.943	1431.257	1454.548	1441.348	1414.943	1433.78	1446.581	1457.538	1482.577
1	1755.035	1741.25	1733.538	1720.135	1761.864	1711.853	1738.409	1714.577	1760.162	1724.428	1711.853	1721.208	1735.974	1751.589	1761.864

AEP	Critical duration										Min	Q1	Mean	Q3	Max
50	24	24	24	24	24	24	24	24	18	24	303.939	314.1698	319.963	322.5485	328.794
20	24	24	24	24	24	24	24	24	24	18	595.582	608.08	614.8905	621.6353	632.77
10	24	24	24	24	24	24	24	24	24	24	831.839	836.392	842.5405	844.357	858.456
5	24	24	24	24	24	24	24	24	24	24	1073.83	1085.066	1086.879	1087.658	1099.031
2	24	24	24	24	24	24	24	24	24	24	1414.943	1433.78	1446.581	1457.538	1482.577
1	24	24	24	24	24	24	24	24	24	24	1711.853	1721.208	1735.974	1751.589	1761.864

Range	IQR		
24.855	7.8%	8.37875	2.6%
37.188	6.0%	13.55525	2.2%
26.617	3.2%	7.965	0.9%
25.201	2.3%	2.59175	0.2%
67.634	4.7%	23.75775	1.6%
50.011	2.9%	30.3805	1.8%

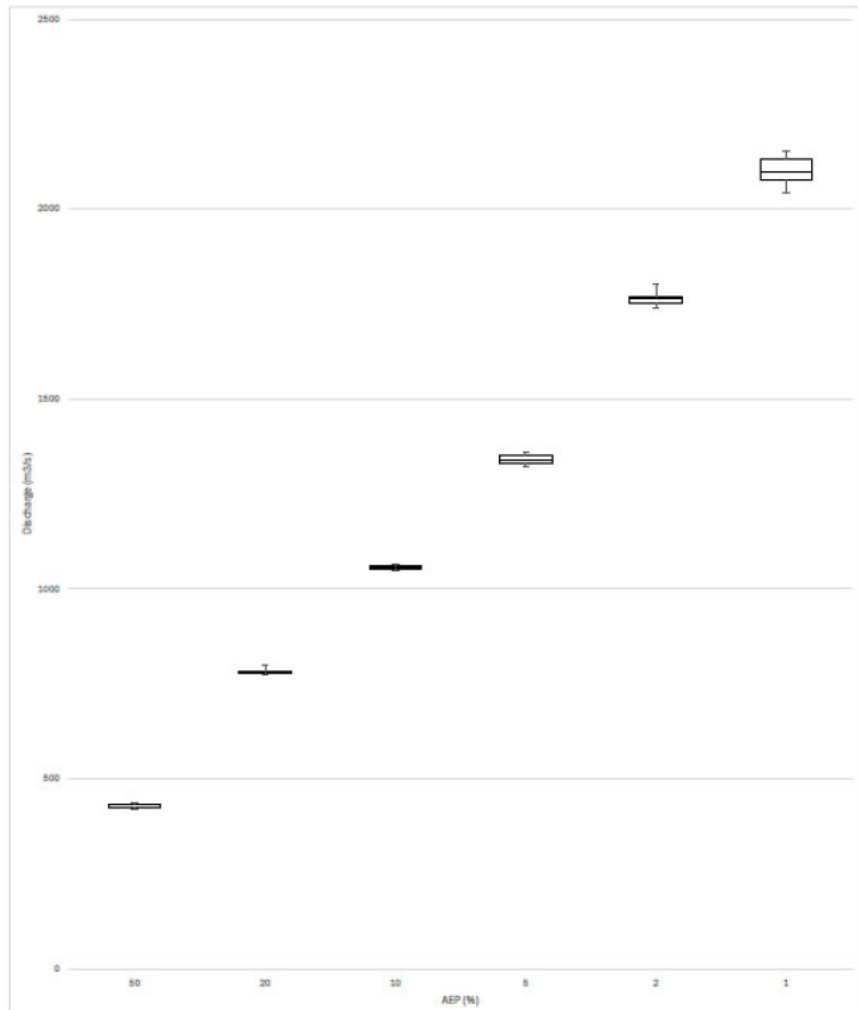


2090 RCP 8.5 SIMULATION SET

Discharges recorded on run number															
AEP	1	2	3	4	5	6	7	8	9	10	Min	Q1	Mean	Q3	Max
50	418.545	437.249	422.722	433.491	427.758	436.873	429.571	434.062	420.436	434.824	418.545	423.981	431.531	434.6335	437.249
20	777.576	779.586	782.225	783.326	779.327	775.941	785.369	797.521	782.985	777.437	775.941	778.0138	780.9055	783.2408	797.521
10	1065.422	1058	1055.335	1057.668	1063.591	1053.946	1049.779	1060.085	1054.102	1051.896	1049.779	1053.985	1056.502	1059.564	1065.422
5	1341.792	1328.513	1330.331	1354.01	1360.997	1322.794	1358.015	1340.611	1348.761	1338.661	1322.794	1332.414	1341.202	1352.698	1360.997
2	1760.247	1768.78	1741.547	1746.478	1751.995	1780.313	1754.184	1765.281	1766.999	1800.726	1741.547	1752.542	1762.764	1768.335	1800.726
1	2098.645	2071.13	2045.3	2089.062	2139.595	2093.962	2061.251	2109.047	2151.331	2149.215	2045.3	2075.613	2096.299	2131.958	2151.331

AEP	Critical duration											Min	Q1	Mean	Q3	Max
50	24	24	24	24	18	18	24	18	24	24	18	418.545	423.981	431.531	434.6335	437.249
20	18	18	18	18	24	18	18	18	24	18	18	775.941	778.0138	780.9055	783.2408	797.521
10	24	24	24	24	24	18	18	18	24	24	18	1049.779	1053.985	1056.502	1059.564	1065.422
5	24	24	24	24	24	24	24	24	24	24	24	1322.794	1332.414	1341.202	1352.698	1360.997
2	24	24	24	24	24	24	24	24	24	24	24	1741.547	1752.542	1762.764	1768.335	1800.726
1	24	24	24	18	24	24	24	24	144	24	24	2045.3	2075.613	2096.299	2131.958	2151.331

Range	IQR		
18.704	4.3%	10.6525	2.5%
21.58	2.8%	5.227	0.7%
15.643	1.5%	5.57875	0.5%
38.203	2.8%	20.28425	1.5%
59.179	3.4%	15.7925	0.9%
106.031	5.1%	56.345	2.7%



RCP 4.5 PROJECTION ANALYSIS

AEP	Median discharge (m ³ /s)				% by 2030	% by 2050	2090%
	2020	2030	2050	2090			
50	223.0011	281.1	296.2	330.0	26%	33%	48%
20	467.1143	547.5	580.1	630.4	17%	24%	35%
10	661.8612	767.4	799.5	865.8	16%	21%	31%
5	868.4268	992.7	1044.5	1116.7	14%	20%	29%
2	1164.494	1315.1	1383.0	1483.7	13%	19%	27%
1	1411.44	1587.9	1659.5	1772.3	12%	18%	26%

Formation of charts

Q1-min

AEP	2020	2030	2050	2090
50	10.85775	4.43325	5.11425	0.84575
20	5.282	4.454	4.4085	5.699
10	5.51675	10.444	6.17225	5.3195
5	32.196	10.11275	6.538	17.549
2	6.2855	7.31875	13.56325	3.27925
1	12.79775	7.254	21.20525	20.35725

Q1

AEP	2020	2030	2050	2090
50	221.2738	276.0593	293.5853	327.1218
20	462.919	544.79	576.0435	625.884
10	654.9088	763.452	797.8323	856.3405
5	865.855	982.7728	1042.861	1107.363
2	1155.7	1311.807	1367.901	1472.204
1	1394.114	1574.504	1637.702	1767.107

Med-Q1

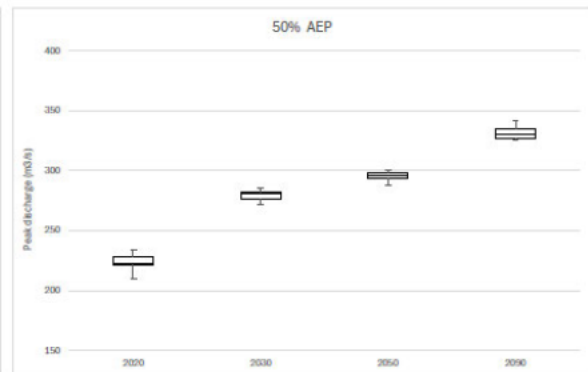
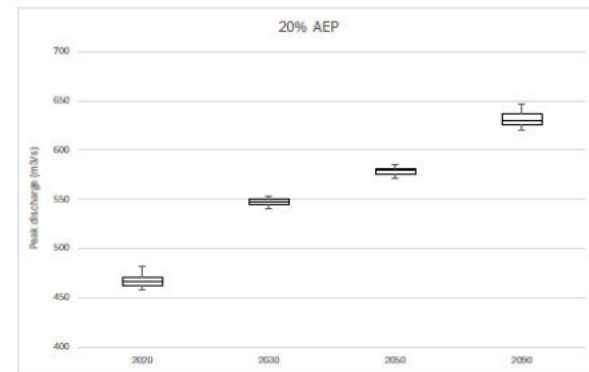
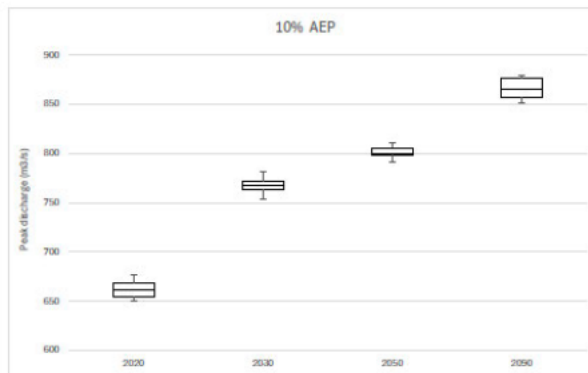
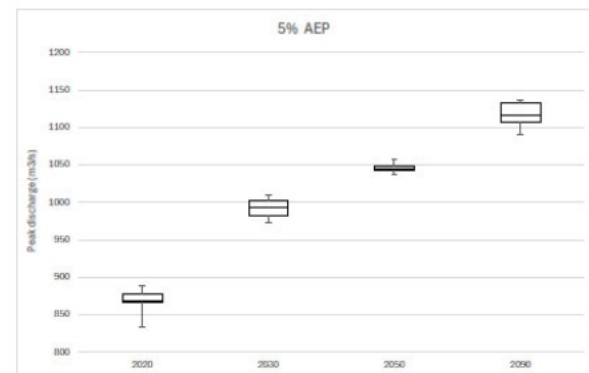
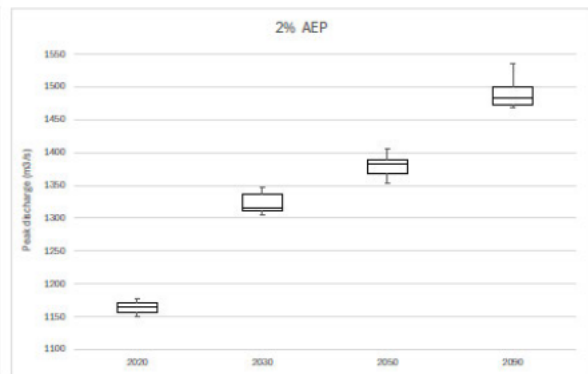
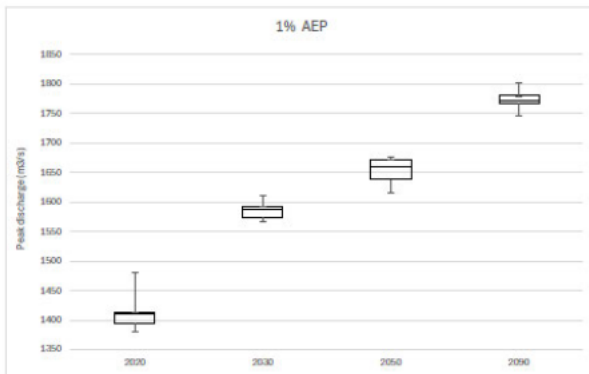
AEP	2020	2030	2050	2090
50	1.72735	5.05175	2.63675	2.91225
20	4.1953	2.731	4.0255	4.4865
10	6.95245	3.917	1.65775	9.4555
5	2.5718	9.96275	1.6745	9.3235
2	8.7945	3.29125	15.10275	11.49675
1	17.32595	13.35	21.82825	5.19675

Q3-Med

AEP	2020	2030	2050	2090
50	5.1449	1.3285	2.296	5.3835
20	3.2142	2.44475	1.58575	7.08525
10	6.8233	4.6955	6.4225	10.57525
5	9.6027	9.91	3.49475	16.46175
2	6.0715	20.99875	4.99525	17.36
1	2.5348	4.12725	12.9725	8.19775

Max-Q3

AEP	2020	2030	2050	2090
50	5.585	3.7405	1.607	6.2905
20	11.8885	3.26225	3.98625	9.69425
10	7.8555	9.7425	4.7595	2.49675
5	9.9515	6.2935	9.81575	3.85375
2	7.4025	11.93725	18.09875	35.121
1	65.9165	19.04575	4.778	22.39225



RCP 8.5 PROJECTION ANALYSIS

Median discharge (m3/s)							
AEP	2020	2030	2050	2090	% by 2030	% by 2050	% by 2090
50	223.0011	280.3	320.0	431.5	26%	43%	94%
20	467.1143	555.5	614.9	780.9	19%	32%	67%
10	661.8612	779.5	842.5	1056.5	18%	27%	60%
5	868.4268	1010.4	1086.9	1341.2	16%	25%	54%
2	1164.494	1340.7	1446.6	1762.8	15%	24%	51%
1	1411.44	1612.4	1736.0	2096.3	14%	23%	49%

Q1-min

AEP	2020	2030	2050	2090
50	10.85775	7.282	10.23075	5.436
20	5.282	12.96375	12.498	2.07275
10	5.51675	8.138	4.553	4.206
5	32.196	2.58325	11.23625	9.6195
2	6.2855	6.321	18.83675	10.99525
1	12.79775	14.8265	9.35525	30.313

Q1

AEP	2020	2030	2050	2090
50	221.2738	276.045	314.1698	423.981
20	462.919	546.7698	608.08	778.0138
10	654.9088	774.137	836.392	1053.985
5	865.855	999.4223	1085.066	1332.414
2	1155.7	1337.857	1433.78	1752.542
1	1394.114	1598.215	1721.208	2075.613

Med-Q1

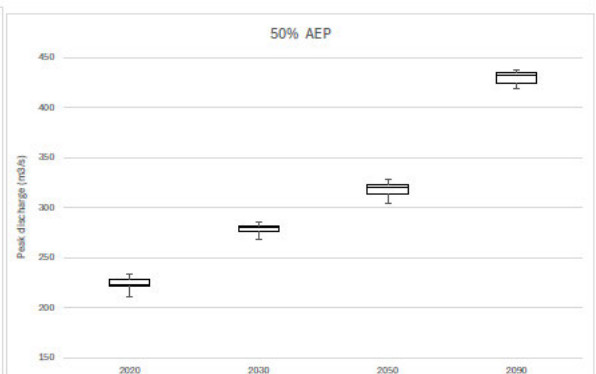
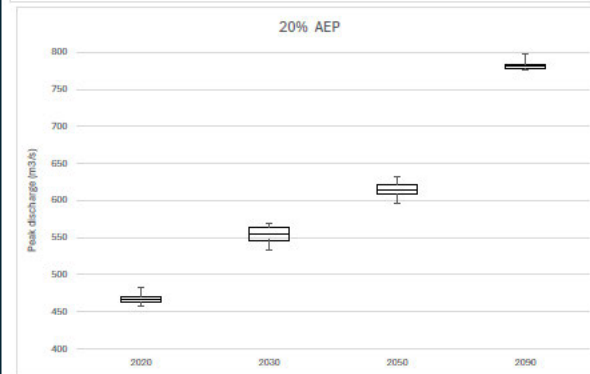
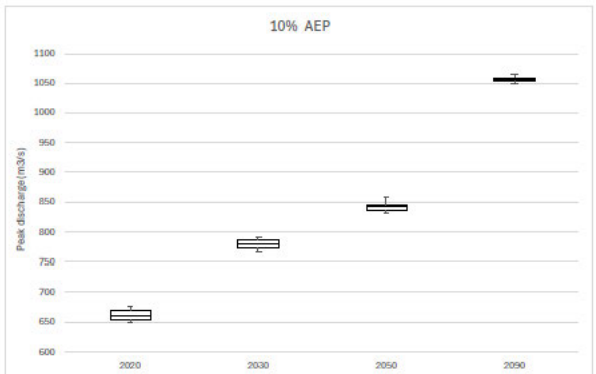
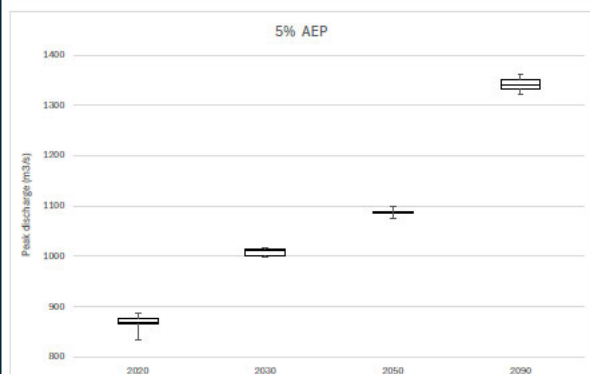
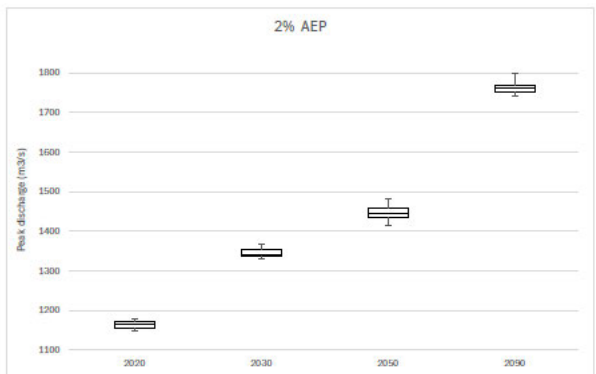
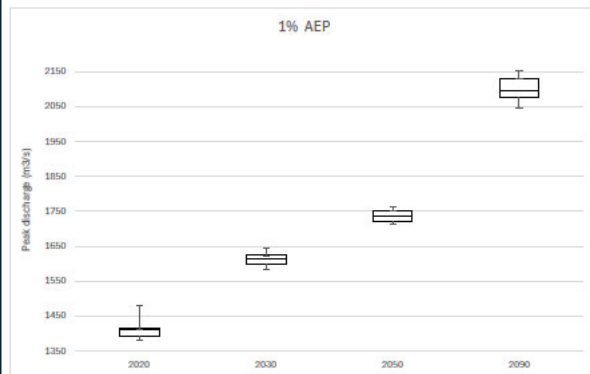
AEP	2020	2030	2050	2090
50	1.72735	4.2625	5.81325	7.55
20	4.1953	8.77875	6.8105	2.89175
10	6.95245	5.391	6.1485	2.5165
5	2.5718	10.95575	1.81225	8.788
2	8.7945	2.8595	12.80075	10.22175
1	17.32595	14.1775	14.76525	20.6855

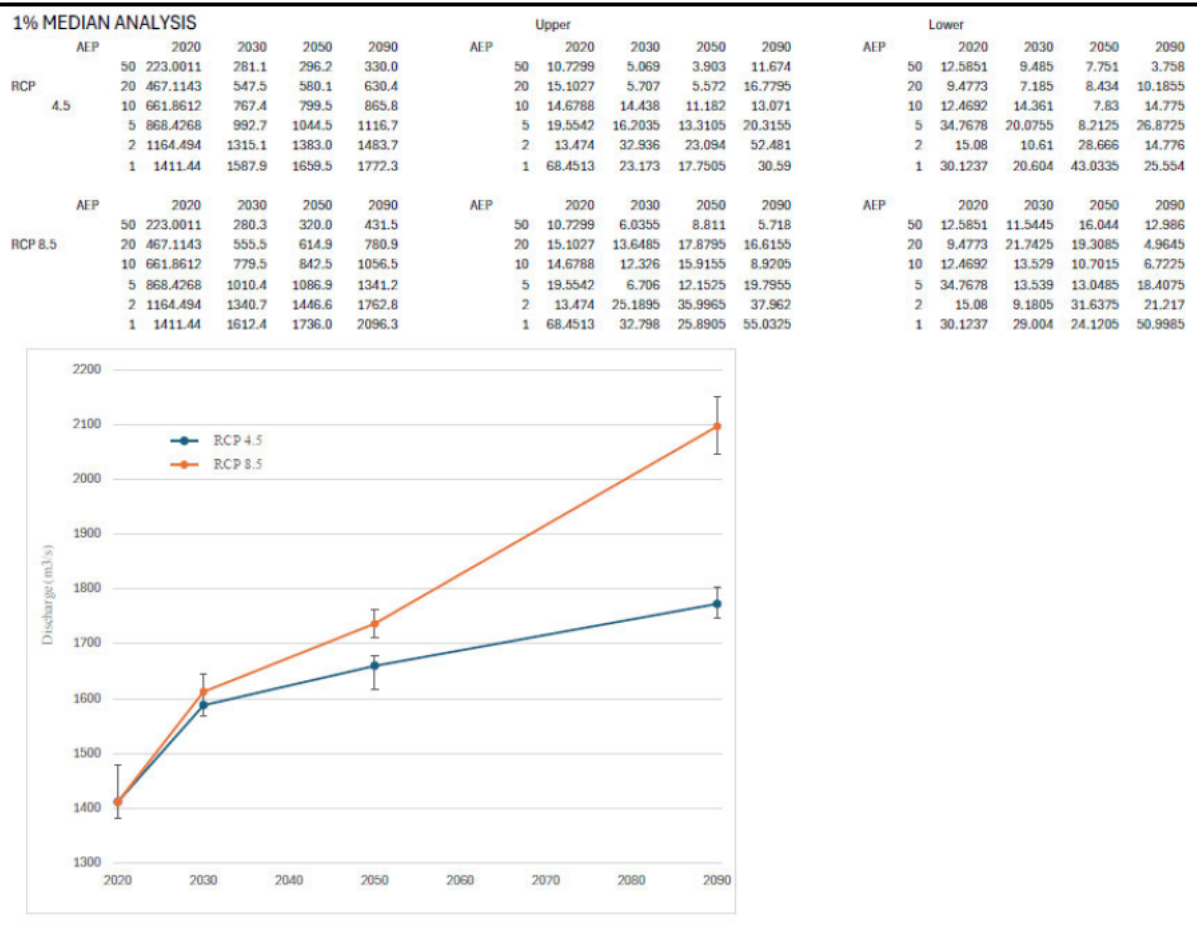
Q3-Med

AEP	2020	2030	2050	2090
50	5.1449	1.65975	2.5655	3.1025
20	3.2142	7.438	6.74475	2.33525
10	6.8233	6.32975	1.8165	3.06225
5	9.6027	2.35625	0.7795	11.49625
2	6.0715	14.0855	10.957	5.57075
1	2.5348	11.88825	15.61525	35.6595

Max-Q3

AEP	2020	2030	2050	2090
50	5.585	4.37575	6.2455	2.6155
20	11.8885	6.2105	11.13475	14.28025
10	7.8555	5.99625	14.099	5.85825
5	9.9615	4.34975	11.373	8.29925
2	7.4025	11.104	25.0395	32.39125
1	65.9165	20.90975	10.27525	19.373





Appendix H: Sensitivity analysis of model parameters using 2020 outputs

	AEP	50	20	10	5	2	1
	2020 Med	223.0011	467.1143	661.8612	868.4268	1164.494	1411.44
KC + 10%							
		Discharges recorded on run number					
29.7	AEP	1	2	3	4	5	
	50	207.646	201.794	210.813	207.298	206.731	
	20	429.236	433.287	431.989	425.173	439.986	
	10	609.539	615.113	604.845	611.945	632.865	
	5	795.006	795.82	800.967	799.57	796.256	
	2	1089.774	1072.127	1091.725	1077.384	1078.033	
	1	1319.796	1278.987	1302.257	1323.576	1325.423	
Critical duration							
	50	24	24	24	24	24	
	20	24	24	24	24	24	
	10	24	24	24	24	24	
	5	24	24	24	24	24	
	2	24	24	24	24	24	
	1	144	36	144	144	144	
2 5 10 20 50 100							
Min		201.794	425.173	604.845	795.006	1072.127	1278.987
Q1		206.731	429.236	609.539	795.82	1077.384	1302.257
Med		207.298	431.989	611.945	796.256	1078.033	1319.796
Q3		207.646	433.287	615.113	799.57	1089.774	1323.576
Max		210.813	439.986	632.865	800.967	1091.725	1325.423
% Med		-7.0%	-7.5%	-7.5%	-8.3%	-7.4%	-6.5%
KC - 10%							
		Discharges recorded on run number					
24.3	AEP	1	2	3	4	5	
	50	248.204	247.846	238.181	241.67	249.848	
	20	501.201	525.346	517.537	511.331	514.045	
	10	714.851	712.187	712.198	713.91	720.462	
	5	925.99	925.64	920.191	926.845	926.279	
	2	1321.966	1238.915	1242.945	1253.216	1219.809	
	1	1489.297	1481.676	1471.374	1484.852	1490.037	
Critical duration							
	50	24	24	18	24	24	
	20	24	24	24	24	24	
	10	24	24	24	24	24	
	5	24	24	24	24	24	
	2	24	24	24	24	24	
	1	24	24	24	24	24	

		2	5	10	20	50	100
	Min	238.181	501.201	712.187	920.191	1219.809	1471.374
	Q1	241.67	511.331	712.198	925.64	1238.915	1481.676
	Med	247.846	514.045	713.91	925.99	1242.945	1484.852
	Q3	248.204	517.537	714.851	926.279	1253.216	1489.297
	Max	249.848	525.346	720.462	926.845	1321.966	1490.037
	% Med	11.1%	10.0%	7.9%	6.6%	6.7%	5.2%
IL + 20%	Discharges recorded on run number						
30	AEP	1	2	3	4	5	
	50	187.822	205.803	181.439	202.17	174.577	
	20	438.508	443.731	446.777	435.953	442.622	
	10	616	630.757	648.222	627.861	638.67	
	5	840.256	823.341	843.599	807.55	844.047	
	2	1128.232	1124.892	1130.449	1144.134	1162.218	
	1	1365.584	1370.686	1365.428	1382.754	1398.218	
	AEP	Critical duration					
	50	24	24	24	24	24	
	20	24	24	24	24	24	
	10	24	24	24	24	24	
	5	24	24	24	24	24	
	2	24	24	24	24	24	
	1	144	24	24	24	24	
		2	5	10	20	50	100
	Min	174.577	435.953	616	807.55	1124.892	1365.428
	Q1	181.439	438.508	627.861	823.341	1128.232	1365.584
	Med	187.822	442.622	630.757	840.256	1130.449	1370.686
	Q3	202.17	443.731	638.67	843.599	1144.134	1382.754
	Max	205.803	446.777	648.222	844.047	1162.218	1398.218
	% Med	-15.8%	-5.2%	-4.7%	-3.2%	-2.9%	-2.9%
IL - 20%	Discharges recorded on run number						
20	AEP	1	2	3	4	5	
	50	256.727	259.23	254.511	253.411	242.078	
	20	477.754	486.612	496.778	487.586	484.723	
	10	675.883	678.458	678.925	663.704	666.605	
	5	878.994	868.96	879.912	895.299	882.655	
	2	1168.352	1159.404	1188.191	1166.783	1177.99	
	1	1424.556	1426.25	1422.658	1420.323	1414.927	
	AEP	Critical duration					
	50	24	24	24	24	24	

		20	18	24	24	24	24	
		10	24	24	24	24	24	
		5	24	24	24	24	24	
		2	24	24	24	24	24	
		1	24	24	24	24	144	
			2	5	10	20	50	100
	Min		242.078	477.754	663.704	868.96	1159.404	1414.927
	Q1		253.411	484.723	666.605	878.994	1166.783	1420.323
	Med		254.511	486.612	675.883	879.912	1168.352	1422.658
	Q3		256.727	487.586	678.458	882.655	1177.99	1424.556
	Max		259.23	496.778	678.925	895.299	1188.191	1426.25
	% Med		14.1%	4.2%	2.1%	1.3%	0.3%	0.8%
CL + 20%								
Discharges recorded on run number								
1.68	AEP		1	2	3	4	5	
		50	201.511	204.143	208.242	207.489	209.44	
		20	442.092	448.996	432.011	442.721	431.231	
		10	627.779	641.15	645.251	630.201	619.669	
		5	811.347	833.331	838.689	841.085	825.414	
		2	1120.388	1128.164	1129.2	1123.612	1122.786	
		1	1369.412	1368.971	1358.419	1357.874	1369.012	
	AEP		Critical duration					
		50	24	24	24	24	24	
		20	24	24	24	24	24	
		10	24	24	24	24	24	
		5	24	24	24	24	24	
		2	24	24	24	24	24	
		1	24	24	24	144	24	
			2	5	10	20	50	100
	Min		201.511	431.231	619.669	811.347	1120.388	1357.874
	Q1		204.143	432.011	627.779	825.414	1122.786	1358.419
	Med		207.489	442.092	630.201	833.331	1123.612	1368.971
	Q3		208.242	442.721	641.15	838.689	1128.164	1369.012
	Max		209.44	448.996	645.251	841.085	1129.2	1369.412
	% Med		-7.0%	-5.4%	-4.8%	-4.0%	-3.5%	-3.0%
CL - 20%								
Discharges recorded on run number								
1.12	AEP		1	2	3	4	5	
		50	251.854	259.237	246.195	233.374	243.009	
		20	487.583	501.438	503.088	493.858	503.779	
		10	664.993	690.326	703.129	699.209	692.585	

	5	901.453	902.064	903.799	918.103	909.428	
	2	1179.473	1201.824	1193.772	1175.215	1217.703	
	1	1435.125	1432.342	1427.53	1409.079	1452.443	
AEP	Critical duration						
	50	24	24	24	24	24	
	20	24	24	24	24	24	
	10	24	24	24	24	24	
	5	24	24	24	24	24	
	2	24	24	24	24	24	
	1	24	24	24	144	24	
		2	5	10	20	50	100
Min		233.374	487.583	664.993	901.453	1175.215	1409.079
Q1		243.009	493.858	690.326	902.064	1179.473	1427.53
Med		246.195	501.438	692.585	903.799	1193.772	1432.342
Q3		251.854	503.088	699.209	909.428	1201.824	1435.125
Max		259.237	503.779	703.129	918.103	1217.703	1452.443
% Med		10.4%	7.3%	4.6%	4.1%	2.5%	1.5%

Appendix I: Flood frequency analysis – RMC outputs

INPUT DATA

Summary statistics

Measure	Unit	All data	Low outliers excluded
Record Length	years	33	26
Low Outliers	number	7	7
Minimum	m3/s	0	7.41
Maximum	m3/s	1,387.11	1,387.11
Mean	m3/s	182.86	225.96
Std Dev	m3/s	343.08	370
Skewness		2.5122	2.2935
Kurtosis		8.2562	4.3783
Mean (of log)		1.023	1.8928
Std Dev (of log)		1.8592	0.6591
Skewness (of log)		-1.2953	0.232
Kurtosis (of log)		3.4322	-0.6233
5%	m3/s	0	7.77
25%	m3/s	7.62	22.88
50%	m3/s	53.5	67.54
75%	m3/s	182.1	193.19
95%	m3/s	1,094.35	1,083.66

Annual Maximum series input 143229A

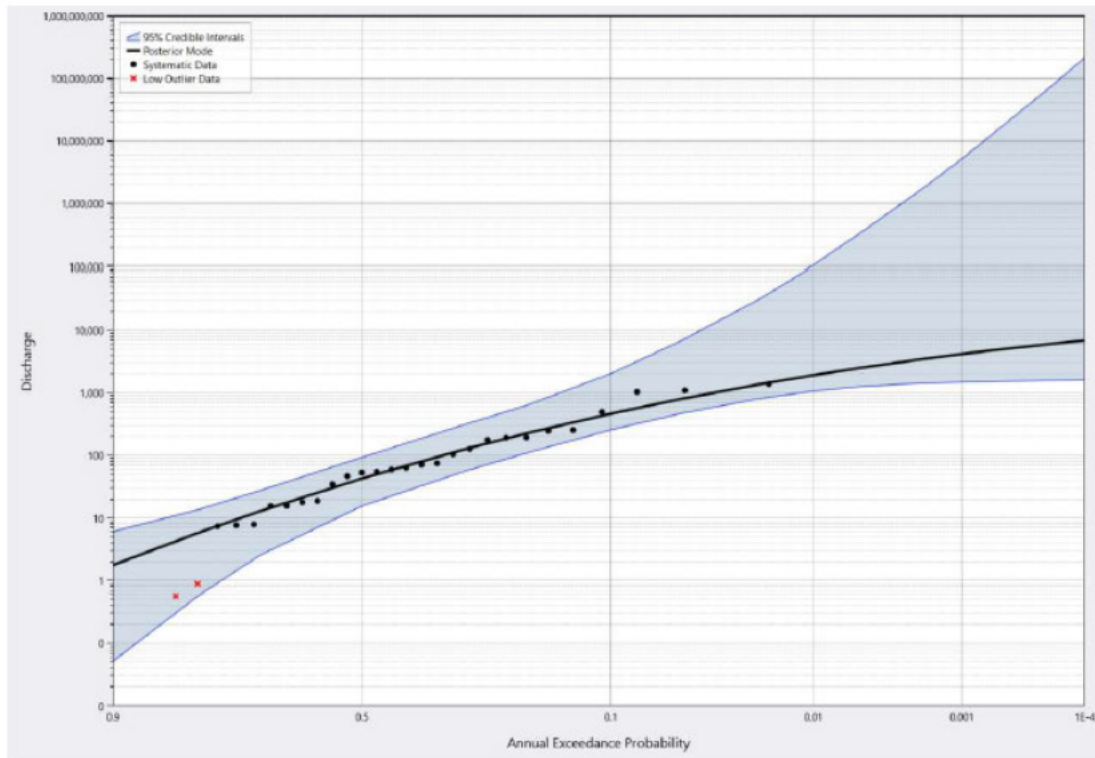
Year	charge (m ³ /s)	Plotting position	Is low outlier
1991	127.376	0.2892	FALSE
1992	192.208	0.2289	FALSE
1993	0.567	0.8313	TRUE
1994	0	0.8916	TRUE
1995	7.406	0.7711	FALSE
1996	496.592	0.1084	FALSE
1997	18.882	0.5904	FALSE
1998	0	0.9217	TRUE
1999	105.039	0.3193	FALSE
2000	15.564	0.6807	FALSE
2001	193.514	0.1988	FALSE
2002	0	0.8614	TRUE
2003	7.709	0.7410	FALSE
2004	75.116	0.3494	FALSE
2005	55.205	0.4699	FALSE
2006	17.919	0.6205	FALSE
2007	0	0.9819	TRUE
2008	53.504	0.5000	FALSE
2009	255.854	0.1386	FALSE
2010	46.94	0.5301	FALSE
2011	1387.11	0.0181	FALSE
2012	63.378	0.4096	FALSE
2013	1041.5	0.0783	FALSE
2014	59.687	0.4398	FALSE
2015	15.68	0.6506	FALSE
2016	0.891	0.8012	TRUE
2017	248.682	0.1687	FALSE
2018	7.939	0.7108	FALSE
2019	0	0.9518	TRUE
2020	34.855	0.5602	FALSE
2021	177.775	0.2590	FALSE
2022	1097.72	0.0482	FALSE
2023	71.705	0.3795	FALSE

RMC DISTRIBUTION FUNCTION OUTPUT

Measure	Exp.	Gamma	GEV	GL	GP	EVI	In-Norm	Logistic	Log-Norm	LP3	Norm	P3	Weibull
Location	-6.955	N/A	19.4518	40.8376	-12.1712	27.0431	393.1046	81.3885	1.5213	1.3769	119.0687	180.0819	N/A
Scale	193.9176	601.6235	48.3992	53.8431	57.3812	201.1046	4,636.17	180.7966	0.9655	1.3011	406.6537	240.8627	89.613
Shape	N/A	0.3115	-1.1258	-1.1281	-0.962	N/A	N/A	N/A	N/A	-1.32	N/A	2	0.475
Minimum	-6.96	0	-23.54	-6.89	-12.17	-∞	0	-∞	0	0	-∞	-60.78	0
Maximum	∞	∞	∞	∞	∞	∞	∞	∞	∞	2,230.07	∞	∞	∞
Mean	186.96	187.44	N/A	N/A	1,498.53	143.12	393.1	81.39	97.14	182.2	119.07	180.08	197.94
Std Dev	193.92	335.81	N/A	N/A	N/A	257.93	4,636.17	327.93	266.98	304.98	406.65	240.86	476.21
Skewness	2	3.5832	N/A	N/A	N/A	1.1396	1,675.80	0	29.008	2.5842	0	2	7.4164
Kurtosis	9	22.2586	N/A	N/A	N/A	5.4	#####	4.2	6,822.84	10.4196	3	9	112.4556
AEP													
Discharge (m3/s)													
0.001	1,267.65	2,479.65	93,424.96	105,911.07	49,172.71	1,290.47	17,405.19	1,224.51	17,405.52	4,009.67	1,335.97	1,464.99	4,017.38
0.002	1,139.82	2,162.72	42,522.57	48,125.26	24,452.42	1,164.11	11,417.36	1,109.16	11,417.57	3,322.33	1,252.59	1,313.50	3,267.72
0.005	970.83	1,751.10	15,001.49	16,930.62	9,692.82	996.91	6,259.16	956.4	6,259.27	2,473.37	1,133.74	1,113.25	2,392.95
0.01	843	1,446.91	6,805.21	7,657.16	4,798.85	870.19	3,811.54	840.38	3,811.60	1,890.71	1,035.66	961.76	1,819.69
0.02	715.17	1,151.02	3,073.49	3,442.50	2,362.56	742.99	2,216.79	723.52	2,216.82	1,371.83	928.49	810.27	1,323.19
0.05	546.18	777.82	1,057.81	1,172	907.95	573.26	983.25	566.09	983.26	801.45	767.74	610.02	785.68
0.1	418.35	515.83	458.76	500.41	425.63	442.13	477.49	441.93	477.5	468.34	624.92	458.53	469.91
0.2	290.52	282.17	186.87	198.1	185.52	305.43	199.12	307.17	199.12	225.71	451.97	307.04	233.46
0.3	215.74	165.99	103.33	106.59	105.78	219.99	105.98	217.61	105.98	126.01	327.26	218.43	132.43
0.5	121.54	54.19	40.36	39.64	42.16	98.95	37.36	76.81	37.36	43.13	121.1	106.79	45.04
0.7	59.48	11.73	14.31	14.08	14.98	-1.63	13.17	-63.98	13.17	12.81	-85.05	33.25	12.3
0.8	34.86	3.61	5.92	6.85	6.49	-54.5	7.01	-153.55	7.01	5.73	-209.76	4.07	4.92
0.9	13.13	0.49	-1.27	1.69	-0.1	-119.75	2.92	-288.3	2.92	1.71	-382.71	-21.67	1.14
0.95	3.16	0.07	-4.97	-0.25	-2.87	-167.68	1.42	-412.47	1.42	0.58	-525.54	-33.49	0.28
0.98	-2.57	0	-7.75	-1.21	-4.4	-216.3	0.63	-569.89	0.63	0.16	-686.29	-40.28	0.05
0.99	-4.44	0	-9.08	-1.49	-4.89	-246.01	0.37	-686.76	0.37	0.06	-793.45	-42.5	0.01

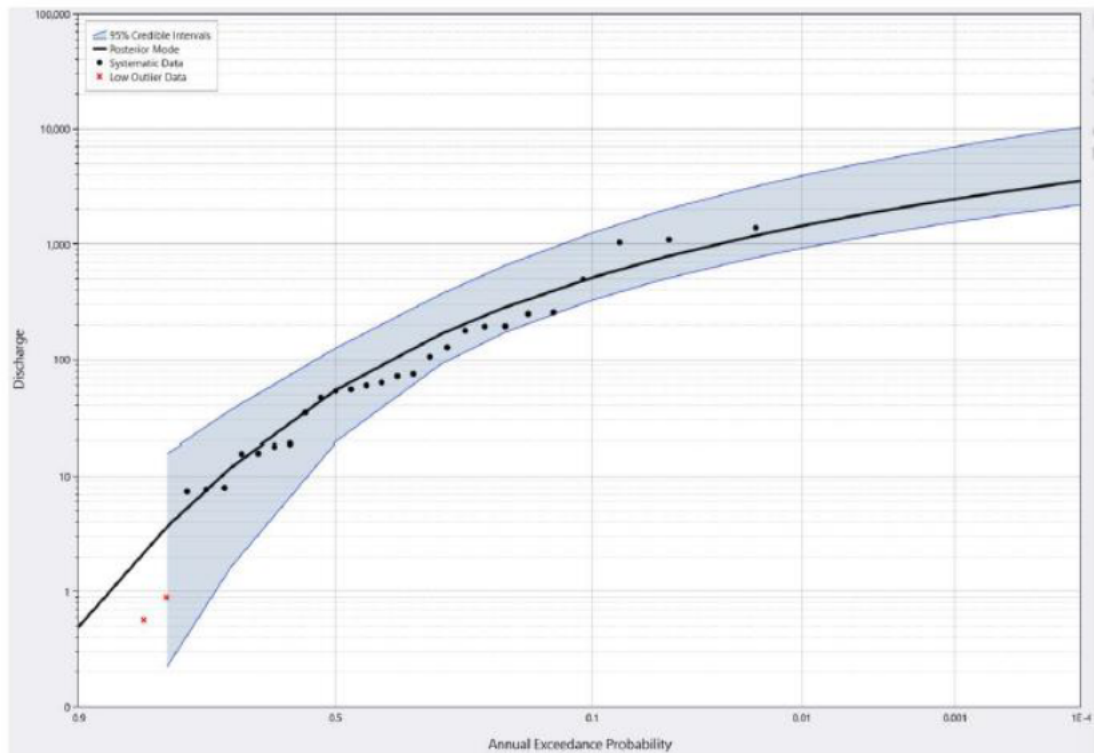
RMC BAYESIAN POSTERIOR MODE - LP3

AEP	Discharge (m3/s)			Mode
	97.5% CI	2.5% CI	Predictive	
0.001	5240689.83	1488.16	109219.71	4194.77
0.002	1668918.40	1424.46	38659.31	3447.99
0.005	357245.13	1272.14	11976.74	2539.62
0.01	106610.37	1072.56	5152.30	1925.76
0.02	32580.86	816.35	2735.94	1386.27
0.05	6874.96	471.30	1253.12	802.04
0.1	2033.24	256.41	616.71	465.77
0.2	624.97	108.70	270.52	223.55
0.3	310.27	55.50	133.05	124.77
0.5	93.38	15.61	39.81	42.91
0.7	27.56	2.55	11.37	12.90
0.8	13.69	0.58	4.92	5.83
0.9	6.08	0.05	1.44	1.77
0.95	3.83	0.00	0.39	0.61
0.98	2.68	0.00	0.06	0.17
0.99	2.23	0.00	0.01	0.07



RMC BAYESIAN POSTERIOR MODE - Gamma

AEP	Discharge (m3/s)			
	97.5% CI	2.5% CI	Predictive	Mode
0.001	7021.57	1556.93	4330.94	2470.27
0.002	6046.19	1360.50	3761.11	2154.79
0.005	4827.33	1110.27	2734.50	1745.04
0.01	3928.33	923.26	2082.81	1442.20
0.02	3060.20	738.11	1619.81	1147.58
0.05	1991.58	502.40	1010.19	775.92
0.1	1259.64	328.52	629.37	514.93
0.2	651.69	171.27	333.37	282.02
0.3	369.05	91.05	188.56	166.11
0.5	125.69	19.50	58.69	54.40
0.7	36.60	1.62	11.51	11.84
0.8	15.58	0.22	3.15	3.66
0.9	3.82	0.01	0.34	0.50
0.95	0.96	0.00	0.03	0.07
0.98	0.16	0.00	0.00	0.00
0.99	0.04	0.00	0.00	0.00



RMC BAYESIAN POSTERIOR MODE - Weibull

AEP	Discharge (m3/s)			
	97.5% CI	2.5% CI	Predictive	Mode
0.001	21572.69	1835.10	8310.46	4027.14
0.002	16563.08	1548.54	6124.38	3275.27
0.005	10968.21	1188.26	3882.84	2398.06
0.01	7598.81	936.62	2746.78	1823.29
0.02	5048.00	712.02	1836.63	1325.57
0.05	2613.77	451.39	1022.99	786.87
0.1	1400.12	280.50	586.14	470.48
0.2	610.75	140.32	284.39	233.65
0.3	328.24	76.49	158.40	132.50
0.5	112.98	21.99	53.81	45.04
0.7	35.97	4.37	14.40	12.29
0.8	16.92	1.31	5.62	4.92
0.9	5.30	0.19	1.22	1.13
0.95	1.78	0.03	0.28	0.28
0.98	0.44	0.00	0.04	0.04
0.99	0.15	0.00	0.01	0.01

